A Study of the Structural Behaviour of Reinforced Brickwork Pocket-Type Sections

Rotimi K. O. Mebude, B.Sc.(Hons), M.Sc.

A Thesis submitted for the Degree of Doctor of Philosophy

Department of Civil & Environmental Engineering,
The University of Edinburgh, Scotland,
United Kingdom

March 1997

DECLARATION

This thesis is the result of research work undertaken in the department of Civil and Environmental Engineering at the University of Edinburgh, for the degree of Doctor of Philosophy.

I hereby declare that the work in this thesis has been carried out by myself, unless otherwise stated in the appropriate portion, and the thesis has been composed by me under the supervision of Dr B.P. Sinha and Dr R.F. Pedreschi.

Edinburgh, Scotland , March 1997.

Rotimi K. O. Mebude.

DEDICATION

This whole work is dedicated to The Almighty, Everlasting and Awesome God for His abundant supply of grace of mercy, patience and wisdom to me.

To the memory of some members of my immediate extended family who departed this wonderful world, at different times, in the course of this research effort.

My dearest sister, Mrs Morenike Sekinat Ibikunle, who departed from us, rather suddenly, but has gone to rest with the LORD.

My dearest sister-in-law, Miss Temitope Oyejola Oyenuga, who departed from us, again rather suddenly, but has gone to rest with the LORD.

My Father-in-law, His Royal Highness, Oba Alfred Adebambo Oyenuga, who departed from us after having lived to a very ripe age and enjoyed good health over and above several others of our God's numerous blessings, and has gone to rest with the LORD.

Finally, to princess Oyebola Tinuade, "my jewel of inestimable value", for her moral and spiritual support over the years and even in the years to come until the rest of our days are spent and, to God's tremendous blessings : OLUWATOFUNMI (Deborah), OLUWATOSIN (Opeyemi) and OLUWATOBILOBA (Adefolarin).
"For this God is our God for ever and ever : He will be our guide *even* unto death" Psalm 48 (verse 14).

ACKNOWLEDGEMENTS

I acknowledge with thanks the supervision and guidance given by both Dr B.P. Sinha and Dr R.F. Pedreschi, my supervisors, throughout the duration of this research project. Their comments and suggestions at various stages of the research were forthright and most helpful.

Many thanks to Professor M.C. Forde and Dr D.R. Fairbairn and all the other senior members of staff in the department of Civil & Environmental Engineering for their encouragement and helpful advice at different stages of the execution of the project.

My thanks and gratitude go to the Association of Commonwealth University (ACU) through the Commonwealth Scholarship Commission in London, as well as to the Federal Republic of Nigeria, for providing me with the necessary financial support to do this research work. To Mr Alex Galloway of the C.O.T. and Mr Pat Maclaughlin of the "Peoples College", a very big thank you for your help, kindness and forbearance. To my several friends who have given support, both moral and sometimes financial, over the past few years. It is prudent for me not to mention names specifically here, firstly so as not to generate any resentment which the inadvertent ommission of some important names is likely to cause and secondly, for reasons of practicability. I am, nonetheless, very grateful for all your labour of love over me.

Many thanks go to all the technicians in the department, particularly to Mr Jim Hutcheson, the chief technician. To Mr Norrie Erskine, Mr Les Russell, Mr Ron O'Donnell, Mr Alisdair McInnes, Mr Kevin Broughton as well as Mr Ian Fowler, thank you. You were all most helpful and quite willing to give a hand whenever help was needed. The other members of the technical crew, in spite of the usually high strain on you, provided support in various ways directly but, oftentimes indirectly, and to all of you, I am grateful.

Finally, all thanks are due to Almighty God, my Heavenly Father, who gave the grace to make this rather herculian task come to fruition and for making all things possible.

ABSTRACT

This thesis investigates the structural behaviour of reinforced brickwork pocket-type sections using the twin approach of experimental and theoretical studies. The behaviour, in shear, of this type of reinforced brickwork is studied experimentally through tests conducted on eight longitudinally-reinforced, full-scale beams, under four-point loading, and for a range of shear-span/effective depth ratios (a/d = 2.0-6.0) and % reinforcement (ρ = 0.61%-1.60%). Aspects of structural behaviour include (a) the ductility of the sections via their moment-curvature relationships as well as their load-deflection behaviour, (b) the shear behaviour of the sections vis-a-vis cracking development and growth through the various stages of loading up to and including the ultimate point. Since the reality of shear failure is such that the members were acting under both shear and flexural stresses, flexural behaviour of the sections are also investigated for the pocket-reinforced beams.

The theoretical formulations are based on small scale representative brickwork prism tests, which are compared with experimental findings. A summary of existing methods for predicting shear strength is presented. The method proposed is based on an adaptation of the technique based on plastic analysis which was used originally for predicting the shear strength of concrete beam sections. The ultimate shear strength results obtained experimentally for the eight pocket-reinforced beams are compared with theoretical predictions based on the proposed method. This adapted method is based on a rigorous analysis of all known brickwork beams which have been reported to fail in shear.

The flanged behaviour of wall sections are also investigated. To this end, six half-scale simply-supported, reinforced brickwork pocket-type wall specimens, in which the % steel is constant and the pocket spacing varied, are tested to determine the characteristics of flanged-action behaviour. A method is proposed for the calculation of the effective width associated with different pocket stem spacings. This method is

based on an analysis of experimental strain measurements across the pocket stems. Results obtained are compared with Yield-Line theory and the Direct Method. The direct method takes into account the mechanical properties of the brickwork and steel as well as tension stiffening effects and uses the stress-strain curves of the materials. These results are further compared with the provisions in the British Code of Practice (BS 5628 : Part 2 :1995) for these members.

NOTATION

a	span of the slab
a_v	shear span
A	cross-sectional area of beam
A_{st}	area of steel reinforcement
b	breadth of the beam
d	effective depth of steel reinforcement
d_n	neutral axis depth
E	Modulus of elasticity of brickwork
E_s	Modulus of elasticity of steel
f	compressive stress in brickwork
f_t	modulus of rupture of brickwork (N/mm^2)
f_m	compressive strength of brickwork (N/mm^2)
$f(\varepsilon)$	stress-strain relationship of brickwork
$f_s(\varepsilon_s)$	stress-strain relationship of steel reinforcement
F_y	yield force of steel reinforcement
h	total depth of the section
I	second moment of area
I_{cr}	second moment of area of cracked section
$I_{effective}$	effective second moment of area
I_u	second moment of area of transformed uncracked section
m	an index
n	modular ratio
M	bending moment
M_{cr}	cracking moment
M_{ult}	ultimate moment
q	total applied load on slab
q_x , q_y , q_{xy}	random proportions of q
S	spacing of the reinforced pockets
v	relative displacement rate of two rigid parts (I) & (II)

V	shear force at failure
x	major direction of bending
y	direction measured across the pocket stems
w	assumed deflection function in slab
W_E	external work done
W_I	internal work done
X_0 -X_3	coefficients of stress/strain relationship of brickwork
Z	section modulus
α	angle of displacement to yield line
β	angle of yield line to axis of beam
β_1	an empirical factor
$\varepsilon_1, \varepsilon_2$	strains in top and bottom fibres of beam
ε	strain in brickwork
ε_{bw}	applied compressive strain in top fiber of slab section
ε_m	ultimate compressive strain in brickwork
ε_x	compressive strain measured across the pockets
ε_{st}	strain in steel reinforcement
λ_1, λ_2	stress block factors
ϕ	curvature of beam
τ	shear stress, V/bh
σ	stress in compression strut
σ_x	compressive stress across the pocket
θ	angle of inclination of compressive strut
ϑ	effectiveness factor
ρ	% steel, A_{st}/bd
υ	Poisson's ratio
Φ	degree of reinforcement

CONTENTS

CHAPTER 1

INTRODUCTION

1.1 REINFORCED BRICKWORK SECTIONS

Reinforced brickwork sections have been employed for many years in the construction industry. One major factor which has worked against their widespread adoption is the difficulty of introducing reinforcement into them. Several innovations have arisen as a result of this including thickening the bed joints containing the steel reinforcement, as in bed- and collar-joint reinforced brickwork sections and the development of bonding patterns which incorporate the steel reinforcement in concrete grout to enable the steel to be laid continuously throughout the length of a wall. Examples of reinforced brickwork falling into this latter category are found in three types of reinforced brickwork, namely (a) grouted cavity, (b) quetta bond and (c) pocket-type sections.

In grouted cavity construction the reinforcement is embedded inside grout concrete which is enclosed by the two outer leaves of brickwork. The advantage of this method of construction is that it effectively eliminates the need for conventional formwork (Fig 1a). With quetta bond reinforced brickwork, the bonding pattern is designed to create holes in a continuous and regular manner. Reinforcement is placed inside these holes and grouted into position (Fig 1b).

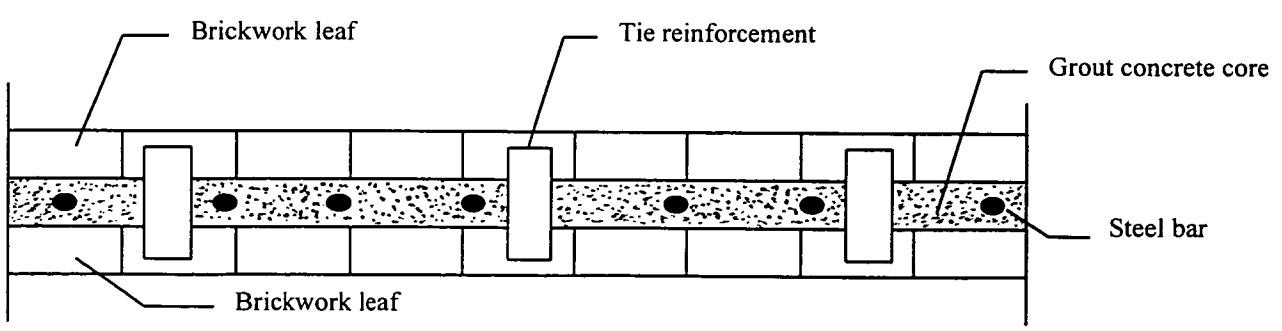

Fig 1a : Grouted cavity reinforced brickwork section

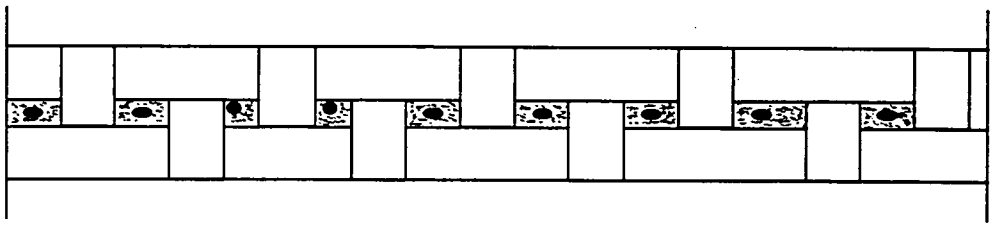

Fig 1b : Quetta bond reinforced brickwork section

Pocket-type construction has similarly emerged as a solution to the problem of reinforcement placement. This type of wall construction is the most efficient of the three in resisting lateral loading. It helps to reduce the overall costs of construction by cutting down on the amount of steel reinforcement (through provision of large effective depth for the steel and at widely spaced intervals), the amount of concrete grout and the amount of formwork required. In this method of construction, the steel reinforcement is placed within holes, called pockets, which are created by the omission of bricks in the arrangement of brickwork courses. Rich mix concrete grout is finally poured into the pockets (containing the steel bars) after the brickwork has cured and attained its strength (Fig 1c).

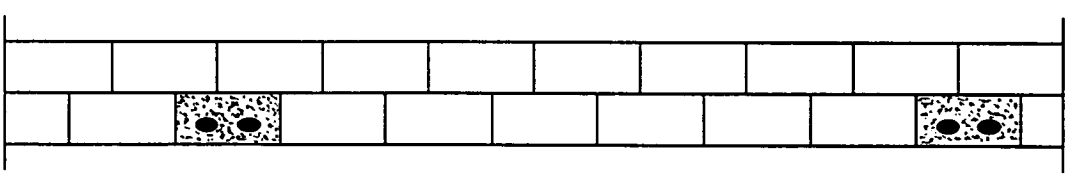

Fig 1c : Pocket-type reinforced brickwork section

Previous cost comparison amongst various designs of retaining wall have shown[1] that pocket type walls are cheaper than the other alternatives, such as grouted-cavity and reinforced-concrete walls. These theoretical cost studies indicate that designing and constructing these walls is economic because it is shown to be only 6% more expensive than the crudest of reinforced concrete walls. It is also, on average, some 15% cheaper than reinforced concrete walls which have an applied aesthetic finish.

Although it has been shown to be cheaper than the other existing alternatives, it has not been exploited because of paucity of data on properties such as shear strength and the limiting pocket spacing. It is for these reasons that the present work has been carried out.

1.2 PRESENT INVESTIGATION

This thesis is mainly concerned with pocket type reinforced brickwork acting as retaining walls.

These walls fall under the classes of brickwork panels which may be subjected to both pre-compressive in-plane and lateral out-of-plane loading. In practice, the precompressive loading in the form of surcharges is usually small in magnitude compared to the lateral loading exerted by the retained material. These walls are predominantly subjected to flexure. This makes plate bending analysis appropriate to them.

In accordance with procedures employed for the limit-state design of reinforced concrete, the current British Code of practice[2] used for designing these walls tried to harmonize the design of reinforced brickwork with those of reinforced concrete (BS 8110). Preliminary investigation reveals that the basis for designing the spacings of the reinforced concrete pockets in pocket-type walls seems too conservative.

This conservative approach was adopted by the Code[2] because of the crucial need to ensure that steel yielding within the concrete pockets always preceded the failure of the panel of brickwork between these pockets. This need also resulted in placing strict limits on the permissible shear strength. This approach arose as a result of paucity of field and experimental data on the structural behaviour of these walls. This problem of inadequate information for design purposes makes this present investigation essential.

The outline of this thesis is as follows :

Chapter 2 presents a literature review which gives a summary of important findings related to this study dating back to the last century.

Chapter 3 presents a summary of experimental procedure and results obtained from small-specimen tests. The mechanical properties as well as stress-strain characteristics of the different constituent materials used for constructing the specimens are presented. The constructional details and procedures for the tests are also given.

Chapter 4 presents a summary of all the theoretical and experimental results obtained from the investigation of shear strength. This chapter also contains other aspects, such as deflection analysis, of the full-scale tests which are incidental to the study of shear strength behaviour and its investigation.

Chapter 5 presents a summary of all the theoretical and experimental results obtained from investigating flanged-member behaviour of these walls and the effect of associated pocket-stem spacings on structural behaviour.

The conclusions of all these investigations are given in Chapter 6. For ease of reference, tables, drawings and photographs are included in appropriate locations.

CHAPTER 2

LITERATURE REVIEW

2.1 INTRODUCTION

This part of the thesis gives a summary review of literature of documented research work on reinforced and prestressed brickwork sections conducted over the past few decades. It is also the aim to give a summary of results of the specific work done in the past on pocket-type reinforced and prestressed sections. Finally, it is aimed to present the areas where further work is required in light of the review carried out.

In parallel with this objective, a brief summary report of results of research dating back to the last century is given. As the work done during this period of time has been carefully summarized by other authors[3,4], detailed report of the specific work done during this interval of time are not included here.

Since reinforced masonry could be considered as a special form of prestressed masonry in which the amount of prestress applied is equal to zero, it is significant to note that results of structural tests done on one category has bearing on the other. Such implications and relevance are better appreciated if the general trend of research as well as what has given rise to the trend is known.

In what follows, therefore, a brief overview of relevant research is given with particular focus on reinforced and prestressed sections. The situation of this particular investigation within the broad field of research is brought forward and highlighted. Finally, the specific work done to study the shear strength of reinforced brickwork is summarized along with the various studies, conducted in the past, to investigate flanged-member action in reinforced brickwork.

2.2 HISTORICAL DEVELOPMENTS IN RESEARCH AND APPLICATIONS

2.2.1 Work Done Prior to 1970

Sir Marc Isambard Brunel's work in 1825 on reinforced brickwork construction is believed to be the first documented work. The details of the feat achieved both as part

of the Thames river tunnel project and the subsequent construction of the "Nine Elms" beam (Fig 2.1) have been previously described[3]. These led to focused attention in the use of reinforced masonry as a structural material.

During the second decade of this century in India, Brebner[5] executed a very substantial programme of testing several reinforced brickwork structural elements. His work paved the way to widespread research in this field both in the USA and in the UK and on such a scale that was unprecedented prior to that time. All these test results confirmed that the theory of reinforced concrete design is applicable to reinforced brickwork, as the behaviour of both of them was similar.

Prior to the 1970s, the vast majority of research papers on reinforced brickwork could be found scattered in several specialist journals and proceedings of conferences, symposia and workshop seminars. These publications were devoted to engineering and applied engineering practice. However, since the commencement of what could be regarded as an annual meeting of masonry professionals in various parts of the world beginning with the one held in Houston, Texas, USA in 1967, several publications devoted specifically to masonry have been documented, co-ordinated and brought to the focus. In particular, the 1967 International conference held in Houston provoked the birth of several other regional and national bodies. The primary objective of these bodies is the dissemination of knowledge on masonry as a structural engineering material. Some of the attempts made to reinforce or prestress brickwork elements are documented in the following section. Such attempts were made in order to enhance structural performance under load as well as to study behaviour and develop methods for predicting them.

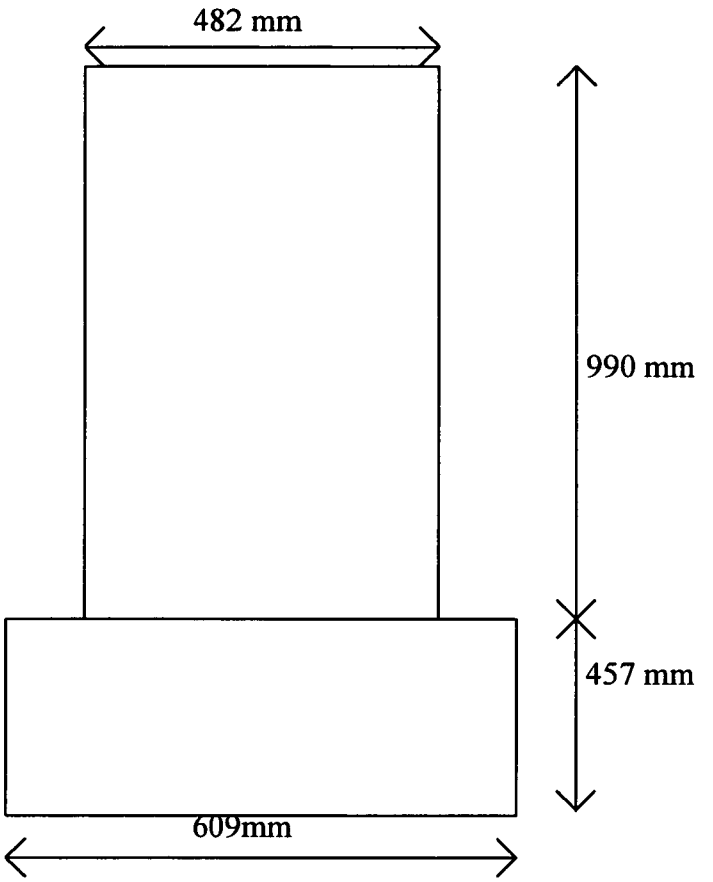

Fig 2.1 : Brunel's "Nine-Elms" Beam (after Foster[3])

2.3 RESEARCH AND DEVELOPMENT WORK DONE ON PRESTRESSED BRICKWORK BEAMS

Mehta and Fincher[6] tested five prestressed grouted masonry beams in their study of the structural behaviour of these beams under load. They varied the coursing pattern as well as the magnitude of the prestressing force. The feasibility of fabricating prestressed grouted cavity brickwork was also explored. The beams were fabricated by laying a brickwork shell in a "U" configuration. The strands passing through the cavity, were stressed and then grouted. The grout constituted at least 25% of the cross-sectional area of the beam and due to its location, it contributed in a significant way to the structural behaviour of the beam at all stages of loading. Only tensioned steel was used and this consisted of three 10 mm diameter seven-wire strands in each beam. The prestressing force was either 187kN or 94kN. The beams were tested under concentrated loading over a span of 1.83 m.

All the beams tested failed in shear. A typical crack at failure showed a stepped crack in the shear span travelling towards the support. There was also a horizontal propagation of this crack towards the loading point once it reached the top bed joint. A typical section used by Mehta and Fincher[6] is given in Fig 2.2.

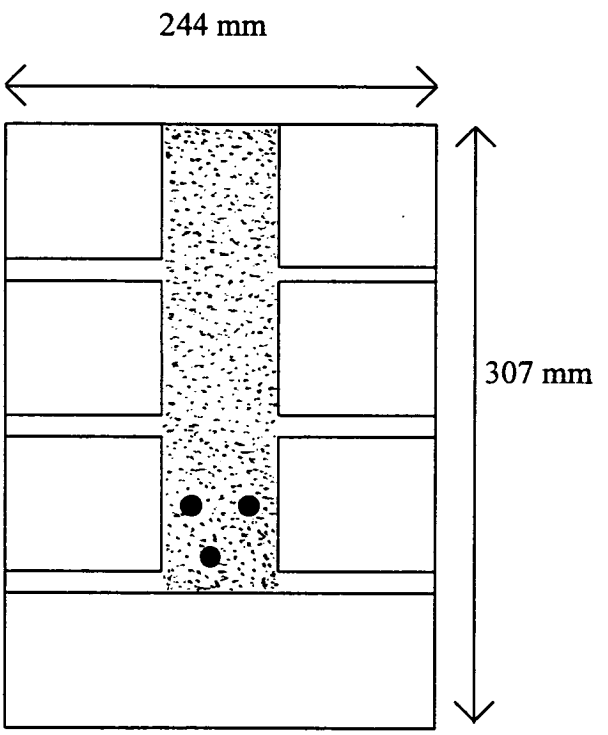

Fig 2.2 : Mehta and Fincher cross-section[6].

Pedreschi[7] tested 51 prestressed brickwork beams containing tensioned reinforcement only. The span used varied from 1.75 m to 6.2 m. The beams were tested under two point loading so that they effectively combine two different test conditions. These conditions are : (a) pure bending between the two loads in the central portion of the beams and (b) constant shear force in the end sections termed the "shear spans". This particular work aimed at studying the effects of

(i) brick strength

(ii) grade of mortar

(iii) area of steel and prestress (or prestressing force) and

(iv) *a/d* ratio

on the deflection, cracking and ultimate load behaviour. The cross sections examined are given in Figs 2.3a and 2.3b. He solved the problem of location and quantity of tensioned steel in the section in a different way than was, much earlier on, reported by Thomas[8]. He conducted several tests on brickwork prisms in order to determine the stress-strain properties of brickwork when compressed parallel to the bed joint. This became necessary because the beam sections tested by Pedreschi developed compressive stresses parallel to the bed joint. This is not in common with the situation in many brickwork structural elements like piers and walls, for which compressive stresses develop normal to the bed joint. This research then led to the formulation of a non-linear expression for the stress-strain relationship for brickwork parallel to the bed joint. Adopting this non-linear stress-strain relationship for brickwork, flexural theory was used to predict the ultimate flexural moment for the sections. Deflection and crack widths were also predicted using the actual stress-strain relationship of brickwork and steel.

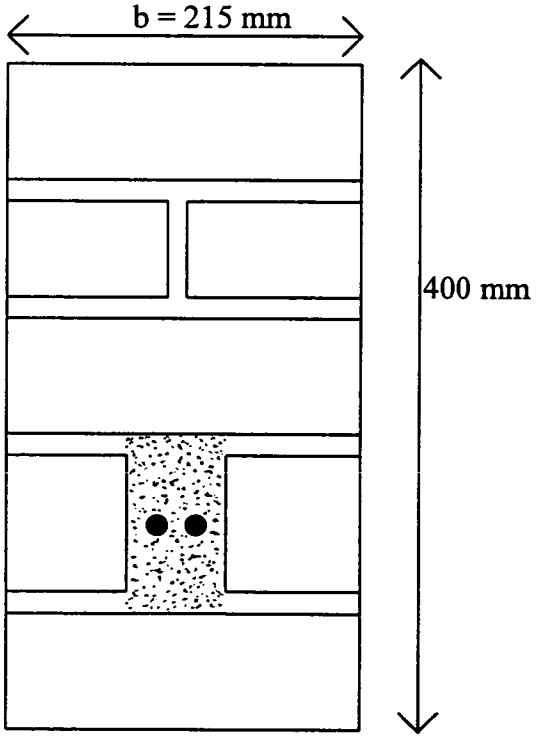

Fig 2.3(a) : Pedreschi's cross section[7]

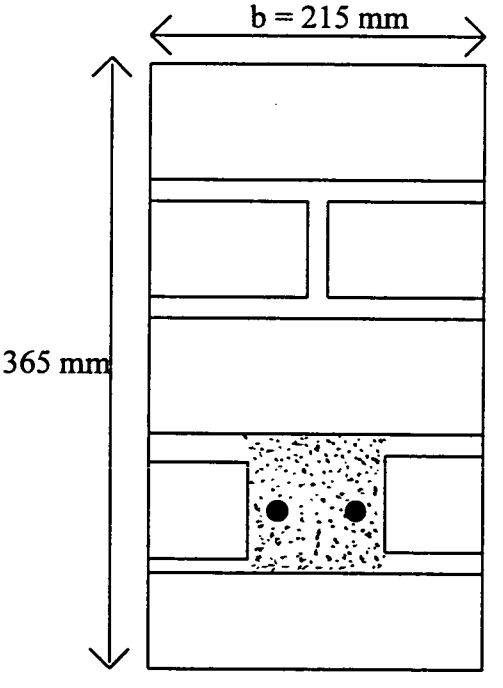

Fig 2.3(b) : Pedreschi's cross-section[7]

Fifteen beams were also tested, varying the *a/d* ratio between 2.0 and 11.21, in order to study the effect of the shear-span to effective depth ratio on the behaviour in shear

of prestressed brickwork beams. He observed two distinct types of shear failure which were dependent on the value of *a/d* ratio. For those beams with low *a/d* ratios, the main feature of the shear failure was the diagonal cracking failure of the brickwork along a line joining the support and load point. Those beams with higher *a/d* ratios showed as their main feature a step-wise propagation of cracks towards the support. On reaching the top bed joint in the direction of the load point, the diagonal crack travelled along the bed joint towards the load point. A similar mode of shear failure was reported by Mehta and Fincher[6].

Pedreschi[7] observed these two basic forms of shear failure. Beams with *a/d* ratios between 4 and 11.2 tended to exhibit shear failure by a splitting of the top bedjoint running from the constant moment zone along the shear span into the support. Beams with $a/d = 2$ failed when a diagonal crack running from support to load point formed. In all the cases, considerable flexural cracking in the constant moment zone occurred before failure. Very little flexural cracking was observed in the shear spans of those beams with low *a/d* ratios (*a/d* ratios between 2 and 4). For beams with high *a/d* ratios, the flexural cracking extended well into the shear spans and progressed upwards through the section at an angle of approximately 45° towards the load point. The diagonal cracks observed in the beams normally moved in a stepwise manner through the mortar joints rather than through the brickwork itself.

In conjunction with experimental results, the shear strength of these beams were predicted based on plastic theory[9] as developed originally for prestressed concrete beams. Pedreschi used the properties of the single course prisms to determine the shear strength in spite of the difference between the neutral axis depth at failure in the beams failing in shear and the thickness of those single course prisms. Also, in determining these shear strength values, no distinction was made between those beams with low and high *a/d* ratios. Regardless of these inherent assumptions, good results were obtained as the actual and predicted shear strengths were quite close. As far as the author knows, this was the first systematic attempt made to study the shear strength of bonded prestressed brickwork beams.

In the work done by Robson et al[10], the prestressing tendons were post-tensioned after grouting so that the tendons remained unbonded. The brickwork prisms were loaded parallel to the bed joint as in the section tested by Pedreschi[7]. A total of eighteen beams were tested, of which six had a high percentage of steel. Of these six, five failed in compression by crushing of the brickwork whilst one failed in shear. The remaining beams failed in tension.

Theoretical results were obtained by using (a) brickwork properties obtained from the prism tests and (b) properties given in the code of practice. When these two sets of results were compared, those obtained using the prism test results gave the better prediction. Also, it was observed that results for those sections which failed in compression are better predicted than those which failed in tension. The reason given was that for those sections which failed in tension, the neutral axis is very small and the prism did not properly represent the situation. On the other hand, the neutral axis depth is larger for those sections which failed in compression and the prism tests adequately represented the situation.

In the early 1980s, Garwood[11] tested three fully and partially-prestressed brickwork beams and demonstrated that prestressing the beams leads to an increased shear strength. This work was later extended by testing eleven beams[12] consisting of two series, each of which had at least five beams from which four had some prestress applied, the fifth represented an ordinary reinforced brickwork beam. Two types of bonding arrangements (course patterns) were tested, one similar to the strecher-quetta bond type of section tested by Robson et al[10] and the other a pier-bond type section. Unlike the previous work done by Garwood[11], shear behaviour became a major focus point of this study.

Walker[13] studied the behaviour of partially prestressed brickwork beams containing tensioned and non-tensioned reinforcement. In his studies he looked at the effect of the percentage of steel; the prestressing force; the partial prestressing ratio; the cover to the non-tensioned steel; the brick strength as well as the mortar strength on the ultimate moment; the deflection and; cracking characteristics of the beams.

The section tested, shown in Fig 2.4, is similar to that of Pedreschi[7], with only a slight modification to accommodate the non-tensioned steel close to the soffit. This arrangement of steel gives better crack control and improves the ultimate moment capacity of the section through an increased lever arm of the resultant tensile and compressive forces. Although the relative area of grout to the beam cross-section is higher than that of Pedreschi's section, this did not contribute to the ultimate moment capacity of the section.

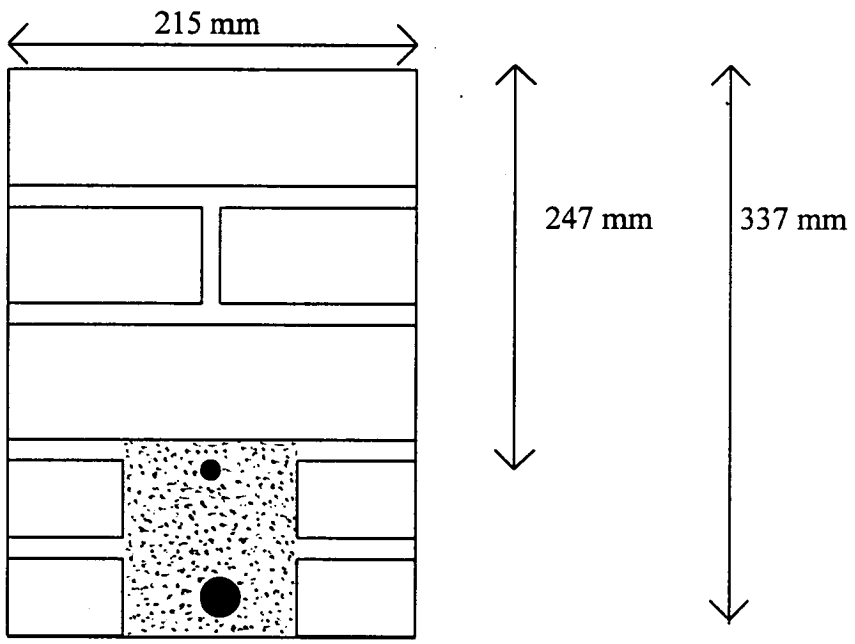

Fig 2.4 : Walker's partially-prestressed brickwork section[13].

Walker[13] tested forty-one beams. As a follow-up to previous work done by Pedreschi[7], he tested several prisms in compression. The compressive force parallel to the bed joint was applied axially and eccentrically to obtain the property of the prisms. He also developed an iterative computer programme which uses the direct method, described in section 4.3.5.4, to calculate the ultimate flexural moment, deflection and cracking based on experimentally determined properties of the brickwork. Tension-stiffening effects as well as the presence of the grout are allowed for in his computer programme which, unfortunately, is incapable of predicting the shear strength of the brickwork beams.

Out of the forty-one full-scale beams tested by Walker, sixteen exhibited some form of shear failure. Thirty-seven of these forty-one beams failed in tension. Of these thirty-seven, twelve exhibited secondary shear failures. Only four of the total number of beams tested failed primarily in shear. It was noted as well that out of the twelve partially-prestressed beams which exhibited secondary shear failure, two categories could be deduced, namely : (i) Category A, made up of eight out of these twelve, in which all the steel had yielded and (ii) Category B, made up of four out of these twelve, in which only part of the steel had yielded. Although shear investigation was not the focus of this research, nonetheless approximately 40% of all the full-scale beams tested exhibited some form of shear failure, thereby further revealing the relevance of this type of structural behaviour in brickwork.

Garwood[14], Mehta and Fincher[6], Pedreschi[7] and Walker[13] have all reported the same phenomenon of a diagonal shear crack which preceded shear failure (note that all these beams were either fully or partially prestressed) or a step-wise propagation towards the support and a horizontal propagation along the bed joints towards the loading point.

Roumani and Phipps[15] tested and reported the results on fifteen prestressed I and T-shaped sections (Fig 2.5). They aimed at formulating design proposals for the shear strength of brickwork sections at cracking and ultimate load. They examined the influence of the shear-span to effective depth ratio (*a/d* between 0.8 and 4.5), the depth (between 665 mm and 440 mm), the amount of prestress (varied between 0.5 and 3.0 N/mm^2), the location of prestress (concentric and eccentric prestress) and the shape of the section (I or T) on the behaviour of the beams. The prestress was applied through 40mm unbonded Macalloy bars, placed at the sides of the webs, see Fig 2.5. All the beams failed in shear, and depending on the *a/d* ratio, distinctions were made on the types of shear failure observed.

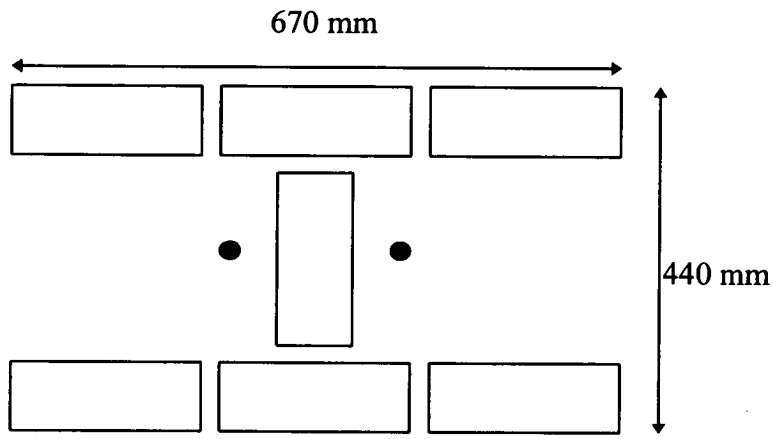

Fig 2.5 : Typical Section of Roumani and Phipps[15,16]

Uduehi[11] compared the structural behaviour of prestressed brickwork beams with that of prestressed concrete beams. Twenty-nine full-scale beams of concrete and brickwork were tested. The cross-sectional properties as well as the compressive brick strengths were identical and the areas of tensioned reinforcement used were similar. The comparisons were conducted in terms of the ultimate flexural strength, deflection, cracking and the ultimate shear strength.

At the time of this study[11], no information existed on the shear strength of partially prestressed brickwork beams, so sixteen partially-prestressed brickwork beams were tested for shear strength by varying the *a/d* ratio of these beams from 1.5 to 6. In this work, concepts developed for predicting shear strength of reinforced concrete beams[17-19] were adapted for reinforced brickwork beams.

Sinha[3] carried out tests on ten full scale post-tensioned brickwork pocket-type retaining walls in order to establish the effect of percentage steel area, prestressing force and brickwork strength on aspects of structural performance such as deflection, cracking and the ultimate moments of the walls. A method was described for predicting the ultimate moment and deflection of beams from prestressing through to cracking and up to ultimate failure. The validity of this method of prediction was established through verification with the experimental results obtained.

Pedreschi and Sinha[21] have also attempted to predict the flexural behaviour of prestressed brickwork sections through correlation with test results from small-scale representative brickwork prisms. Experimental evidence[21] on full-scale beams were correlated with prism test results and it was concluded that, for brickwork sections in which the compressive forces act parallel to the bed-joint, a better approximation of the compression zone is provided by the single course prism formats compared to the corresponding 3-course prism formats.

At failure, the single-course prism is visualized as the compression zone (of a flexural member) which is considered as a series of courses in which the bed-joints between those courses had split. Each course is then regarded as being subjected to progressively greater stresses as one moves away from the neutral axis position in accordance with the classical distribution obtained in flexural elements.

It was noted in line with similar observations made by other investigators[22] that, because of the presence of bed-joints in a direction parallel to the applied loads, a non-uniform strain distribution may result (particularly at high stress levels) due to transverse tensile failure across the bed-joint. This has the potential of generating a spurious stress distribution which fails to reproduce the true distribution being sought. Using, therefore, the single-course prism precludes this undesirable effect from occurring since no physical bed-joint parallel to the applied load then existed. This experimental evidence lent support to the adoption of the single-course prism rather than the corresponding three-course prism as a better approximation of the compression block zone of the brickwork beams.

2.4 RESEARCH AND DEVELOPMENT WORK DONE ON REINFORCED BRICKWORK BEAMS

There exists three basic ways of introducing reinforcing steel into brickwork construction and these have been classified[23-26] as follows :

(a) placing within the mortar joints as in bed-joints or collar (perpend) joints of the brickwork;

(b) placing in specially formed pockets and;

(c) placement in a grouted-cavity between skins of brickwork.

Different types of reinforced brickwork beams falling into one of these three categories have been studied for shear strength by several investigators[7,11,27,23,24,28,29,30]. A feature of the premise which most of these investigators used was to assume that the shear strength of reinforced brickwork beams are largely influenced by the same set of variables affecting the shear strength of reinforced concrete beams. For instance, it has been previously established[31,32] that, for reinforced concrete beams, shear strength is influenced by the ratio of the shear span to effective depth, the amount of tensile reinforcement and the compressive strength of the compression zone. It should be noted that more test results have been documented for brickwork sections in which the reinforcement is embedded in concrete than for brickwork sections in which the reinforcement is embedded in mortar joints[23]. Within the former category, quite a few results are available for reinforced brickwork sections in which the reinforcement is placed in specially formed pockets.

Attempts have been made to evaluate and also predict the shear strength of reinforced brickwork in which only longitudinal reinforcement is provided in a grouted concrete core to resist shear forces[18,27,33]. Tests were usually conducted on beams and based on the observed cracking and other structural behaviour throughout the various stages of loading, theoretical models were formulated and used to predict shear strength. Concepts employed have varied from the traditional method used to predict shear strength of similar reinforced concrete members[27,34,35], those involving "tied arch" behaviour formulation[33], through to those involving the "compressive force path" method[11] and methods based on plastic analysis[7,11], which were developed originally for reinforced and prestressed concrete members respectively.

Suter and Hendry[36] studied the shear strength of bed-joint reinforced brickwork beams and concluded that for this category of reinforced beams, shear strength generally increased with decreasing ratio of shear span to effective depth (a/d). Twelve reinforced brickwork beams were tested with shear span/effective depth

varying from 1 to 7 and the beams were built from common frogged bricks. The percentage of tensile reinforcement was varied from 0.24 to 1.46. When the results of this set of beams were combined with others, they suggested that a characteristic shear strength of 0.35 N/mm^2 be adopted for *a/d* ratio greater 2 and that this value be increased to 0.8 N/mm^2 if the *a/d* ratio is less than 2. In other words, they concluded that the effect of *a/d* ratio on shear strength is accentuated at *a/d* ratios of less than 2 and attributed this marked effect to the mode of failure of the sections by noting that at higher *a/d* ratios, shear failure often follows the development of a typical diagonal crack whereas for those beams with a low *a/d* ratios, cracking is usually followed by the development of a tied-arch effect. Thus, they observed that the lower the shear span ratio the greater the arching strength and thus the apparent shear strength recorded by such beams. Unlike reinforced concrete beams, it was also observed that bed-joint reinforced beams show no significant evidence of a relationship between the amount of tensile reinforcement and ultimate shear strength. Moreover, these beams gave no significant correlation between compressive strength of the brickwork and ultimate shear strength.

Osman and Hendry[27] carried out tests on reinforced grouted-cavity brickwork beams in order to assess the contribution of compression zone, aggregate interlock and dowel effect on shear strength.

The beams tested had an overall cross-section of 450 mm deep by 295 mm wide and 5.34 m span. Two types of brick and hence brickwork were used in constructing them. One set of the beams used common clay bricks and the other set used high strength 3-hole bricks. The % steel was also varied between 0.9 % and 1.42 % while the *a/d* ratio was kept constant at 6 throughout. Compressive strength tests on prism specimens 213 mm by 100 mm by 440 mm gave the following respective results for the low and high strength bricks : 12.24 N/mm^2 and 22.63 N/mm^2. The Young's modulus parallel to the bed joints for the two types of brickwork were 11.97 kN/mm^2 and 18.50 kN/mm^2 respectively.

Strains in the relevant portions of the beams were measured using the mechanical "demec" strain gauges. Longitudinal strain measurements, over a 150 mm gauge length, located at different depths from the top of the beam were used for the determination of the neutral axis depth and to provide an estimate of the compression zone contribution to shear resistance. Gauges were also used as rosettes to determine movements across cracks using 50 mm gauge length. Vertical and horizontal displacements across cracks were measured in order to obtain an estimate of the contribution of aggregate interlock and dowel effect to shear resistance. Some tests were carried out on beams of lower strength masonry in which an artificial crack had been introduced so as to provide a means of measuring shear transmission due to dowel effect. In these tests, the load was applied centrally to the lower part of the beam through a steel plate passing through the brickwork.

In estimating the contribution to shear resistance due to aggregate interlock, it was assumed that shear transmission by this mechanism takes place only in the grouted section of the beam and none by the interface between brick and mortar provided by the brickwork. This assumption was used because the interface of mortar and brickwork is considered to be relatively frictionless when compared to the grouted section. The shear force contribution by aggregate interlock had been estimated from measurements of vertical displacements across shear cracks and from crackwidth-measurements.

The authors[27] found that no significant difference in the shear resistance exists between beams built with weak and strong brickwork. It was also found that shear resistance of these beams could be accounted for by the three mechanisms of compression zone transmission, dowel effect and aggregate interlock and that these contributions varied with the applied load. The results obtained also gave an approximate indication of the relative magnitude of these mechanisms and suggested that compression zone transfer provided the largest single contribution to shear resistance.

The deflection of grouted-cavity beams were also satisfactorily predicted using two different methods[27,37,38] previously used successfully for reinforced concrete beams. The first procedure is based on the calculation of an effective second moment of area. This method provides a transition value between well defined limits in the uncracked ($I_{uncraked}$ or I_g) and fully cracked ($I_{cracked}$) states. The second procedure, on the other hand, involves the use of a fictitious reduced value for the second moment of area. This second method involved estimating this reduced value by multiplying the uncracked second moment of area, $I_{uncracked}$, by a factor. This factor was found to be equal to 0.85 for the beams tested.

Suter and Keller[28] studied the shear strength of grouted-cavity reinforced brickwork beams vis-à-vis reinforced brickwork beams and showed, using the results of reinforced concrete beams[31], that the shear strength of grouted-cavity beams are intermediate between those of reinforced concrete and reinforced brickwork beams with reinforcement provided in bed or collar joints. They also indicated that it is possible to calculate the shear capacity of these beams by adding together the separate shear capacities of the grouted core and the brickwork sections in accordance with their relative widths. Based on the section tested, good agreement between derived and the experimental results were obtained for *a/d* ratios greater than 2. The universal applicability of this latter result has, however, been questioned[4] on the basis of the structural response of such a composite section to load. In their tests[28], the shear span/effective depth ratio of the beams was varied from 1 to 7. However, the percentage area of tensile reinforcement for the reinforced brickwork beam was fixed at 1.49% while that of the reinforced grouted-cavity beam was fixed at 1.41%.

Sinha[39] also tested grouted-cavity brickwork beams and arrived at results which agreed with those of Suter and Keller[28] in terms of the dependence of shear strength on the *a/d* ratio. Unlike mortar-bed reinforced beams, the shear strength of grouted-cavity beams increases with the amount of tension steel. Sinha also tested twelve grouted-cavity brickwork slabs[40], fixing the percentage of tensile reinforcement at 0.88 and varying the shear arm/effective depth ratio from 2 to 5. Results for these slabs also show that the ultimate shear stress increased as the shear arm/effective

depth ratio decreased. Different shapes of the compression stress blocks, i.e., triangular, rectangular and parabolic were assumed in the analysis of the test results. In a further comprehensive test on grouted-cavity brickwork beams and slabs[29] in which the variables were :

(i) *a/d* ratio (1.5 to 10),

(ii) % area of tensile steel (0.88 to 2.54),

(iii) brick strength (21.55 to 88.33 N/mm^2),

(iv) effect of shear reinforcement and,

(v) the mortar grade (1: ¼ :3, 1: ½ :4.5 cement:lime:sand)

the conclusion was made that shear strength is strongly influenced by the *a/d* ratio, the % area of tensile steel as well as the amount of shear reinforcement and the thinness of the section. This was indicated by the higher shear strength sustained by the slabs compared to the beam sections over a wide range of *a/d* ratios (2 to 7). From these results, it was also concluded that the mortar grade has only a slight influence, while the brick strength does not exert any influence on shear strength.

Garwood and Tomlinson[41] tested eight beams of which four were reinforced with both longitudinal tension steel and shear reinforcement and the remaining four were reinforced with only longitudinal tension steel. The amount of tension steel used varied from 0.34% to 1.33%. The sections were 328 mm wide, 290 mm deep and the length of the beams was 3905 mm. All the beams were laid in 4 courses, the first two courses in stretcher bond while the last two courses were laid in quetta-bond. By omitting the central line of bricks in the second course, a longitudinal cavity, 130 mm wide and 75 mm deep was created inside which the reinforcement cage was placed. This presented a form of grouted cavity brickwork. Special care was taken to avoid a continuous perpend joint particularly in the second and third courses of brickwork, where the interface between the two different bonding patterns coincided.

In spite of some of its other advantages, the special bonding arrangement adopted for these beams was unable to incorporate any longitudinal top bars to anchor the shear stirrups as is conventionally done in reinforced concrete beams. This is basically caused by the inevitable presence of headers in the top course, a special feature

associated with quetta bond. In this case, one sees yet another example of some of the difficulties often encountered in attempting to reinforce brickwork. Although shear strength investigation did not form the focus of this particular study, a sudden shear failure was reported for one of the beams; the one with the highest amount of tension steel (1.33%). Shear failure occurred in this beam in spite of the fact that it was the most heavily reinforced in shear of all the eight beams tested and, compared with one beam having a lower amount of tension steel (0.89%) and a lower level of shear reinforcement, it even failed at a lower bending moment. This sudden shear failure was unexpected, and it was attributed to poor adhesion between the mortar and the bricks. However, as practically six out of the eight beams tested were built with the same workmanship, a similar problem should affect these other beams, but the fact that heavily over-reinforced brickwork beams often fail in shear was not properly reckoned with. Apart from this one, two other beams having 0.89% tension steel (one with and one without shear links) were also reported to have failed suddenly in shear although the shear failures in these cases were combined with yielding of the tension steel.

2.5 RESEARCH AND DEVELOPMENT WORK DONE ON SLABS

Some experiments[42] have been conducted to test the performance of reinforced brickwork masonry box beam structures, in which masonry forms the webs and reinforced concrete floors form the flanges of the box. In these experiments, two types of wall were used, one 9 inches thick (but made with special bricks) and having vertical and horizontal bars, and the other 11 inches thick and having diagonal bars in a grouted cavity. The wall having the diagonal bars performed better in terms of serviceability and ultimate limit states.

Maurenbrecher[43] determined the ultimate design load of a 4 m high reinforced brickwork retaining wall. The wall was a cantilever, anchored into a reinforced concrete base, with a varying elevation and cross-section ; the thickness of the wall was 440 mm at the base, reducing in two steps to 325 mm and 215 mm respectively at the top. Noting that prior to the construction of this particular wall, concrete pockets have usually been spaced at a maximum of 1.22 m intervals. Maurenbrecher's design

allowed a larger spacing by varying the distances between the reinforced pockets from 1.375 m and 1.575 m in the central (more heavily loaded portion) section of the wall to 2 m in the sloping portion. The backfill material retained was mainly hardcore which was spread in layers and covered with earth at the top. Two coats of bitumen were used to paint the back of the wall next to which a single layer of bricks was placed to protect these bitumen coatings.

The pocket wall was considered to be equivalent to a reinforced concrete T-beam where the flange of the beams is replaced by brickwork. For the section tested, the space between the concrete webs is filled with brickwork resulting in a uniform wall thickness. This type of construction increases the interface shear strength between the concrete and brickwork and also the strength of the brickwork panel between the pockets.

This particular wall could be easily divided (in the sectional elevation) into three parts, namely two end trapezoids and one central rectangle. In the actual design of the wall, spacing between the pockets was considered to depend on : (a) the ability of the brickwork to resist lateral loading and transfer it to the reinforced concrete pockets; (b) the magnitude of the anchorage stresses in the bars holding down the wall to the reinforced concrete base and; (c) the amount of steel that could be reasonably accommodated in the pockets.

Aspects of deflection behaviour of the wall which were studied included : (a) the variation of overall deflection measured at three levels, two of which corresponded to the points where the cross-section changed and the third level corresponded to the top of the wall; (b) the profile of deflection over the height of the wall and within regions close to the pocket centerline in order to examine the behaviour around the more heavily loaded portion of the wall and ; (c) the time variation of deflection, again, at three levels in order to assess the angular movement due to wall deformation and tilting.

Both sliding and tilting movements of this cantilever wall were observed and because of the nature of its sectional elevation, the wall exhibited a slight reverse of curvature near the centerline, which was attributed to the relative restraint provided by the more lightly loaded portion of the wall section.

Sinha[44] subjected reinforced brickwork masonry retaining walls, of the grouted-cavity variety, to sustained loading to determine creep in bending, see Fig 2.6.

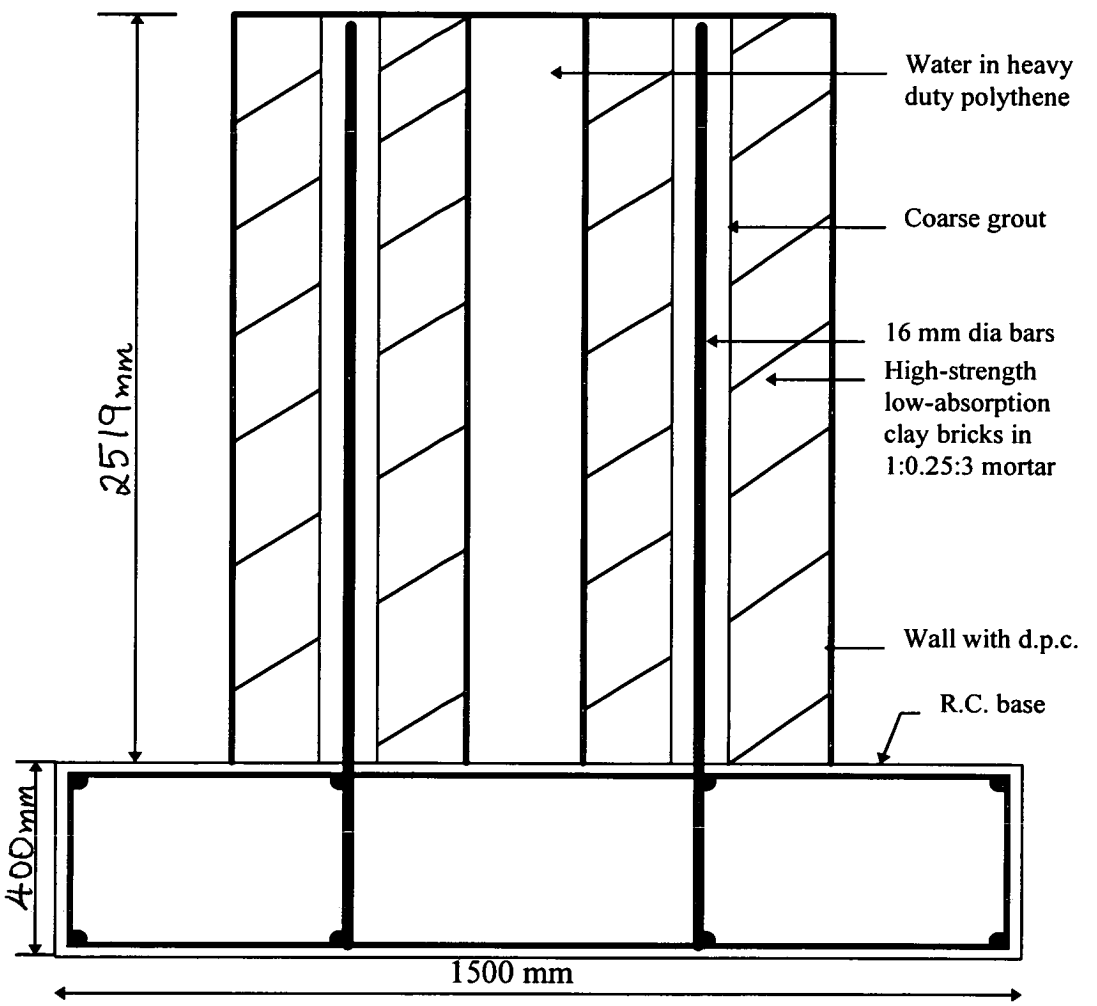

Fig 2.6 : Sinha's Masonry Retaining Wall for Investigation of Creep in Bending[44]

Tellett[45,46] tested pocket-type reinforced brickwork retaining walls and beams. The walls were cantilever structures whilst the beams were simply supported. He also developed a Finite Element Model (FEM) for reinforced brickwork acting under

flexural stresses. His objective was to investigate the performance of pocket-walls in relation to the requirements of the then British draft code for the design of reinforced masonry. Six walls and fifteen beams were tested, for which the parameters examined were : brick type; % of reinforcement; slenderness and; shear span ratio. It was reported that flexural failure occurred in all the walls and in the light-medium reinforced beams whilst only the heavily reinforced beams failed in shear. Wall thicknesses of 215 mm and 330 mm were tested with pocket spacings equal to 1 m. The reinforcement percentages used varied from 0.28%-0.92% through to 1.25%-1.44% and the effective depth varied from 167 mm through 289 mm. The wall heights were 3 m and the length, 2 m. Two types of bricks were used, denoted A and B. For the beam tests, the shear span ratios varied from $a/d = 2$ for short beams to $a/d = 4{,}5$ for long beams. Three types of bricks of wide ranging compressive strength were used for the beams and these were named A,B, and C.

Since the objective of this work[45,46] was to check the adequacy or otherwise of the draft code provisions, the focus was not to investigate the flanged-member behaviour of these walls. The results obtained confirmed that the code stipulations were adequate in matters of flexural behaviour but it was concluded that conditions imposed on shear strength was too restrictive[30]. However, the shear strength results reported were incorrect, although it was indicated that shear is often the limiting condition for design of these walls except for cases where the degree of reinforcement is very low[30]. These authors tried to validate their FEM by using it to predict the deflection at the top of two reinforced brickwork retaining walls previously tested at the B.C.R.A. The model was used to predict the deflection at the top of some laterally loaded reinforced and unreinforced brickwork panels previously tested at the BCRA[47]. In addition, a parametric study on the basis of this FEM was conducted to predict the behaviour of alternative designs for reinforced brickwork retaining walls. The parameters varied include : slenderness; pocket spacings; panel thickness and; % of tensile reinforcement. Some qualitative guidance were provided to show areas where wall designs might be made more efficient and economical. In their parametric study, May and Tellett[46] predicted that wall aspect ratio (wall height : pocket spacing) could be reduced to 1.25, for stems designed as rectangular sections, by increasing the pocket

spacing and that wall slenderness (height : wall thickness) could be increased subject to satisfactory serviceability (deflection) performance. In these parametric studies, two types of panel were distinguished namely, internal and external as well as two types of designs for the stem namely, rectangular and flanged.

The Finite Element Analysis carried out by May and Tellett[47] was meant to predict flexural failure of the brickwork elements tested. Since their formulation was based on thin plate theory, it ignored the effects of out-of-plane shear stresses and consequently was incapable of predicting shear failure. The results which they obtained from testing these sections for shear strength were incorrect as they are out by a factor of 2 as revealed in Table 2.5.1 and Table 2.5.2. These Tables are given as Table 5 and Table 6 respectively in the corresponding reference. The corrected values are given in the ninth column of Table 2.5.2. Nonetheless, he further concluded that (a) the requirements of the draft code were adequate for pocket spacings of up to 1 m and, (b) that for greater pocket spacings, further experiments were needed to confirm the adequacy of code provisions.

The beauty of parametric studies is that they help to point the way towards possibilities but their major drawback is that, when not backed with detailed experimental data, they cannot be fully relied upon since they are usually based on, what may sometimes be spurious, extrapolation of existing knowledge. They have the potential, therefore, of creating one of two major classes of errors often made by researchers, namely : (a) insisting that something exists when, in fact, it does not and (b) insisting that something does not exist when, in fact, it does. Against this background, the conservative approach adopted by the British Code of practice[2] is understandable but not justifiable especially as it concerns matters of pocket spacings. The code imposed a limit of 1 m on allowable pocket spacings if walls were to act as homogeneous sections and that if spacings greater than this value are to be used, the ability of the masonry to span horizontally between the ribs should be checked.

Table 2.5.1[30] Beam Details and Test Results

Beam No	1	2	3	4	5	6	7	8	9	10	11	12	13	14	15
Length (mm)	3960	3970	3950	3372	2196	3995	3980	4010	3985	3995	3980	2152	2140	2190	2580
Breadth (mm)	1010	1005	1025	1050	1004	1020	1010	1010	1005	1010	1007	1005	1000	1005	1002
Depth (mm)	332	327	330	330	328	330	330	327	330	327	330	327	327	330	330
Span (mm)	3400	3400	3400	2800	1700	3400	3400	3400	3400	3400	3400	1680	1680	1680	1680
Effective depth (mm)	275	280	295	280	280	275	265	270	280	270	265	270	270	285	275
Mean concrete cube strength (N/mm^2)	29.2	29.2	31.5	21.5	31.5	37.1	40.3	35.5	35.5	37.1	37.1	35.9	35.9	35.9	35.9
Reinforcement Type	3T25	3T32	4T16	4T16	4T16	3T32	3T40	3T32	4T16	4T16	3T40	3T32	3T32	3T32	3T40
Reinforcement %	0.53	0.86	0.27	0.28	0.28	0.87	1.42	0.89	0.28	0.29	1.42	0.89	0.89	0.84	1.37
Code characteristic steel strength (N/mm^2)	425	425	460	460	460	425	425	425	460	460	425	425	425	425	425
Failure moment (kNm)	170	240	117	129	123	305	326	263	121	121	281	132	208	172	257
Shear force at failure (kN)	253	352	178	240	451	446	476	384	182	182	403	493	720	617	956

Table 2.5.2[30] : Comparison of predicted and ultimate bending moment capacities

Beam No	a/d	Predicted[1] b.m. capacity M_{flex} (kNm)		Ultimate b.m.	Predicted[2] Shear Capacity		Shear Stress (N/mm^2)		Moment Ratio		Failure Mode	
		Brickwork	Steel	M_{ult} (kNm)	Average stress (N/mm^2)	b.m.[2] M_{shear} (kNm)	Experim -ental	Correct values	M_{ult} /M_{flex}	M_{ult} /M_{shear}	Predicted	Actual
1	5.09	825	163	170	0.45	175	0.46	0.91	1.04	0.97	T	T
2	5.00	308	236	240	0.53	208	0.63	1.25	1.01	1.15	S	T+S
3	4.75	963	103	117	0.39	165	0.30	0.59	1.13	0.70	T	T
4	3.93	889	98	129	0.39	126	0.43	0.82	1.31	1.02	T	T
5	2.00	850	98	123	0.39	60	0.81	1.60	1.25	2.05	S	T+S+L
6	5.09	833	262	305	0.53	208	0.81	1.59	1.16	1.46	S	T+S+L
7	5.28	766	394	326	0.59	221	0.90	1.78	0.82	1.47	S	S+L
8	5.18	636	254	264	0.53	202	0.71	1.41	1.04	1.30	S	T+S+L
9	5.00	680	98	121	0.39	153	0.32	0.64	1.23	0.79	T	T
10	5.18	288	93	121	0.39	148	0.34	0.67	1.30	0.81	T	T
11	5.28	276	318	281	0.59	220	0.84	1.51	0.88	1.27	S	S+L
12	2.00	286	226	132	0.53	77	0.91	1.82	0.58	1.71	S	S+L
13	2.00	629	253	208	0.53	77	1.33	2.67	0.82	2.70	S	S+L
14	1.89	881	273	172	0.55	84	1.08	2.15	0.63	2.04	S	S+L
15	1.96	818	396	257	0.53	78	1.71	3.47	0.65	3.29	S	S

Notes : 1 the lesser value governs
2 equivalent bending moment
3 T = tension failure of reinforcement, S = shear failure,
L = Longitudinal cracking along the pocket boundary

It is prudent to have some experimental validation before such parametric survey prediction is exploited. This is particularly relevant for a material of such heterogeneity as reinforced brickwork and this matter forms a major focus of study in this thesis. For a pocket-type retaining wall of 3 m height, the code recommends a pocket spacing of 1 m if walls are to act as a homogeneous unit. Although this value is considered as rather conservative and walls of similar heights[43] have tended to have pocket spacings of between 1.2 and 1.5 m, implying aspect ratios of 2.5 to 2.0. Reducing the aspect ratio to a value of 1.25, as predicted by this parametric study, implies that for such a wall, we could have spacings as wide as 2.4 m apart. This kind of result would lend weight to the economic performance of these walls and result in increased competitiveness with reinforced concrete walls, for example.

These parametric survey results suggest that pocket reinforced walls would still be governed by stem failure rather than panel failure so long as the aspect ratio is greater than 1.25 for interior walls which have been designed as rectangular sections. In other words, if reinforcement located within the pockets were to always fail before the panel between brickwork pocket failed, then for a 3 m high wall, the maximum spacing between the pockets should not exceed 2.4 m. Also, according to the results of this survey, the code is conservative in eighteen out of the forty-one cases examined. They[47] also established similar limiting conditions for failure to be governed by stem failure rather than panel failure in the case of exterior panels. In this latter case, no unique aspect ratio value was found but when a somewhat similar variable, namely, the ratio of spacing to the thickness of the wall, was substituted for the aspect ratio, a unique value was again obtained regarding the limiting condition for stem failure. This situation probably arose due to the assumption made in modelling the response of the exterior panels which did not account for any in-plane restraint as was done for the corresponding interior panels. The modelling was done this way in order to achieve a simple but functional formulation.

Aspects of the influence of spacing on wall behaviour were, therefore, only indirectly addressed by May and Tellet[47] through parametric studies. They tried to establish

limits for this variable through investigating the respective aspect ratios, for both rectangular and flanged sections and for both interior and exterior wall panels, which would ensure that stem failure rather than panel failure is critical. Values were established for these different cases through results obtained from these parametric studies. For instance, it was concluded as part of this parametric survey that for interior panels which are designed as flanged sections, aspect ratio should be taken greater than 2.5. Therefore, for a flanged interior panel, of height h = 3 m, the suggested maximum spacing permissible for a flanged section is 1.2 m. It was concluded here, in essence, that for interior panels with spacing greater than 1.2 m, the design of a 3 m high wall, should be based on a rectangular section. However, more recent experimental evidence[48], obtained from tests conducted on two full-scale pocket-type reinforced brickwork retaining walls, suggests that this is not necessarily true and that some measure of flanged member behaviour could be considered. The limitations of parametric studies have been highlighted earlier on and for these reasons, confirmatory tests to establish the validity of these results in order to know the true limits of pocket spacings are still required.

At Redland Bricks Ltd., research was carried out[1] on pocket-type reinforced walls which were built to represent the lower 3 m of a 5 m-high wall. In this wall, the ratio of bending moment to shear force (M/V) at the base of the wall was made to represent an earth pressure distribution at the base of the 5 m-high wall. The walls are the stepped-type (that is, cross-section changes with height), similar to that tested by Maurenbrecher[43].

The first two stepped pocket-type walls tested by Redland Brick Ltd., as part of this company's research project gave way to the Market-Led Research Initiative undertaken by The Brick Development Association, BDA. This resulted in the testing of a third wall under lateral loading which is applied by hydraulic jacks in such a manner that M/V at the base (that is, lever arm to the centre of applied force) represents that from an earth pressure distribution at the base of a 5 m-high wall. In the third wall therefore, experience at Redland Bricks formed the background and the objective remained largely the same : To demonstrate that with a stepped pocket-type

construction, large retaining walls could be built that did not require high strength bricks to achieve the required engineering performance. This became necessary at that time so as to be able to properly address both aesthetic and structural considerations pertaining to these types of walls.

The first wall in this series failed in shear. The wall sheared across a crack stretching from the first step to the base. Cracking was also recorded across the pockets on the tension face of this wall. This first wall had no shear reinforcement. The base bending moment at which the wall sheared was recorded as more than twice the calculated working load of the wall. Although this wall had to be loaded twice; first when the capacity of the loading rig was reached and second, after making necessary adjustments to the loading rams. The two sets of readings were, however, reported to correlate well. As mentioned above, this first wall failed in shear through a large shear crack observed at the first change in wall thickness. This happened in spite of taking necessary precaution to guard against reducing the percentage reinforcement too close to the thickness change; the reason adduced for a similar failure observed in an earlier test programme.

As a consequence of this type of failure, another wall was tested in which shear reinforcement was provided in every bed joint. The capacity of the test frame was not sufficient to apply the load required to fail this wall because of the excessive reinforcement and impractical design adopted. Following this experience, a third wall was built with a moderate amount of shear reinforcement and an amount of tensile steel which ensured that a reasonably practical load could be sustained. All these walls were built with moderately strong bricks (for instance, the average compressive strength of the bricks used for the third wall in the series was 47.2 N/mm^2) to demonstrate that good engineering performance is achievable from building stepped pocket-type walls using such moderately strong bricks.

The walls were designed as cantilevers anchored to reinforced concrete footings. For the third wall in this series, this stepped wall is constructed such that the bottom portion, 975 mm high, had a thickness of 550 mm, the middle portion, 1050 mm high,

had a thickness of 440 mm while the top portion, 975 mm high, had a thickness of 325 mm, see Fig 2.7(a), 2.7(b). This third wall, which is basically an improvement on the earlier two in terms of the moderate shear resistance as well as the tensile steel provided, was found to perform well structurally. It is considered as the most reasonable in terms of practical design. This wall failed in shear but both the steel and the brickwork were effectively utilized as shown by the recorded steel and brickwork strains at failure. The shear failure was first detected in the perpend joint at the end of the wall which later developed gradually into diagonal cracks emanating from the first step in the thickness of the retaining wall. These shear cracks became evident at both ends of the wall. It is worthy of note that in spite of the high level of steel strains recorded which were almost at the yield point, the steel did not actually show serious signs of yielding (usually associated with the acceleration of the steel strains). The highest brickwork strains recorded were also much higher than that required to crush the brickwork in direct compression, yet the brickwork in the compression zone did not collapse. This situation probably arose due to an underestimation of the strength of the wall in calculations by failure to accurately account for the contribution made to section capacity by the moderate amount of shear reinforcement provided. The wall failed as a result of diagonal shear cracks combined with the excessive deflection recorded which was considered significant in relation to the height of the wall.

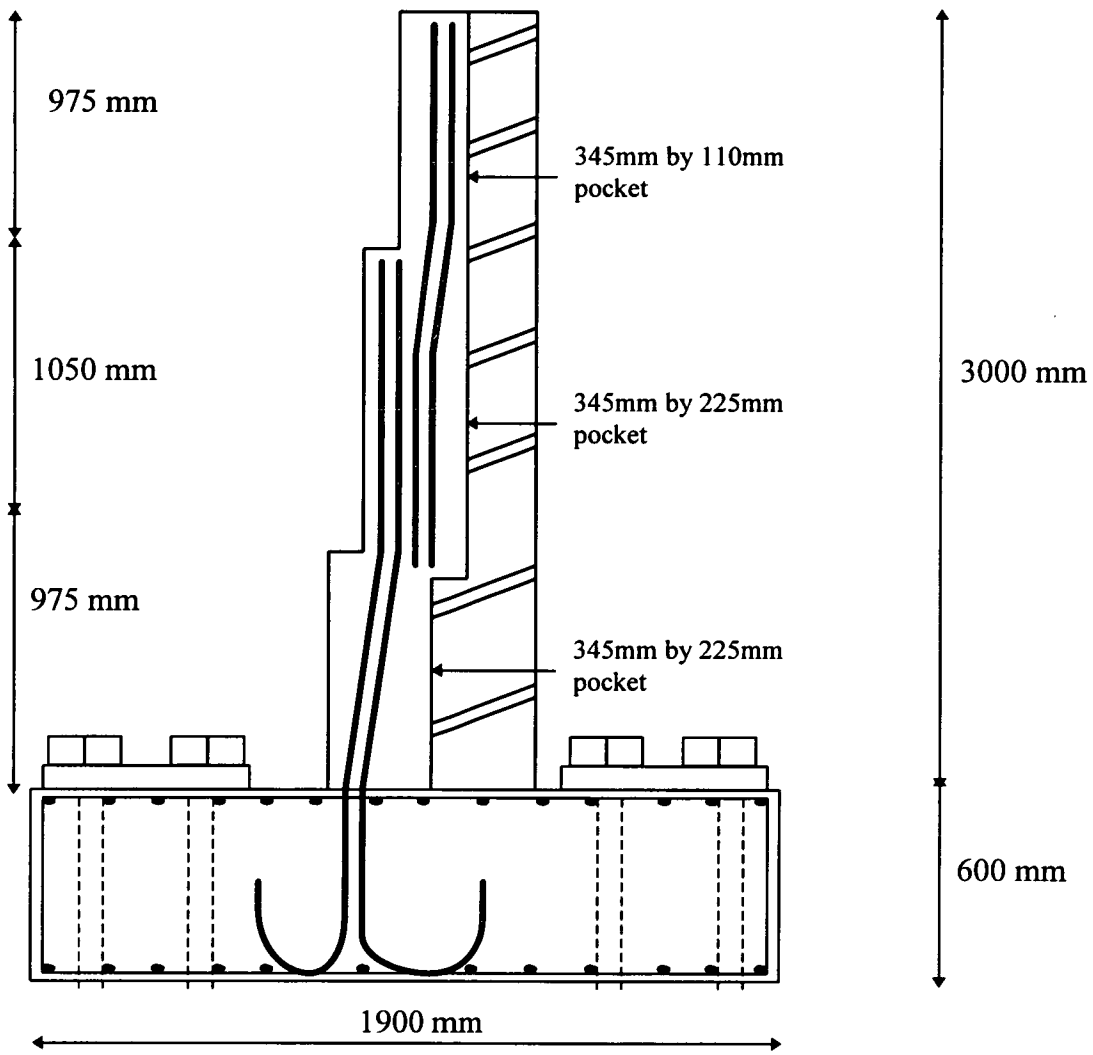

Fig 2.7(a) : Cross-Section through Pocket-Wall[1].

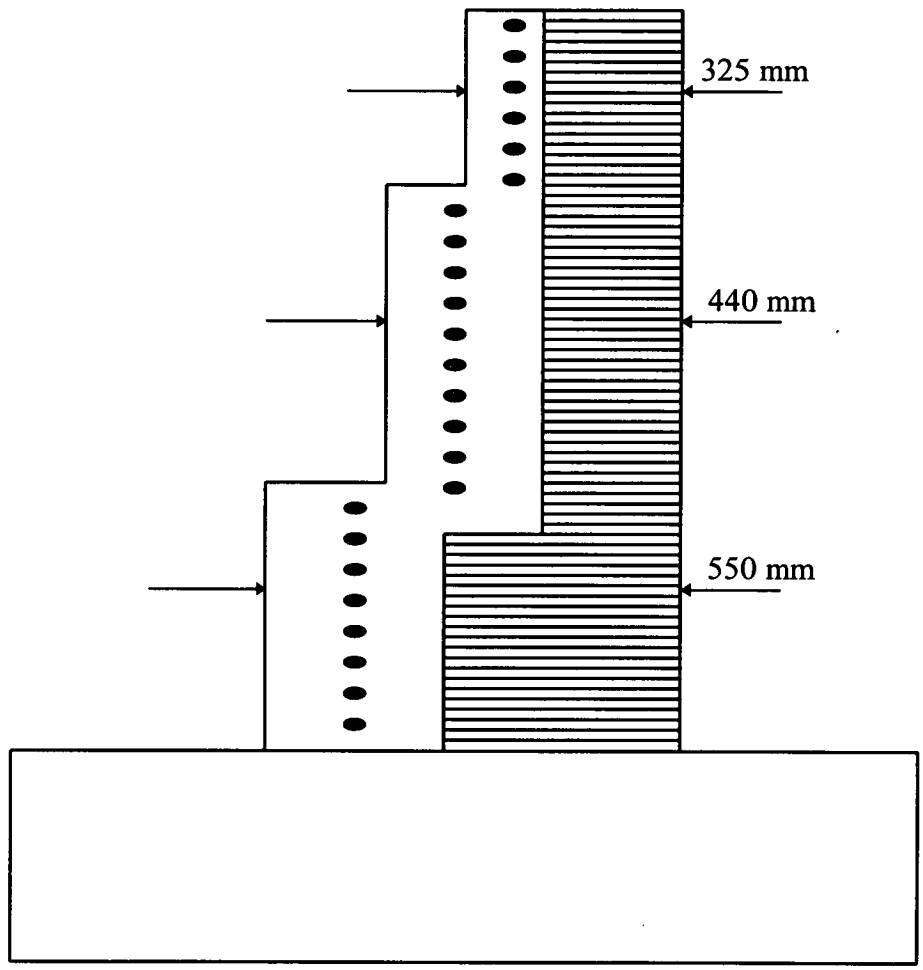

Fig 2.7(b) : Cross Section Through Pocket-Wall Showing Bed-Joint Reinforcement

Work continued at BDA[48] after the results obtained on the third wall proved quite successful. The objective this time was to test a series of slender reinforced pocket brickwork retaining walls with wide pocket spacings to generate experimental data from which the Finite Element Model (FEM) predictions given by an earlier work[45,46] could be validated. It was proposed that if such tests were successful in that respect, it would be safe to recommend walls with wide pocket spacings much in excess of those currently being used.

Two full-scale walls have been tested and reported out of this series, each a 215 mm solid rectangular section construction, 3m high. Each of the two walls were loaded with three 1m wide horizontal air bags along the whole length of the wall, which ensured a distributed stepped load to simulate triangular loading. The load was monitored using a mercury manometer graduated in kN/m^2. The air bags were restrained against the pocket side of the wall by reaction boards fixed to an A-frame bolted to a strong laboratory floor.

The first wall was 4.87 m long with a pocket spacing of 2.4 m (aspect ratio=1.25) while the second wall was 5.35 m long with a pocket spacing of 3 m (aspect ratio=1.0). Both were cantilever walls anchored to a reinforced concrete base. Similar reinforcement were provided within the two walls but the second wall also contained "Brickforce" ladder-type bed joint reinforcement and nominal shear-link stirrups. Each wall was fully instrumented with strain guages, demec and portal guages, deflection transducers and conductive paint stripes. The first wall attained a maximum base moment of 60.8kNm/m which resulted in a maximum deflection at the top of the wall of 69.4 mm. Cracking occurred at the joint between the wall and the concrete base on the tension face and this spread from the centre of the wall towards each end.

For the second wall, a maximum base moment of 76kNm/m was attained which resulted in a maximum deflection of 80.3 mm at the top of the wall. The cracking pattern was similar to that of the first wall. At all other positions on the two walls, no cracking was observed. In the first wall, the demec and portal strain readings on the compression face all show that the highest compressive strains occur in line with the concrete pockets compared to other points far removed from the pockets. Also, no damage was observed on the panel of brickwork between the pockets in spite of the absence of shear reinforcement in this wall. This result gave way to the conclusion by the authors that flanged-member action had taken place and that wall pockets were behaving as flanged members and providing adequate edge support to the masonry panel between the pockets. Shear resistance of this wall was provided purely by the bond between the brick and the concrete and, in spite of this, no evidence of shear failure was observed. Walls behaved as an under-reinforced section with failure

occurring by yielding of the reinforcing steel with a considerable reserve of shear and flexural strength than predicted by theory being retained at the point of failure.

In the design calculation pertaining to the second wall, an over-reinforced section is indicated. However, this wall also behaved as an under-reinforced section with failure governed by yielding of the reinforcing steel. The maximum brickwork strains at the end of the tests were of the same order as those associated with the limits of the brickwork used for the wall. The fact that the brickwork did not fail was attributed, by the authors, to the presence of the bed-joint reinforcement which is thought to possibly allow higher brickwork strains, than would normally occur, to develop prior to the compressive failure of brickwork. A similar phenomenon was observed concerning the shear strength of this wall. The shear strength exceeded the design value by as much as 81%, a situation which was explained by (a) the fact that the presence of nominal stirrups and bed-joint reinforcement have made contributions to the shear strength of the wall section in a manner which the design calculation could not adequately reflect (an attempt to incorporate such contribution by the authors only reduced this margin by about 33% leaving the remaining 48% unaccountable) and (b) if a review of the shear strength calculation for reinforced elements is done so as to incorporate the strengthening effect of shear reinforcement, based on the premise that the compression block is strengthened by the presence of shear reinforcement, in almost the same manner that prestressing (as in post-tensioned structures) to strengthen the section in compression improves shear strength, then the reserve shear strength exhibited by the wall would be accounted for.

For the two walls, the strength was governed by ultimate strength rather than deflection limits and both of them showed that flanged-member action had taken place. This is supported by the experimental brickwork strain distribution from cracking to the ultimate point. Much higher compressive brickwork strains were observed around the pockets compared to the strains at points far removed from the pockets. There was also no evidence of brickwork crushing between the pockets and it was concluded that the pocket stems provided adequate edge support for the brickwork. The tests also indicated that no significant benefits have resulted from the

use of bed-joint reinforcements except perhaps an increased moment of resistance of the brickwork and the authors recommended that tests be conducted on over-reinforced walls where failure occurs in the brickwork rather than in the pocket reinforcement so as to investigate if such bed-joint reinforcement (used in the second wall) actually leads to an increase in the brickwork moment of resistance. The issue of whether such reinforcement leads to an improved shear resistance for the wall was also considered worthy of further investigation and the authors recommended that work should be furthered to ensure the possibility of reflecting this much more realistically in design calculations.

2.6 METHODS USED FOR PREDICTING SHEAR STRENGTH OF LONGITUDINALLY REINFORCED BEAM SECTIONS

Broadly speaking, three different theoretical methods have been employed by previous investigators to predict the shear strength of longitudinally-reinforced and/or prestressed brickwork members. These three methods are distinct by virtue of the totality of the underlying assumptions associated with them respectively. Each of these methods are hereby briefly discussed in turn.

2.6.1 Method Based on the concept of "Compressive Force Path" or CFP

This method was also originally developed for reinforced concrete members. It assumes that a path exists through which compressive forces "flow" from the support to the load point and that the development of a critical stress state along this path ultimately determines the shear strength of the section rather than on any stress conditions below the neutral axis. In other words, the necessary and sufficient condition for shear failure to occur would normally take place along this path of compressive forces. The shear failure of the member is attributed to the development of tensile stresses, along the path, which creates a region of weakness in the surrounding material, then propagates from there to other surrounding areas and eventually results in the ultimate collapse of the structure.

This method gives no account of the stress conditions below the neutral axis for members having only longitudinal reinforcements. Its proponents insist that shear

failure is neither dependent on aggregate interlock or on stress conditions below the neutral axis of the section for that matter but rather, only on the stress situation along the "path" of compressive forces. The method further assumes that the uniaxial stress conditions traditionally assumed for the compression zone is trivial and that the actual stress conditions ensuing within this zone is much more complex.

It is further argued that its greater understanding is found in a triaxial stress-state consideration of an element of material within the compression zone of the beam. Much experimental evidence have been used to support this concept and failure of most of the sections examined have been attributed to the development of tensile stresses in the "region of the compressive force path". Based on this premise, models of the path have been formulated with both horizontal and inclined parts, the relative dimensions of which are functions of the *a/d* ratio and the observed failure modes of the beams tested. This method has been successfully applied to predict shear strength of both reinforced concrete[17-19,49,50] and partially prestressed brickwork[11] beams that have no shear reinforcement incorporated into them.

It appears that the method of CFP is best suited for brickwork sections in which the bed-joint planes are coplanar with the induced compressive forces and, in order for the method to be relevant, one needs to be sure that the crack immediately responsible for ultimate failure in shear actually grows towards and terminates in the constant bending moment region of the beam. This way, the subsidiary condition needed to complete the governing equations can be associated with results obtained from relevant prism formats. This method is therefore not well suited for the pocket-type sections tested by the author since the compressive forces developed perpendicularly to the bed-joint planes.

2.6.2 Method Based on the "Tied-Arch" Formulation

Another approximate method which has been used to predict the shear strength of reinforced brickwork beams is contained within the confines of Arching Theory. In this theory, the reinforced brickwork beam is assumed to behave as a tied-arch and the following assumptions are made for the brickwork within the shear span, namely : (1)

plane stress conditions exists within this region of the beam, (2) brickwork/grout interface within the shear span is subject to precompression and (3) ultimate failure in shear is due to one of the following three reasons, namely : (a) compressive stress acting in the compression zone exceeds the compressive strength of the brickwork used in beam construction or the tension failure of the "arch rib"; (b) the tie stress exceeds the tensile strength of the steel used or ; (c) tie force is equal to or exceeds the ultimate shear strength (force) of the brickwork used so that the bond between the steel and grout is destroyed.

This formulation includes writing the equation of equilibrium which incorporates conditions at the boundary between the constant shear and maximum bending moment zones of the beam. Such an equation ensures that the physical condition of continuity of the beam, prior to ultimate collapse, is not violated. Equations for predicting shear strength are then developed based on the compatibility condition at failure as well as on the manner with which failure actually occurred. In other words, any of the possible conditions given above, which actually result in ultimate failure in shear, are then incorporated in the formulation.

This theoretical prediction of failure stress is then compared with actual failure stress of the beam in shear to examine the accuracy of the model. The model itself dictates the condition under which it is valid. This type of model has been successfully used to predict the shear strength of brickwork of the grouted-cavity variety as well as for results previously obtained for ordinary reinforced brickwork sections[33].

This method is also best suited to brickwork sections in which the compressive forces develop parallel to the bed-joints in view of the assumptions inherent in its formulation. In such sections, the bed joint is assumed to be under precompressive stress which enhances the shear strength. This method has not been used in the present work since the bed joint planes are perpendicular to the compressive forces.

2.6.3 Method Based On Plastic Analysis

The beam is assumed to be made up of compression and tension stringers which behave in a rigid-perfectly-plastic manner. The concrete in the web is also assumed to be rigid-perfectly-plastic with yielding controlled by a modified Coulomb yield criterion which assumes a tensile strength value of zero. This assumption has been considered reasonable for brickwork beams on the basis of the experimental evidence supplied by Page[51] which showed that, under biaxial compression, the failure criterion could be approximated by a square surface which is independent of the orientation of the principal stresses relative to the bed joints of the brickwork.

In order to account for the somewhat unrealistic assumption of unlimited ductility made by this method, the compressive strength of the brickwork is multiplied by an effectiveness factor, ϑ ,which varies between 0 and 1.

After formulating a simple model which satisfies the requirements of perfect plasticity, this method proceeds to determine the ultimate load which was calculated, in accordance with the theory of plasticity, as the lowest upper bound or the highest lower bound. As for the upper bound, the solution was found by assuming a failure mechanism and equating the rates of external and internal work. The lower bound solution, on the other hand, was obtained by assuming a stress distribution and calculating the load corresponding to it.

Although the validity of the assumptions made by this technique of prediction is questionable, its adherents[9] nonetheless insist that the correct plastic solution to the shear prediction problem has been found. They[9] argued that this is so because both the upper and lower bound analysis gave the same value of the ultimate shear load.

This method is also not exact. First, on the basis of the assumptions made and secondly, because of its absolute reliance on the empirically-determined parameter called the effectiveness factor. This latter reason would equally qualify the method as a semi-empirical one at best. However, to its credit, the method has been successfully

employed by previous investigators to predict the shear strength of reinforced concrete beams[9] and those of fully[7] and partially[11] prestressed brickwork beams.

From these three theoretical methods, the method based on plastic analysis seemed very promising in view of its successful application in reinforced concrete. Hence the method has been adapted to predict the shear strength of the pocket-type reinforced brickwork beams tested by the author. The underlying theory as well as the predictions resulting thereof are presented in chapter 4.

2.7 SCOPE OF THIS RESEARCH

After critically examining earlier works, it became very clear that very limited work has been done to understand the behaviour or establish the shear strength of reinforced pocket-type walls. Mostly, the research has been done on reinforced brickwork beams with reinforcement parallel to the longitudinal bed-joints and not normal to the bed joint as in the case of pocket-type walls. There is also complete dearth of experimental data on flanged-member behaviour. Hence, the investigation sets out to achieve the following aims :

(i) To investigate the behaviour and ultimate shear strength of reinforced pocket-type walls and thus to add to the existing database of information.

(ii) To investigate flange-member action and spacing of the pockets in reinforced pocket-type walls. Flanged member action occurs when the panel of brickwork between the reinforced concrete pockets act effectively with the pockets to resist the applied load from initial cracking to the ultimate point.

Some associated small scale tests are also done to establish the strength of the brickwork and steel as well as their mechanical properties.

Full-scale tests are performed to obtain the shear strength of the pocket-type walls for enhancement of BS 5628 recommendations. Full-scale tests are expensive and time consuming, hence half-scale bricks are used to establish the flange-member action.

CHAPTER 3

MATERIAL PROPERTIES

3.1 INTRODUCTION

This chapter presents a summary of the results obtained from testing the constituent materials used for the construction of the reinforced brickwork beam and slab specimens. As reinforced brickwork is made up of different materials, i.e. brick units, mortar, grout and steel reinforcement, it is usual to determine the structural properties of these basic materials as a prerequisite to understanding the structural properties and behaviour of the combined product. Reinforced brickwork beam and slab sections are examples of such finished products. In flexural elements such as beams and slabs, the compression zone properties of the brickwork are determined by studying the behaviour of relevant brickwork prism formats under compressive loads whereas the tension zone properties are determined from modulus of rupture tests, again on relevant brickwork prism formats. The tensile properties of the steel specimens are obtained from uniaxial tests following standard recommended procedures in codes of practice.

As for the mortar and grout constituents, cube tests have been used to characterize the strength of these materials. Oftentimes, a good estimate of the strength properties of the brickwork is gained by testing and establishing the strength properties of the brick unit itself in various loading directions as may be relevant (that is, on bed, on edge and on end). This result is then combined with the strength properties of the mortar, obtained from cube test results, to determine the overall strength properties of the brickwork. This latter approach is adopted in the current British Code of practice employed for the design of masonry structures[2], in which various tables and graphs have been drawn to cater for different combinations of strength of these materials.

The essence of these small-scale tests is to determine the strength properties of the final composite material, both in tension and compression and the strains associated

with ultimate failure of the elements. These tests also enable the stress-strain characteristics in the tension and compression zones of a typical flexural element to be obtained. These properties are thereafter used to formulate equations governing the strength and serviceability behaviour of the structural elements. As a result of the variable nature of these test results, the stress-strain characteristics are often given in non-dimensional form. This form gives a generalized picture of the properties of these constituent materials pertaining to the final product in question. This procedure is followed in this thesis. The construction of these materials as well as the test methods subsequently employed are now described. The beam and slab sections, constructional details and the reinforcing and grouting procedures are described subsequently in this chapter. The instrumentation and test methods used for the beams and slabs are described in the next chapter.

3.2 MATERIALS

3.2.1 Steel Reinforcement : Standard testing procedures conforming to BS 4449[52] were used to test the steel bars. The yield strength and ultimate strength of these bars were, thereafter, determined. Hot rolled high yield deformed bars were used for the reinforcement. The resulting strain on the specimens was recorded by electrical resistance strain gauges mounted on them.

The summary of results obtained from tensile tests on the steel specimens are given in Table 3.1 and Figs 3.1(a), 3.1(b) and 3.1(c).

Table 3.1 : Properties of the Steel Reinforcements

Diameter of bar (mm)	$\sigma_{0.2\%}$ (Nmm^{-2})	σ_{ult} (Nmm^{-2})
16	515	607
20	520	618
25	483	580

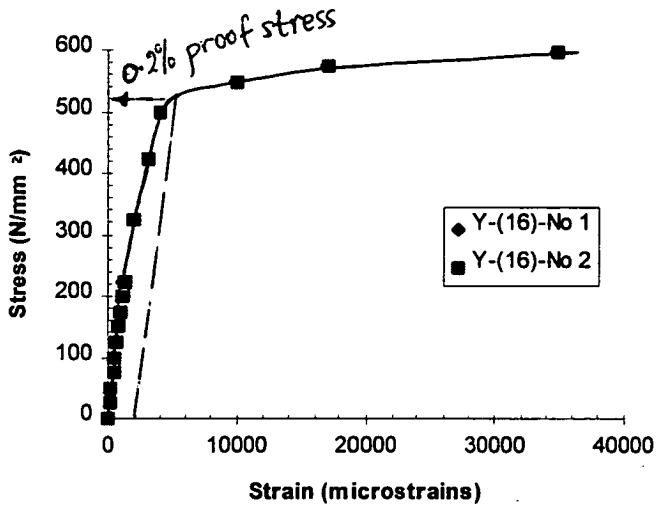

Fig 3.1(a) : Stress-Strain curve for T-16 diameter steel bars

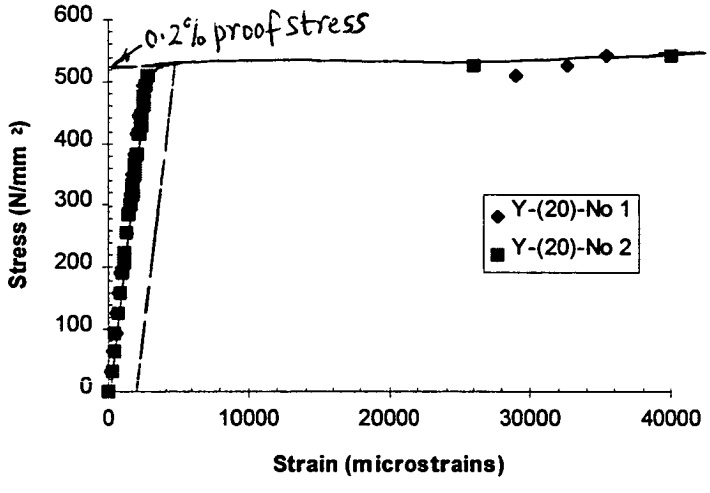

Fig 3.1(b) : Stress-Strain curve for T-20 diameter steel bars

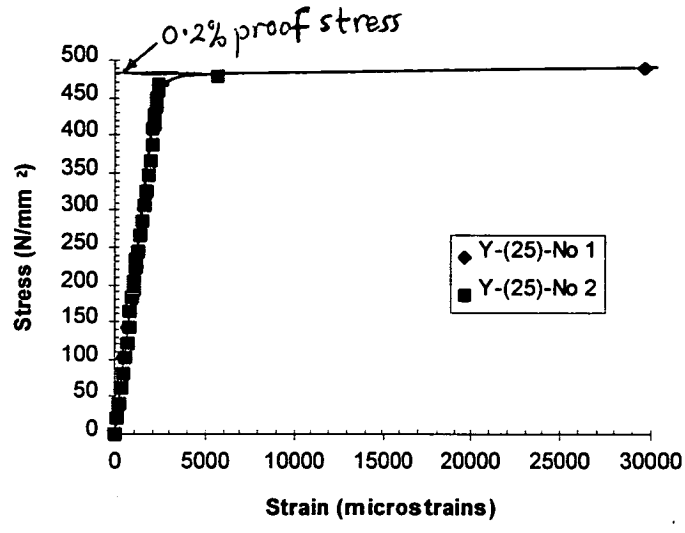

Fig 3.1(c) : Stress-Strain curve for T-25 diameter steel bars

3.2.2 Bricks : Extruded class A engineering bricks with three holes were used throughout for the beams. The average area of perforations was 14.9 %. It has an average compressive strength, on bed, of 84 Nmm^{-2}.

3.2.3 Mortar : Grade I mortar was used throughout for the test. The mix proportion being $1:\frac{1}{4}:3$ (cement : lime : sand by volume). Gauging boxes were used to obtain these mix proportions and the water content was adjusted by the bricklayer to achieve a consistent, workable mix. The same bricklayer was employed throughout the duration of construction of the test specimens. 100 mm control cubes were taken during construction, cured in water and tested at 28 days. The mortar strength thus obtained are given in Table 3.2 for each beam.

Table 3.2 : Compressive Strength of Mortar Cubes

Cube strength	B1 (kN)	B2 (kN)	B3 (kN)	B4 (kN)	B5 (kN)	B6 (kN)	B7 (kN)	B8 (kN)
1st	242.0	215.0	158.0	170.0	211.0	249.0	223.0	230.0
2nd	237.5	224.0	154.0	196.0	229.0	258.0	251.0	243.0
3rd	241.5	214.5	221.0	185.0	255.0	252.0	246.0	248.0
Average compressive strength (N/mm^2)	24.03	21.78	17.77	18.37	23.17	25.30	24.00	24.03

3.2.4 Cement and Lime : Ordinary Portland Cement conforming to B.S. 12[53] and lime conforming to B.S. 890[54] were used throughout for the construction of these structural elements.

3.2.5 Sand : The sand used for the construction conforms to the grading limits of B.S. 1200[55] for reinforced brickwork.

3.2.6 Grout : A grout mix of 1:2½:2 (cement : sand : aggregate by volume) was used throughout. The same sand and cement as used in the production of the mortar was used for the grout. 100 mm cubes were also cast during each grouting session, cured in water and tested at 7 days. The result of compressive strength tests are as given in Table 3.3.

Table 3.3 : Compressive Strength of Grout Cubes

Cube strength	B1 (kN)	B2 (kN)	B3 (kN)	B4 (kN)	B5 (kN)	B6 (kN)	B7 (kN)	B8 (kN)
1st	342.2	202.0	240.0	263.0	287.0	243.0	225.0	211.0
2nd	317.0	212.0	236.0	249.0	281.0	248.0	230.0	189.0
3rd	287.0	220.0	245.0	263.0	282.0	232.0	222.0	193.0
Average compressive strength (N/mm^2)	31.53	21.13	24.03	25.83	28.33	24.10	22.57	19.77

3.2.7 Brickwork Properties : The compression zone properties of the reinforced elements were determined by testing prism specimens which adequately represent this zone. Both concentric and eccentric uniaxial loading were applied to these prisms, shown in Figs 3.2(a) and 3.2(b) respectively. The eccentric loading was used to represent the strain-gradient which is normally associated within the compression zone of flexural elements. For axially-loaded prisms, there is no strain gradient. In brickwork elements in which compression forces are coplanar with the bed joints, tests done previously on relevant prism formats have shown that this strain gradient has no effect on the attainable ultimate strength[11,13]. This result is not necessarily transferable to brickwork elements in which the compressive forces are developed in a perpendicular direction to the bed joint planes. Therefore, in order to find out the possible influence of the strain gradient on the ultimate strength of the compression zone for the brickwork used in this work, both eccentric and concentric loading were applied to some prism specimens.

The dimensions of the prism are given in Fig 3.2(a). The height of the prism was set so that 'machine platen' effect was negligible. All the test specimens were built by the same person, an experienced bricklayer, and cured under polythene for 28 days prior to testing.

For the eccentrically-loaded prisms, the set up was arranged (Fig 3.2(b)) such that the line of action of the load was at an eccentricity of $\frac{t}{6}$. Strain measurements were taken at positions across the width of the section using a mechanical "demec" strain gauge, of gauge length *200 mm*, at regular load intervals.

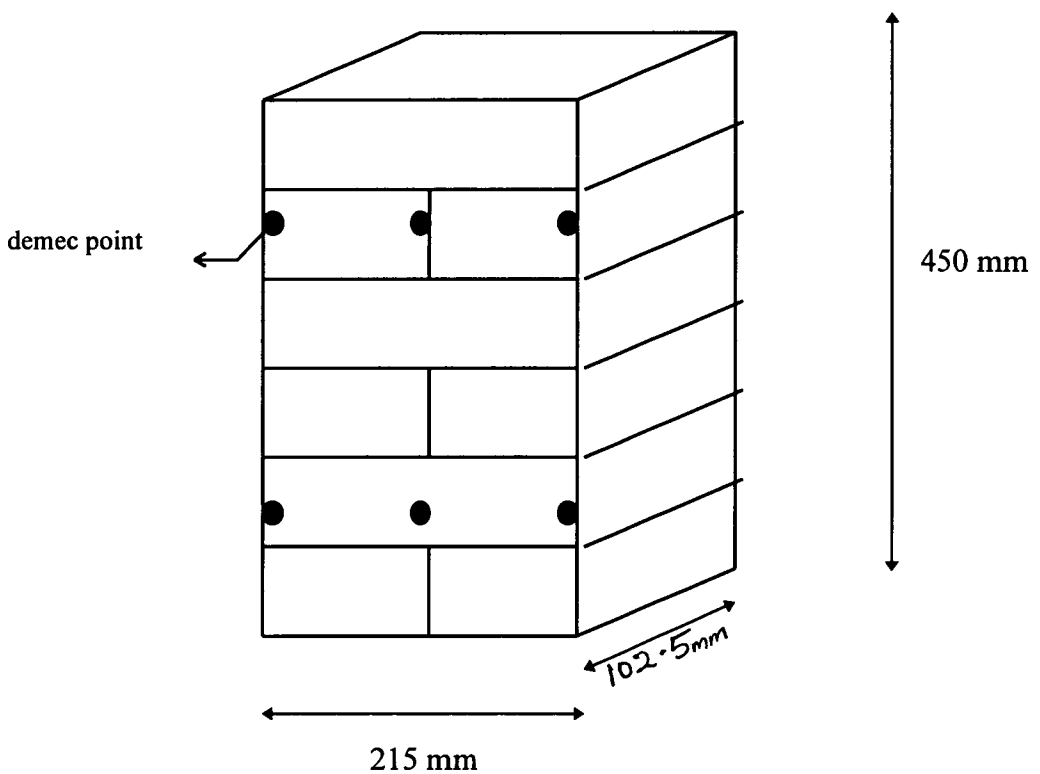

Fig 3.2(a) : Prism of brickwork ("Demec point" for axially-loaded specimen)

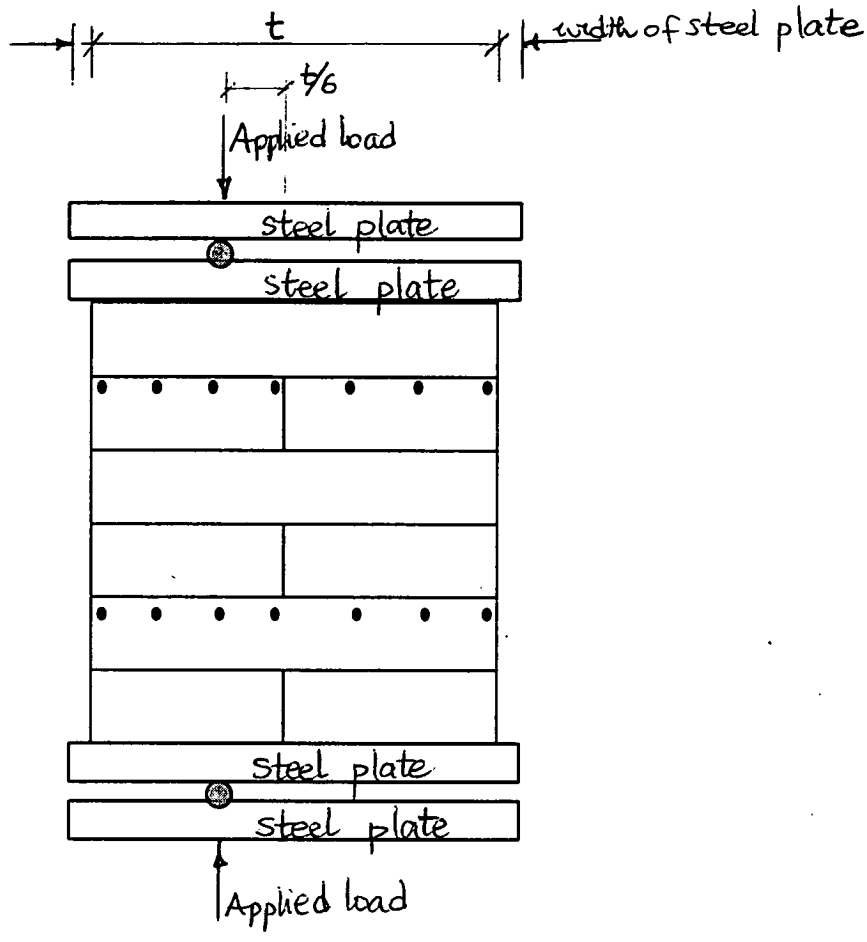

Fig 3.2(b) : Test Set-Up for Eccentrically-loaded Prism Specimen

3.3 EXPERIMENTAL OBSERVATIONS

3.3.1 Single Course Prisms : The single course prisms are those prisms which represent the compression zone in such a way that no physical bed-joint exists in the same plane as the applied compressive force. In all the prisms tested, failure was due to vertical tensile cracks which developed parallel to the axis of loading. Collapse was caused by explosive spalling of the brickwork.

3.3.2 Modes of failure : Prior to failure, vertical tensile cracks of the bricks occurred in both the axially and eccentrically-loaded prisms. For the axially-loaded prisms, splitting of the bricks was at the center of the prisms whereas, it was along the line of action of the load in the eccentrically-loaded prisms. For the eccentric prisms, the strain distribution prior to cracking was linearly varying from a maximum value at the loaded end and reducing to approximately zero at the opposite end furthest removed

from the loaded end. The properties of the brickwork used for the full-scale tests have been deduced from these single course prisms.

3.3.3 Results :

3.3.3.1 The compressive strength of axially-loaded brickwork Prisms : The summary of results obtained from testing the brickwork prisms is given in Table 3.4.

Table 3.4 : Compressive Strength Test Results (Axially-loaded prisms)

Prism No	Maximum Load (kN)	Maximum Stress (Nmm^{-2})	Ultimate Strain ($\mu\varepsilon$) (10^{-6})
1	676	28.0	2577
2	620	26.3	2421
3	474	18.7	2070
4	665	28.2	2360
5	480	19.9	2124
Average compressive stress		24.22	

3.3.3.2 Stress-Strain Relationship

The stress-strain relationships for the high strength brickwork with grade I mortar tested by the author is given in Fig 3.3(a-e). In these, f represents the stress, the strain and R^2 represents the correlation coefficient.

The ultimate strain occurring in the specimens could not be measured by the technique employed, nonetheless, measurements were taken up to within the range 85%-97% of the ultimate strain. A curve was, therefore, fitted to the experimental observations. The ultimate strain, ε_m, was then obtained by extrapolation of the stress-strain curve up to the failure stress.

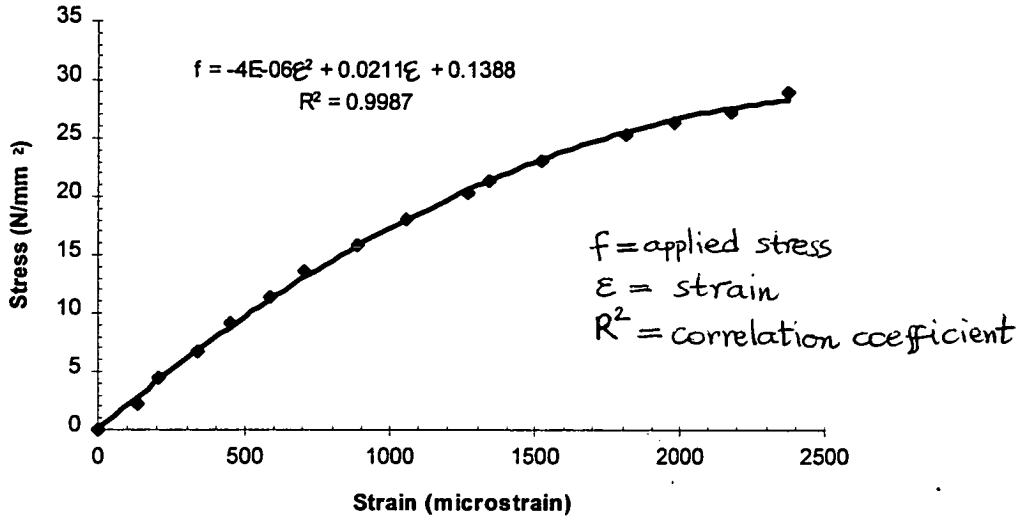

Fig 3.3(a) : Stress-Strain relationship for axially-loaded prism (No 1)

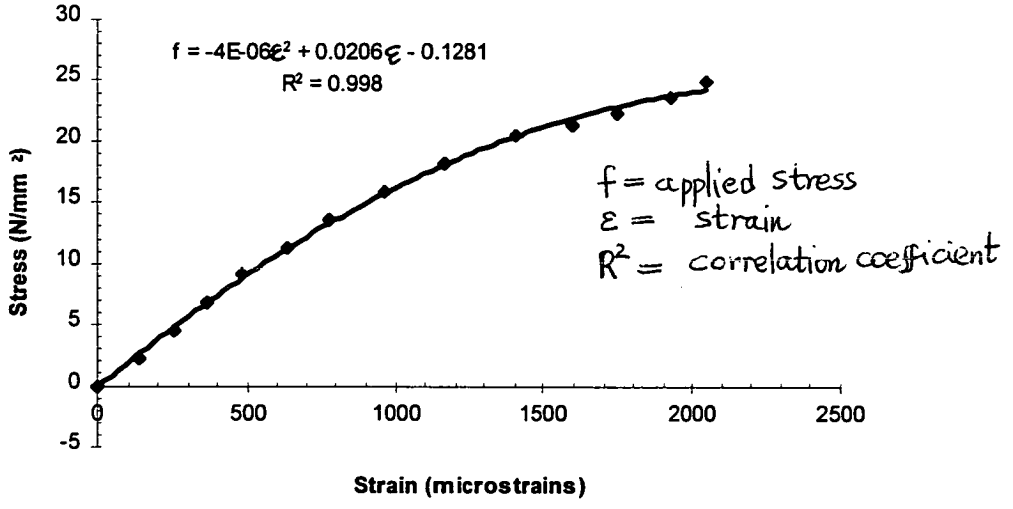

Fig 3.3(b) : Stress-Strain relationship for axially-loaded prism (No 2)

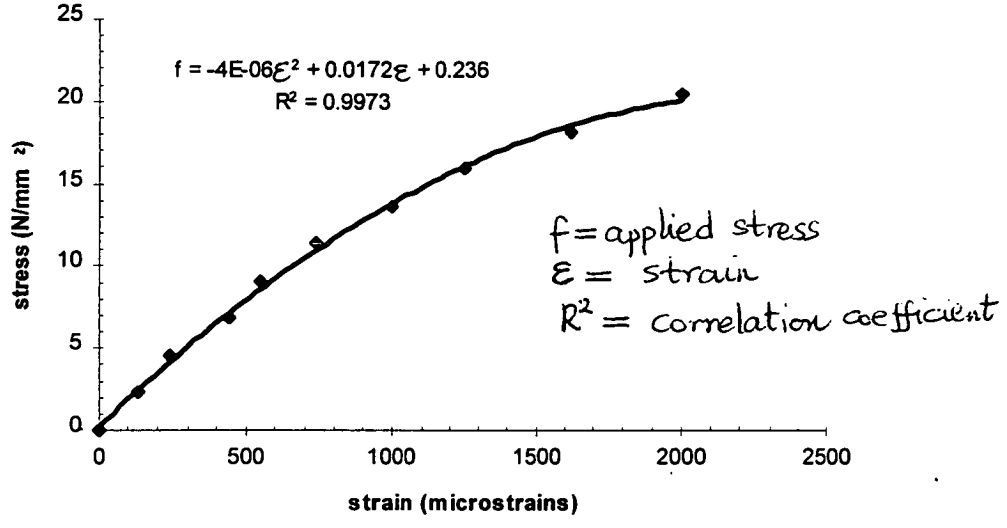

Fig 3.3(c) : Stress-Strain relationship for axially-loaded prism (No 3)

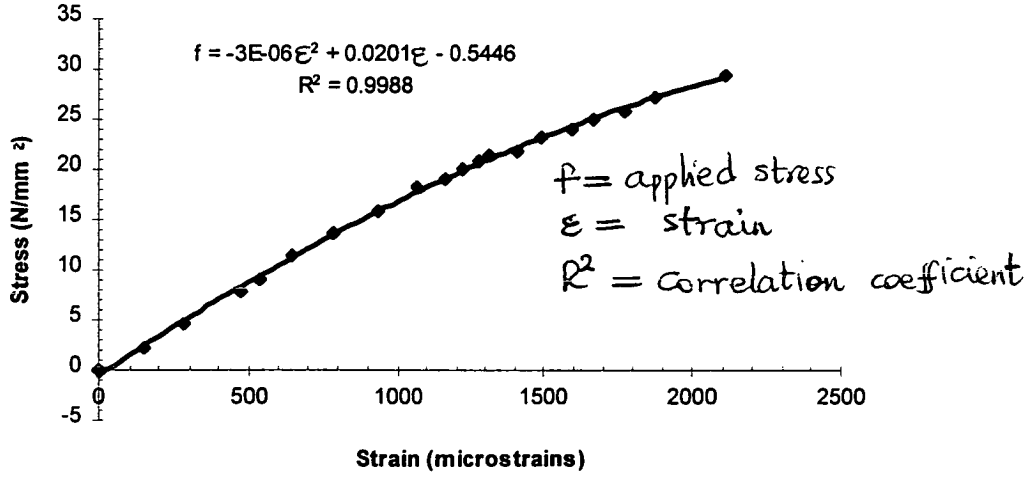

Fig 3.3(d) : Stress-Strain relationship for axially-loaded prism (No 4)

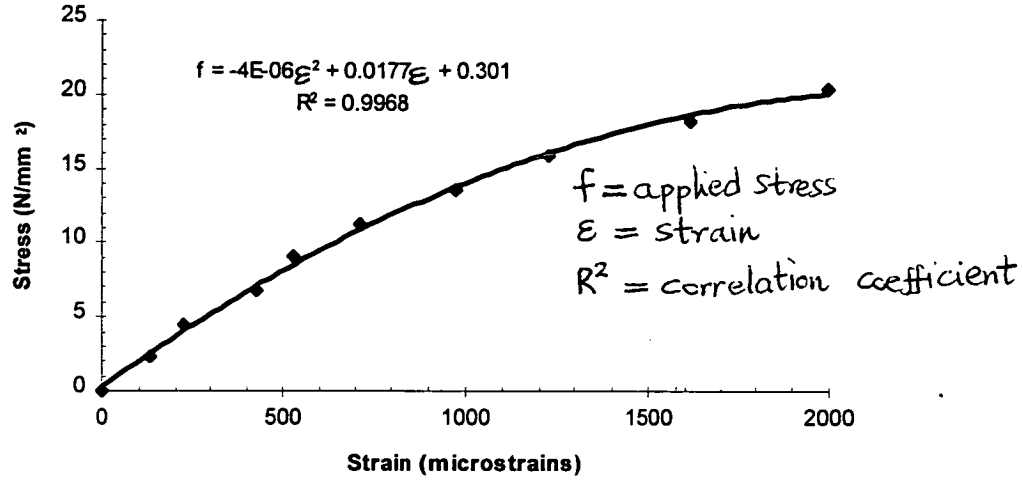

Fig 3.3(e) : Stress-Strain relationship for axially-loaded prism (No 5)

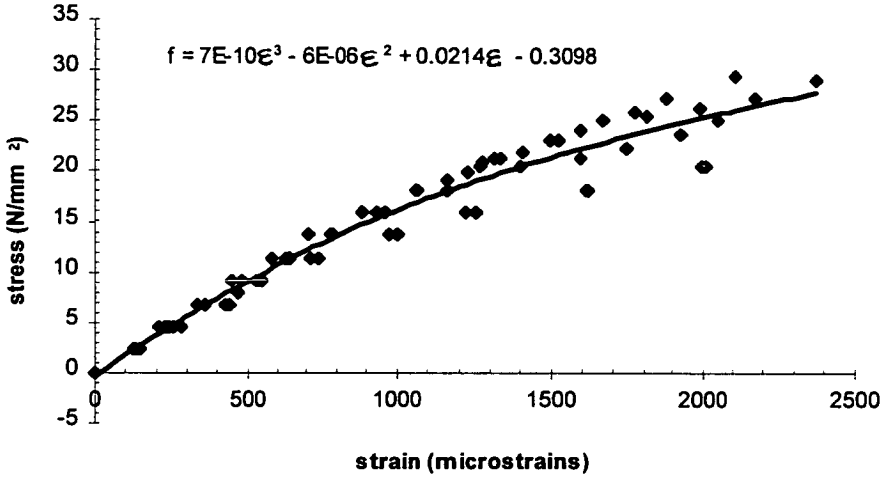

Fig 3.3(f) : Average Stress-Strain relationship for brickwork

For the purposes of analysis and also in order to minimize the variation recorded in the prism test results, the stress-strain relationship of the brickwork is given in non-dimensional form. This was done by normalizing the stress and strain by their maximum values, f_m and ε_m respectively, for the individual prism test results. The non-dimensional, normalised stress-strain relationship is given in Fig 3.3(g).

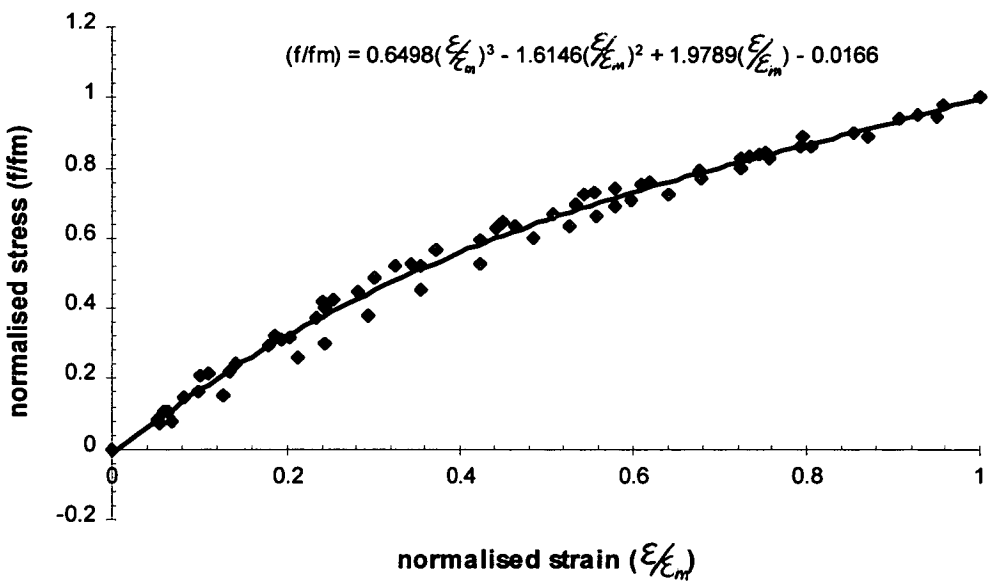

Fig 3.3(g) : Non-dimensional Stress-Strain relationship for brickwork

This relationship is found to be adequately represented by a third degree polynomial of the form given by equation 3.1 :

$$f/f_m = X_0 + X_1\left(\varepsilon/\varepsilon_m\right) + X_2\left(\varepsilon/\varepsilon_m\right)^2 + X_3\left(\varepsilon/\varepsilon_m\right)^3 \qquad \text{----------(3.1)}$$

Other investigators[7,11,13,56,57] have previously expressed the stress-strain relationship for brickwork in a similar manner. Pedreschi obtained coefficients for various brickwork and prism types with loading applied parallel to the bed-joints. For instance, the coefficients which he obtained for high strength bricks in grade I mortar are as given, along with those of other workers, in Table 3.5. Walker[13] subsequently obtained constants for a large number of tests on single and three course prisms of high and medium strength bricks in grade I and II mortar. Again, this result is for

brickwork loaded parallel to the bed-joint. Uduehi[11] also obtained coefficients for high strength single course brickwork prisms loaded parallel to the bed joints as given in Table 3.5. The coefficients obtained from the brickwork used in this investigation are given alongside all those obtained by previous investigators. However, the brickwork reported here is loaded in a direction perpendicular to the bed-joint. From a comparison of these various coefficients, it is seen that the non-dimensional relationships for brickwork loaded parallel and perpendicular to the bed-joints have close correlation. This is confirmed when the stress-block characteristics, defined later, relating to each of these separate results are compared (Table 3.8).

Table 3.5 : Non-Dimensional Stress-Strain Characteristics

Coefficients	Pedreschi[7]	Walker[13]	Uduehi[11]	Present work
X_0	-0.05	0	0	-0.0166
X_1	+2.373	+2.12	+1.67	+1.9789
X_2	-2.095	-1.78	-0.665	-1.6146
X_3	+0.776	+0.66	-0.017	+0.6498

3.3.3.2(a) Brickwork Prisms loaded eccentrically

The possible effect of the strain gradient on the stress occurring at the point of failure was also investigated by analysing the results obtained from the eccentrically loaded prisms. Firstly, the average stress-strain curve obtained from all the concentrically-loaded prism specimens was derived by fitting a curve through all the experimental observation points (Fig 3.3(f)). The equation derived from this curve-fitting procedure was used to work out the stress at every point across the breadth of the eccentrically-loaded prism from the strain measurements obtained at these points see Fig 3.3(h-j).

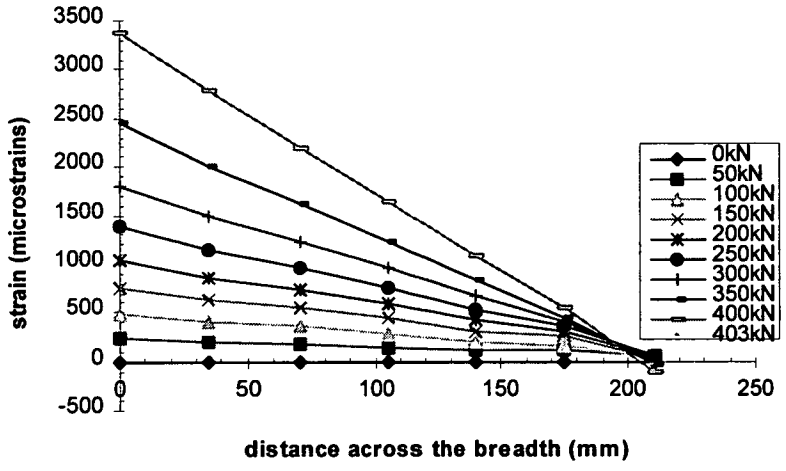

Fig 3.3(h) : Strain distribution in eccentrically-loaded prism (No 1)

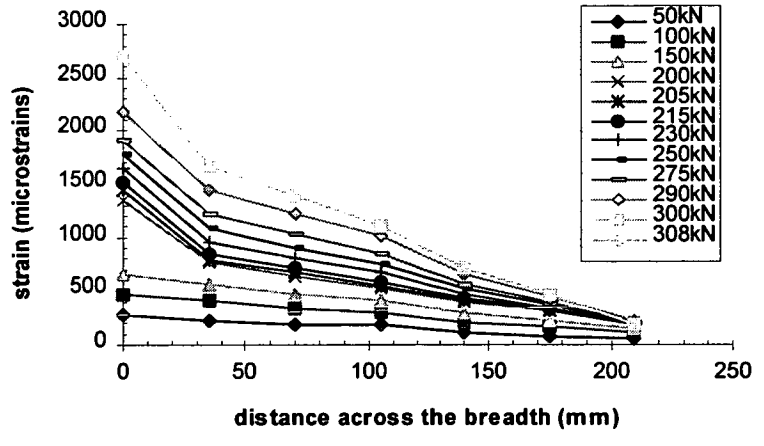

Fig 3.3(i) : Strain distribution in eccentrically-loaded prism (No 2)

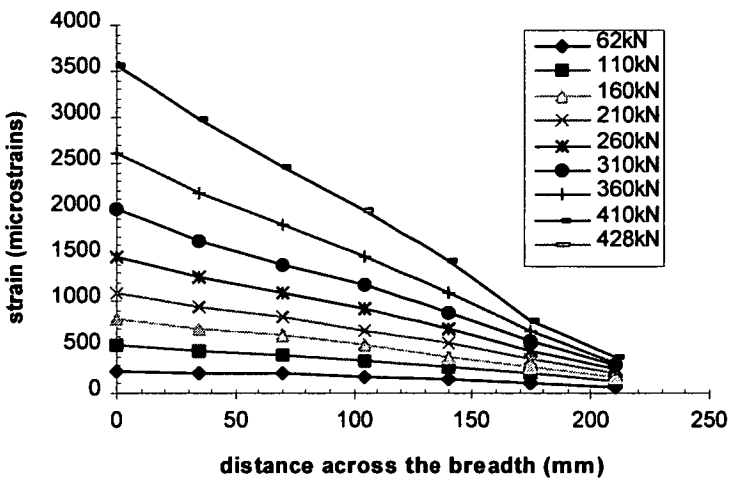

Fig 3.3(j) : Strain distribution in eccentrically-loaded prism (No 3)

Therefore, at every stage of applied loading, the stress distribution across the breadth of the eccentrically-loaded prism specimen was derived. Again, this stress-distribution was obtained by a curve-fitting procedure.

Secondly, equilibrium was checked at every stage of applied loading by integrating the stress diagram across the breadth of the prism for the particular level of loading. These calculation gave comparable results between the applied external load and the derived load for all the prism specimens (Table 3.6). This demonstrates the accuracy and validity of the technique to determine the stress distribution in eccentrically-loaded prisms.

Table 3.6 : Comparison of Experimental and Predicted Loading for Eccentrically-loaded prism

Load Level	50% of Ultimate Load (kN)			75% of Ultimate Load (kN)			95% of Ultimate Load (kN)		
Prism No	Theor	Expt	% diff	Theor	Expt	% diff	Theor	Expt	% diff
1	198	200	1%	315.6	300	5%	419.4	400	5%
2	153	150	2%	222.2	215	3%	318.5	290	9%
3	291.4	260	11%	418	360	14%	476	410	14%

3.3.3.2(b) Maximum stress at failure (Eccentrically-loaded prism)

The distribution of maximum stress throughout the loading history of the prism was used to obtain the maximum stress occurring at failure for the eccentrically-loaded prism specimens. This was done because the strain at the point of failure could not be recorded by use of a demec gauge. A curve-fitting procedure was used to arrive at these values. In other words, a regression analysis was done on the distribution of maximum stress. The maximum stress for every individual prism, loaded eccentrically, was taken as the stress corresponding to the ultimate load for that particular prism (Table 3.7).

Table 3.7 : Maximum stress at failure (Eccentrically-loaded prisms)

Prism No	Maximum stress ,f_{max} , (N/mm^2)
1	29.64
2	26.96
3	31.76
Maximum stress (average value)	29.45

When the maximum stress at failure was calculated from experimental data for the three eccentrically-loaded prisms tested, the results revealed that stresses were approximately the same order of magnitude for both the eccentrically-loaded specimens and axially-loaded prisms (compare Table 3.4 & Table 3.7). The strain

gradient therefore has no discernible effect on the attainable ultimate stress for the brickwork format reported in this work. In view of these findings and because it is very difficult to obtain results from eccentrically-loaded test specimens, it may be appropriate to adopt results from the axially-loaded prisms as adequately representing the compression zone characteristics in flexure.

3.3.3.3 Stress block characteristics

To predict the ultimate strength of beam in flexure, the magnitude and relative position of the resultant force in the compression zone are both required; They are defined, respectively, as :

$$\lambda_1 = \int_0^1 \left[X_0 + X_1\left(\varepsilon/\varepsilon_m\right) + X_2\left(\varepsilon/\varepsilon_m\right)^2 + X_3\left(\varepsilon/\varepsilon_m\right)^3 \right] d\left(\varepsilon/\varepsilon_m\right) \quad \text{---------- (3.2)}$$

$$\lambda_2 = 1 - \frac{\int_0^1 \left[\left(\varepsilon/\varepsilon_m\right)\left(X_0 + X_1\left(\varepsilon/\varepsilon_m\right) + X_2\left(\varepsilon/\varepsilon_m\right)^2 + X_3\left(\varepsilon/\varepsilon_m\right)^3 \right) \right] d\left(\varepsilon/\varepsilon_m\right)}{\lambda_1} \quad \text{---(3.3)}$$

where λ_1 relates the average stress to the compressive strength of the brickwork and λ_2 relates the depth of the centroid of the stress block to the neutral axis depth.

These two characteristics, λ_1 and λ_2 are geometric properties of the non-dimensional stress-strain curve. Both of them combine together to describe, completely, the distribution of compressive stresses in the compression zone.

These characteristics have been compared for axially-loaded and eccentrically-loaded brickwork prisms (Table 3.8). Since the variation of these two characteristics for the different brickwork prisms is not significant, it may be reasonable to take them as independent of the prism format and type of loading used. In view of these observations, it is correct to adopt results from the axially-loaded prism specimens as sufficient to estimate the compression zone properties of the brickwork.

Table 3.8 : Comparison of the Stress Block Characteristics λ_1 and λ_2 for Different Types of Brickwork

	Axially-loaded Prism		Eccentrically-loaded Prism	
Authors	λ_1	λ_2	λ_1	λ_2
Pedreschi (Ref 7)	0.652	0.390	-	-
Walker (Ref 13)	0.606	0.372	0.672	0.333
Uduehi (Ref 11)	0.61	0.387	-	-
Present work	0.60	0.38	0.64	0.41

3.4 THE MODULUS OF RUPTURE FOR BRICKWORK

To obtain the moment at which first cracking appears in reinforced brickwork beams, the modulus of rupture test is often conducted. The modulus of rupture has been obtained for the combination of brick unit and mortar grade reported in this investigation. The average modulus of rupture, obtained from three specimens (Table 3.9), for the brickwork is 1.42 N/mm^2. For the tested sections, three 10-courses high, two-and-a-half brick wide wallettes were built and tested as a beam subjected to a four-point loading arrangement.

Table 3.9 : Modulus of Rupture for Brickwork

Sample No	Modulus of Rupture (M.O.R) N/mm^2
1	1.48
2	1.42
3	1.36
	Average = **1.42** N/mm^2

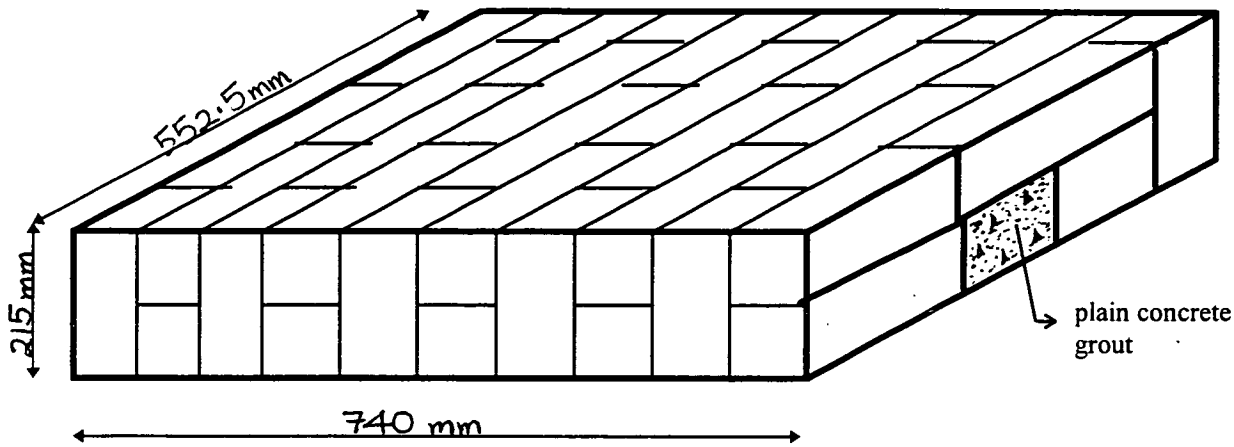

Fig 3.4 : Modulus of rupture specimen

3.5 MODULUS OF ELASTICITY OF BRICKWORK

The tangent modulus of brickwork varies significantly depending on the type of brickwork as well as the direction of loading relative to the bed-joint of the brickwork. Walker[13] obtained equation (3.4) based on brickwork loaded parallel to the bed-joint.

$E_m = 1308 f_m^{0.74}$ (N/mm^2) ----------(3.4)

Pedreschi[7] obtained equation (3.5) based on a large number of tests on prisms loaded normal and parallel to the bed joint.

$E_m = 1180 f_m^{0.83}$ (N/mm^2) ----------(3.5)

The Code of practice gives the relationship as (3.6) :

$\boldsymbol{E_m = 0.9 f_k}$ (kN/mm^2) ---------- (3.6)

In this investigation, the initial tangent modulus of elasticity obtained for the brickwork was 15 kN/mm^2. This result was obtained from prisms loaded perpendicular to the bed joints. The modulus of elasticity obtained from equations (3.4) and (3.5) is approximately 6% lower and 14% higher than the initial tangent modulus respectively. The value of f_m used is the overall average taken from Table 3.10. i.e f_m = 25 N/mm^2. The results were compared with the code of practice, from which the value of f_k was obtained from the test results of Sinha[58] (Table 3.10) and this work. The value of f_k for the brickwork used is 21.5 N/mm^2. Thus, the modulus

of elasticity obtained from equation (3.6) gives 19350 N/mm^2, which is much higher than the test results. This suggests that the code provision is not conservative.

Table 3.10 : Compressive strength of 6-course brickwork prisms after Sinha[58]

Beam No with Prism	Compressive strength (N/mm^2)
3-1	25.6
3-2	25.6
3-3	24.6
4-1	23.3
4-2	25.1
4-3	30.3
5-1	25.2
5-2	27.9
5-3	26.5
6-1	24.4
6-2	26.0
6-3	26.0
7-1	23.0
7-2	24.0
7-3	23.0
8-1	24.9
8-2	25.1
8-3	24.4
Prism 1	28.0
Prism 2	26.3
Prism 3	18.7
Prism 4	28.2
Prism 5	19.9
Average stress (f_m)	25.0

The average moduli of elasticity for brickwork, loaded perpendicular to the bed joint, were obtained from another extensive investigation[59]. These values were used for the slab specimens.

3.6 SUMMARY AND CONCLUSIONS

(1) The technique of using results from axially-loaded prisms to determine the stress distribution in eccentrically-loaded prisms is shown to be valid for the brickwork used in the present work.

(2) The stress block factors λ_1 and λ_2 are not significantly different for brickwork loaded axially or eccentrically. Therefore, axially-loaded brickwork prisms provide a reliable description of the compressive properties of brickwork beams. Also, the experimental procedure and data processing pertaining to the axially-loaded brickwork prisms are comparatively simple.

(3) The modulus of elasticity for brickwork is dependent on the direction of stressing relative to the bed-joint. For the brickwork used in this work, the modulus appears to be reasonably predicted by existing equations derived for (a) brickwork loaded parallel to the bed-joint and (b) brickwork in which loading is applied normal and parallel to the bed joint. It appears that the code provision for estimating this property of brickwork is not conservative.

CHAPTER 4

ULTIMATE SHEAR CAPACITY OF BEAMS

4.1 INTRODUCTION

In design, shear strength seems to be an important criterion in defining the ultimate strength of reinforced brickwork beams and retaining walls. Studies conducted in the past indicate that shear strength depends on variables like a/d ratio, % longitudinal steel, brick masonry strength, mortar strength but the first two variables affect shear strength more than the others. A lower bound value of 0.35 N/mm^2 was derived for shear strength of brick masonry beams in which the reinforcement is embedded in mortar, either in the bed or collar joint of the brickwork. In BS5628 : Part 2, the relevant British Code of Practice pertaining to this subject, this lower bound value is allowed to be increased by a factor $2a/d$ when the shear span ratio is less than 2 for brickwork employing mortar mixes of 1:0.25:3 and 1:0.5:4.5 with a maximum shear strength of 0.7 N/mm^2. It should also be noted that this lower bound value was originally derived for brickwork masonry based on the analysis of tests carried out to investigate the shear strength and the associated failure criteria for storey-height shear walls, employing mortar mixes 1:0.25:3, subjected to the biaxial stress state of shear and precompressive loading.[60] BS5628 recognises that the shear strength is influenced by the *a/d* ratio and also by the % steel for reinforced brickwork masonry in which the reinforcement is placed within pockets, cores or cavities filled with concrete. This relationship is presented in the code by the following expression : $(0.35+17.5\rho)\left[2.5-0.25\frac{a}{d}\right] \nleq 1.75\text{N/mm}^2$.

The quantity inside the first bracket caters for the shear strength for shear span ratios greater than 6. Whenever the *a/d* ratio is less than 6, shear strength is enhanced by the multiplier quantity within the square bracket up to a maximum of 1.75 N/mm^2.

It may be argued that a considerable amount of information exists on the shear strength of reinforced brickwork in general, nonetheless gaps still exist in knowledge of the shear strength of pocket-type sections since only a limited amount of tests have

been conducted on this type of reinforced brickwork[61]. In other words, until now, only a limited number of pocket-type beams have been investigated for shear strength. These few results do not give a clear indication of the order of shear strength of pocket-type beams or how to estimate them. The British Code of Practice[2] dealing with these members recognised the enhancement provided by the % steel and *a/d* ratio as shown in the above expression, but placed a limit of 1.75 N/mm^2 on the characteristic shear strength of simply supported reinforced beams and cantilever retaining wall sections. If the partial safety factor for shear[2], $\gamma_{ms} = 2$, is applied to this characteristic value, conservative values of design shear strength results. This conservative approach is a direct result of paucity of experimental data on shear strength of pocket-type beams, hence the need for this experimental investigation.

This chapter presents the details of experimental set-up and results obtained from testing eight full-scale beams in order to investigate the shear behaviour of pocket-reinforced sections. These experiments examine the effects which the two salient variables, namely, the shear span to the effective-depth ratio a/d and the degree of longitudinal reinforcement, ρ, have on ultimate shear strength. Although, shear strength behaviour investigation forms the major focus of this aspect of the research, other investigations of behaviour, like deflection and cracking analysis, remained a necessary part of these tests. These incidental aspects of the shear investigation were also used to classify and categorise the shear behaviour of these beams. The beams were designed to fail primarily in shear and the effect of *a/d* ratio on shear strength was studied by keeping all variables constant and varying the *a/d* ratio from 2 to 6. The effect of % steel was studied by varying the % steel from 0.6% to 1.6% while all other variables were kept constant and *a/d* ratio was fixed at a value of 3.2.

A summary of existing methods of predicting shear strength has been presented in chapter 2. The theoretical basis which was adopted for analysing these beams is not entirely new but could be considered as an extension of that developed originally for prestressed concrete beams. Finally, a comparison of the experimental results obtained by the author with recommendation for shear strength in the current British Code of practice[2] is presented.

4.2. SHEAR FAILURE IN BEAMS WITHOUT SHEAR REINFORCEMENT

The reality of shear failure is that they occur under combined shear forces and bending moment. They are characterised by small deflections and lack of ductility since they often occur before the flexural capacity of the member is attained and can take place quite unexpectedly. They are undesirable because they often occur with little or no prior warning. Shear failures are mostly associated with diagonal tension and diagonal cracking.

Diagonal failure in shear is usually studied by testing reinforced beams under two-point loading. The major advantage of a set-up like this is that it combines two different test conditions, namely pure bending between the two loads in the central portion of the beam and constant shear force in the end sections termed the "shear spans".

4.3 THEORETICAL ANALYSIS

4.3.1 Analysis of Beam Test Results Using Method Based on Plastic Analysis

As noted in chapter 2, this method has been successfully applied to predict the shear strength of both fully and partially prestressed brickwork sections in which the compressive forces were applied parallel to the bed-joints. Since reinforced brickwork could be considered to be only a special form of prestressed brickwork in which zero prestress is applied, it is considered reasonable and useful to assess the shear strength of these pocket-type reinforced brickwork beams by this technique.

The method predicts the shear strength by employing an empirical factor on compressive strength. The plastic methods proposed by Nielsen et al.[9,62] are detailed elsewhere but those aspects of the theory pertaining to the shear strength of beams without shear reinforcement are considered here. Using the plastic theory, per se, assumes implicitly that the material exhibits a reasonable degree of ductility. This implicit assumption is not apparent in materials such as brickwork or concrete. The limited ductility of these materials are allowed for by the effectiveness factor, ϑ, which is empirically determined and applied to the compressive strength of the

material. In this section, the equations governing the plastic method of analysis are summarised.

It is assumed that :

(i) the beam is in a state of plane stress ;

(ii) the reinforcement behaves in a rigid-perfectly plastic manner ;

(iii) the brickwork is rigid-perfectly plastic and obeys a modified Coulomb's failure surface in which the compressive strength is equal to ϑf_m and the tensile strength is zero.

The modified Coulomb failure criterion, developed for concrete, is shown in Fig 4.3.1. Experimental work done in the past by Page[51], in which a large number of brickwork panels were tested under biaxial compression at varying ratios of principal stresses and orientations to the bedjoint, infers that the failure surface is square, Fig 4.3.2, and not significantly affected by the angle of the bedjoint. This is why it is reasonable to apply the same yield locus, used by Nielsen and Braestrup[9], to brickwork.

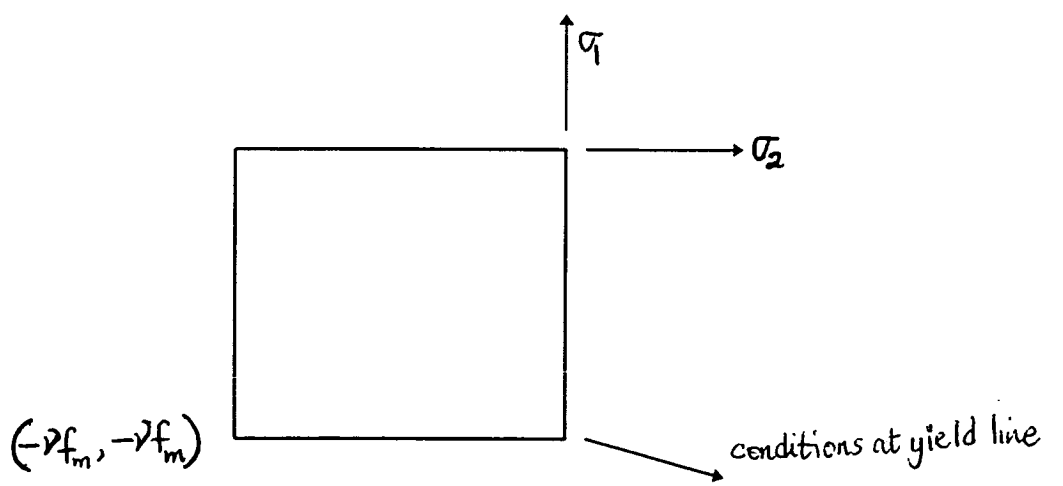

Fig 4.3.1 : Modified Coulomb Yield Criterion

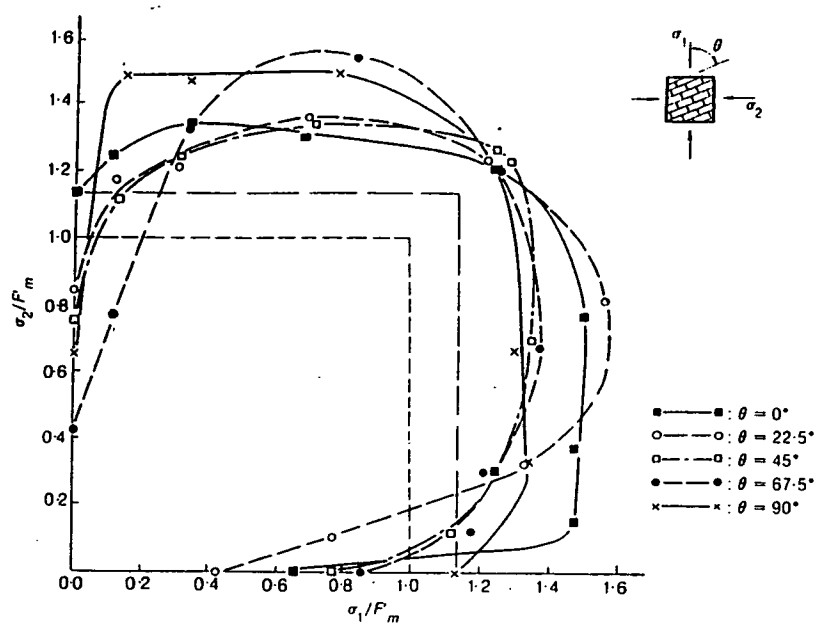

Fig 4.3.2 : Failure surface for brickwork in bi-axial compression (after Page[51])

4.3.2 Upper Bound Solution

The failure mechanism assumed by Nielsen and Braestrup[9] is shown in Fig 4.3.3. This consists of a yield line running from support to load point, separating two rigid parts of the beam. The relative displacement of the two parts, v, is inclined at an angle, α , to the yield line, which in turn is inclined at an angle, β , to the beam axis. The yield line, or more accurately, the yield surface is the area of deformation between the two rigid parts, (I) and (II) as shown in Fig 4.3.3. By consideration of the principal strains in this deforming zone and applying the normality condition[63], which states that the principal rates of strain are normal to the yield surface, it was shown that the only stress state which satisfies this condition corresponds to the corner of the yield surface shown in Fig 4.3.1

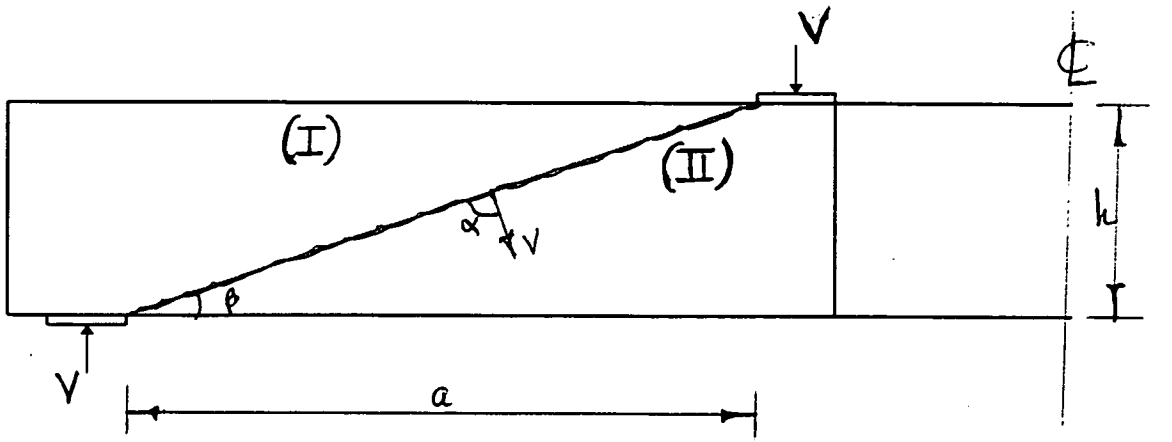

Fig 4.3.3 : Assumed Failure Mechanism for an Upper-Bound Solution

From these considerations, the following expressions for the rate of internal work dissipated per unit area of the yield line was derived :

$$W_1 = \frac{1}{2} v \vartheta f_m (1 - \sin\alpha) \qquad \text{---------- (4.3-1)}$$

where W_1 = rate of internal work dissipated per unit area of the yield line.

$$-\pi/2 \le \alpha \le \pi/2 \qquad \text{---------- (4.3-1(b))}$$

It is assumed that the steel yields in tension, that is,

$$\alpha + \beta \ge \frac{\pi}{2} \text{ or } \alpha \ge \frac{\pi}{2} - \beta \ . \qquad \text{---------- (4.3-1(c))}$$

The rate of internal work done by the failure mechanism is :

$$W_I = \frac{1}{2} v \vartheta f_m (1 - \sin\alpha)\left(b \frac{h}{\sin\beta}\right) - F_y v \cos(\alpha + \beta) \qquad \text{---------- (4.3-2)}$$

In deriving equation (4.3-2), the contribution of the web material was computed based on equation (4.3-1).

The rate of external work done is

$$W_E = Vv \sin(\alpha + \beta) \qquad \text{---------- (4.3-3)}$$

Furthermore, the average shear stress is defined as

$$\tau = \frac{V}{bh} \qquad \text{---------- (4.3-4)}$$

and the mechanical degree of reinforcement, Φ ,as :

$$\Phi = \frac{F_y}{bhf_m} \qquad \text{---------- (4.3-5)}$$

where F_y is the force in steel at yielding. Applying the work equation $W_E = W_I$ and substituting equations (4.3-4) and (4.3-5) into equation (4.3-2) yields the upper bound for the ultimate shear stress :

$$\left(\frac{\tau}{f_m}\right) = \frac{\vartheta(1-\sin\alpha) - 2\Phi\sin\beta\cos(\alpha+\beta)}{2\sin\beta\sin(\alpha+\beta)} \qquad \text{---------- (4.3-6)}$$

which becomes

$$\left(\frac{\tau}{f_m}\right) = \frac{\vartheta - \vartheta\cos\beta\sin(\alpha+\beta) + (\vartheta - 2\Phi)\sin\beta\cos(\alpha+\beta)}{2\sin\beta\sin(\alpha+\beta)} \qquad \text{---------- (4.3-7)}$$

The lowest upper bound is determined by minimising equation (4.3-7) with respect to the variable α , which yields :

$$\frac{d\tau}{d\alpha} = 0 \text{ at } \vartheta\cos(\alpha+\beta) = -(\vartheta - 2\Phi)\sin\beta \qquad \text{---------- (4.3-8)}$$

By putting equation (4.3-8) into equation (4.3-7), it was found that the minimum is given by equation (4.3-9) :

$$\left(\frac{\tau}{f_m}\right) = \frac{1}{2}\left(\sqrt{\vartheta^2\cot^2\beta + 4\Phi(\vartheta - \Phi)} - \vartheta\cot\beta\right) \qquad \text{---------- (4.3-9)}$$

and with $\cot\beta = \frac{a}{h}$, the lowest upper bound is :

$$\left(\frac{\tau}{f_m}\right) = \frac{\vartheta}{2}\left(\sqrt{\left(\frac{a}{h}\right)^2 + \frac{4\Phi(\vartheta - \Phi)}{\vartheta^2}} - \frac{a}{h}\right) \qquad \text{---------- (4.3-10)}$$

The limit on the degree of steel arises from the condition given by equation (4.3-1(c)) by virtue of equation (4.3-8). Whenever $\Phi > \frac{\vartheta}{2}$, the minimum is obtained with $(\alpha+\beta) < \frac{\pi}{2}$ and, in such a case, equation (4.3-2) is invalidated as this means that the steel is no longer in tension.

If the reinforcement is sufficiently strong, such that $\Phi > \frac{\vartheta}{2}$ then from equation (4.3-8), equation (4.3-10) does not apply. In other words, as Φ increases, the angle $(\alpha + \beta)$ decreases as seen in equation (4.3-8). When $\Phi > \frac{\vartheta}{2}$, $(\alpha + \beta) < \frac{\pi}{2}$; the steel does not yield. It was furthermore shown[9] that when $(\alpha + \beta) \leq \frac{\pi}{2}$ the lowest upper bound is obtained when $(\alpha + \beta) = \frac{\pi}{2}$.

Putting the condition $(\alpha + \beta) = \frac{\pi}{2}$ into equation (4.3-7), it was found that :

$$\left(\frac{\tau}{f_m}\right) = \frac{\vartheta}{2}\sqrt{\left(\frac{a}{h}\right)^2 + 1} - \left(\frac{a}{h}\right) \qquad \text{---------- (4.3-11)}$$

Equation (4.3-11) is also obtained if $\Phi = \frac{\vartheta}{2}$ is put into equation (4.3-10).

4.3.3 Lower Bound Solution

The stress distribution in Fig 4.3.4 is assumed. The compressive force is transmitted via a brickwork strut running from the load point to support. This distribution is similar to a "tied arch" and it is assumed that the reinforcement is bonded only at the support. The regions of the beam immediately above and below the support and load points are assumed to be in a state of biaxial compression of depth *y*.

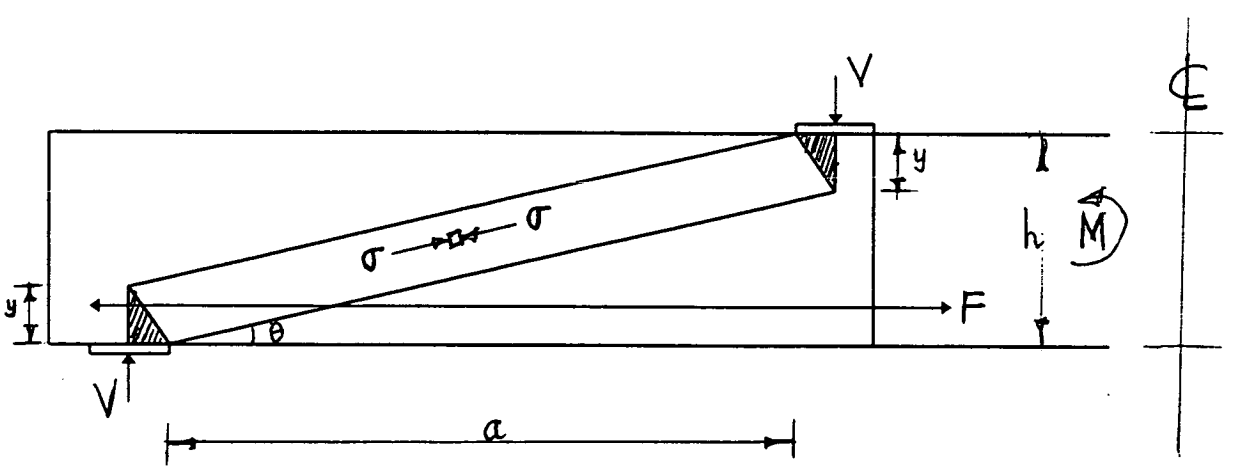

Fig 4.3.4 : Stress Distribution in the Shear Span Subject to Concentrated Loading (Lower Bound Solution)

At the support this implies a small moment which is ignored in the analysis. From Fig 4.3.4, the strut inclination is determined by the following geometrical relation :

$$h - y = (a + y\tan\theta)\tan\theta \qquad \text{----------(4.3-12)}$$

This equation gives a quadratic in **tan**θ , the relevant solution of which is given in equation (4.3-13)

$$\tan\theta = \frac{1}{2y}\left(\sqrt{a^2 + 4y(h-y)} - a\right) \qquad \text{----------(4.3-13)}$$

By considering equilibrium of horizontal forces, the depth y may be obtained. F is the force in the longitudinal reinforcement :

$$by\sigma = F$$

Therefore, $y = \dfrac{F}{b\sigma}$ ----------(4.3-14)

Considering equilibrium of vertical forces, the load V, corresponding to the stress distribution is found :

$$V = \sigma by\tan\theta = \frac{1}{2}b\sigma\left(\sqrt{a^2 + 4y(h-y)} - a\right) \qquad \text{----------(4.3-15)}$$

Putting equation (4.3-14) into (4.3-15) results in equation (4.3-16), which gives the lower bound :

$$V = \frac{1}{2}\left(\sqrt{a^2b^2\sigma^2 + 4F(hb\sigma - F)} - ab\sigma\right) \qquad \text{----------(4.3-16)}$$

Differentiating equation (4.3-16) with respect to the static variables σ and F, it was found that $\dfrac{dV}{d\sigma}$ is always greater than zero and also that

$$\frac{dV}{dF} > 0 \text{ for } F < \frac{1}{2}hb\sigma \text{ and } \frac{dV}{dF} < 0 \text{ for } F > \frac{1}{2}hb\sigma \qquad \text{----------(4.3-17)}$$

The maximum lower bound is obtained when σ is a maximum, that is $\sigma = \vartheta f_m$

When $F < \dfrac{1}{2}hb\vartheta f_m$, the steel is yielding and F is determined from the maximum force in the reinforcement : That is,

$$F = \Phi bhf_m \qquad \text{----------(4.3-18)}$$

If $F > \frac{1}{2} bh\vartheta f_m$, the maximum force in the steel is governed by the brickwork and the maximum lower bound is found with : $F = \frac{1}{2} bh\vartheta f_m$ ----------(4.3-19)

Putting equations (4.3-18) and (4.3-19) into equation (4.3-16), two separate expressions are obtained for $\left(\frac{\tau}{f_m}\right)$ as follows :

$$\left(\frac{\tau}{f_m}\right) = \frac{\vartheta}{2}\left\{\sqrt{\left(\frac{a}{h}\right)^2 + \frac{4\Phi(\vartheta - \Phi)}{\vartheta^2}} - \left(\frac{a}{h}\right)\right\} \text{ valid for } \Phi \le \frac{\vartheta}{2} \quad \text{---------- (4.3-20)}$$

$$\left(\frac{\tau}{f_m}\right) = \frac{\vartheta}{2}\left\{\sqrt{\left(\frac{a}{h}\right)^2 + 1} - \left(\frac{a}{h}\right)\right\} \text{ valid for } \Phi \ge \frac{\vartheta}{2} \quad \text{----------(4.3-21)}$$

These two preceding expressions are identical to those two expressions obtained from the upper bound solutions given by equations (4.3-10) and (4.3-11). The method therefore asserts that the exact plastic solution to the problem has been found.

4.3.4 The effectiveness factor ϑ

To be able to use this method of prediction, the effectiveness factor has to be evaluated first. This parameter is dependent on the outcome of the shear strength test results and gives a measure of the ductility of the concrete or brickwork. In concrete, an average effectiveness factor of 0.455 has been reported[9] for beams failing in shear.

The successful application of this method to reinforced brickwork requires the correct evaluation of the effectiveness factor. In the experiment it was observed that shear cracks were always extensions of flexural cracks, hence the effectiveness factor must be influenced by the flexural strength of the brickwork. In addition, in some cases the shear and flexural failure happened almost simultaneously, hence the upper limit of the shear failure is influenced by the compressive strength. It was, therefore, felt that these two properties of masonry will have significant effect on the effectiveness factor. In statistical terms, the effectiveness factor can be expressed as a function of :

$$\vartheta = \Psi f_m^a f_t^b \qquad \text{---------- (4.3-22)}$$

where Ψ, a and b are constants to be determined.

This will make the plastic method much more acceptable and less dependent on specific experimental findings. A way of doing this would be to analyse several experimental results of similar categories and extract an overall average value, much like a global average effectiveness factor for that category, which would later be used in analysing different results of shear tests carried out on sections falling strictly within that category. This will then drive the method away from its current rigid, semi-empirical form.

All previous shear test[7,11,13,23,24,27,33,40,45,58] results on reinforced and prestressed brickwork were analysed by performing a regression analysis. The analysis gave the following expressions, with 73 % and 80 % correlation coefficients for reinforced and prestressed brickwork respectively :

$$\vartheta = \frac{0.41 f_t^{0.29}}{f_m^{0.08}} \quad \text{(reinforced brickwork)} \qquad \text{---------- (4.3-23)}$$

$$\vartheta = \frac{1.41 f_t^{0.10}}{f_m^{0.41}} \quad \text{(prestressed brickwork)} \qquad \text{---------- (4.3-24)}$$

On close examination of the two expressions it can be seen that the compressive strength of masonry becomes the dominant factor for prestressed brickwork with the increasing tensile strength. The effectiveness factor for the present test was obtained substituting the known values of flexural tensile and compressive strength. The value of the effectiveness factor was used in equation 4.3-20 or 4.3-21 to predict the shear strength of the pocket-type reinforced walls tested in the present work. These results are given later in Table 4.5.2.

The variation of effectiveness factor with tensile and compressive strength considered in this analysis are given in Appendix (I). In this appendix, Nos 1-82 are reinforced

brickwork sections with no prestress applied to them. Nos 83-116 are prestressed brickwork sections.

4.3.5 Load deflection response of pocket-type reinforced beams

4.3.5.1 Introduction

Deflection measurements of these beams were carried out to examine the deflections accompanying failure in shear. Measurements of deflection are needed so as to know if the full cross-section is mobilized to resist the applied load up to the point of failure in shear.

Deflection measurements and prediction is important for serviceability limit state calculations. In serviceability terms, limits may be placed on the value of deflection permitted such that the structure does not become unserviceable. If, for example, cracking is not permitted in these members, the calculation of deflection becomes a straightforward process, following standard procedures in which either tangent or secant modulus of elasticity of the brickwork material is used. However, when cracks are allowed to occur, calculation of deflection becomes much more involving because, at a cracked section, the stiffness properties of the section change such that stresses in the brickwork increase more rapidly. Noting that the basic behaviour of brickwork itself is non-linear, the non-linearity due to cracking makes the calculation of deflections slightly complicated.

For these reasons, various techniques[30,35] have been proposed for the calculation of deflection in brickwork members, and these techniques have tried to incorporate the loss of material stiffness in different ways, thus producing different levels of accuracy that depend on the method adopted. It is also noted that a basic prerequisite to any deflection calculation is the Moment-Curvature relationship.

4.3.5.2 Theoretical Methods Used For The Calculation of Deflections

Only two methods are described here. A crucial step in the theoretical calculation of deflection is the determination of the moment-curvature M-ϕ relationship. This relationship also provides useful information on the ductility of the member.

In the case of simple bending of a beam, the following relationship holds between the moment M and the curvature ϕ :

$$\phi = M/EI \qquad \text{----------} \qquad (4.3\text{-}25)$$

where E = Young's Modulus of Elasticity.

I = Second Moment of Area.

For the calculation of deflection, one needs to know the distribution of bending moment along a member. With this knowledge, the curvature at any section can be extracted from the equation given above. The deflection y, is then obtained from the differential equation :

$$\phi = -d^2y/dx^2 \qquad \text{----------} \qquad (4.3\text{-}26)$$

where

x = distance along the beam

Brickwork has low flexural tensile strength and therefore cracks at very low applied load in flexure. Whenever cracking occurs, the second moment of area, I , changes. The Young's modulus of elasticity also varies with stress level. This situation has led to different methods for calculating the curvature in bending and consequently, the deflection of their members. The differences inherent in these methods has to do with the way the varying nature of the flexural rigidity, EI , is accounted for. The two methods are :

(1) The second moment of area method

(2) The direct method

4.3.5.3 The Second Moment of Area Method

In this method, the section is assumed to behave in an elastic manner. A bi-linear or tri-linear relationship is then obtained between the moment and curvature. Up to the point of cracking, the second moment of area is based on an uncracked section analysis. This quantity is calculated either by using the gross or transformed section. The transformed section accounts for the presence of the reinforcement. Beyond the point of cracking, the second moment of area is obtained from the area of brickwork in compression and the transformed area of steel. For under-reinforced sections, this method also calculates the second moment of area at a third stage which corresponds to the yielding of the tensile reinforcement. At each of these different stages of member structural behaviour, a value of the elastic modulus is chosen to reflect the level of stress in the beam.

The effective moment of inertia is calculated by using methods close to that originally proposed by Branson[37] for reinforced concrete beams.

$$I_{effective} = \left(\frac{M_{cr}}{M}\right)^{m} I_u + \left[1 - \left(\frac{M_{cr}}{M}\right)^{m}\right] I_{cr} \qquad \text{----------} \qquad (4.3\text{-}27)$$

where

$I_{effective}$ = effective second moment of area.

I_u = second moment of area of transformed uncracked section.

I_{cr} = cracked transformed second moment of area.

M_{cr} = cracking moment.

M = the applied moment.

m = an index. The value of m =3 has been found to give reasonably good results.

The Moment-Curvature relationship is often idealized as a bi-linear curve. Each part of this relationship is based on cracked and uncracked second moments of area.[35]. However, due to the fact that the transition between these stages is smoother than would be indicated by the bi-linear idealization, results based on this model tend to overestimate the deflections. This is due to the well-known tension stiffening effect. This "extra" stiffness due to tension stiffening is incorporated in different ways for

calculating deflections, i.e. by multiplying the deflection itself by a reduction factor or by using an effective second moment of area which is greater than that based on the cracked second moment of area. Methods of this type generally require information from experimental work on beams[7,13,38].

Some limitations of this method are as follows :

-- The non-linear behaviour of brickwork is not taken into account.

-- The elastic modulus varies continually with stress level.

4.3.5.4 The Direct Method

The direct method uses the actual stress-strain relationship of the brickwork as well as that of the tensile reinforcement. This, therefore, eliminates most of the limitations associated with the moment of inertia method. However, the beams are also considered to be elastic up to the point of cracking and the curvature is obtained from equation (4.3-25).

After cracking, the curvature is obtained by applying increments of compressive strain to the extreme compression fiber. Assuming a cracked section, the tensile strain required for the equilibrium of the internal forces is obtained. Using the strain profile, the curvature is determined. For any loading, the distribution of curvature along the beam is obtained from the computed moment-curvature relationship. To obtain the average curvature using this method, tension stiffening is accounted for. Finally, the deflection is obtained from double integration along the span.

Pedreschi[7] applied the direct method to prestressed brickwork beams by incorporating the stress-strain relationship for brickwork from prestressing to failure. This procedure was further improved by Walker[13] who accounted for the properties of the composite section. It has also been used successfully by Uduehi[11] to predict the load-deflection relationship for prestressed brickwork and concrete beams which failed in flexure.

As mentioned above, the deflection is evaluated from the M-ϕ relationship. The relationship between the curvature ϕ and the deflection y along the span of the beam is given by equation (4.3-26).

Since the analytical solution of this equation is not possible, the numerical finite difference method was used to obtain the deflection. The finite difference method is an approximate method for solving differential equations and this method of numerical integration is only applicable to problems in which the values of the independent variable is known. In this situation, the independent variable is the curvature, ϕ. The aim is to find the values of the dependent variable, y, by first of all converting the problem to that of solving a set of linear simultaneous equations. A knowledge of the shape and magnitude of the bending moment diagram is required to determine the curvature, ϕ.

4.3.5.5 Predicting Deflections By the Direct Method

Since the direct method has been successfully used to predict the deflection of both fully- and partially- prestressed brickwork beams, it is assumed that it would equally predict the deflection of pocket-reinforced beams tested by the author.

Results obtained on the basis of the first method as well as all the experimental deflection measurements are compared with those based on this method. These are given in Fig 4.5-39 to Fig 4.5-42.

4.4 TEST ARRANGEMENT

The arrangement for testing the beam as well as the various measurements carried out during the test are described in this section.

The beams were tested under two point loading in a specially-designed rig which provided pin and roller supports. The typical test beam was placed on the supports which were previously positioned at the correct span (compare Figs, 4.4.1, 4.4.2 and 4.4.3). The load was applied to the beam by means of two hydraulic jacks attached by a single feed to a hydraulic pump.

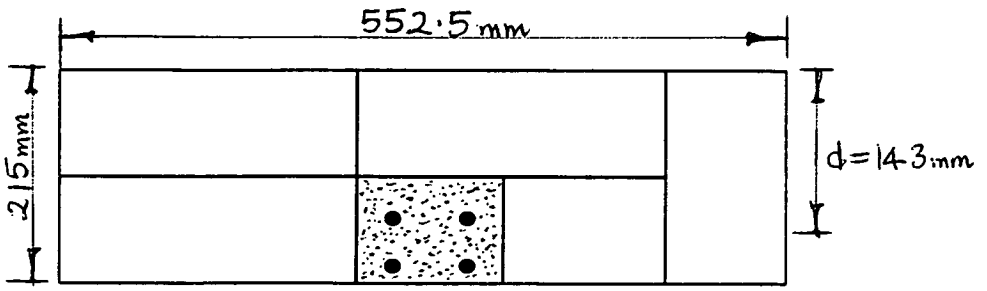

Fig 4.4.1 : Cross-section of the pocket-type reinforced brickwork beam (B1-B4)

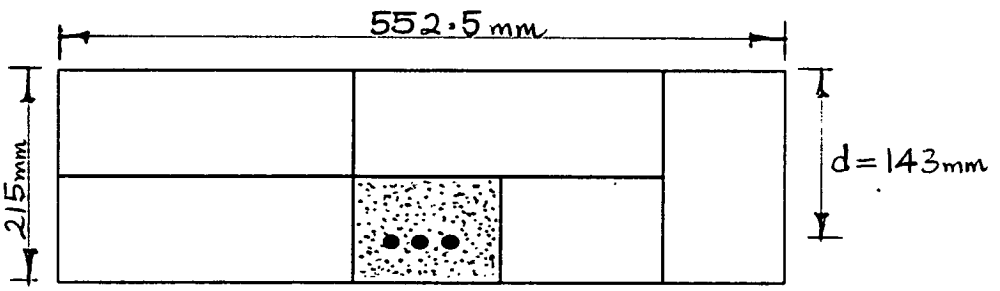

Fig 4.4.2 : Cross-section of the pocket-type reinforced brickwork beam (B5-B8)

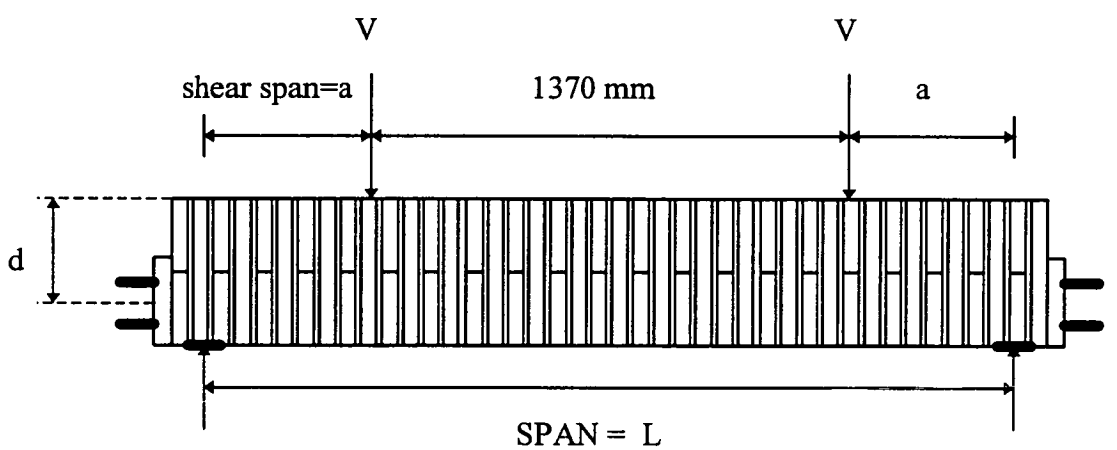

Fig 4.4.3 : Test set-up for pocket-type reinforced brickwork beam

4.4.1 Test Procedure

The minimum age of the beams at the time of test was 28 days. This age allowed 21 days before placing the longitudinal reinforcements and a further 7 days curing after grouting. Before placing the beam in the testing rig, the self weight was taken by a load cell attached to the lifting crane and connected to a digital voltmeter which recorded the weight in millivolts. The cross heads and the jacks of the rig were removed and the beam was lifted onto its supports. The cross heads and the jacks were then replaced. The ends of the beam were jacked off the supports and bearing plates placed onto the supports. The beam was then very carefully bedded onto the plates using a rich mortar mix. Steel bearing plates were also bedded on top of the beam beneath the jacks. Before applying any load to the beam, initial readings were taken from the dial gauges, strain gauges and load cells. The load was thereafter applied slowly in small increments. For most of these beams, failure occurred after about 10-12 increments. At every increment, the load was held constant while deflection and strain measurements were taken. As the failure point was reached, the loading increment was reduced and strain and deflection measurements were taken as close as possible to the ultimate load.

4.4.2 Measurement of Strain in Brickwork and Steel

Strains were measured on the faces of the brickwork beams using demountable "demec" gauges having gauge lengths of 200 and 305 mm. Measurements were taken in the constant moment zone of the beams at various depths using 200 mm gauge length as shown in Fig 4.4.2-1. The strains were measured on both faces at a particular depth thereby obtaining the average strain across the section. More points were located at the top parts of the beam surface to enable the migration of the neutral axis to be determined and help in the calculation of experimental curvatures of these beams. Longitudinal strain measurements were also taken at the top surface of the beams in the maximum bending moment regions at points located as shown in Fig 4.4.2-2. Similarly, points were located centrally within the shear span zones to measure the longitudinal strains occurring in these zones.

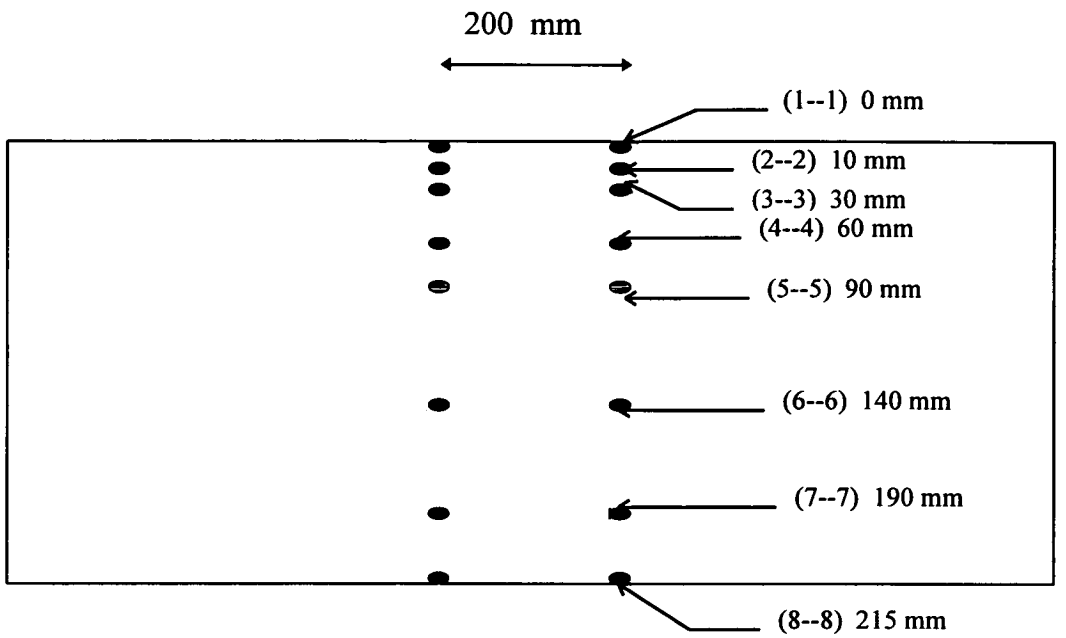

Fig 4.4.2-1 : Showing the position of the demec points along the depth of the beam in the constant bending moment zone

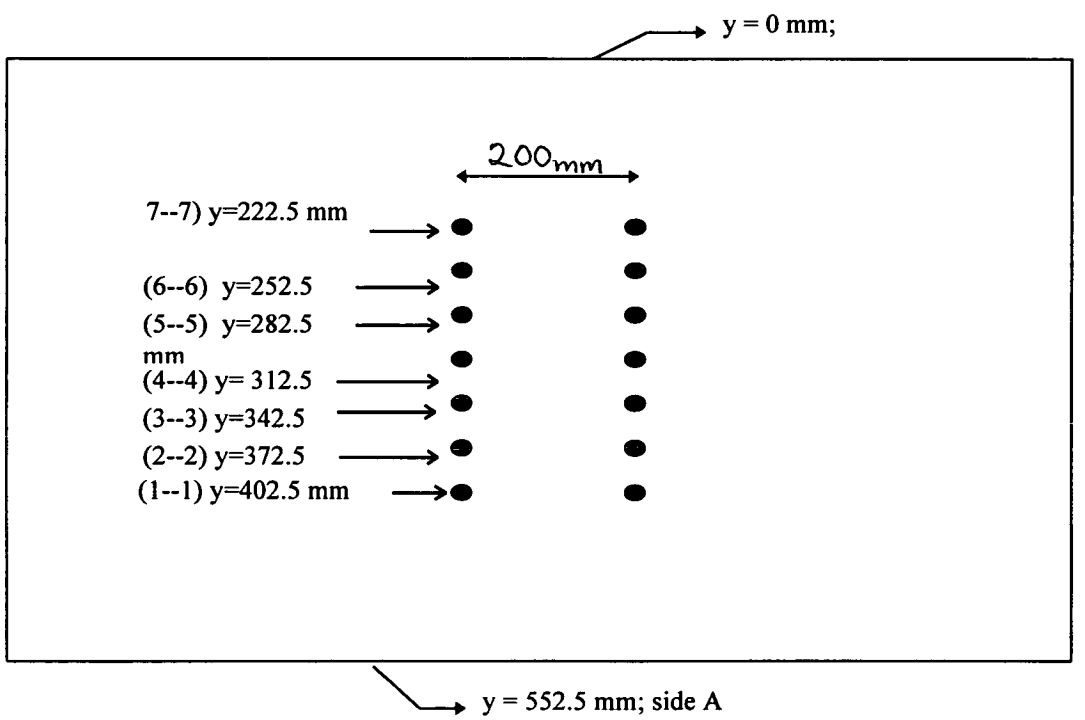

Fig 4.4.2-2 : Showing the position of the demec points along the width of the beam in the constant bending moment zone.

Attempts to measure the corresponding transverse strains at these locations in order to determine the tension developing there were not successful because the strain gauges were not sensitive enough to measure the order of strains developing prior to failure of these beams.

Strains were measured on the steel reinforcement using electrical resistance strain gauges. The strain gauge was attached to a well prepared and smoothened surface of the steel reinforcement. In order to achieve proper bonding, an epoxy resin was used to stick the electrical resistance strain gauge to the surface within the gauge length appropriate to the diameter of the steel reinforcement. After the gauge is cured in the laboratory for about one day, it is carefully protected by a nylon tape from the abrasive forces normally induced by the subsequent grouting operation. For every beam tested, initial readings were taken of all strain gauges before the external load was applied. For a given applied load, therefore, the actual strain is obtained by subtracting this initial reading.

4.4.3 Measurement of Deflection

The deflections of the beams were measured using mechanical dial gauges. The deflections were measured at midspan and at the two supports in all the beams. The support measurements were necessary in order to check if any support settlement occurred and these were accounted for in the determination of the actual midspan deflections of these beams. Dial gauges reading to 0.01 mm were used for these midspan deflection measurements whereas gauges reading to 0.002 mm were used to record support settlements.

4.4.4 Load Measurements

The applied load to the beam was measured at the jacking point using 200 kN load cells. The power supply to the load cells was from a 10 volt power supply and the measurements taken by each load cell was monitored by a digital voltmeter. The load cells used in the test arrangement had been calibrated previously in a compression testing machine using the same voltmeter and power supply as in the beam tests.

4.5 EXPERIMENTAL RESULTS

4.5.1 Summary of experimental results :

The summary of experimental results is given in Table 4.5.1.

Table 4.5-1 : Experimental Results

Beam No	Length (mm)	Span (mm)	Shear Span, a (mm)	a/d ratio	% steel	Self Weight (kN/m)	Ultimate Load, V (kN)	Ultimate Average shear stress (N/mm^2)
B1	2105	1960	293	2.05	1.59	2.76	146.46	1.86
B2	2090	1960	292	2.04	1.59	2.71	171.57	2.18
B3	2480	2310	468	3.27	1.59	2.69	88.44	1.14
B4	2495	2325	475	3.32	1.59	2.65	84.33	1.08
B5	2435	2325	475	3.32	0.61	2.59	76.33	0.98
B6	2495	2310	468	3.27	0.61	2.62	63.22	0.82
B7	3245	3115	870	6.08	1.64	2.67	46.88	0.62
B8	3245	3115	870	6.08	1.64	2.67	45.67	0.61

4.5.1.1 Discussions of Experimental Results : The experimental results are discussed in this section.

4.5.1.2 Brickwork strain

The relationships between the moment and top fibre strain for all the beams are shown in Fig. 4.5-1 to Fig 4.5-8. In beams B1 & B2 and B3 & B4(Figs.4.5-1 to 4.5-4), the curves remained approximately linear prior to ultimate failure. The compressive strain at the time of the beam failure was much lower than the ultimate strain as obtained from prism tests.

In beams B5 and B6 (Figs 4.5-5 & 4.5-6), the curves show a continuous increase up to the failure point. Except for beam 5, the relationship between moment and strain remains linear and the magnitude is much lower than the ultimate strain. These results confirm that the failure of beams was due to shear not in flexure. This trend also holds true for the strains within the shear spans, that is sides A1 and A2 respectively, recording much smaller maximum brickwork strains in comparison, as would be expected.

For beams B7 and B8 (Figs. 4.5-7 & 4.5-8), the growth of top brickwork strains in these beams could be approximated by linear curves. Again, the brickwork in the compression zone was underutilized.

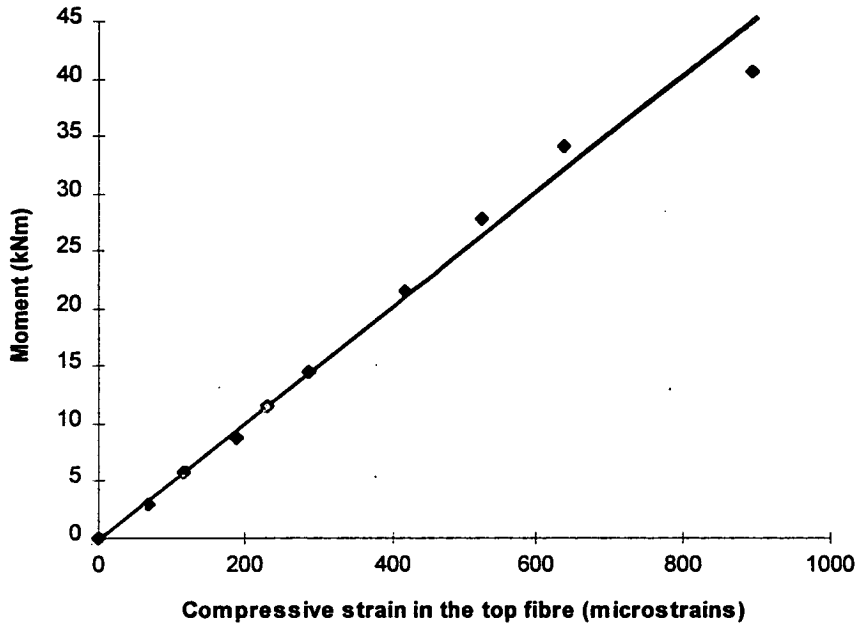

Fig 4.5-1 : Relationship between moment and the average top fibre strain in brickwork (Beam 1)

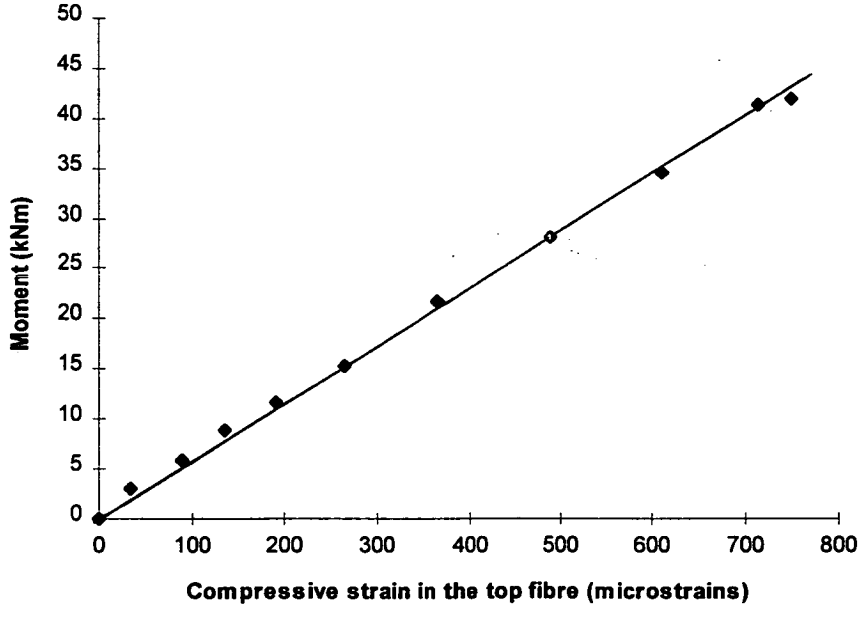

Fig 4.5-2 : Relationship between moment and the average top fibre strain in brickwork (Beam 2)

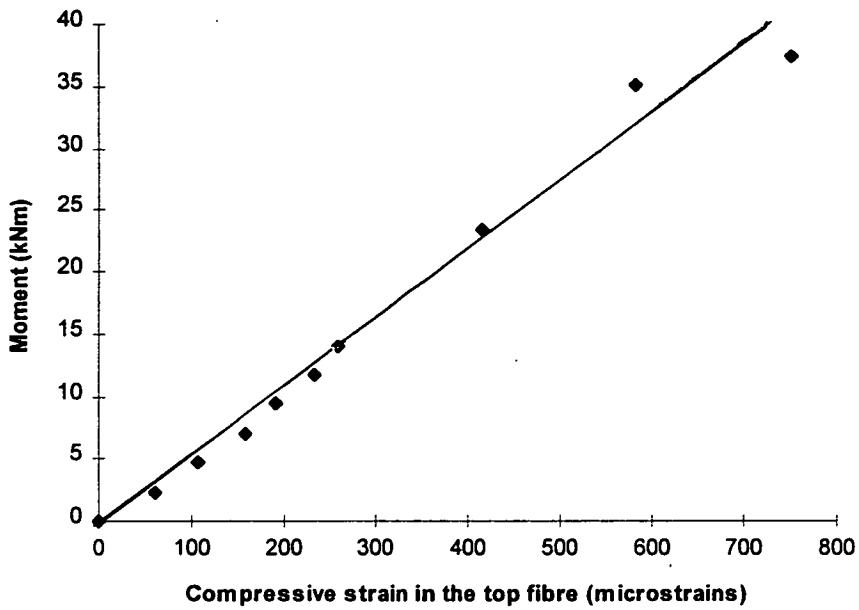

Fig 4.5-3 : Relationship between moment and the average top fibre strain in brickwork (Beam 3)

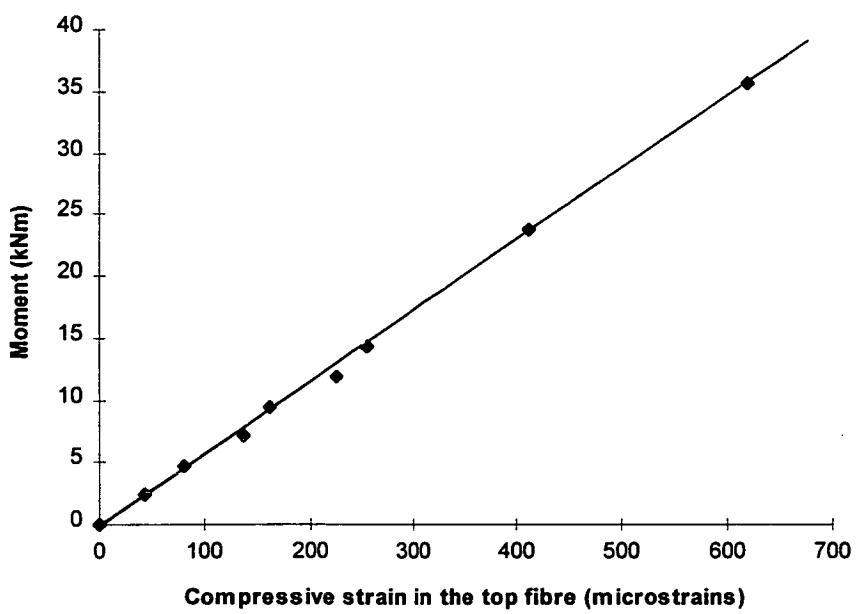

Fig 4.5-4 : Relationship between moment and the average top fibre strain in brickwork (Beam 4)

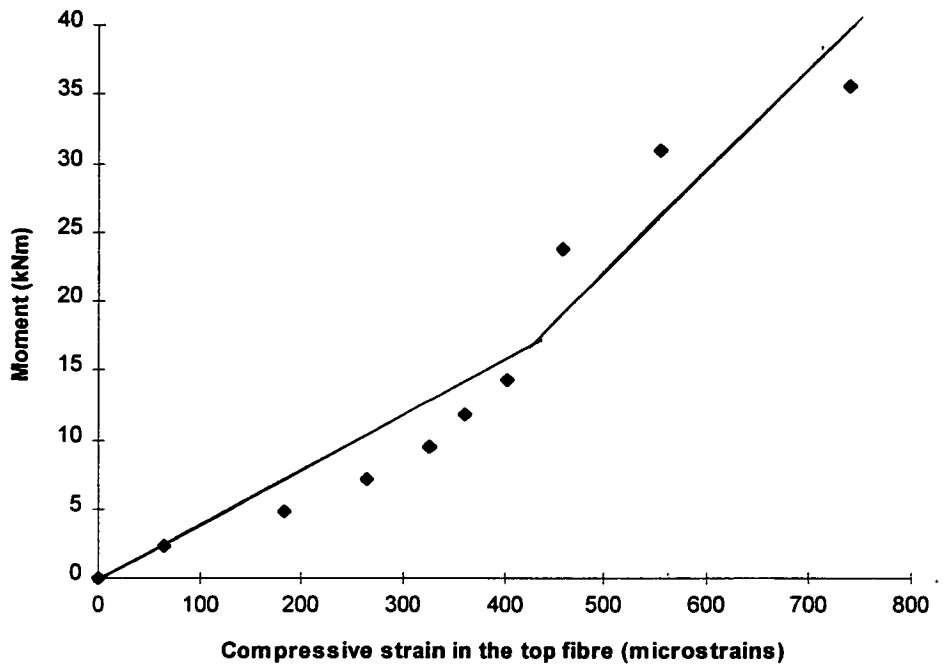

Fig 4.5-5 : Relationship between moment and the average top fibre strain in brickwork (Beam 5)

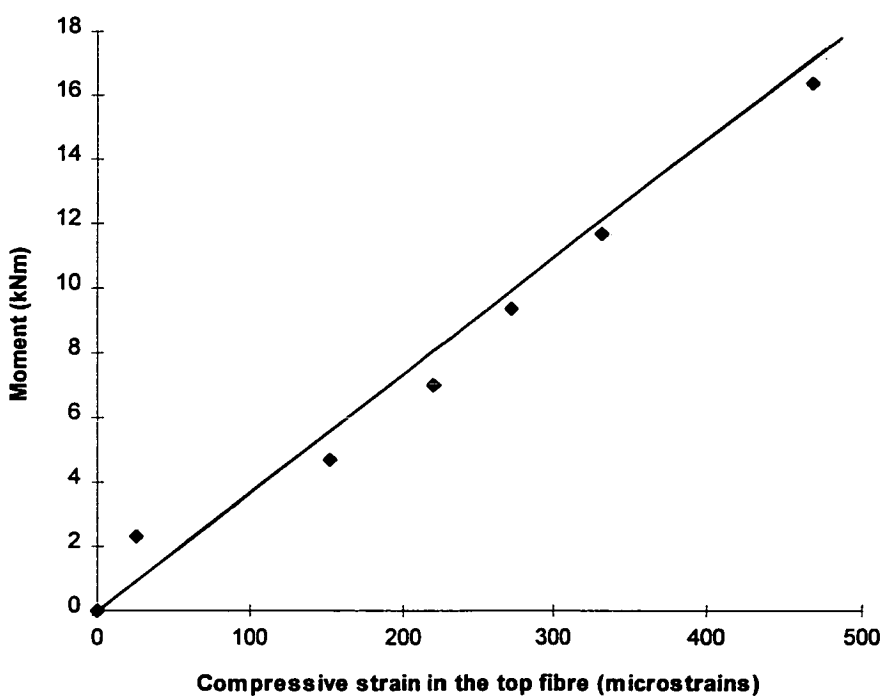

Fig 4.5-6 : Relationship between moment and the average top fibre strain in brickwork (Beam 6)

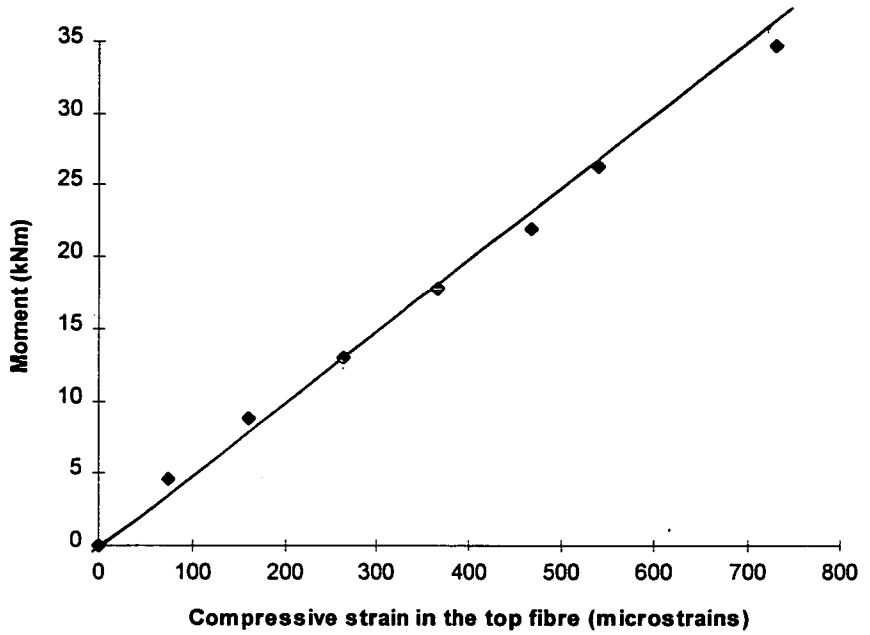

Fig 4.5-7 : Relationship between moment and the average top fibre strain in brickwork (Beam 7)

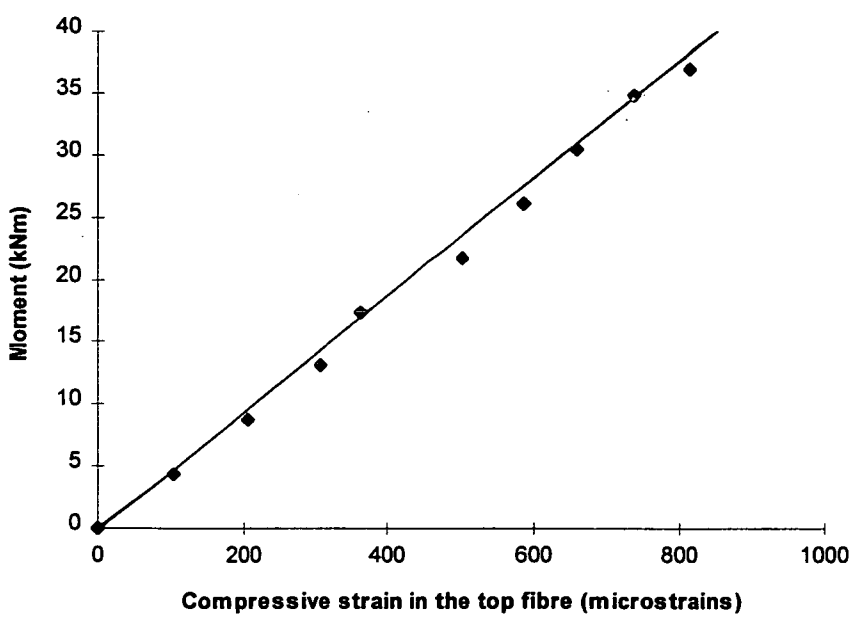

Fig 4.5-8 : Relationship between moment and the average top fibre strain in brickwork (Beam 8)

4.5.1.3 Variation of brickwork strain through the depth

The variations of strain through the depth of the section for all the beams are given in Figs. 4.5-9 to 4.5-19. As is seen from these set of curves, the strain distribution within the constant bending moment regions of the beams remained linear just prior to ultimate collapse. This confirms the theoretical prediction that a straight line relationship exists between the strain and depth of the beam, thus validating the classical assumption that "plane cross-sections remain plane before and after bending of the beams". Another major feature of these results is that the neutral axis depths for beams B5 and B6 (Figs 4.5-13 and 4.5-16) are smaller than those of the other beams having a higher degree of longitudinal steel.

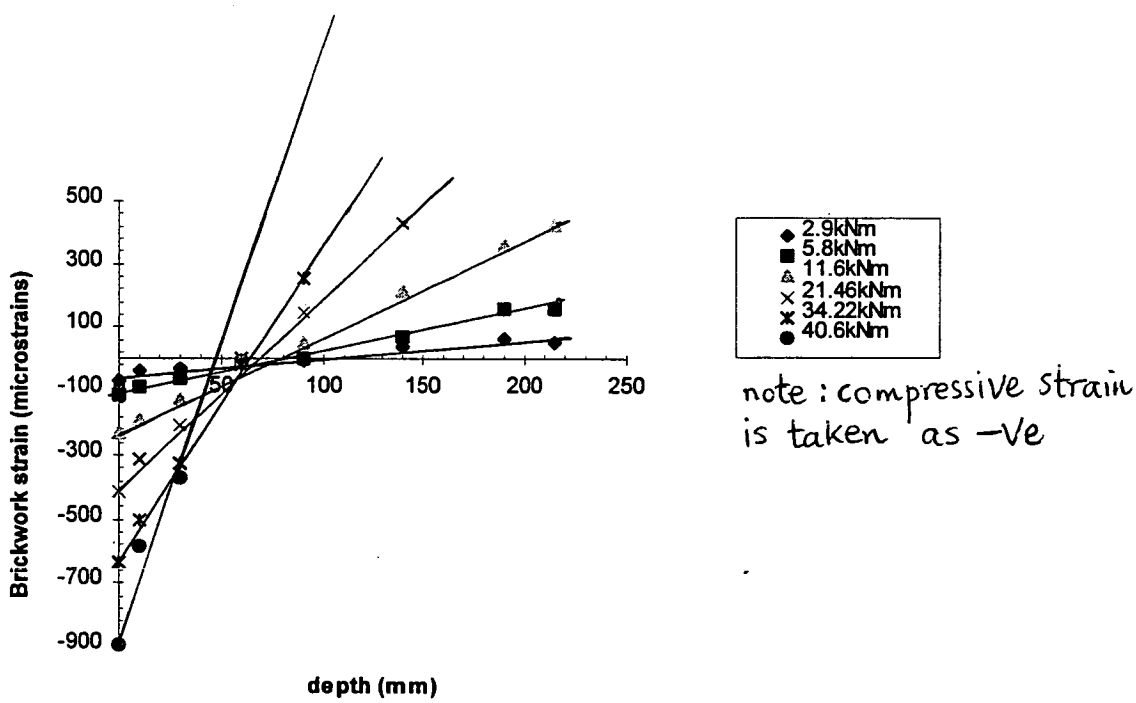

Fig 4.5-9 : Variation of average brickwork strain with depth (Beam 1)

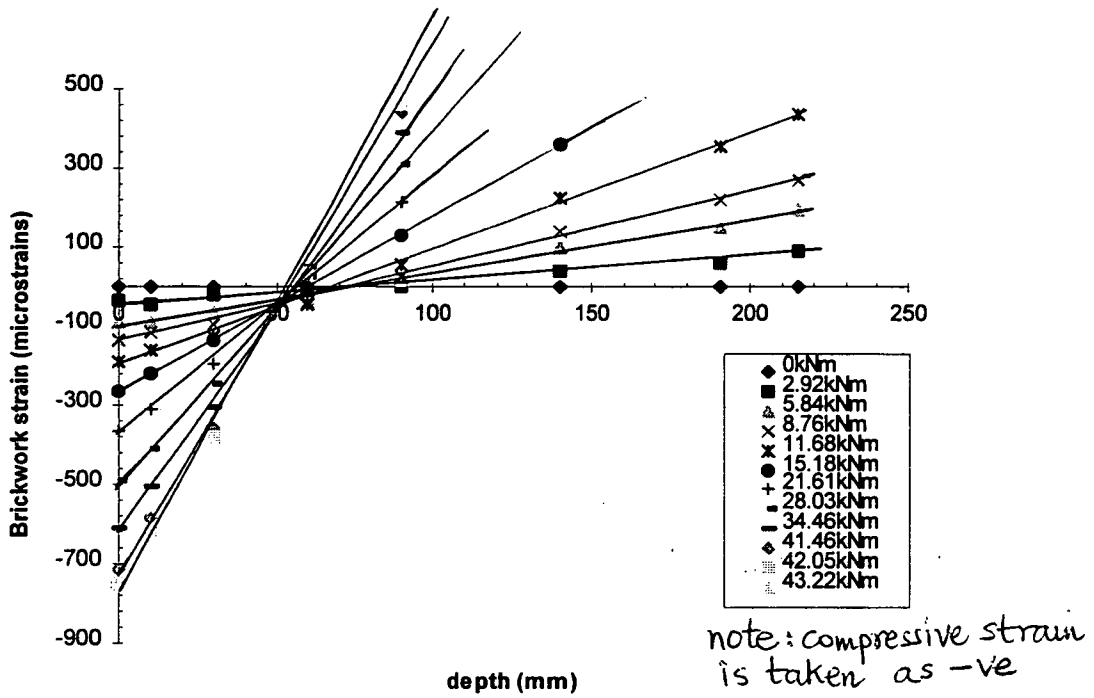

Fig 4.5-10 : Variation of average brickwork strain with depth (Beam 2)

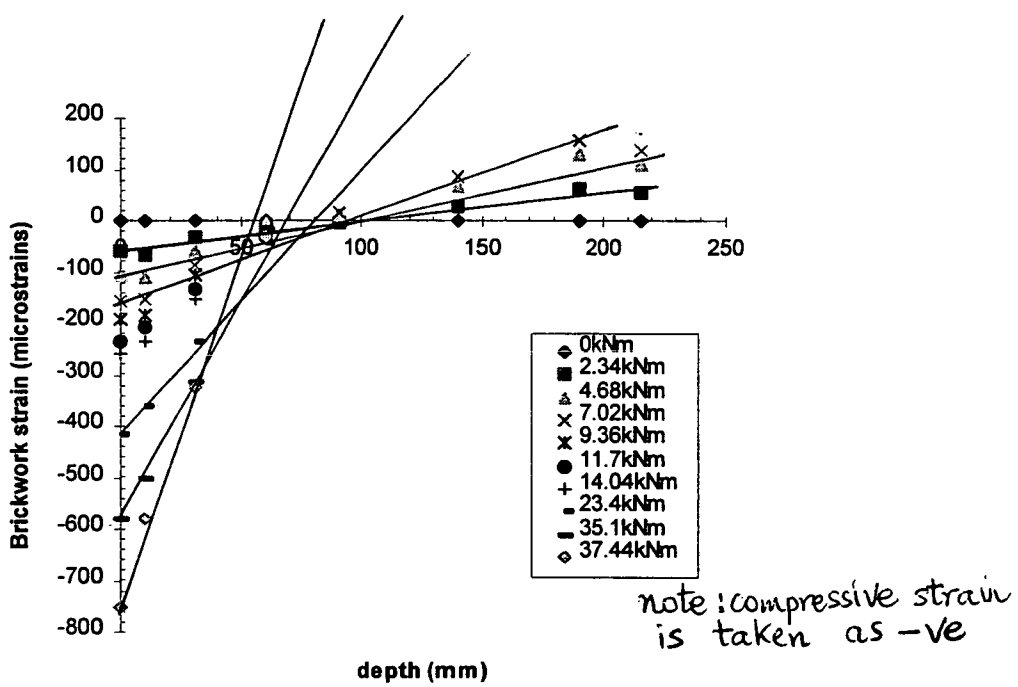

Fig 4.5-11 : Variation of average brickwork strain with depth (Beam 3)

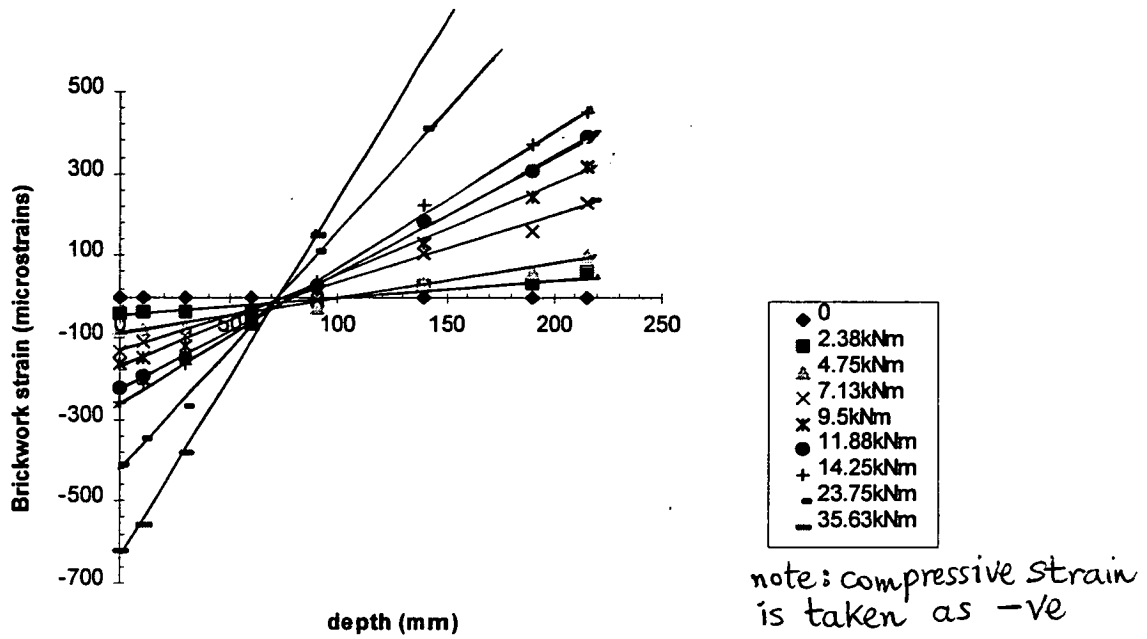

Fig 4.5-12 : Variation of average brickwork strain with depth (Beam 4)

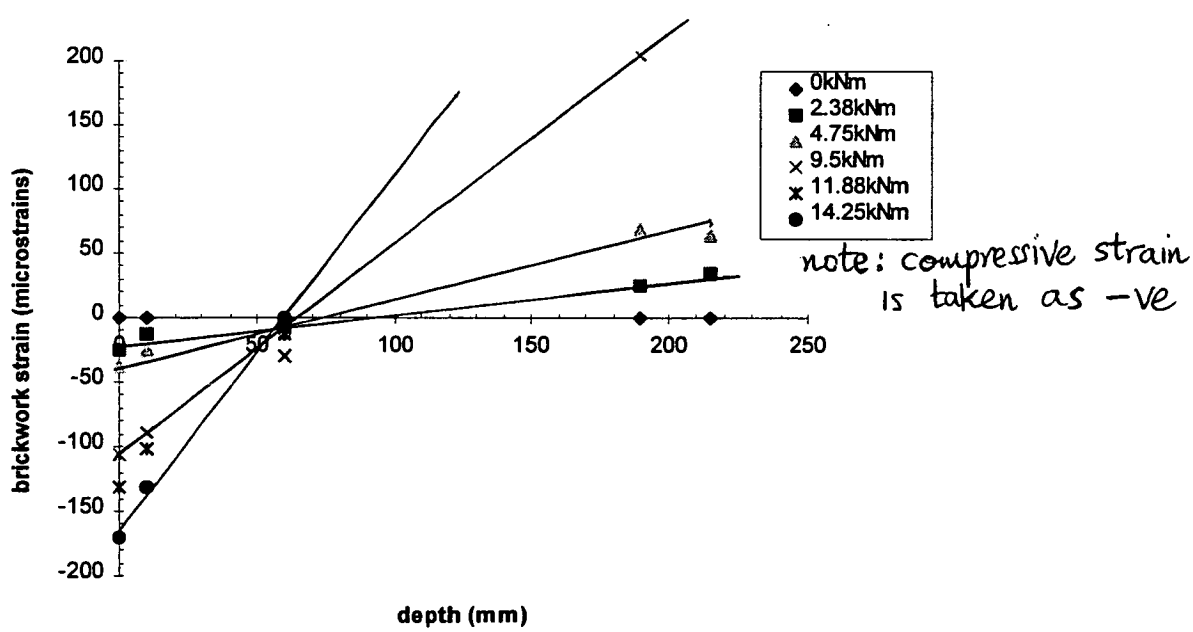

Fig 4.5-13 : Variation of average brickwork strain with depth (Beam 4)-left shear span

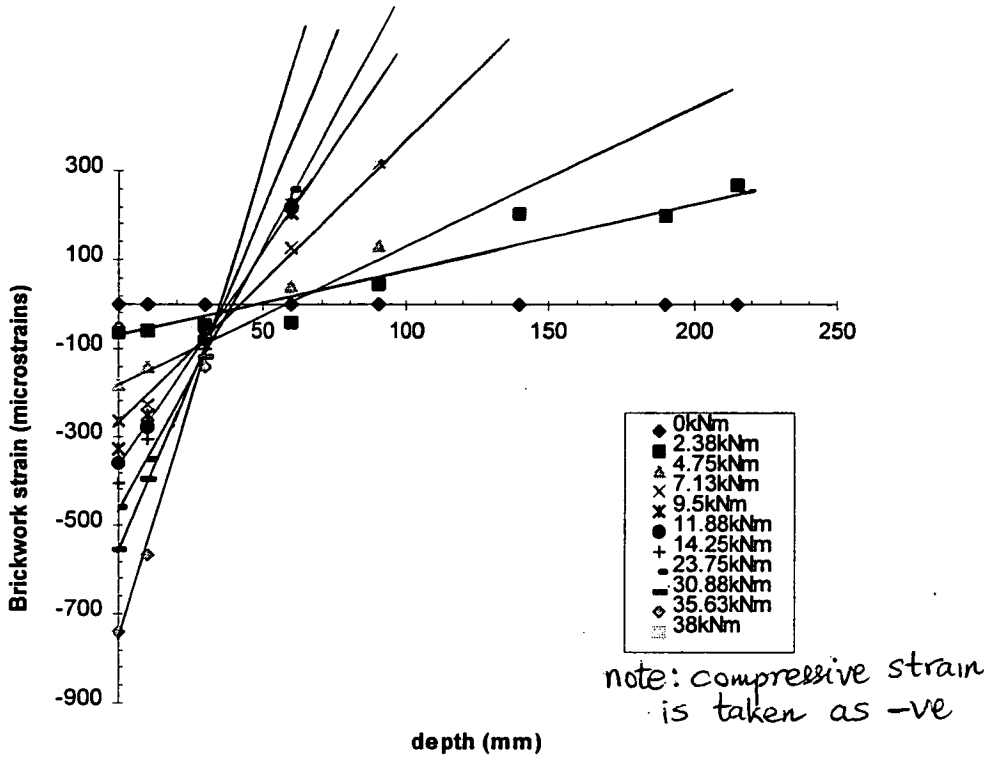

Fig 4.5-14 : Variation of average brickwork strain with depth (Beam 5)

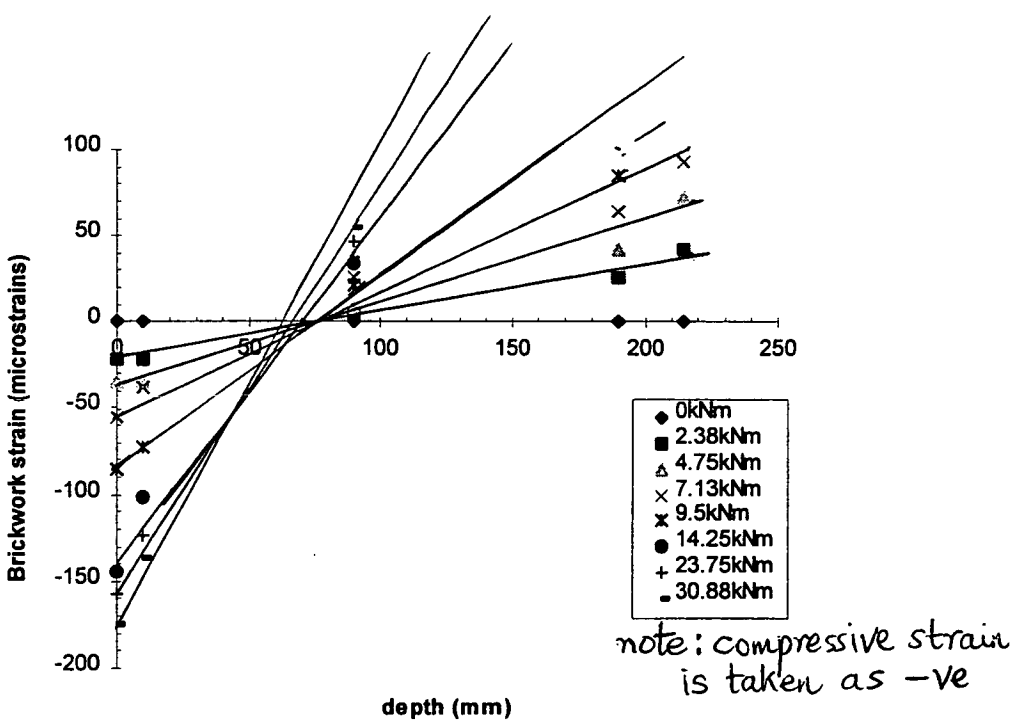

Fig 4.5-15 : Variation of average brickwork strain with depth (Beam 5)-left shear span

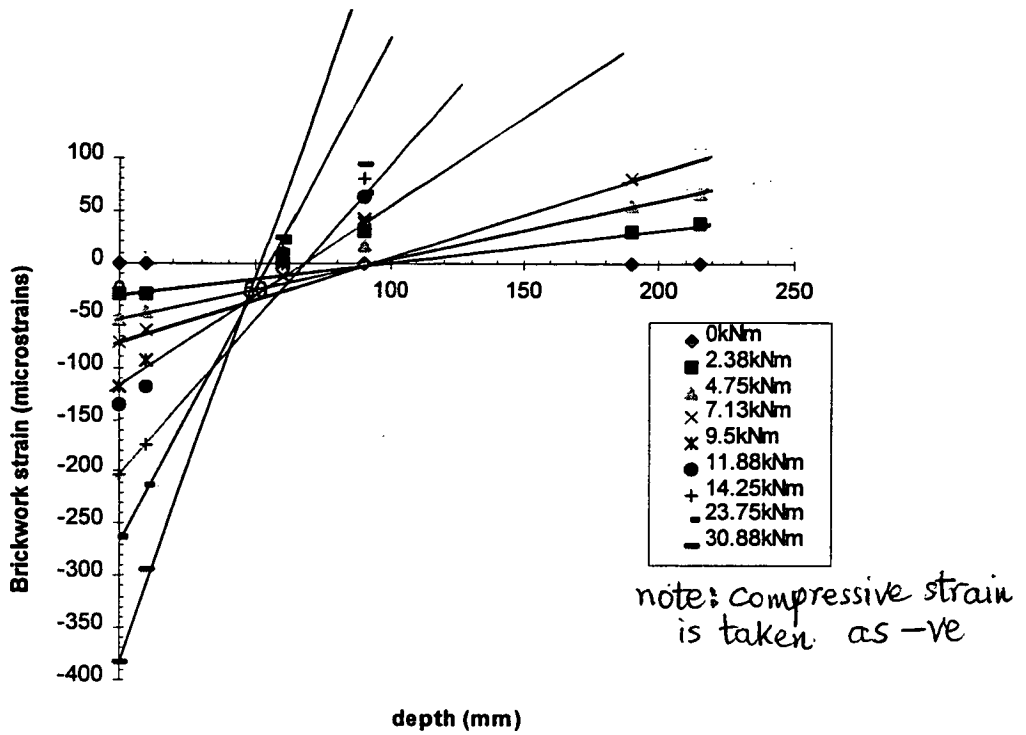

Fig 4.5-16 : Variation of average brickwork strain with depth (Beam 5)-right shear span

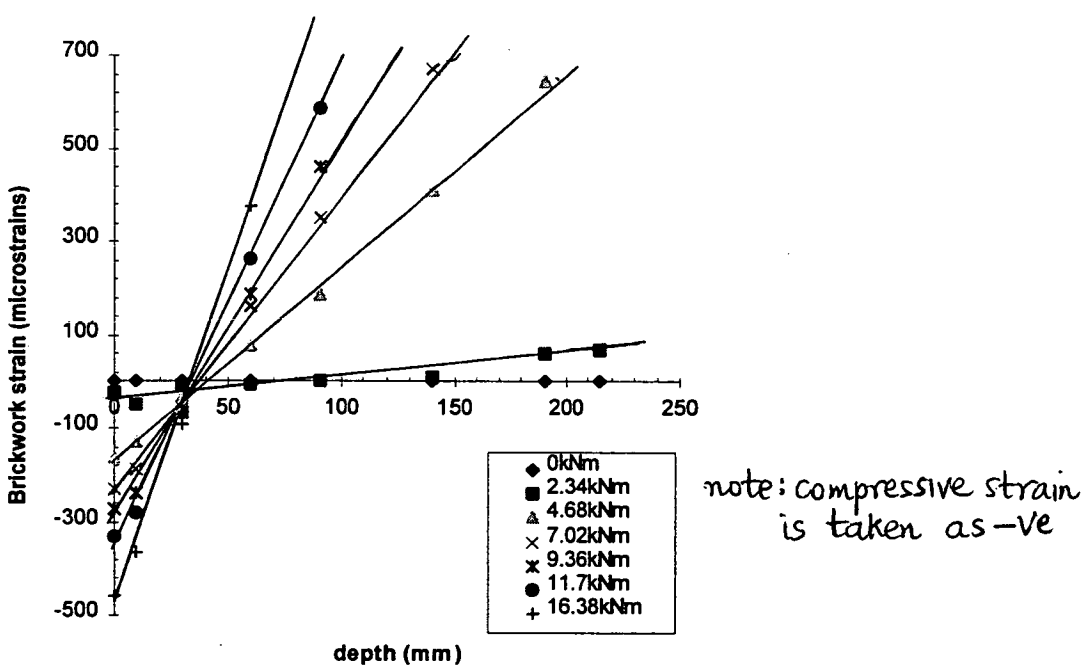

Fig 4.5-17 : Variation of average brickwork strain with depth (Beam 6)

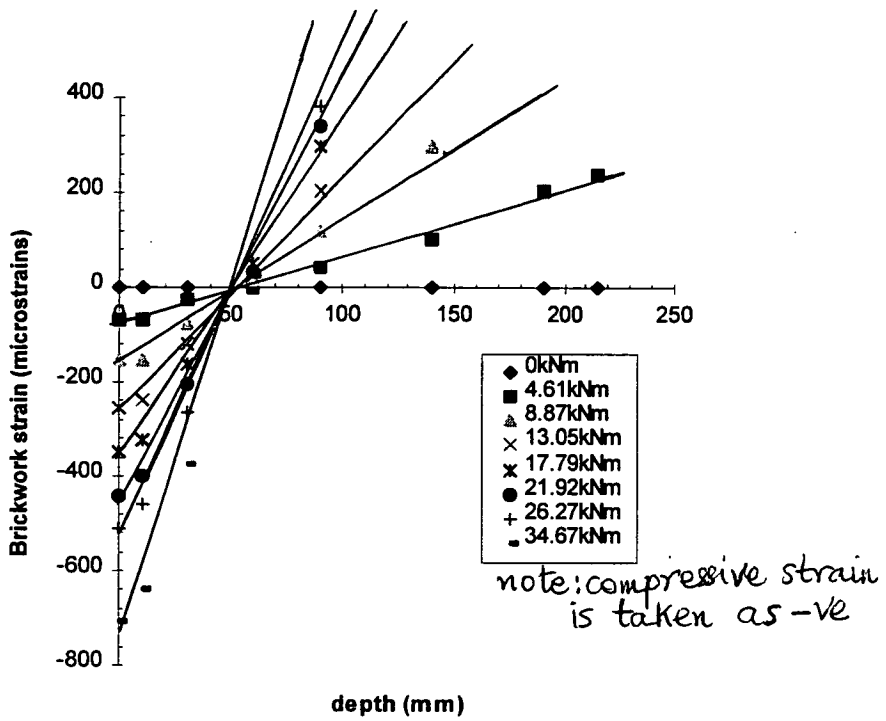

Fig 4.5-18 : Variation of average brickwork strain with depth (Beam 7)

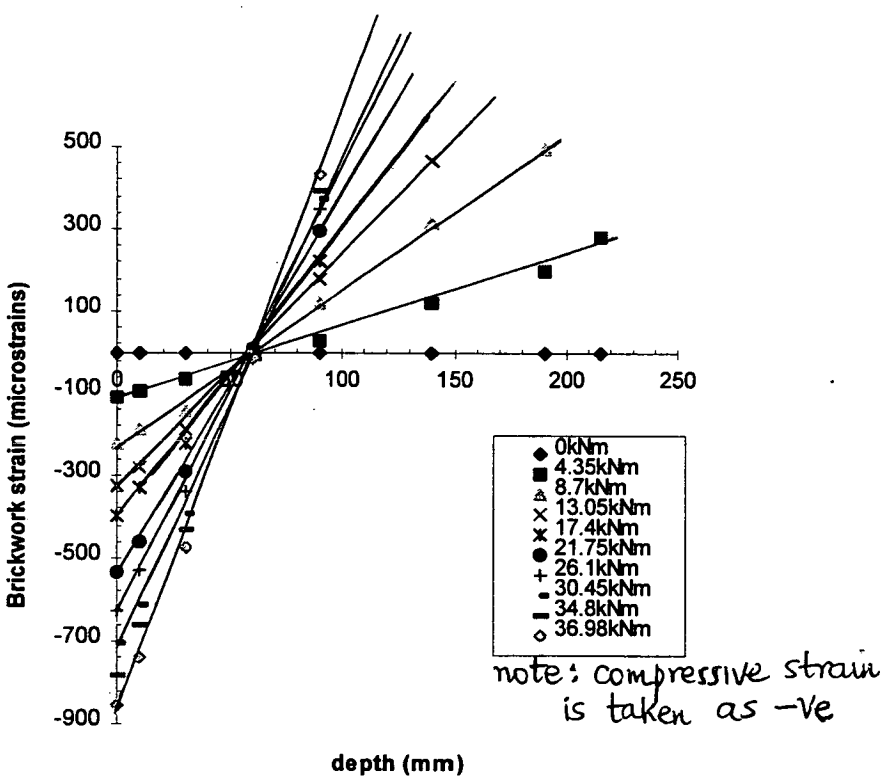

Fig 4.5-19 : Variation of average brickwork strain with depth (Beam 8)

4.5.1.4 Variation of steel strains with bending moment

The variations of steel strain are shown in Figs 4.5-20 to 4.5-27. The order of steel strains for all the beams, except for beams B5 and B6, are much smaller than the yield strain associated with the reinforcement used. Figs. 4.5-(20-23), 4.5-(26-27) show these results for beams with the higher degree of steel reinforcement. However, just prior to ultimate failure in shear, the order of steel strains in beams B5 and B6 (Fig 4.5-23 & Fig 4.5-24) were at the yield threshold. It is quite possible that steel yielding and shear failure coincided in the case of these beams but what is more likely is that shear failure occurred just when the steel was at the onset of yielding. If shear failure had not taken place, the beam would have carried some extra load since the steel is capable of sustaining higher strains than those recorded in these experiments. Furthermore, the steel reinforcement had not shown any serious sign of yielding, which is often associated with accelerating strains.

Thus, the measurements confirm that the failure of most of the beams were in shear with no yielding of steel except for two cases. In these two cases, the brickwork strains were much lower than the ultimate strain, hence the stress blocks were not fully developed.

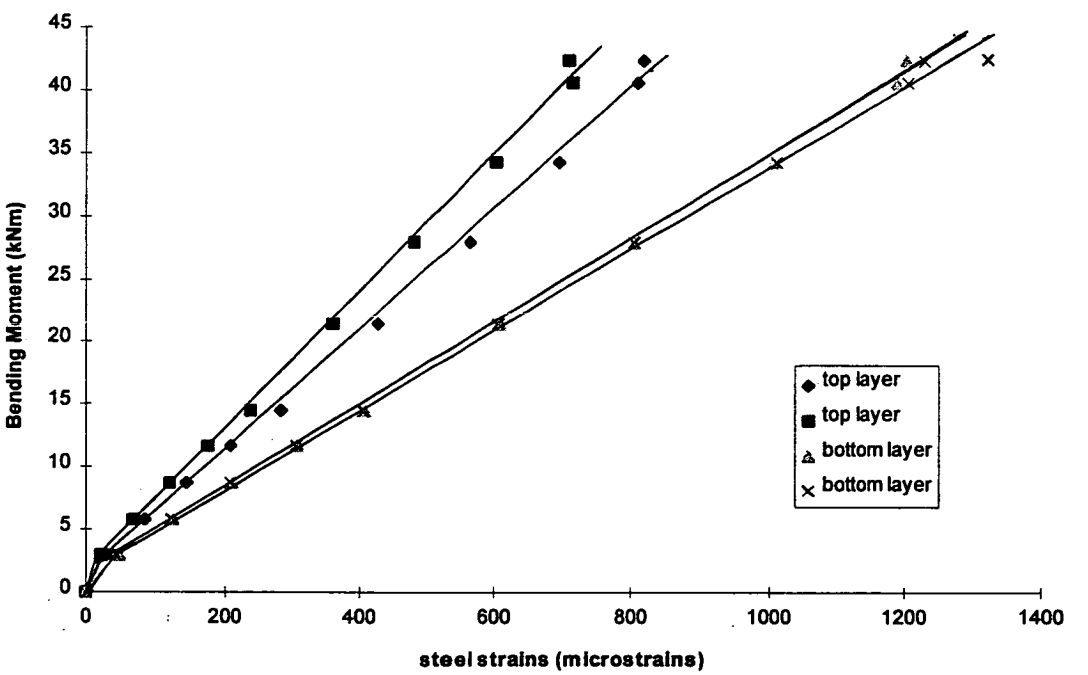

Fig 4.5-20 : Variation of steel strains with bending moment (Beam 1)

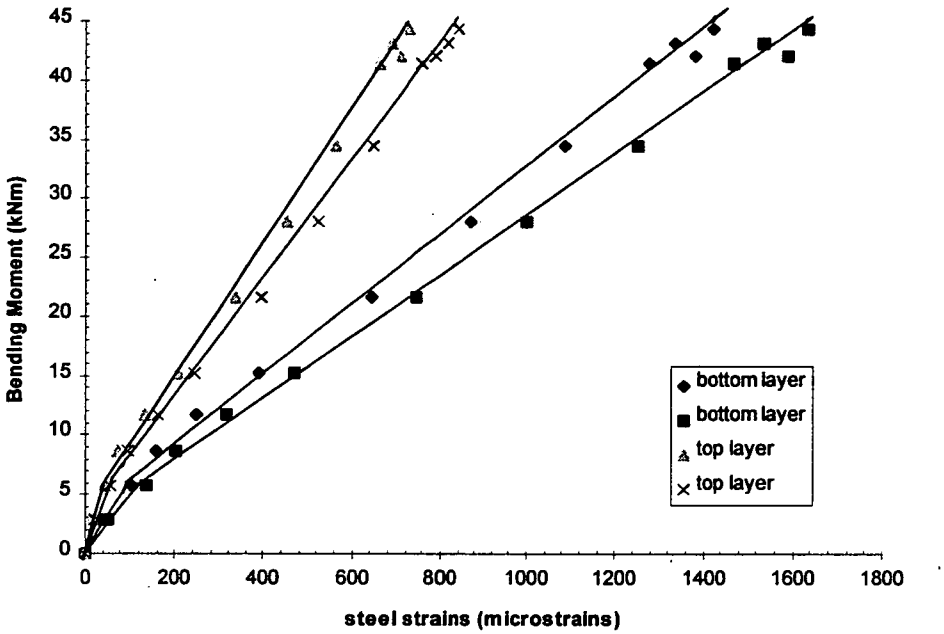

Fig : 4.5-21 : Variation of steel strains with bending moment (Beam 2)

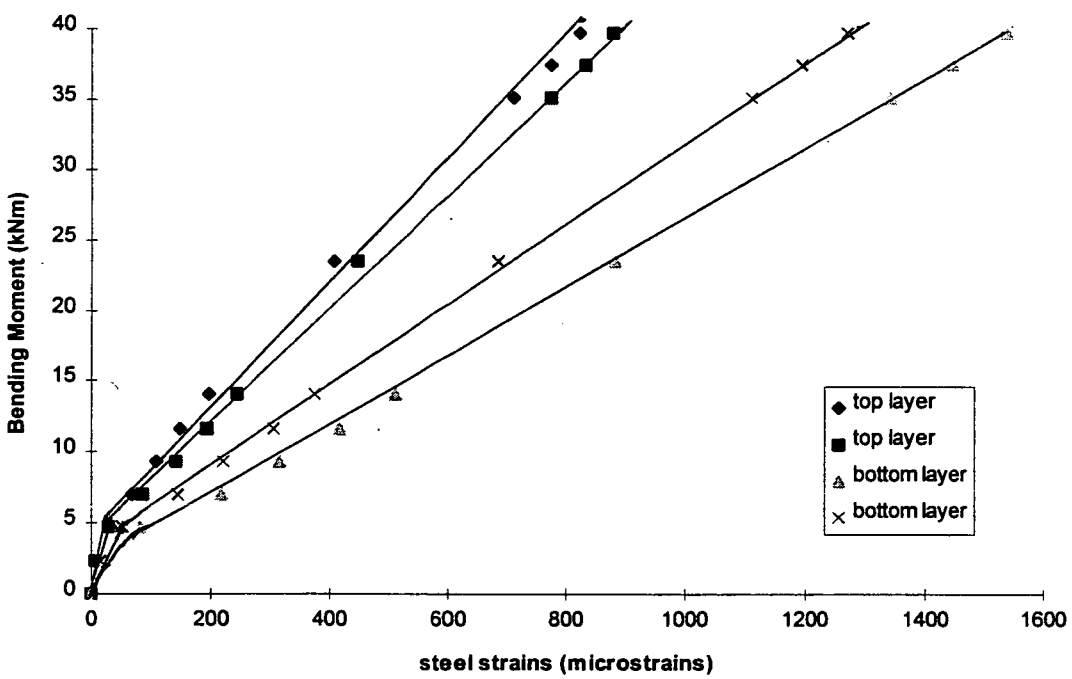

Fig 4.5-22 : Variation of steel strains with bending moment (Beam 3)

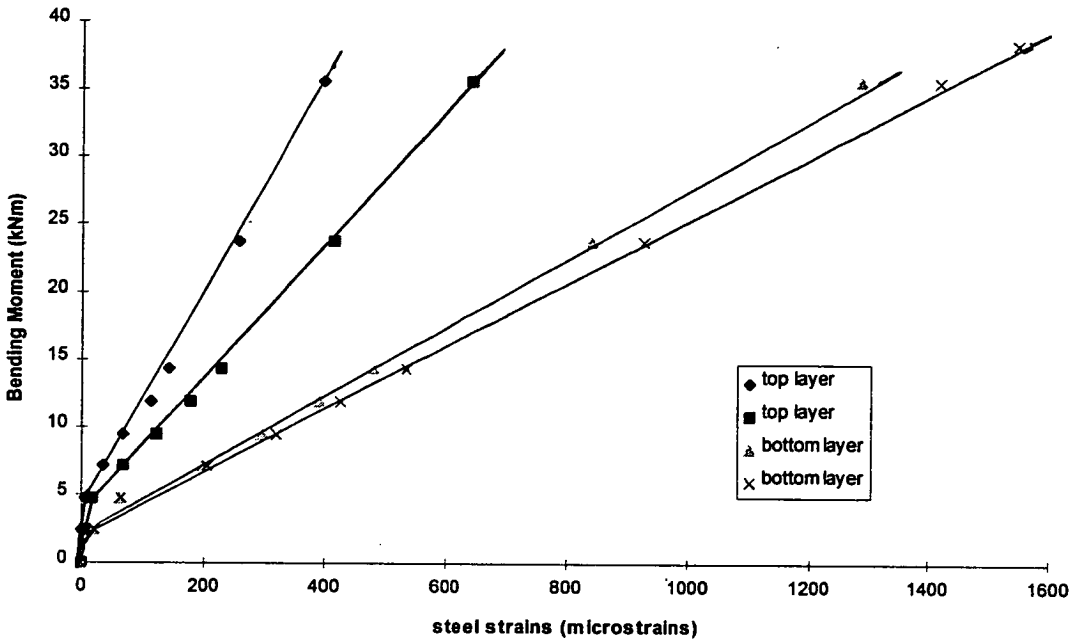

Fig 4.5-23 : Variation of steel strains with bending moment (Beam 4)

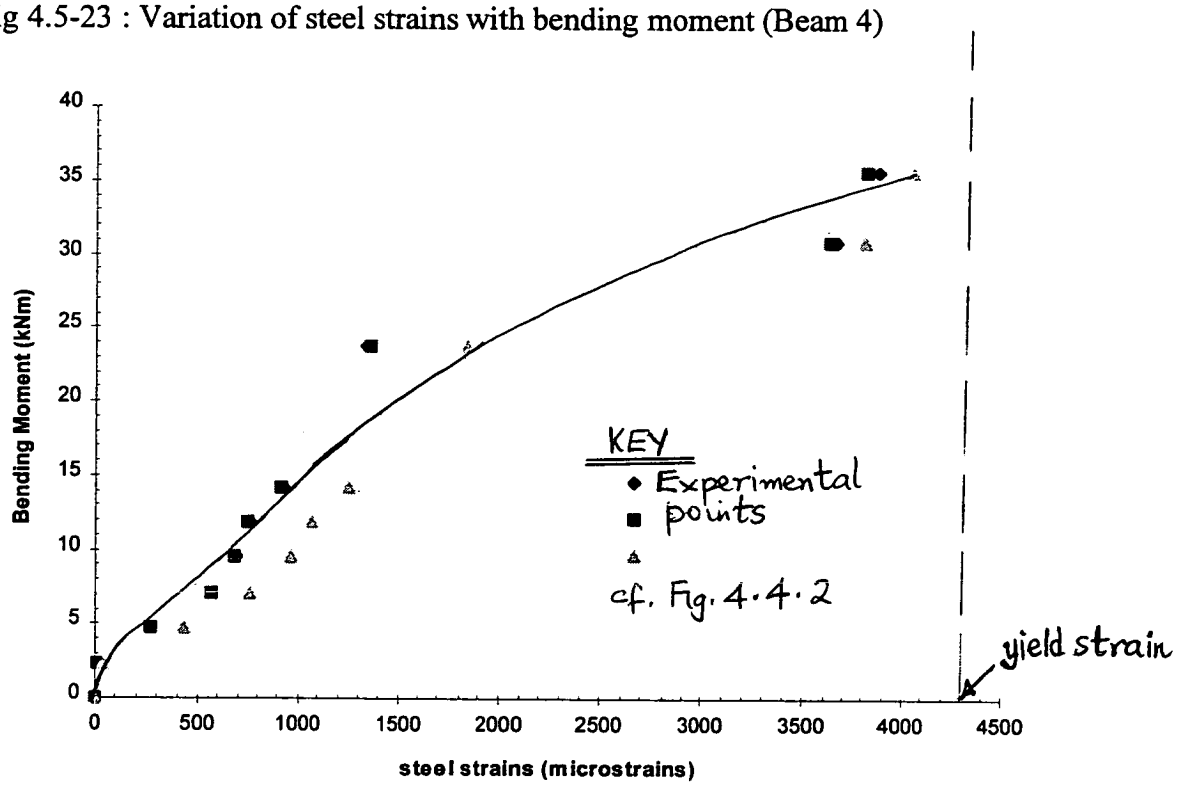

Fig 4.5-24 : Variation of steel strains with bending moment (Beam 5)

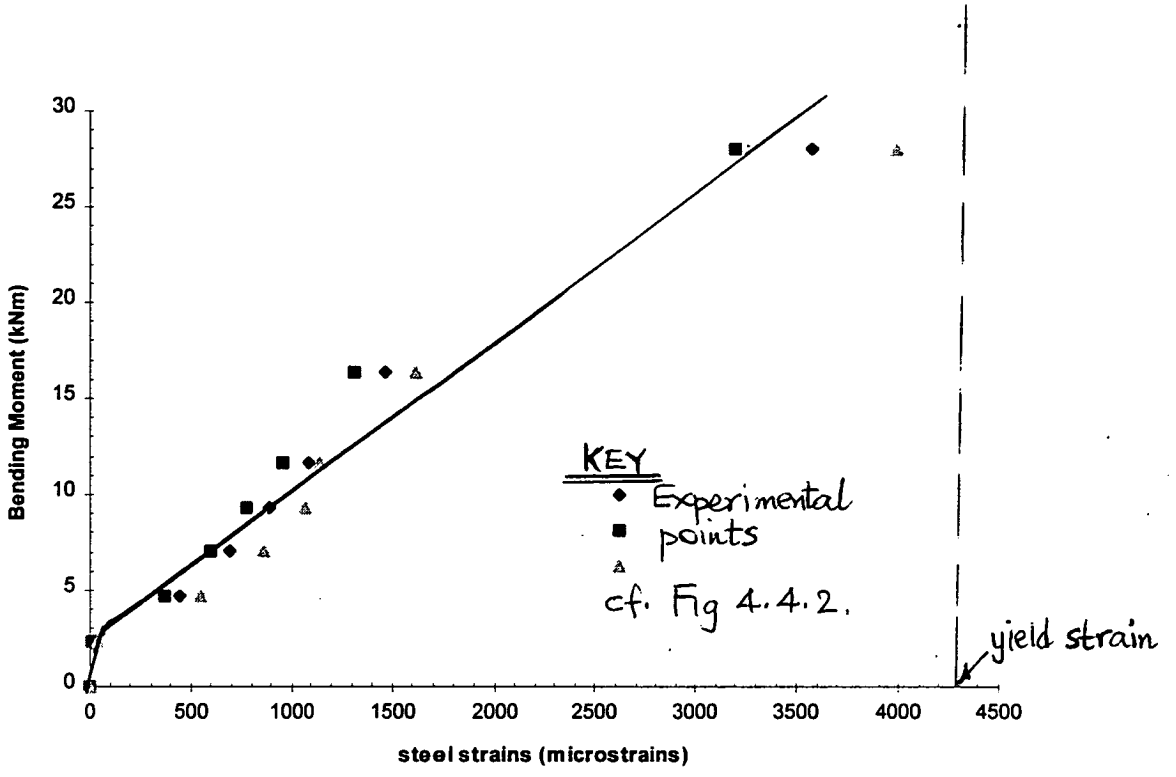

Fig 4.5-25 : Variation of steel strains with bending moment (Beam 6)

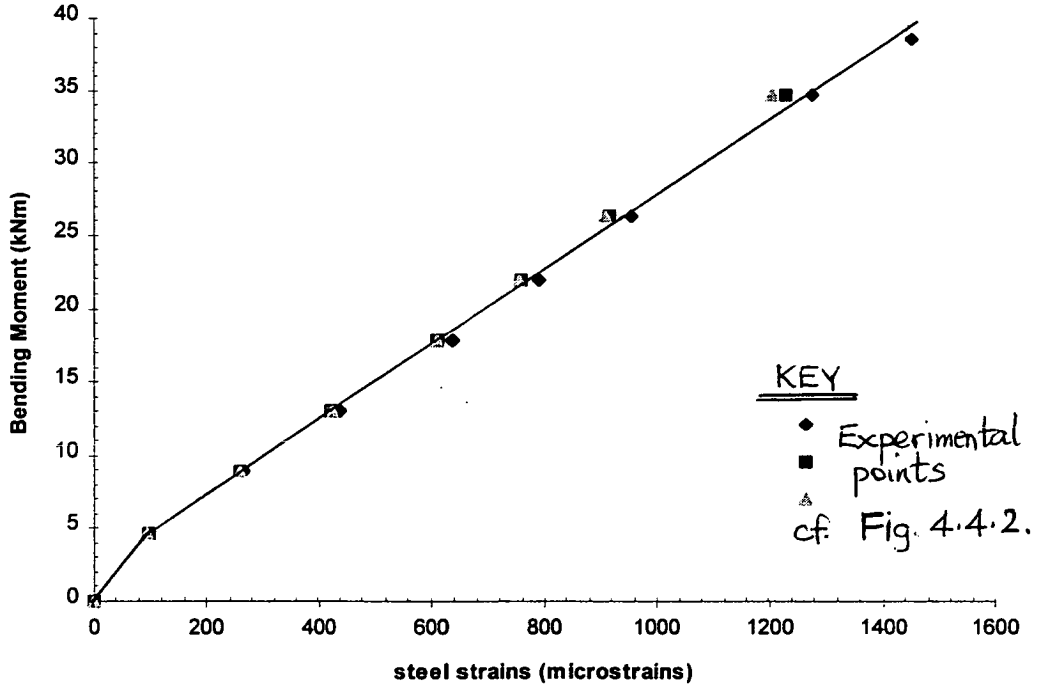

Fig 4.5-26 : Variation of steel strains with bending moment (Beam 7)

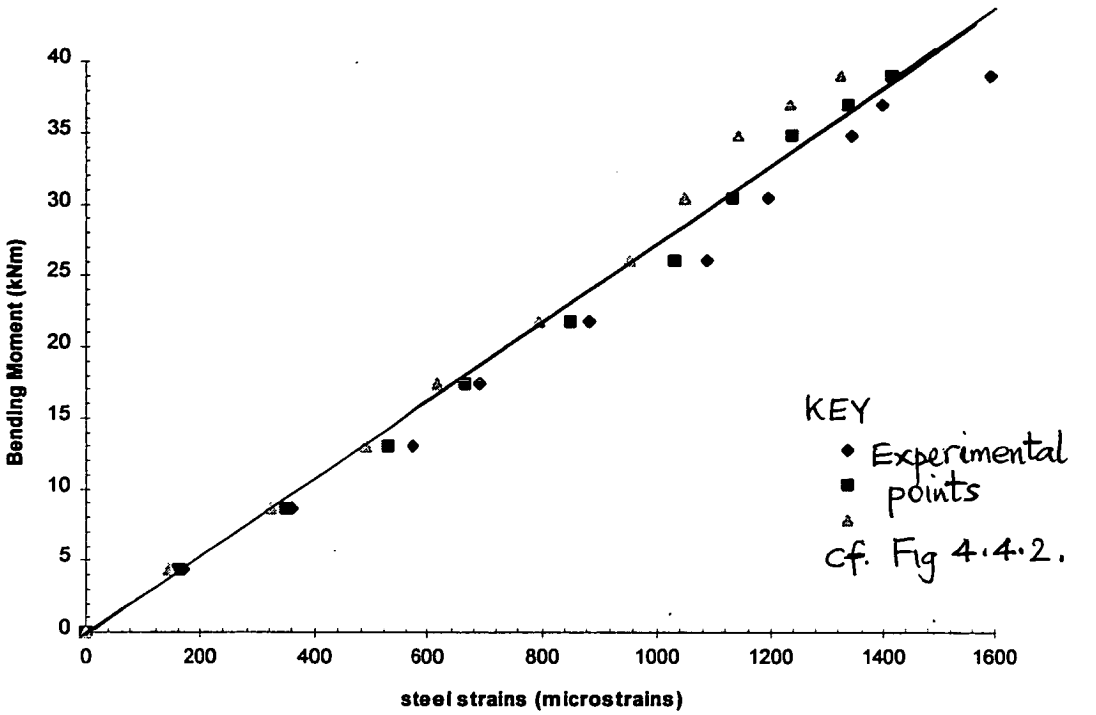

Fig 4.5-27 : Variation of steel strains with bending moment (Beam 8)

4.5.1.5 Variation of top longitudinal strains along the breadth

These curves are given by Figs. 4.5-28 to 4.5-36. They are plotted to examine the situations within both the maximum bending moment regions and the shear spans throughout the different regimes of loading and also to compare with measurements taken along the depth. For beams B1 and B2, the longitudinal strains measured along the breadth (that is, across the spans) gave a uniform distribution throughout the loading regimes (Fig 4.5-28 and Fig 4.5-29). In beam B5, the longitudinal strains are compressive both within the shear spans and the constant bending moment regions (Fig 4.5-31). In beam B6, similar results were obtained (Fig 4.5-32 to Fig 4.5-34).

In beams B7 and B8, a uniform longitudinal strain distribution along the breadth was obtained within the constant bending moment regions of the beams (Fig 4.5-35, Fig 4.5-36). Within the shear spans of these beams, the longitudinal strains were compressive. The shear failure of these beams were also accompanied by a longitudinal crack. This longitudinal crack developed subsequent to shear failure and travelled from the maximum moment zone to the end section of the beam. A typical

longitudinal crack accompanying shear failure as well as a typical shear failure within the shear span are shown, respectively, in Figs 4.5-37 and 4.5-38. These results correspond well with strain measurements taken along the depth of the beams {Figs 4.5-9 to 4.5-19}.

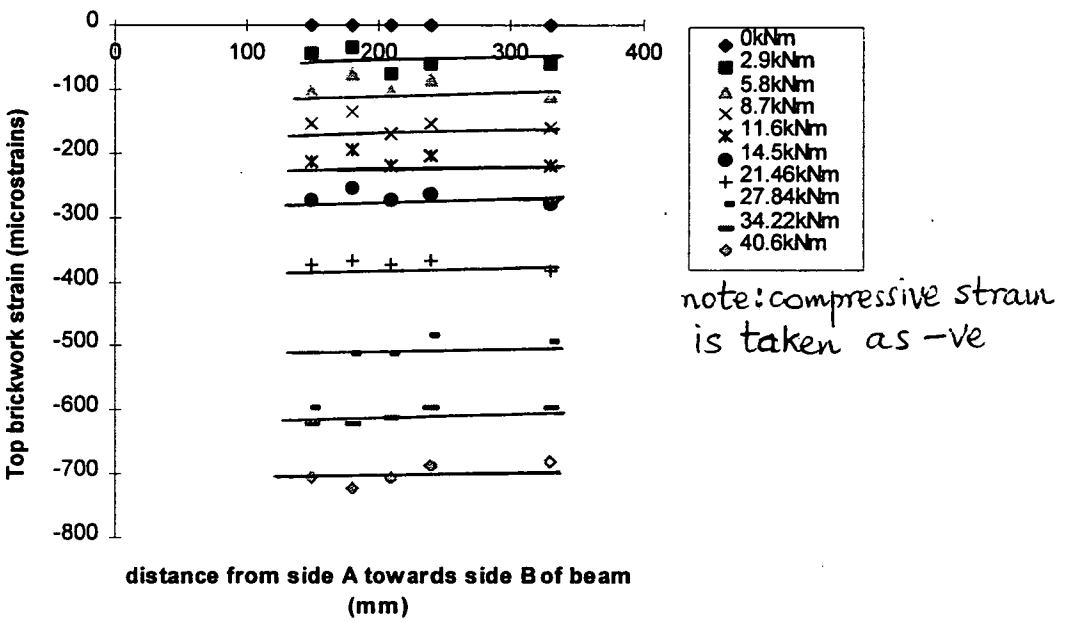

Fig 4.5-28 : Variation of Top Longitudinal Strain along the Breadth (Beam 1)

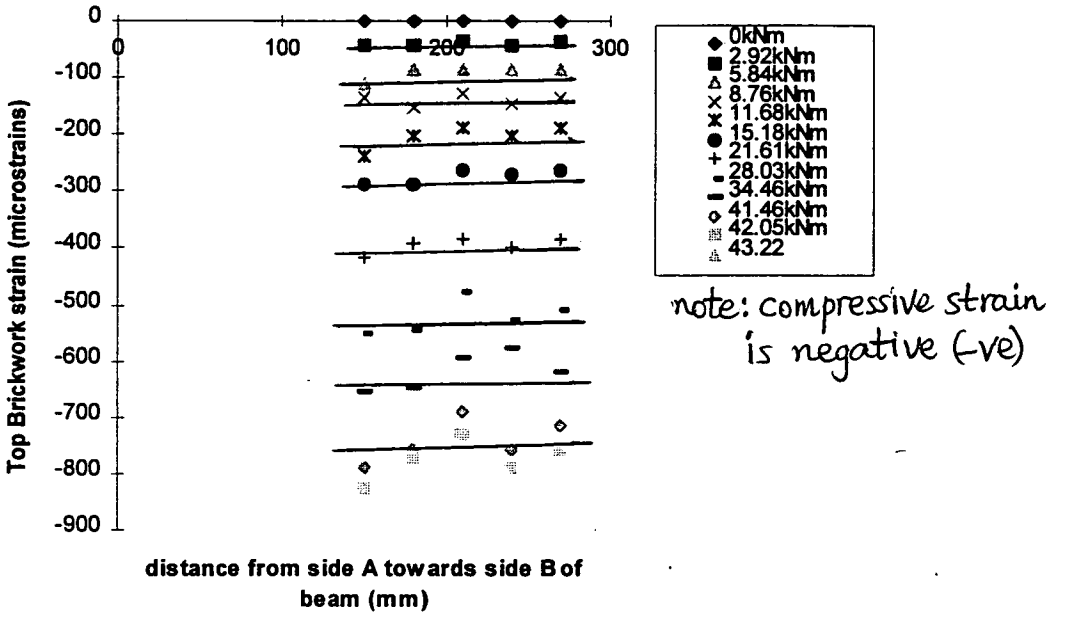

Fig 4.5-29 : Variation of Top Longitudinal Strain along the breadth (Beam 2)

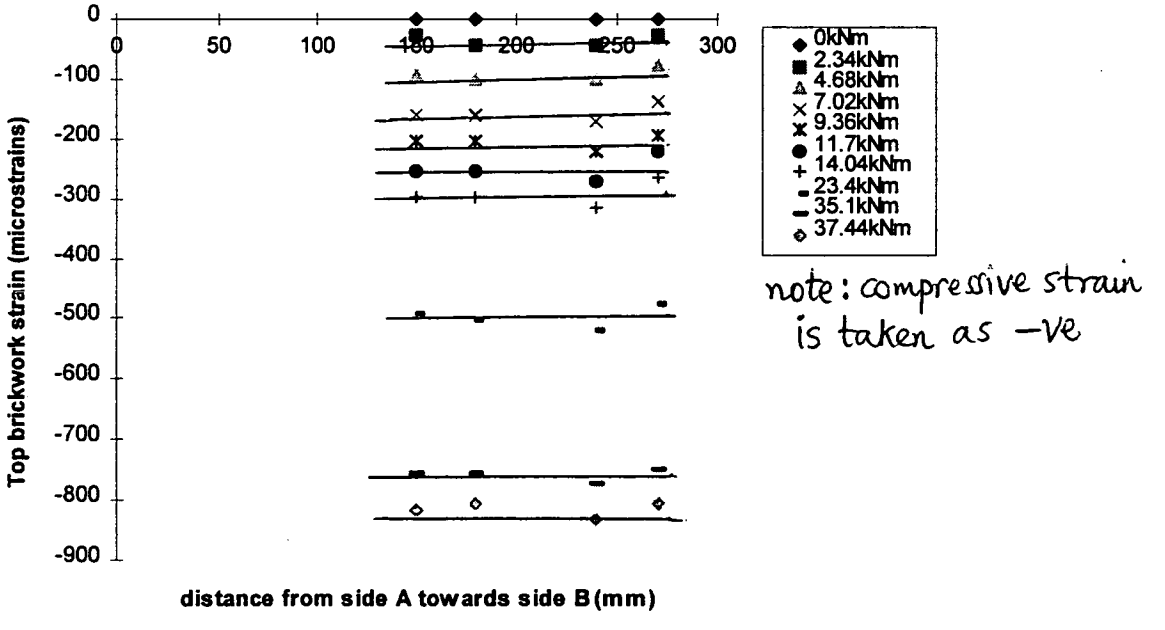

Fig 4.5-30 : Variation of Top Longitudinal Strain along the Breadth (Beam 3)

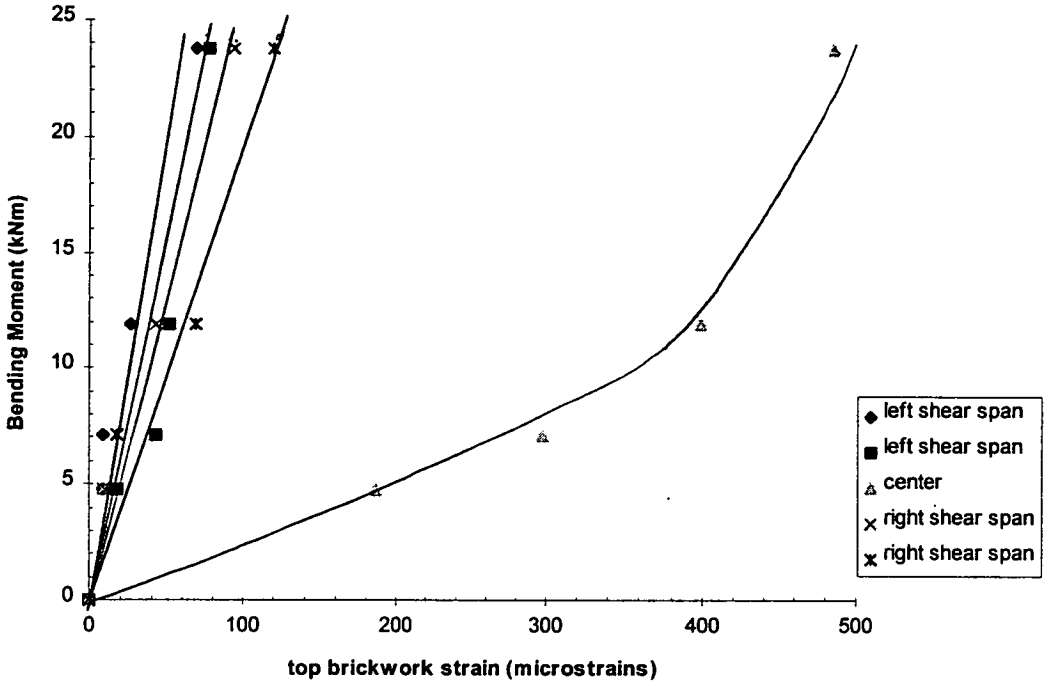

Fig 4.5-31:Variation of Longitudinal Strain with B.M. along the top surface (Beam 5)

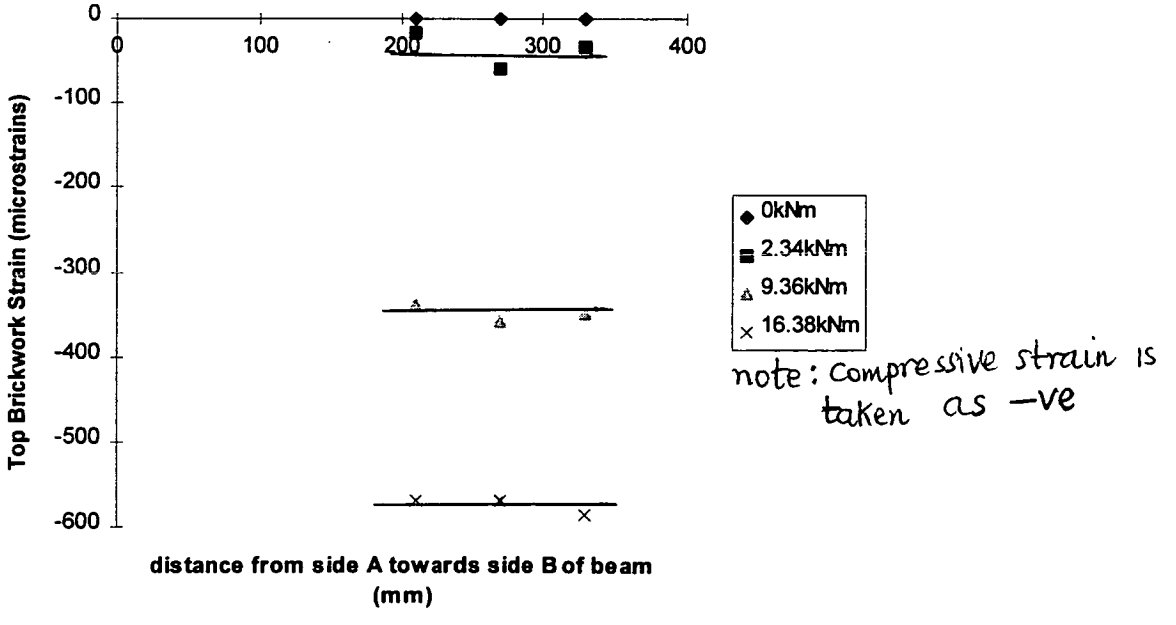

Fig 4.5-32 : Variation of Top Longitudinal Strain along the breadth (Beam 6)-Top center

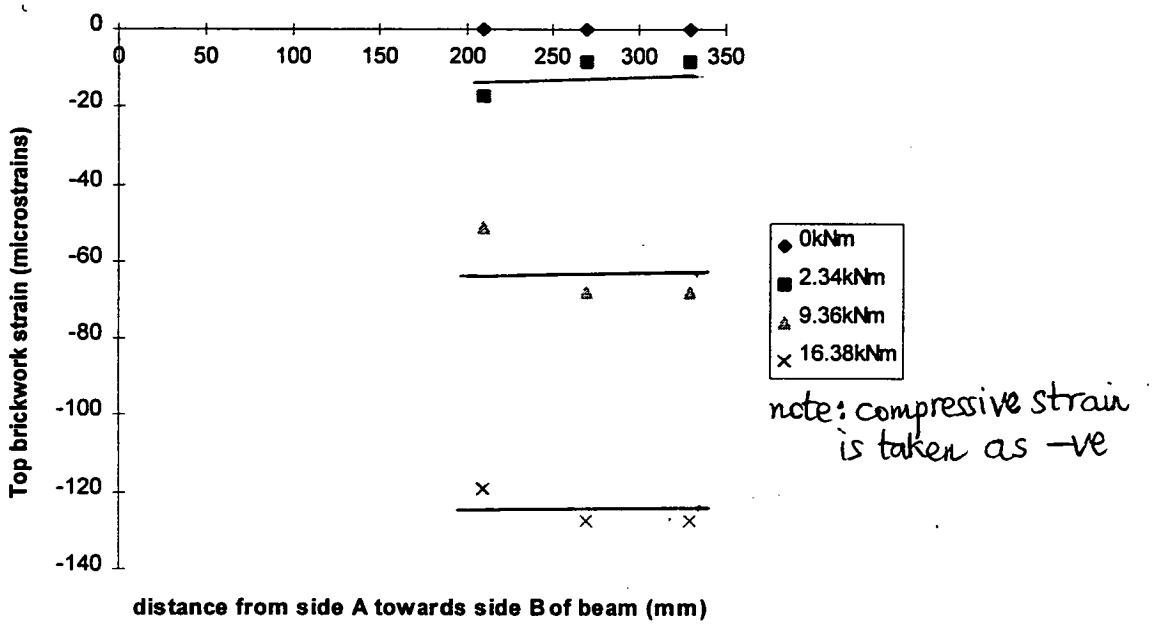

Fig 4.5-33 : Variation of Top Longitudinal Strain along the Breadth (Beam 6)-Top (1)

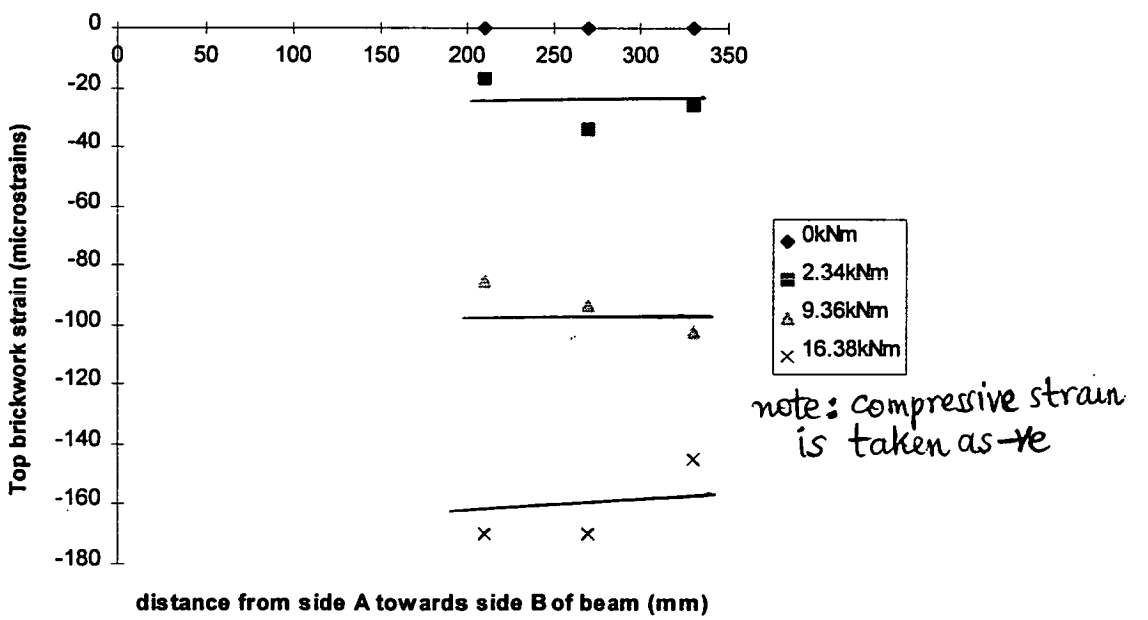

Fig 4.5-34 : Variation of Top Longitudinal Strain along the Breadth (Beam 6)-Top (2)

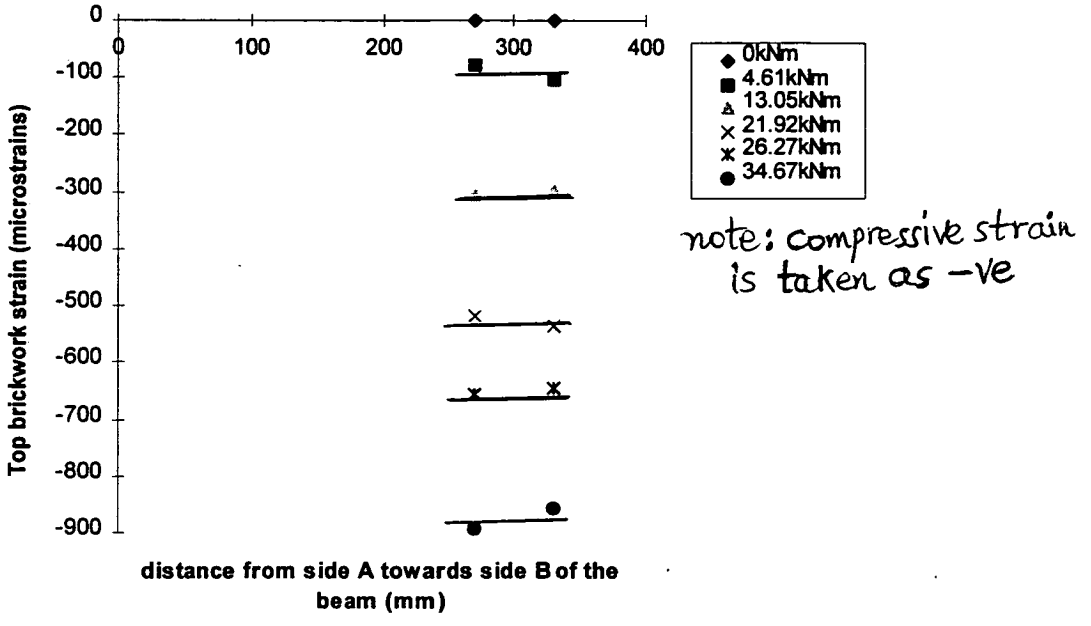

Fig 4.5-35 : Variation of Top Longitudinal strain along the breadth (Beam 7)

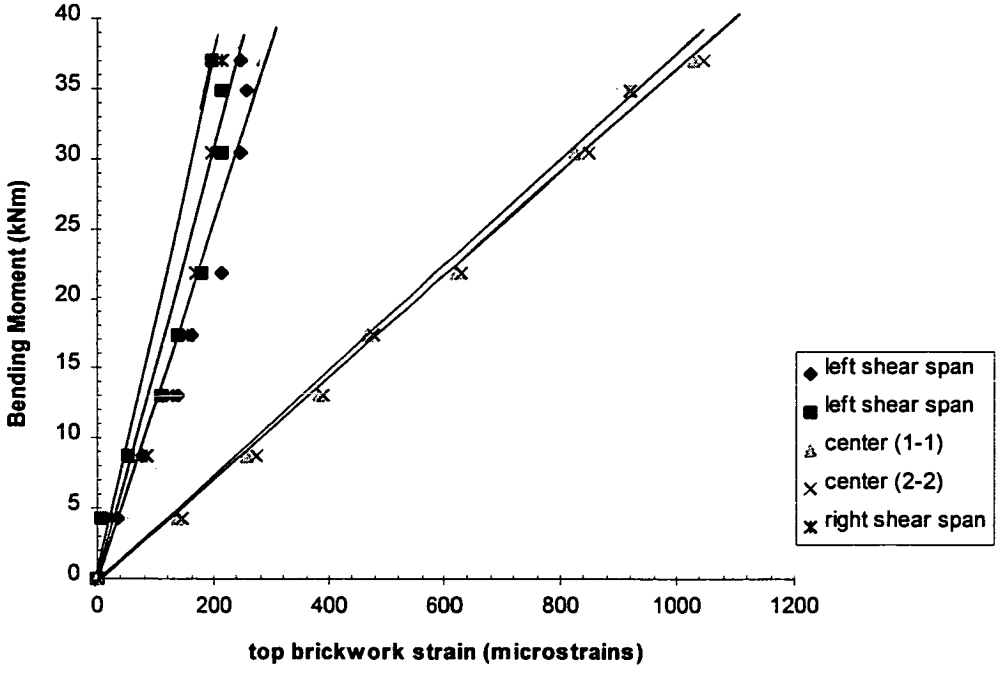

Fig 4.5-36 : Variation of Top longitudinal Strain with Bending Moment at points along the breadth (Beam 8)

Fig 4.5-37 : Longitudinal shear cracks accompanying shear failure

Fig 4.5-38 : A typical diagonal shear failure within the shear span

4.5.1.6 Relationship between Moment and Central Deflection

The deflection measurements as well as the strain measurements were taken to check if the whole of the cross-section in compression was used up before failure in shear. Also, the deflection measurements are required to classify the beams in terms of relative stiffness. Theoretical methods were used to predict the deflections occurring in these beams. These beams were designed to fail in shear so they are not expected to reach ultimate moment capacities when loaded to failure.

These experimental results have been compared with the predictions based on : (a) the direct method, which was incorporated into an interactive computer programme developed by Walker[13] and ; (b) on Branson's procedure[37] as proposed originally for calculating deflections in reinforced concrete members. Predictions given by both methods are reasonable as shown in Fig 4.5-39 to Fig 4.5-42.

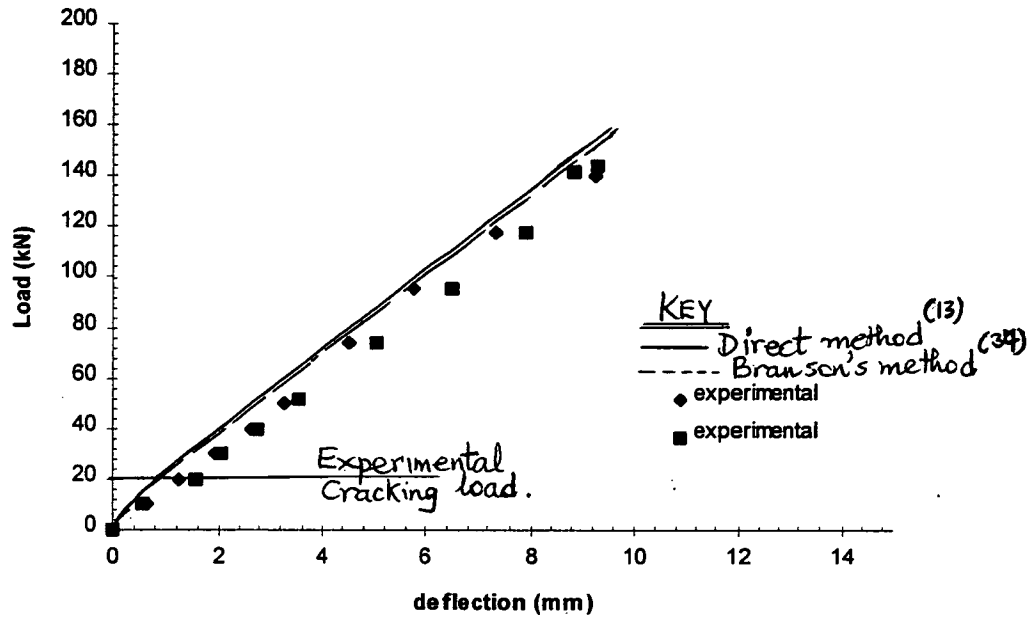

Fig 4.5-39 : Load Vs Central Deflection (a/d=2; ρ =1.6%)

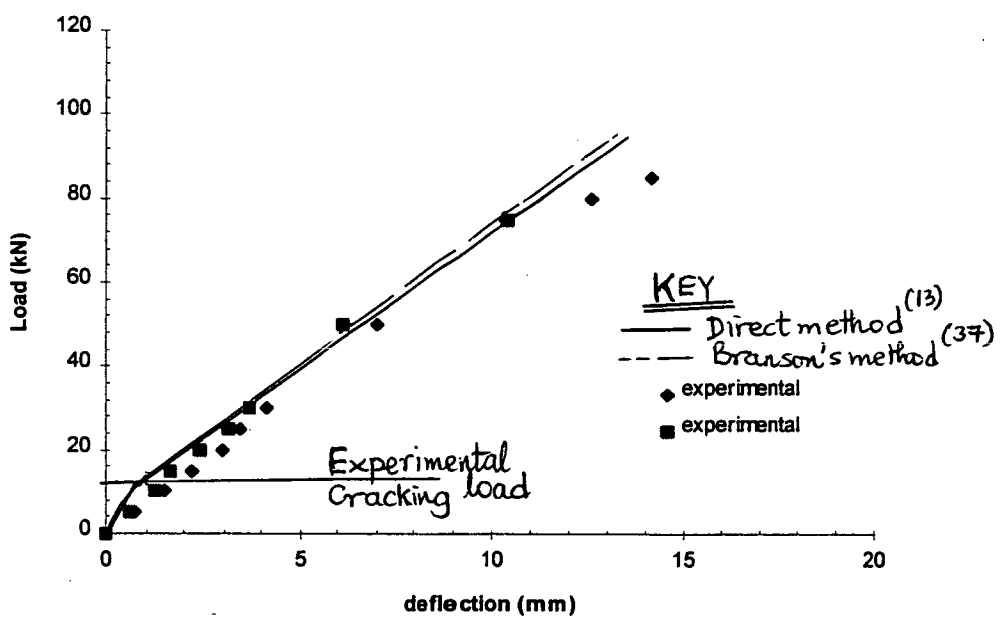

Fig 4.5-40 : Load Vs Central Deflection (a/d=3.2; ρ =1.6%)

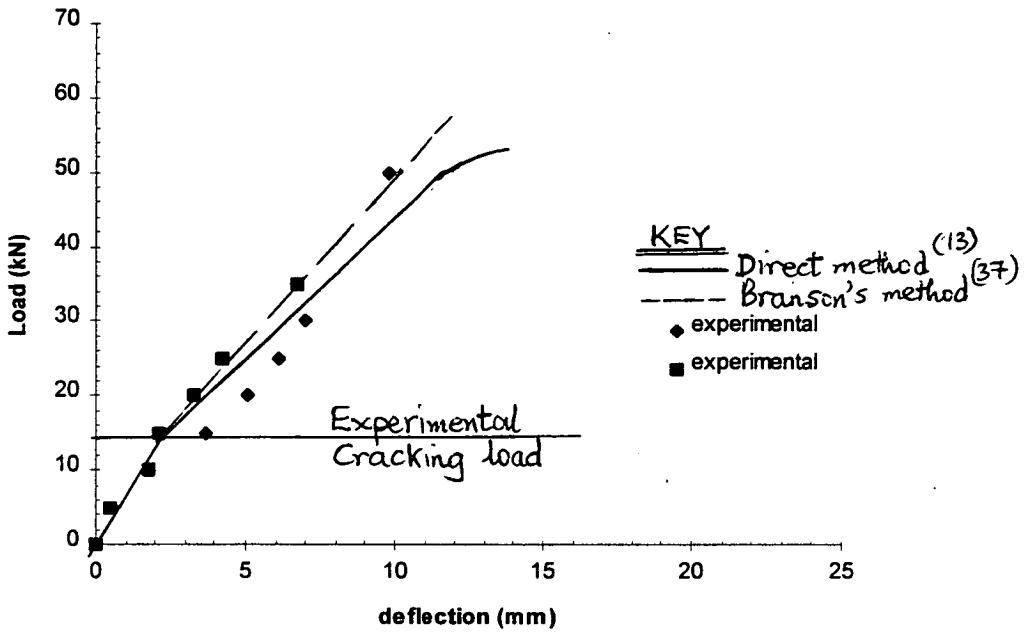

Fig 4.5-41 : Load Vs Central Deflection (a/d=3.2; ρ =0.61%)

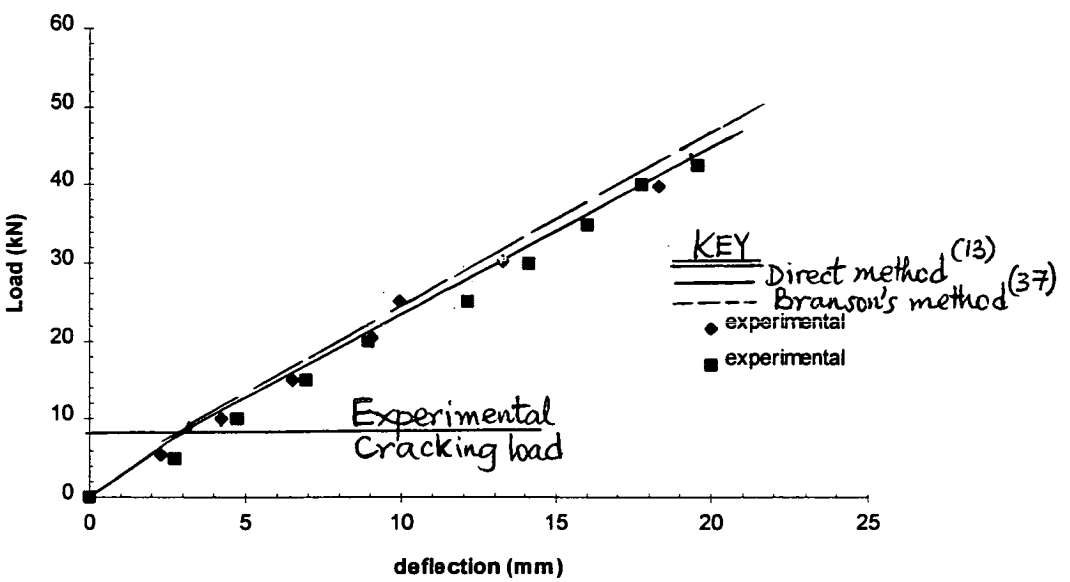

Fig 4.5-42 : Load Vs Central Deflection (a/d=6; ρ =1.6%)

4.5.1.7 General Characteristics of the test results

(1) The strains in both the constant bending moment zone and shear span are directly proportional to the distance from the neutral axis. This means it follows the assumption made in bending.

(2) The compression zone is not fully developed prior to and at the instant of failure in shear.

(3) The neutral axis depth had not shifted significantly prior to failure of the specimen. The brickwork crushing strain, ε_m, is much higher than the brickwork strain at the time of beam failure ; this shows that the compression zone is underutilized. The strains in the steel at failure are also much smaller than the yield strain of the reinforcement. These characteristic features show that shear failure is associated with an under utilization of the materials making up the beam namely, brickwork and steel.

(4) This type of failure is characterized by small deflections. The beams which are close to flexural failure exhibited more ductility.

Strain measurements in the steel and the maximum compressive strain prior to failure of the beams gave an indication of the type of failure which had occurred as well as the degree of ductility of the beams relative to one another. The maximum strains in the steel are compared with the strains corresponding to the proof stress of the reinforcement in order to determine if the latter strain is exceeded and also if yielding of the steel had occurred. Attempts to measure the transverse strains at the top of the beams, in order to check any tension developing there, were not successful as the instrument used was not sensitive enough to measure such strains.

In all the beams, the compressive strains at the top fibers within the maximum bending moment region showed a practically linear increase throughout the various loading stages prior to ultimate collapse. The distribution could be appoximated by a linear curve in most cases. As shear failure tended to occur rather suddenly with very little prior warning, the strains could not be measured up to failure as this was considered unsafe. Nonetheless, attempts were made to take measurements as close to the ultimate failure point as was practicable.

4.5.2-(a) Influence of a/d ratio on shear strength

From Table 4.5-1, it can be seen that the a/d ratio has a marked influence on the shear strength of the pocket-reinforced beams. The shear strength decreases with increasing a/d ratio.

4.5.2-(b) Influence of steel area on shear strength

The experimental results show that the levels of steel in these pocket-reinforced beams fall within the threshold where the degree of longitudinal reinforcement, Φ, still counts in resisting shear forces. This explains the enhanced shear strength recorded by the beams B3 and B4 relative to B5 and B6, though similar, but with a higher reinforcement ratio. From these results, it is seen that the influence of steel area on shear strength is relatively small compared to that of the a/d ratio.

4.5.2-(c) Comparison Between Theoretical and Experimental shear strengths

Table 4.5.2 compares the experimental and theoretical shear strengths of the pocket-reinforced brickwork beams using the plastic theory[9,62]. There seems to be very good agreement between the experimental and theoretical results. Hence, this method of analysis can be used for calculating the shear strength of the reinforced pocket-type beams. The shear stress obtained in this table (Table 4.5.2) differs slightly from those given in Table 4.5.1 because total depth has been taken into account for theoretical calculation.

These shear strength results have been compared with results obtained in accordance with the British standard[2] recommendations. This comparison is given in Table 4.5.3. A similar analysis was also carried out on the shear test results reported earlier on reinforced brickwork pocket-type beams[61]. This is done so as to ascertain the factor of safety associated with these beams when the allowable shear stress recommendations given by the British Code[2] of practice is used for design. These results are given in the Appendix (Table A2). If the reported results (Table A2) are used, it means that very low factors of safety are provided by the code and, if the corrected values are used, this factor of safety is exaggerated in many cases. A material partial safety factor of 2.0 for shear strength should be adequate. The factor

varies from 1.15 to 2.85 for the pocket-type reinforced brickwork beams tested by Tellett & Edgell[30]. It seems that the code provision is to some extent unsafe.

Table 4.5.2 : Comparison Between Experimental and Theoretical Shear Strengths

BEAM No	Φ (Degree of reinforcement)	(*a/h*)	$\tau_{experimental}$ (N/mm^2)	$\tau_{experimental}$ (C) (N/mm^2) (average)	$\tau_{theoretical}$ (D) (N/mm^2)	(C)/(D)
B1	0.22	1.36	1.26	1.36	1.34	1.01
B2	0.22	1.36	1.47			
B3	0.22	2.18	0.77	0.765	0.88	0.87
B4	0.22	2.21	0.76			
B5	0.08	2.21	0.67	0.62	0.66	0.94
B6	0.08	2.18	0.56			
B7	0.21	4.04	0.43	0.425	0.48	0.89
B8	0.21	4.04	0.42			

Table 4.5.3 : Comparison Between British Standards[2] and Experimental Shear Strengths

BEAM No	Characteristic shear strength (N/mm^2), f_v	f_v/γ_{mv} Design shear stress (N/mm^2)	Average experimental shear strength (N/mm^2)	Experimental Design shear stress
B1	1.23	0.615	2.02	3.28
B2	1.23	0.615		
B3	1.03	0.515	1.11	2.16
B4	1.03	0.515		
B5	0.76	0.38	0.90	2.37
B6	0.76	0.38		
B7	0.62	0.31	0.615	1.98
B8	0.62	0.31		

4.6 ANALYSIS OF BEAM BEHAVIOUR IN THE MAXIMUM BENDING MOMENT REGION

Results of theoretical and experimental measurements are presented in this section. A summary of the analysis carried out on the experimental results obtained in the constant bending moment regions of these beams are tabulated. These results are also used to draw conclusions on the structural behaviour of the beams.

4.6.1 Strain Measurements in the Maximum Bending Moment Regions

In this shear strength investigation, brickwork strain measurements were taken in the constant bending moment regions so as to establish the exact cause of failure of the beams. If, on one hand, compressive flexural failure occurred rather than shear failure, then this would be indicated by a fully developed compression block and would be easily confirmed by the strain measurements of the brickwork. On the other hand, if tensile flexural failure occurred rather than shear failure, then this would be indicated by the post-yield behaviour of the tensile steel and this would also be easily confirmed by the strain measurements in the steel reinforcements. These experimental measurements obtained from brickwork and the steel reinforcements were used to work out the internal moment of resistance mobilized just prior to failure of these beams. Since for all these beams, the compression block zone was not fully developed prior to ultimate failure, the experimental measurements were used to work out the stress block characteristics just prior to failure. These results are compared with the ultimate moments predicted based on beam properties as well as those predicted by the BS5628 [2] provisions for these members.

4.6.2 Ultimate strength prediction based on moment capacity

In this sub-section, the failure of these beams based on flexural strength is analysed with the objective of comparing the failure predicted by theory with experimental observations within their constant bending moment regions.

It is known that beams may fail in bending because of weakness in the tension steel or weakness in the compression brickwork. Several ultimate strength theories have been proposed for reinforced and prestressed brickwork[7,11,13,64]. These theories are different from one another basically in the shape assumed for the stress block and consequently, the characteristics associated with these blocks. Once these

characteristics are expressed in general terms, the equations pertaining to ultimate strength predictions are derived using the principles of mechanics. The two relevant characteristics of this block are the ratios λ_1 and λ_2, as defined in section 3.3.3.3.

4.6.3 Comparative Analysis of Theoretical and Experimental Results

In this section, the experimental results have been compared with the theoretical predictions given by BS 5628 [2], those given by the stress block factors λ_1 and λ_2 obtained in this work as well as those given by the direct method[7,11,13]. These results are given in Table 4.6.1. The experimental results were also analysed on the basis of experimentally-derived compression block properties. The measurements, obtained just prior to the ultimate failure of the beams in shear, were examined and used to calculate the internal moment of resistance, at that level of loading, in the maximum bending moment region of these beams. These results are compared with the measured applied bending moment (that is, just prior to ultimate failure) and this comparative analysis is given in Table 4.6.2.

Table 4.6.1 : Comparison of Experimental and Failure Moment Based on BS5628 [2], λ_1 and λ_2 obtained in this work and also by the direct method[7,11,13]

Beam No	Experimental Moment (Average) (kNm)	Failure Moment based on BS5628[2] (kNm)	Failure Moment based on λ_1 and λ_2 derived in this work.	Failure Moment based on Direct Method
B1	46.5	80.7	66.5	65.3
B2	46.5	80.7	66.5	65.3
B3	40.7	80.7	66.5	65.3
B4	40.7	80.7	66.5	65.3
B5	35	38	36	32
B6	35	38	36	32
B7	40.3	77	66.5	65.7
B8	40.3	77	66.5	65.7

Table 4.6.2 : Comparison of Derived and Experimental Moment prior to Ultimate Failure

Beam No	MOR (kNm) (Based on strain measurements in brickwork and steel)	Experimental BM (kNm)	Ratio {MOR}/{BM}
B1	36.52	40.6	0.90
B2	37.26	41.46	0.88
B3	34.50	37.44	0.91
B4	32.07	35.63	0.88
B5	32.90	35.63	0.88
B6	17.08	16.38	1.05
B7	38.39	34.67	1.11
B8	41.42	36.98	1.10

Results given in Table 4.6.1 indicate that for all the beams, the flexural capacity was not reached. The code of practice gives a much higher values for the flexural failure than is obtained either by the direct method or by the stress block method. It also shows that the flexure capacity of beams was not reached due to premature shear failure. Even for beam B5 where flexural failure seems to have coincided with shear failure, the experimental results indicate that shear was still the primary reason for failure and it only coincided with the onset of yielding of the steel reinforcement. This is so because the steel had not shown any serious sign of yielding, often associated with accelerating steel strains, when ultimate failure in shear occurred. When these experimental results are then compared with predictions based on the properties of brickwork and steel used for the beams, flexural failure was not indicated. Results given for the other beams with high % steel also show that there is moment degradation due to shear failure. The analysis confirms that the failure of these beams was due to shear and not due to flexure except for the direct method which predicts flexural failure for beams with low % steel. However, experimental evidence had shown that shear failure had occurred prior to flexural failure in these beams.

Also, when the internal moment of resistance was calculated from the experimental measurements of both brickwork compressive strains and the steel strains and the results were compared with the applied moment at the instant just prior to failure, the observed results were reasonable as given in Table 4.6.2.

4.7 CONCLUSIONS

From the work done, the following conclusions can be drawn :

(1) For pocket-type reinforced brickwork, shear strength is strongly influenced by the *a/d* ratio. Shear strength of these beams decreases with increasing shear span/effective depth ratio.

(2) From the limited tests, it appears that the shear strength of pocket-reinforced brickwork beams is not significantly affected by the % steel.

(3) The plastic method originally developed for predicting shear strength of concrete beams can be used successfully for predicting the shear strength of pocket-type reinforced masonry beams provided the effectiveness factor is obtained from the expression developed in this work.

(4) Both the direct method and the method based on Branson's[37] procedure gave good prediction of deflections of pocket-reinforced beams tested in this work. The method based on the direct method gave a closer prediction than Branson's method, in most cases especially at higher bending moments.

(5) The test results show that the partial safety factor for material on shear stresses for the pocket-type reinforced brickwork beams appears to be lower than 2, hence the code provision is not very safe. The code provisions for shear strength may therefore be revised to reflect this.

CHAPTER 5

BEHAVIOUR OF REINFORCED BRICKWORK POCKET-TYPE SLABS

5.1 INTRODUCTION

The problem of deciding on the maximum spacing at which to place the pocket stems, while ensuring that flanged-action takes place from cracking to the ultimate point is yet to be resolved. This is further compounded by paucity of experimental data on the actual flanged-action behaviour of these walls. This paucity of data has led to conservative code provisions[2] on this matter, notably, the restrictions placed on the maximum flange width of the section, which the code assumes for the behaviour of reinforced brickwork pocket-type walls. This present investigation has therefore been carried out to attempt to determine the existence or otherwise of the structural action, its possible extent and characteristics. To this end, six slab specimens were tested, keeping all variables constant except the pocket stem spacings.

This chapter reports on the experimental and theoretical investigation into the structural behaviour of reinforced brickwork pocket-type slabs subjected to lateral loading and in which the spacings of the pockets were varied.

In the experimental work, the effect of pocket stem spacing as a variable on the structural behaviour of these walls was investigated. The deflection and ultimate strength behaviour were investigated and used to characterize wall behaviour. The effect of varying the pocket spacing on the ultimate load carrying capacity is also studied in a theoretical analysis. The experimental results were compared with the provisions of the code[2].

The concept of effective width of the walls is discussed based on the experimental results and against the backdrop of some theoretical considerations. Furthermore, a

method of calculating the effective widths associated with the different spacings is presented.

A brief description of the design procedure[2] for pocket-reinforced wall sections is included. Also, the details of the experimental set-up for this investigation are described. Finally, on the basis of the experimental results obtained and the theoretical analysis carried out, suggestions for further improvement of the design of these walls are given.

5.1.1 Programme of test

For all the six slab specimens tested, the span was maintained constant at 1200mm. The pocket stem spacing of the specimens was varied between 0.5 m and 1.8 m, that is, 1.0 m and 3.6 m respectively in a corresponding wall that uses full-sized brick units. The specimens were, therefore, simply increased in length to accommodate the respective spacings between the reinforced stems.

5.2 DESIGN OF REINFORCED BRICKWORK POCKET-TYPE WALLS BY THE CODE PROVISIONS

The British Standard which gives guidance on the design of brickwork pocket-type walls is BS5628:Part 2 (1995)[2]. Prior to the formulation and adoption of this code of practice here in the UK, publications by the BCRA (British Ceramic Research Association) and the BDA (Brick Development Association) were used mainly as reference sources for the design of these walls. These publications basically considered pocket walls as homogeneous cantilevers (since most of these walls are cantilever structures, anchored to a solid reinforced concrete base) for pocket spacings not exceeding 1 m. For pocket spacings greater than 1 m, these walls were designed as a series of "T"-sections with reduced flanges. In these latter cases, it was considered necessary to check the capacity of the brickwork to span between the reinforced pockets. Previously, design principles incorporating both elastic and load factor methods have been employed for the design of these walls.

The current code of practice adopts the limit state philosophy of design. The code treats pocket-walls as flanged members regardless of pocket spacings. This is a similar approach used in the design of hollow concrete blockwork walls having regularly spaced protruding ribs. Perhaps in order to achieve consistency with methods employed for reinforced concrete members, the design formulae have been given in a similar manner for pocket-reinforced walls. The assumption made is that the ultimate limit state, rather than the serviceability limit state, would be critical. The partial safety factors associated with the ultimate limit state are therefore employed for design purposes. To satisfy the serviceability criteria of cracking and deflection for instance, some recommendations are offered which ensures that certain boundary values, based on the wall geometry, are not exceeded.

In the actual design of these walls, the first task to be performed is the accurate assessment of the load which is most likely to be sustained throughout the wall's useful life. As most of these walls are made to retain earth materials, procedures employed to calculate load in earth retaining structures are used to consider different possible loadings and their combinations. For example, considerations are given to both active and passive earth pressures, calculation of surcharges and implications of possible land-use changes which may subsequently affect load distribution on these walls. Details of these issues are not the subject of this thesis but it is sufficient to state that an accurate determination of the most critical case of loading on the wall has been made. Following this, a preliminary sizing of the element based on the support conditions of the wall is carried out and subsequently, the calculations are based on forces acting on a unit (1m) width of the wall and conducted such that all the capacities are calculated on this basis.

The moment of resistance used in designing the walls is computed on the basis of either of the following two equations :

$$M_d = \frac{f_f}{\gamma_{mm}} b t_f \left(d - 0.5 t_f\right) \qquad \text{---------- (5.2.1)}$$

$$M_d = \frac{f_y}{\gamma_{ms}} A_s\left(d - 0.5t_f\right) \qquad \text{---------- (5.2.2)}$$

where

M_d = design moment of resistance

A_s = area of reinforcement

b = effective width of the flange

d = effective depth of the reinforcement.

f_f = characteristic compressive strength of reinforced masonry in bending

f_y = characteristic tensile strength of reinforcement.

t_f = flange thickness

γ_{mm} = partial safety factor for compressive strength of masonry

γ_{ms} = partial safety factor for strength of steel

t_f is taken as the lesser of t_u and 0.5d, where t_u is the thickness of the unit on the compressive side of the pocket.

b is taken as the lesser of the pocket spacing, the breadth of the pocket plus $12t_u$, or one-third the wall height.

The maximum flange width allowable by the code of practice[2] is the lesser of :

(a) width of the pocket plus 12 times the thickness of the flange,

(b) the spacing of the pockets, or

(c) one-third the height of the wall.

While equation 5.2.1 computes the moment of resistance based on the brickwork, equation 5.2.2. computes the moment of resistance based on the steel. In design parlance, a reinforced pocket wall is said to be under-reinforced when the reinforcing steel moment of resistance is less than the brickwork moment of resistance. Such walls fail by yielding of the steel reinforcement inside the pockets. On the other hand, when the reinforcing steel moment of resistance exceeds the brickwork moment of resistance, these walls are termed over-reinforced. Over-reinforced walls fail by crushing of the brickwork rather than by yielding of the steel reinforcements.

5.2.1 Design for Shear

The overall shear resistance is provided by the whole of the effective depth of the section, except in cases where the brickwork thickness between the pockets is lower. Then, in such instances, the actual thickness of the brickwork in between the pockets is used. At the calculated design load, the member is sized such that the average shear stress does not exceed f_v / γ_{mv} where f_v is the characteristic shear strength and γ_{mv} is the partial safety factor for the shear strength of the brickwork. The procedure just described could be broken into four steps as follows :

(a) Obtain the percentage steel ratio associated with the wall,

(b) Deduce the characteristic shear strength associated with this percentage steel ratio from the relevant equation in the code,

(c) Calculate the characteristic shear load based on the knowledge obtained from step (b) above,

(d) Calculate the design shear load by applying the partial safety factor for shear.

This load is the design shear resistance of the wall section which must not be exceeded in service.

5.3 EXPERIMENTAL DETAILS

Table 5.3.1 gives details of these reinforced walls made of $\frac{1}{2}$-scale bricks, each of which was 1 brick (115mm) thick and spanned 1.2 m . The overall length is determined by the spacing which varied between 0.5 m and 1.8 m for the $\frac{1}{2}$-scale brickwork models. The objective is to investigate structural behaviour when the spacings between the reinforced pockets are varied while other wall parameters remain constant.

Table 5.3.1 : Details of Reinforced Wall Parameters (RW1-RW6)

Wall Type	Width B (mm)	Span L (mm)	t (mm)	Pocket Spacing S (mm)	Steel bar Type per Pocket	effective depth d (mm)	% Steel	Yield Stress (N/mm^2) Ref[13] .
RW1&RW2	800	1200	115	540	1T-10	90	0.2	500
RW3&RW4	1280	1200	115	1000	1T-12	90	0.2	470
RW5&RW6	2030	1200	115	1750	(1T-12) plus (1T-10)	90	0.2	470 & 500

where

L = Span of wall (or Height of wall)

B = Overall width of wall

t = thickness of wall

S = Spacing of reinforced concrete pockets

RW1 - RW6 are the pocket-reinforced walls (Nos 1 to 6)

All the walls were built on a reuseable steel channel base to prepare the pockets for the subsequent reinforcing and grouting operations.

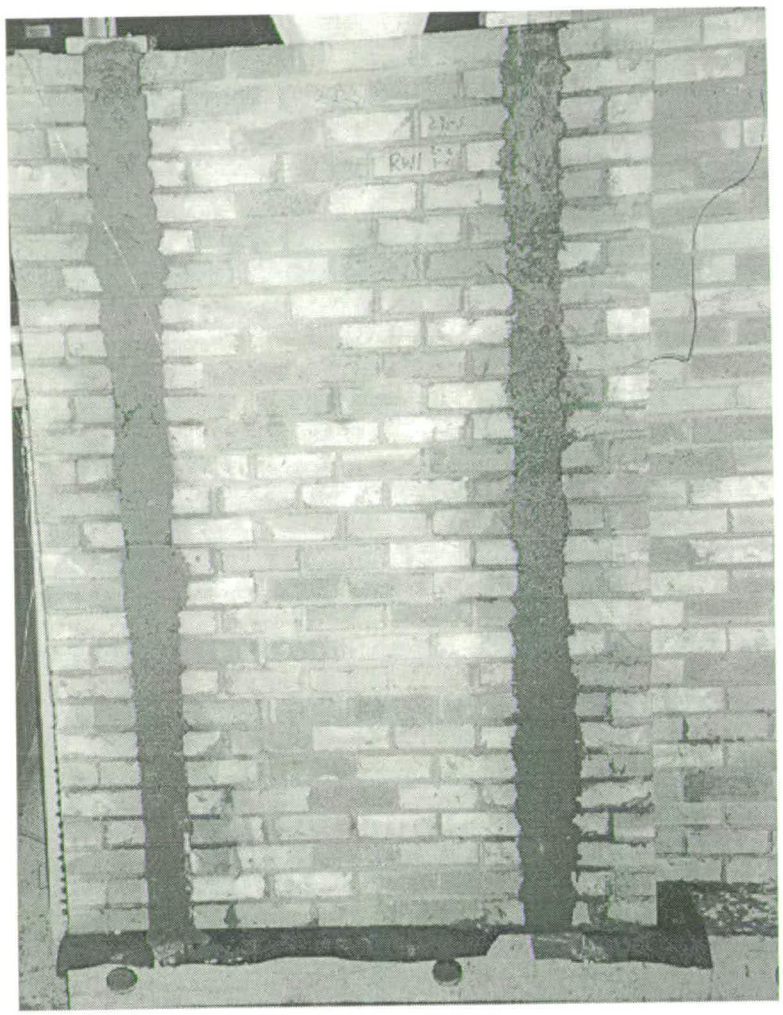

Fig 5.1 : Grouted reinforced brickwork pocket-type wall built on a reuseable steel channel base (RW1)

After the construction and curing was completed, shuttering was clamped to the rear face of the wall and grout poured into the pockets and carefully compacted using a thin steel rod which is easily accommodated by the small hole provided by the pocket (Note : All these walls were built with rapid-hardening portland cement in order to speed up the hardening process and strictly implement the testing programme). The same concrete and mortar mix proportions used for the full-scale beam shear tests were used for the construction of these walls. After the grouting operation was completed, these walls were covered with polythene sheets and curing was allowed

for at least 14 days before final testing was done. Details of part of the construction processes and subsequent testing of these walls are shown in Figs 5.2-5.7.

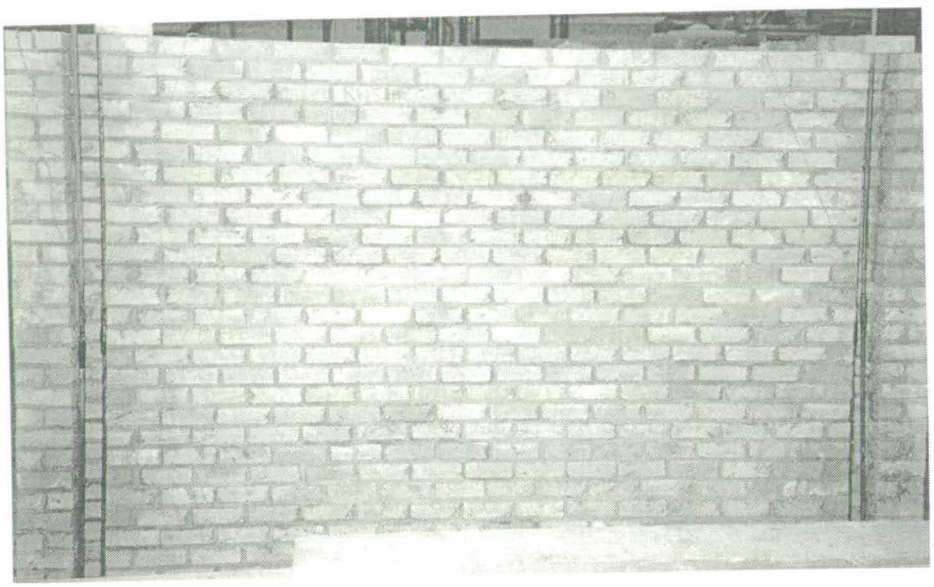

Fig 5.2 : Long wall ready for grouting

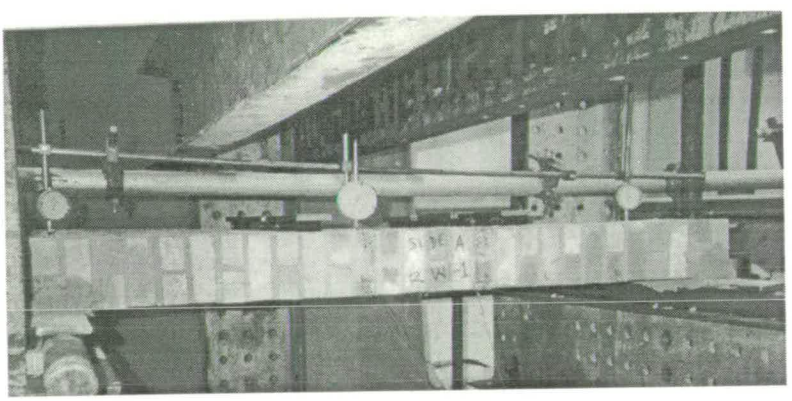

Fig 5.3 : Typical Test assembly for reinforced walls

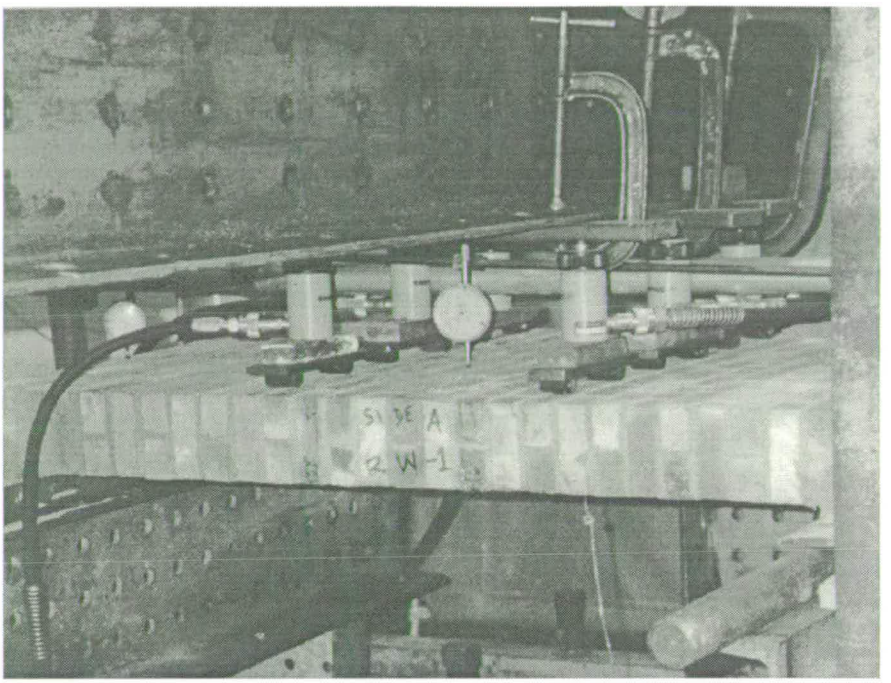

Fig 5.4 : Transverse Loading applied to RW1

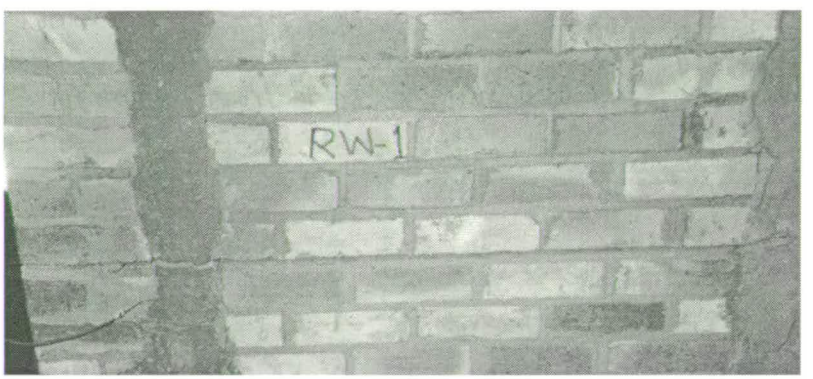

Fig 5.5 : RW1 after test (showing pocket side)

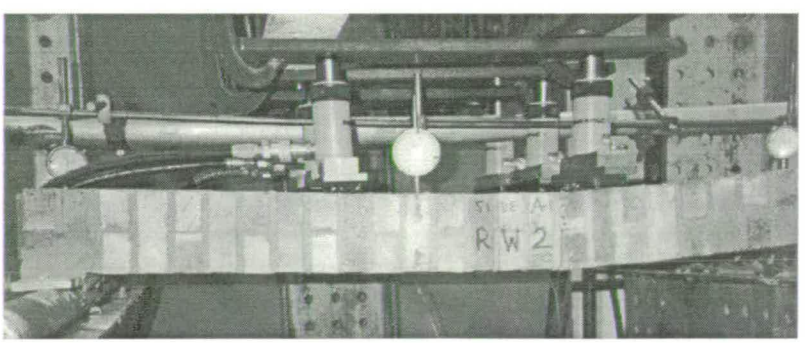

Fig 5.6 : RW2 undergoing testing

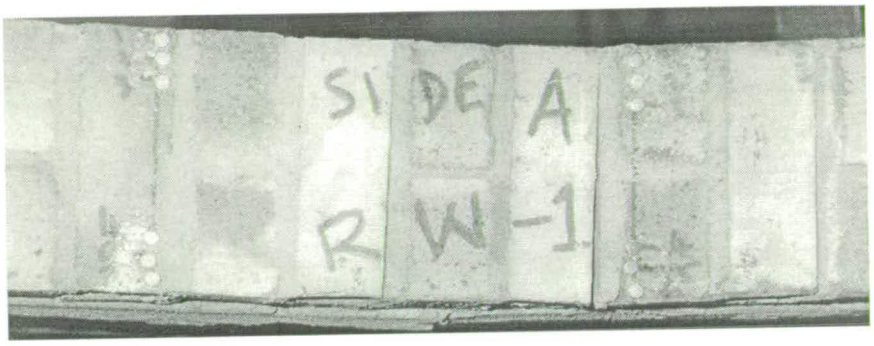

Fig 5.7 : Side Elevation of RW1 showing demec points in the maximum bending moment region

Loading Arrangement

Each of the walls was loaded laterally by a combination of loading jacks applied at the compression face. A system of hydraulic jacks is employed with one of the jacks acting as the control jack to record load measurements via a load-cell. This load-cell has been previously calibrated and was connected to a digital voltmeter. The load itself was applied by a "Losenhausen" machine capable of applying constant and sustained loading for long periods of time. The load combination applied to each wall was such that a distinct region of the slab was created where the flexural effects became critical and where all the measurements required in both the steel and the brickwork were taken. The strains in the steel reinforcement were measured using electrical strain gauges of 5 mm gauge length.

The slab sections were tested in a specially-designed testing rig incorporating both loading and reaction frames which were independently bolted to a strong floor. These two frames were made adjustable so that extensions could be made for testing the longer specimens. The testing rig assembly was completed by an independent deflection-measurement frame used to monitor the deflection of the specimens throughout the loading history until very close to the ultimate point.

The slabs were supported on a frame fixed to a strong floor. The transverse load was applied by hydraulic jacks connected to a reaction frame. The reaction frame is made up of a combination of parallel steel channel sections that anchor independently to the

strong floor. The deflection measurements in the central regions of these slabs were carried out using the third independent frame; made sufficiently rigid, to ensure that accurate deflections were obtained to an accuracy of 0.002 mm. In other words, all the three frames constituting the rig assembly acted independently of each other throughout the testing process.

Incremental loading was applied to the slabs and after each increment, deflection measurements were taken from the dial gauges, while the steel strains were obtained with a "Sangamo" strain-gauge measuring meter. The brickwork strains in the two orthogonal directions of loading were then measured using the mechanical "demec" gauges capable of taking measurements to the order of 10μ. After all the measurements have been taken for a particular loading increment, the slab specimen was observed for any sign of cracking and the location noted. Thereafter, another round of measurements were taken just before the next loading increment was applied so as to monitor any creep effects. When the loading stage was sufficiently advanced and close to the ultimate, recording of the brickwork strain measurements was stopped for reasons of safety. In other instances, when either the deflection or steel strain measurements were judged to be sufficiently large, the testing was also stopped for safety reasons. The deflection measurements were taken by a combination of dial gauges capable of taking readings to either 0.01 mm or 0.002 mm accuracy.

The strain readings in the elevation sections were taken by the 200 mm gauge length strain gauges and were dispersed as shown in Fig 5.7 & Fig 5.8. At the top of the slabs, the strain gauge readings were taken, as shown in Fig 5.9 & Fig 5.10, such that more points were concentrated around the reinforced stems than there were at distances far removed from the stems, up to the midsections of the slabs. The strain gauge length used was 200 mm in the main direction. In a perpendicular direction to this, the strain measurements were taken by a 300 mm-gauge length strain gauge. These strain gauges are more sensitive since the order of strains measured in this perpendicular direction are small in comparison to the main direction of bending. These slabs were all divided up into two halves, respectively named sides A and B,

because of the symmetrical arrangement of loading employed. The same points used for the measurement of strains on side A were used on side B.

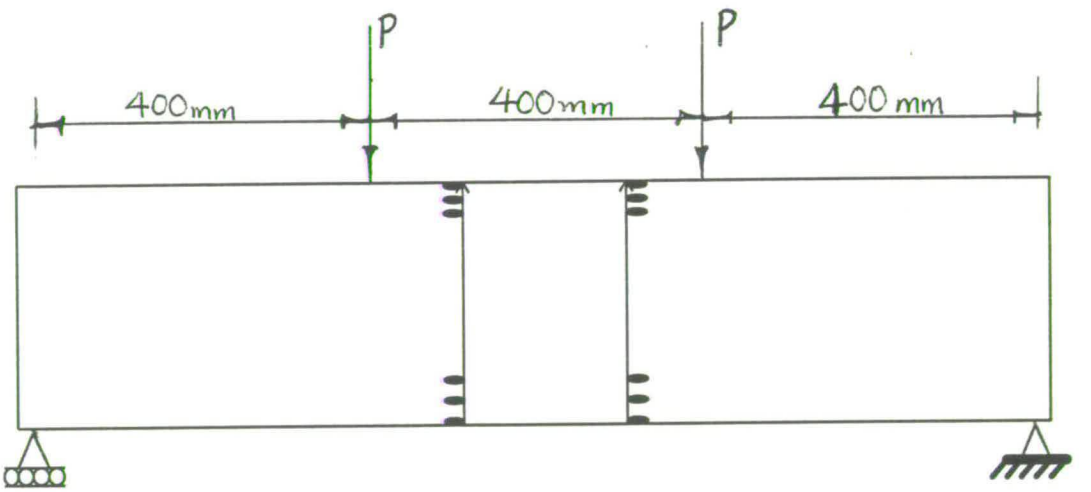

Fig 5.8 : Showing the 'demec' points for measuring the strain on slab's side elevation

Fig 5.9 : Demec point locations on top surface of slab

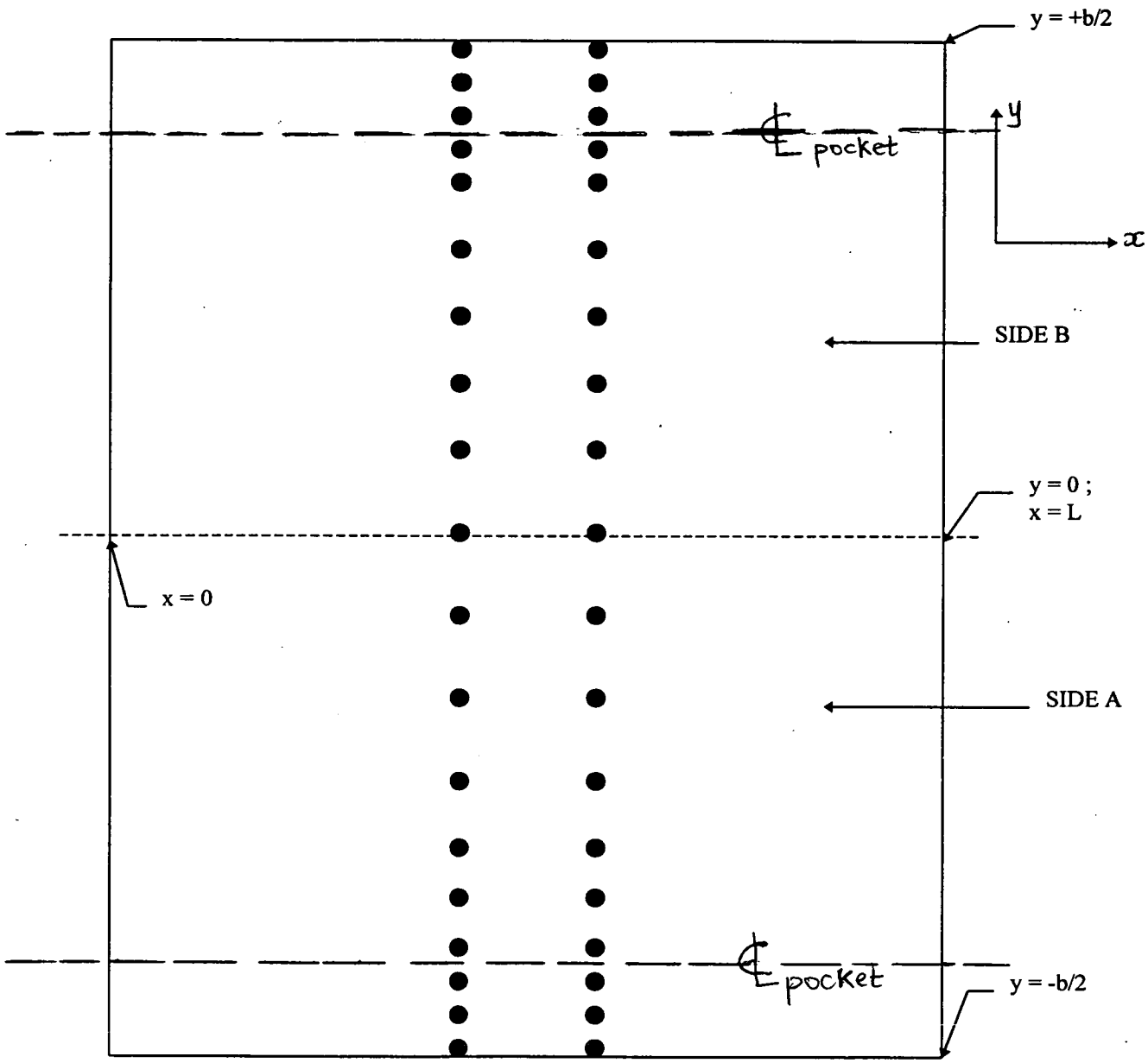

Fig 5.10 : Strain gauge measuring pin points on the top surface of slab

The slabs were all simply supported with a roller and a pinned support provided at each end of the span respectively. This was done so as to have a statically-determinate structure and simplify the experimental setup.

5.4 RESULTS OF THE TEST : The results are shown in Figs 5.11-5.58.

5.4.1 Discussion of the Experimental Results

As the loading and hence the bending moment increased, the steel strains also increased linearly, until the cracking point was reached. Once the specimen cracked, a series of changes occured both in the steel strains and the top brickwork strains measured. The linear, uniform variation of these strains was suddenly changed and various characteristics emerged regarding the structural behaviour of these walls. This was observed to be also closely dependent on the spacing of the reinforced stems. For this reason therefore, and because it is considered reasonable to group together similar slab specimens, the following presentation of the results is given.

5.4.1.1 Walls 1 and 2 (RW1 and RW2)

For RW-1 and RW-2 having the lowest spacings, steel strains grew very slowly at the beginning up to the cracking point, at which stage a sudden jump was recorded. Thereafter, the strain progressed steadily until the yield point was reached. At this stage, a sudden acceleration of the strains was experienced which progressed until the ultimate point was finally reached. The test was stopped when the deflection was growing rapidly towards collapse. For both of these slabs, the steel had yielded extensively as shown in Figs. 5.11 and 5.12.

In the case of RW1, the steel in each pocket behaved in approximately the same way and they both yielded at about the same time, approaching the ultimate failure strain in the same manner. With RW2, the two steel bars behaved in approximately the same way at the beginning up to the cracking point. Thereafter, one of them lagged behind in growth up to the yield point after which it started to drop off. The straining of the other steel bar continued, accelerating rapidly up to a very high value of about 20000 $\mu\varepsilon$ after which it started to fall off as well. This very high strain recorded by the second steel bar indicated that loss of stiffness in a portion of the plate may be accompanied by a stress redistribution.

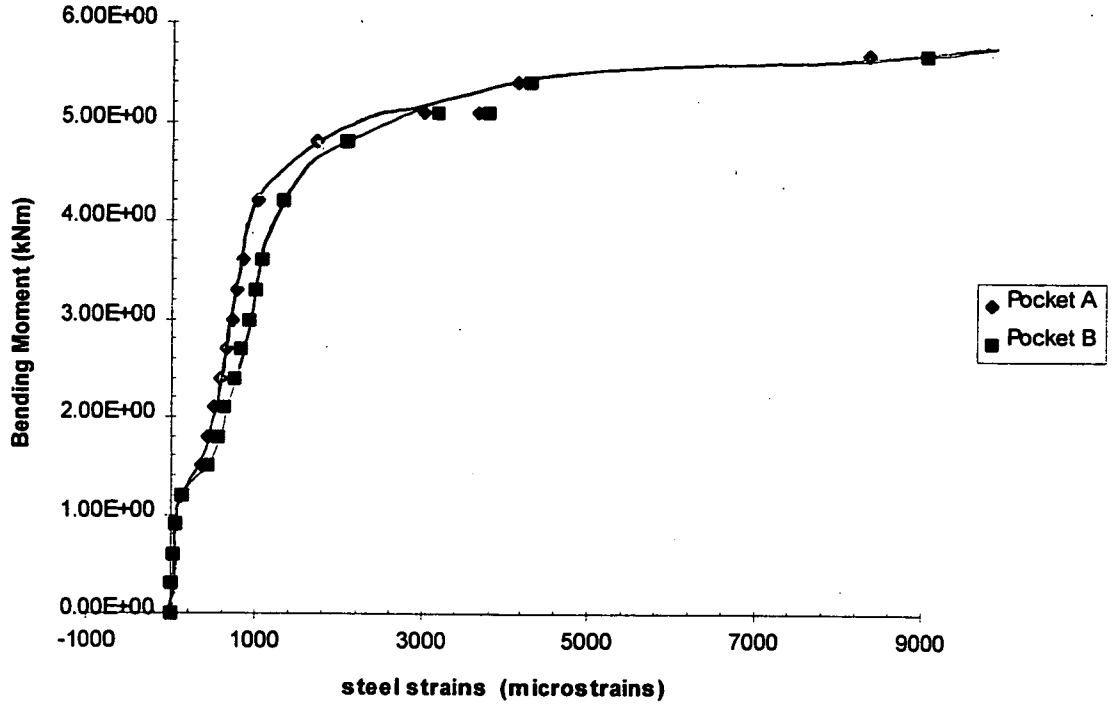

Fig 5.11 : Relationship between the bending moment and steel strains (RW1)

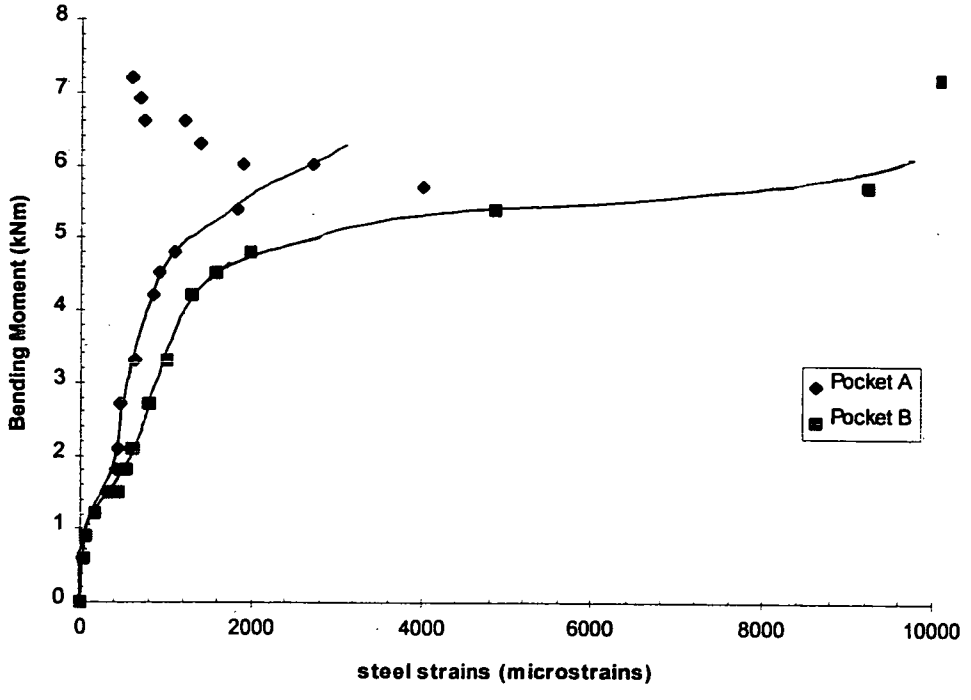

Fig 5.12 : Relationship between the bending moment and steel strains (RW2)

For both of these walls, the compressive strains were approaching the ultimate strain associated with failure, in direct compression, of the brickwork. However, the primary mode of failure of these two walls was due to yielding of the steel reinforcement in the tension zone. Although some evidence of brickwork crushing was seen in the pocket regions of these beams, these were only a secondary effect. The distribution of the compressive strains in the topmost fibre of the brickwork for both of these slabs is nearly uniform, although the strains around the pocket regions of these beams are marginally higher than at distances far removed from the pocket regions (Figs. 5.13-5.18).

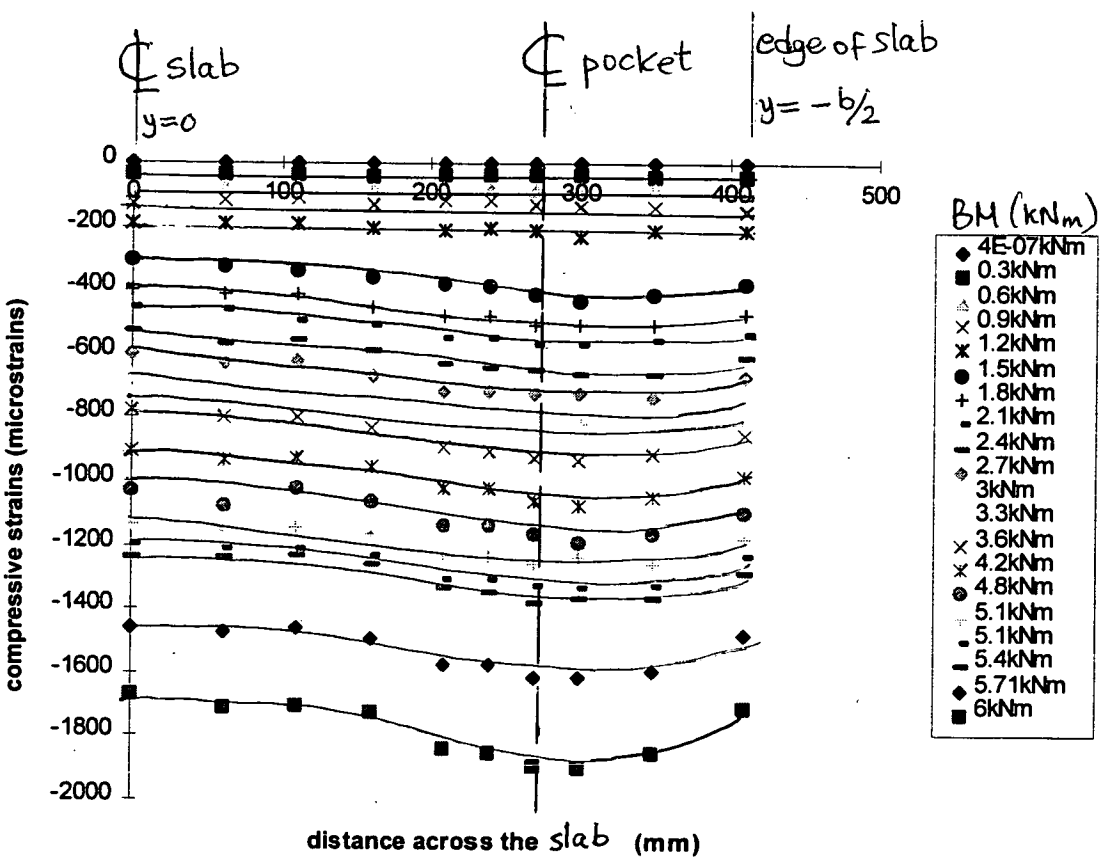

Fig 5.13 : Compressive strains in brickwork across the span (RW1) - side A

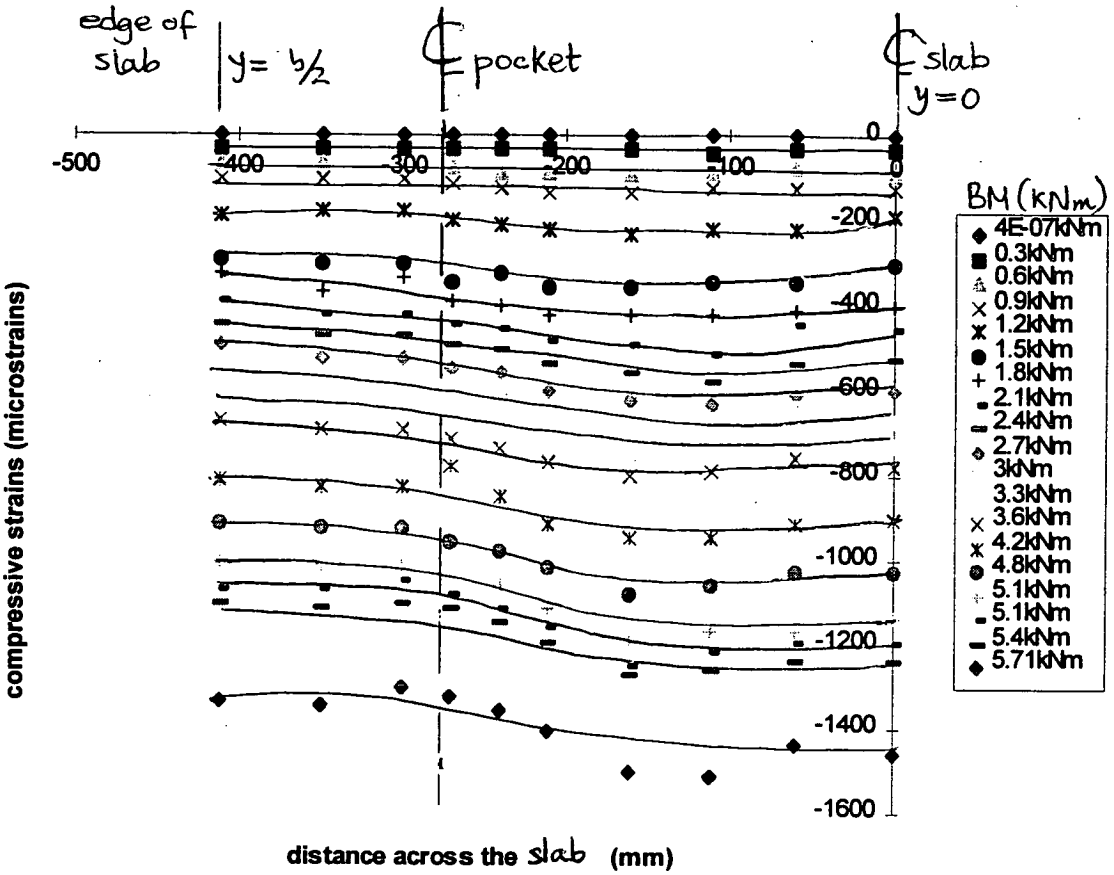

Fig 5.14 : Compressive strains in brickwork across the span (RW1) - side B

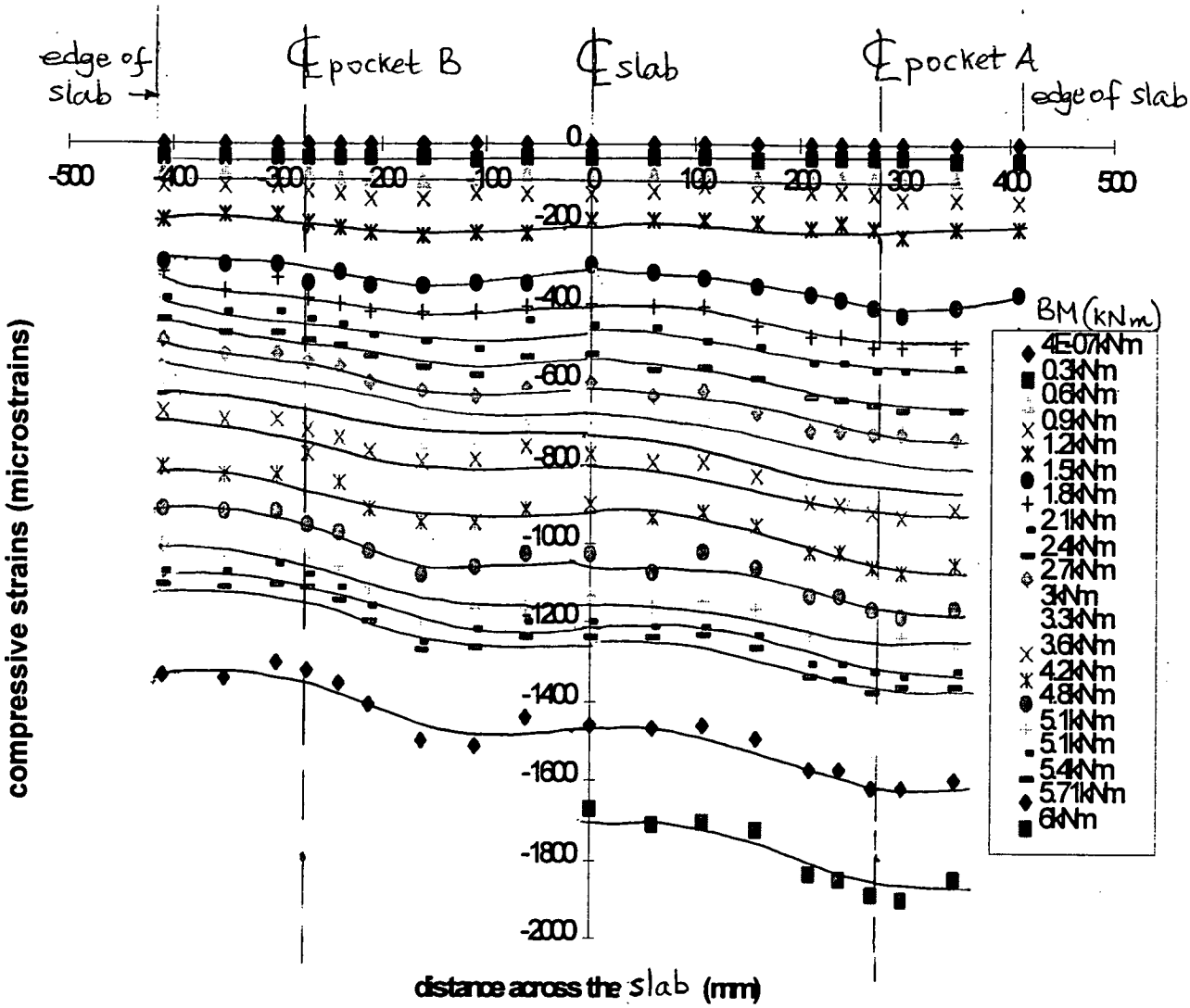

Fig 5.15 : Compressive strains in brickwork across the span (RW1) - sides A & B

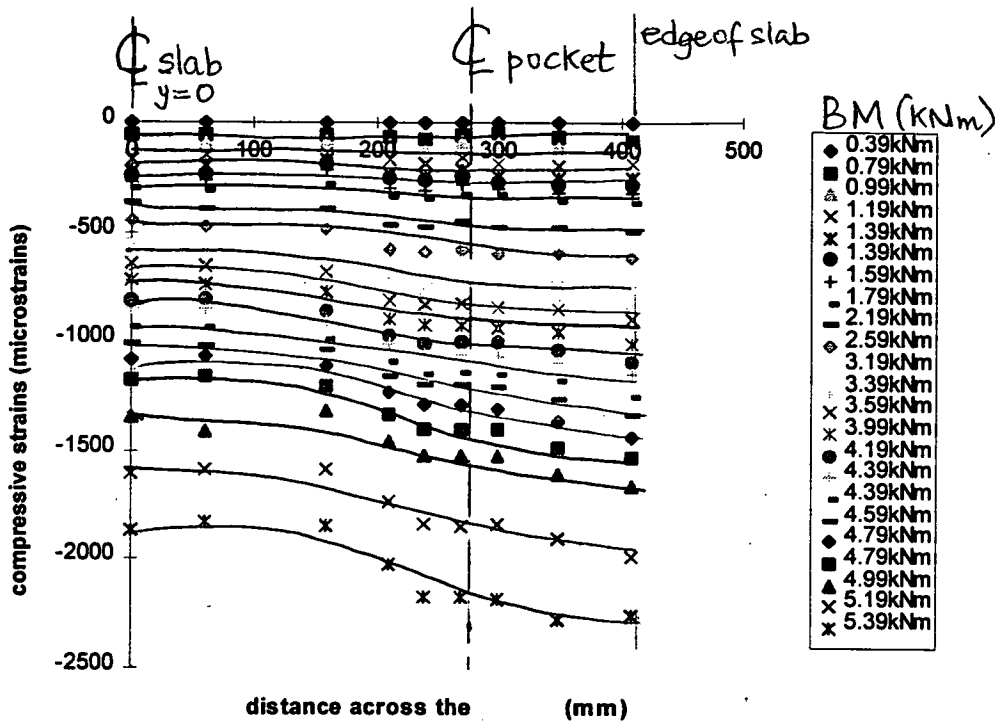

Fig 5.16 : Compressive Strains in brickwork across span (RW2)-side A

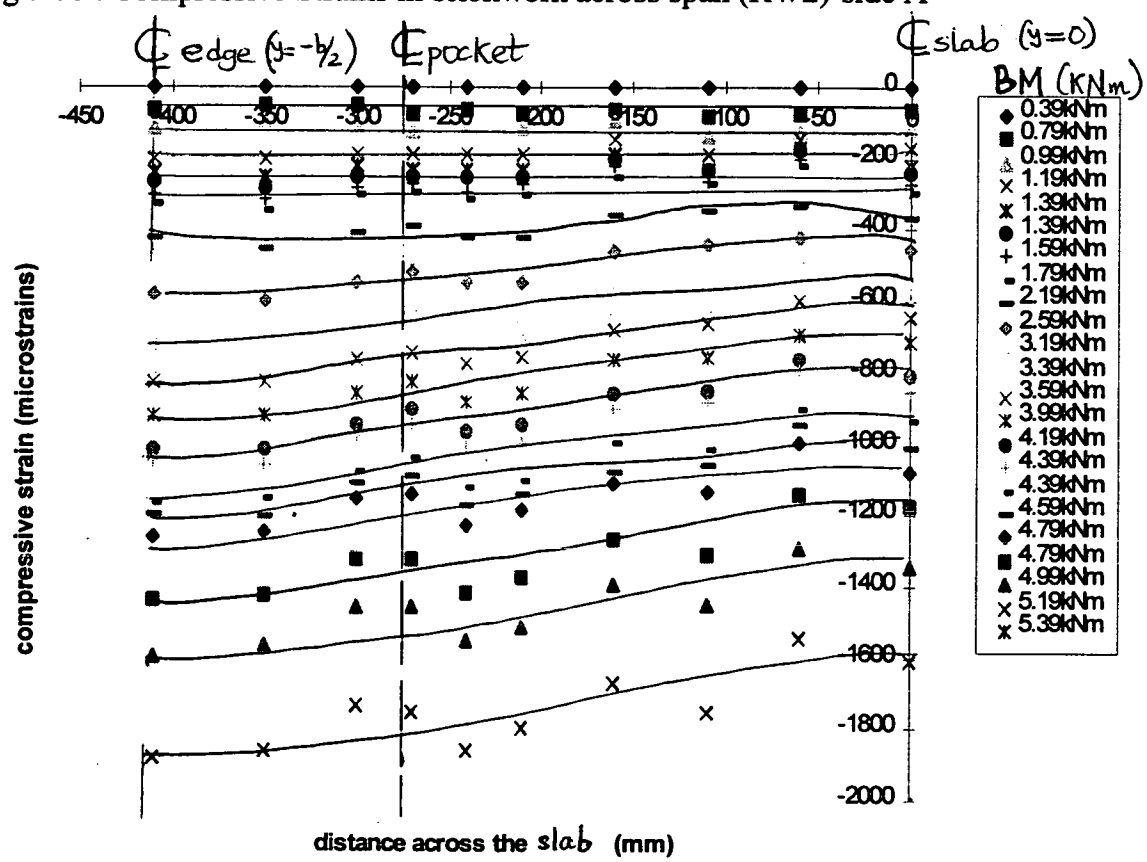

Fig 5.17 : Compressive Strains in brickwork across span (RW2)-side B

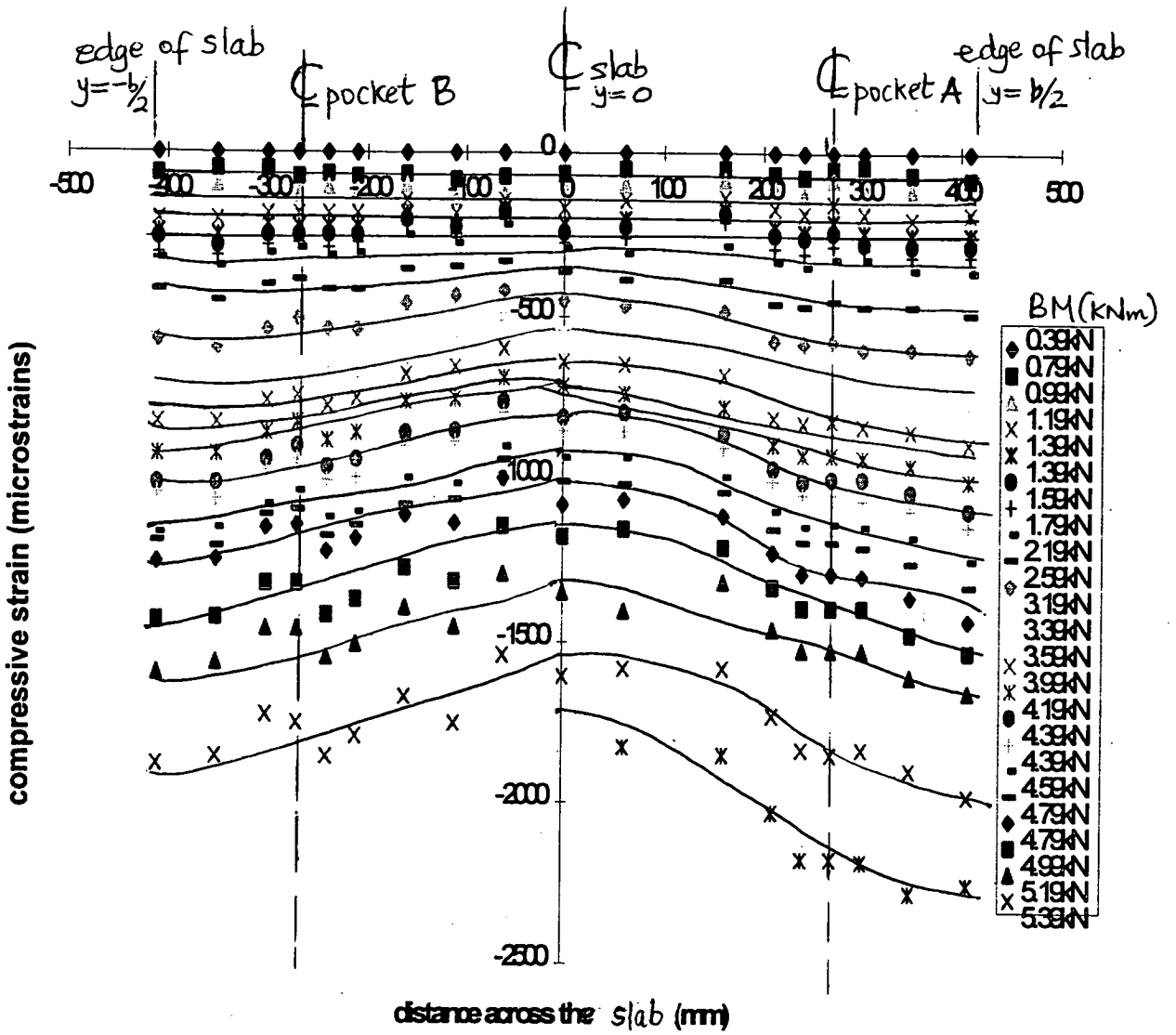

Fig 5.18 : Compressive strain in brickwork across span (RW2) - sides A & B

This distribution is somewhat analogous to that which exists in a simply supported beam of rectangular cross-section of normal breadth as predicted by the simple bending formula. For these two walls, the y-direction strains,(ε_y), are practically non-existent as no change was measured by the 300-mm gauge-length strain gauge despite its more acute sensitivity. If the distribution of ε_x strains are considered, one could observe here that practically the whole flange is active for this level of spacing of the reinforced stems.

The distribution of strains across the depth of these slabs (Figs. 5.19-5.22) show linear variations throughout the various stages of loading.

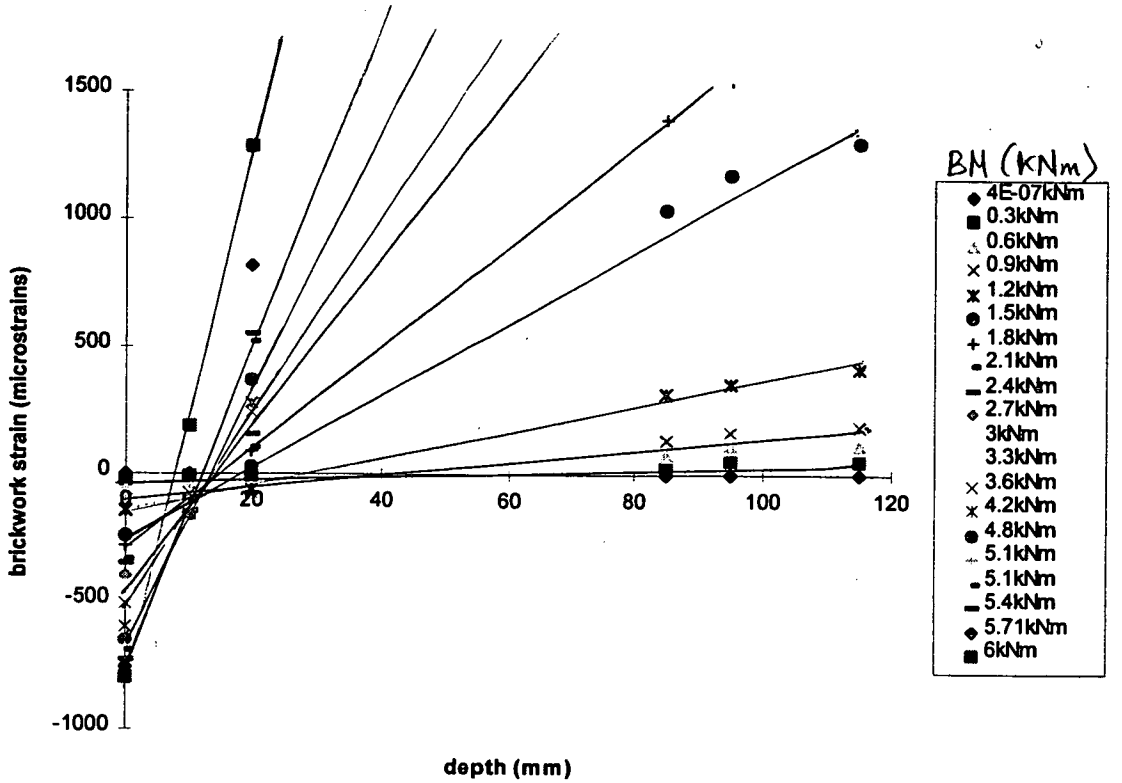

Fig 5.19 : Variation of brickwork strains through the depth (RW1) - side A

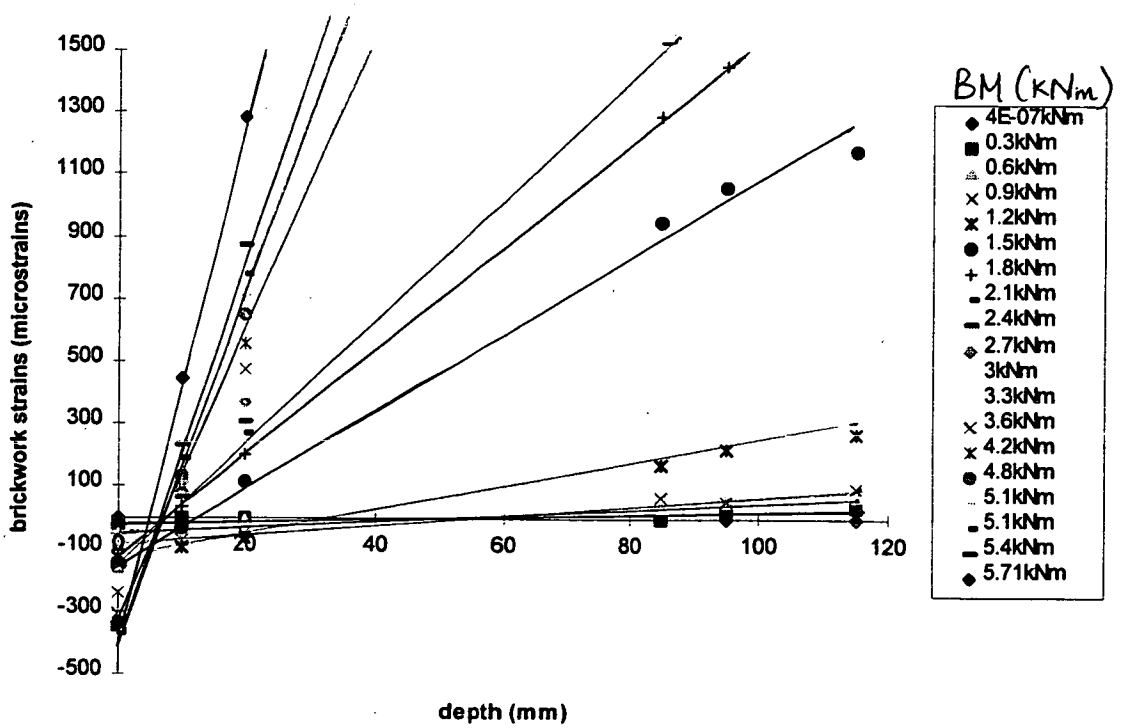

Fig 5.20 : Variation of brickwork strains through the depth (RW1) - side B

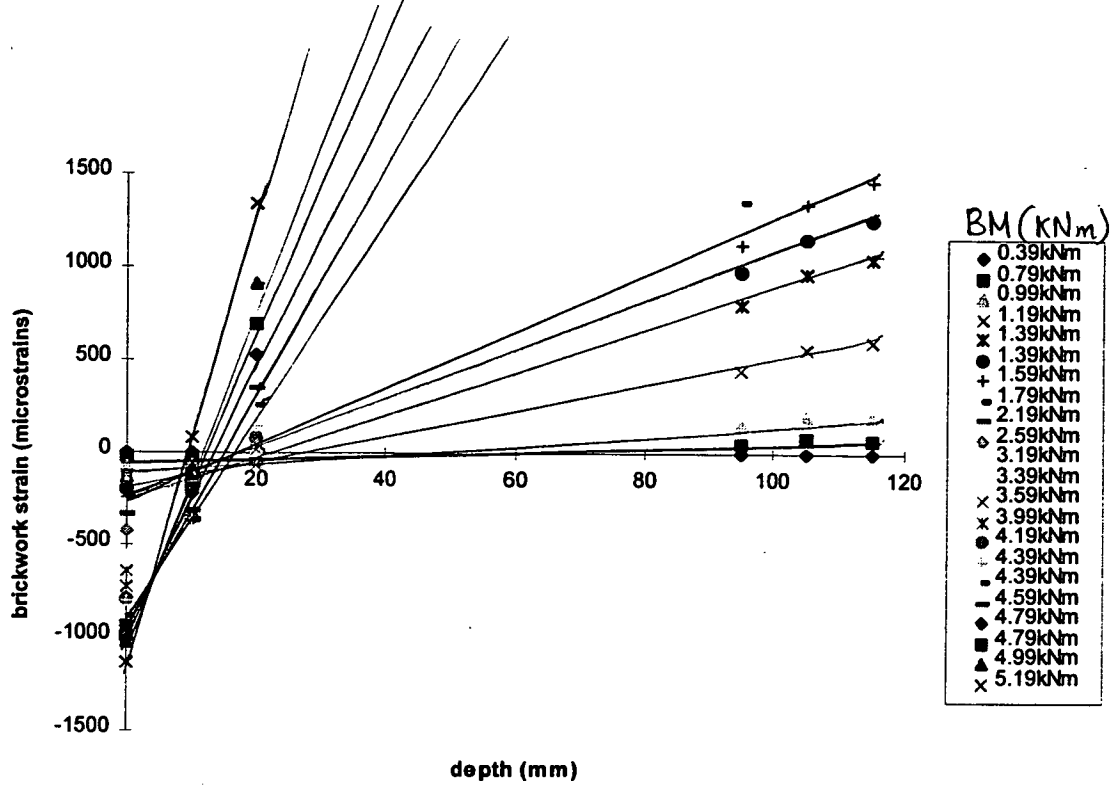

Fig 5.21 : Variation of brickwork strains through the depth (RW2) - side A

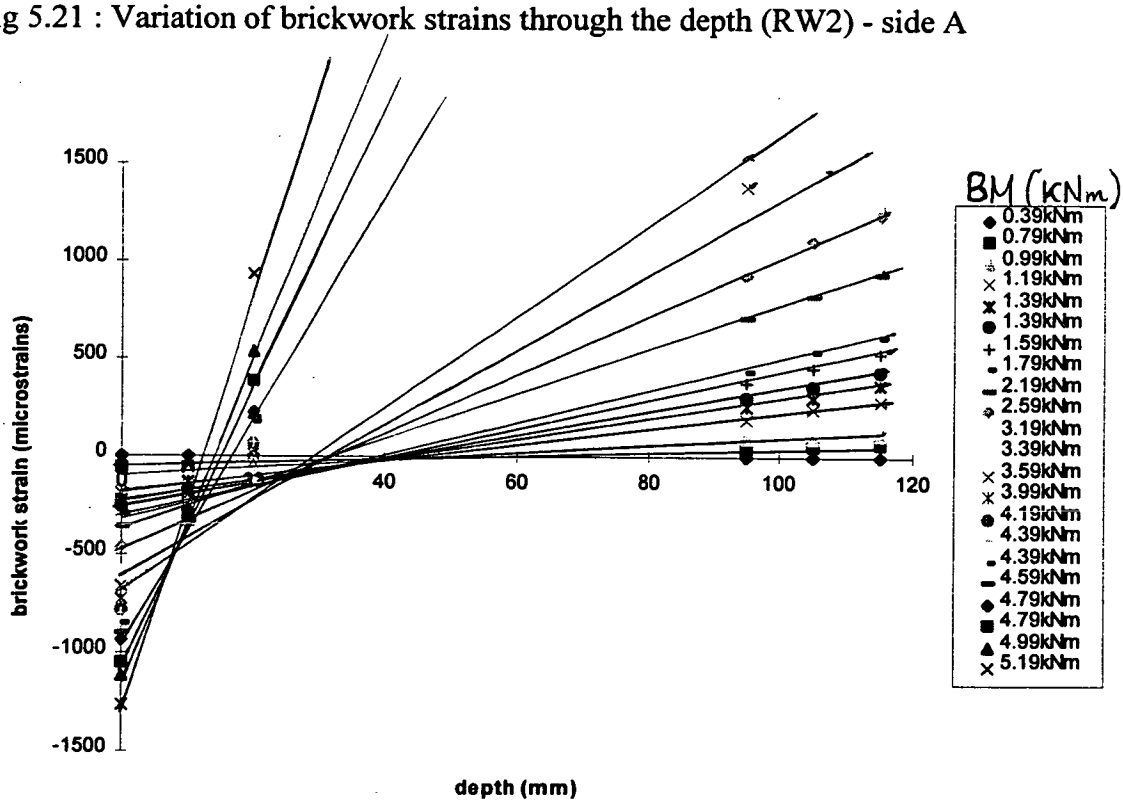

Fig 5.22 : Variation of brickwork strain through the depth (RW2) - side B

These recorded linear distributions give credence to the assumption, made subsequently in the analysis of the structural behaviour of these slabs, that "plane cross sections remained plane prior to and after bending of the slabs specimens". The central deflection behaviour of these walls were also similar (Fig 5.23 and Fig 5.24). These deflections increased slowly from the beginning up to the cracking point. After this point, the rate of growth increased and as the failure point was approached, the rate of increase became much more rapid and was accompanied with excessive rotations at the supports. The structural behaviour of these walls could also be inferred from these deflection measurements.

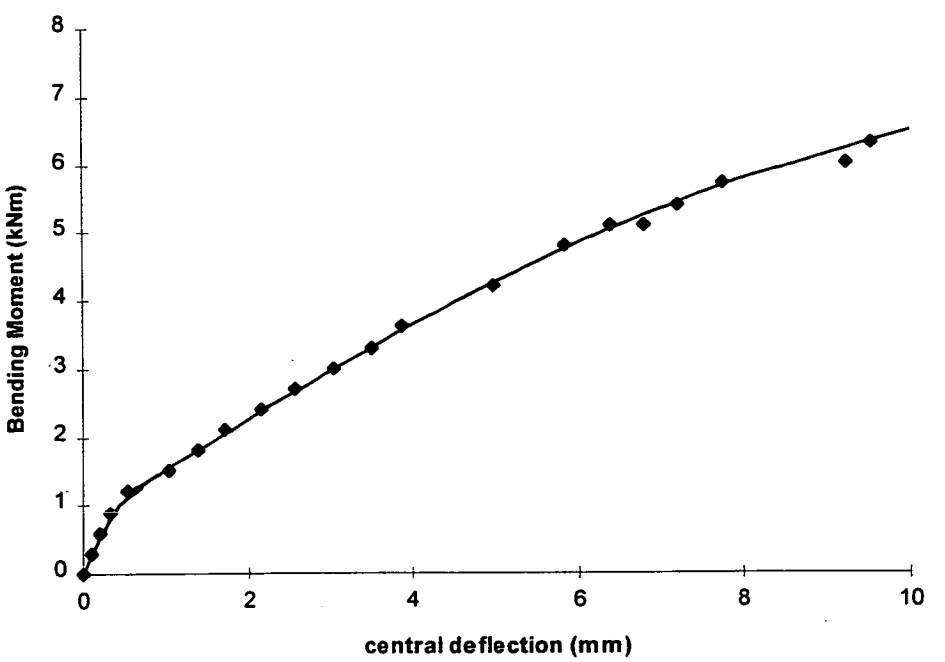

Fig 5.23 : The relationship between bending moment and the central deflection (RW1)

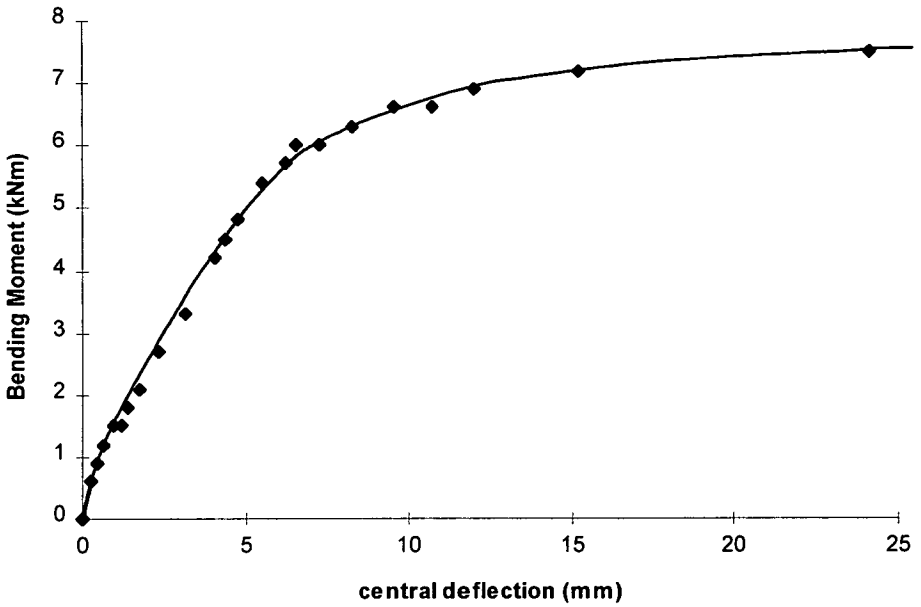

Fig 5.24 : The relationship between bending moment and the central deflection (RW2)

5.4.1.2 Walls 3 and 4 (RW3 and RW4)

When taking deflection measurements for these two walls as done for RW1 and RW2, two additional points located at 250 mm from both supports, were used for recording measurements so as to be able to get a more accurate profile of deflection along the central parts of the plate. The deflection behaviour of these walls (Fig 5.25 and Fig 5.26) was similar in character to those of RW1 and RW2 : The deflection was very small at the beginning and increased linearly up to the cracking point. After cracking, these slabs deflected more rapidly with corresponding bending moments increase. This behaviour is more apparent in wall RW4 (Fig 5.26).

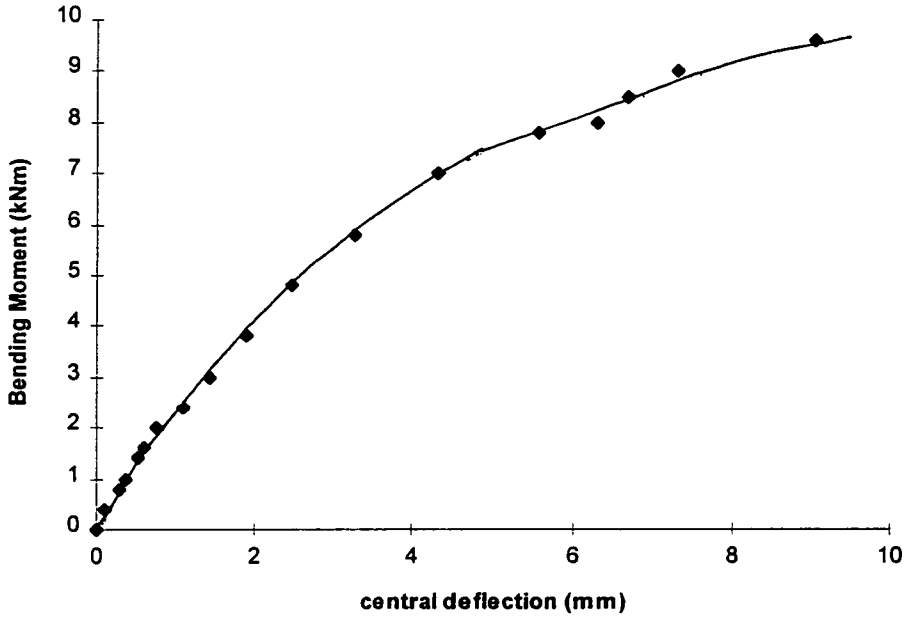

Fig 5.25 : The relationship between bending moment and the central deflection (RW3)

These two walls behaved in practically the same manner. The deflection profiles at the two points located, respectively at 250 mm, from the roller and pinned supports were similar for the same level of applied bending moment (Figs. 5.27 and 5.28).

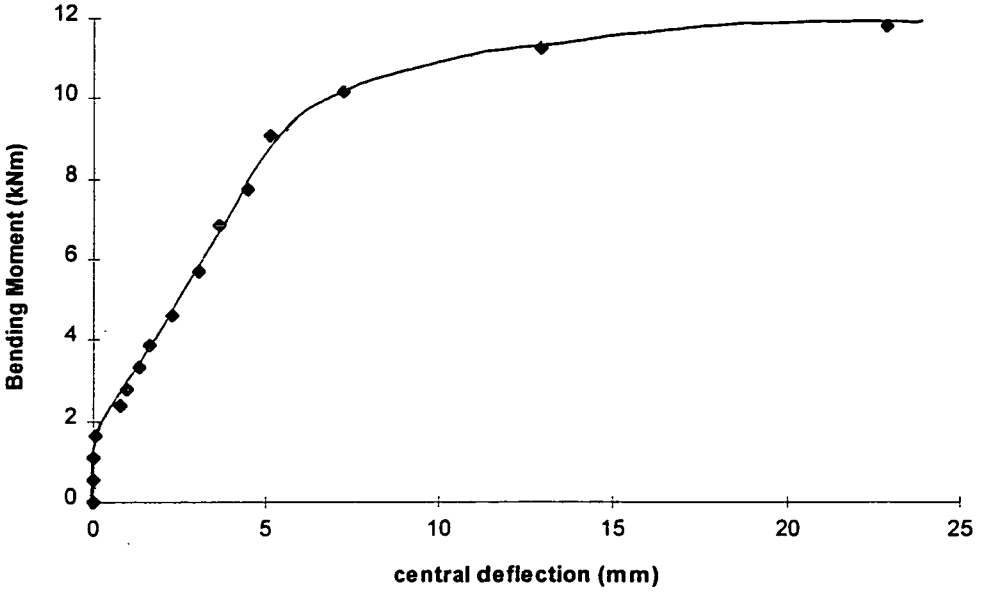

Fig 5.26 : The relationship between bending moment and the central deflection (RW4)

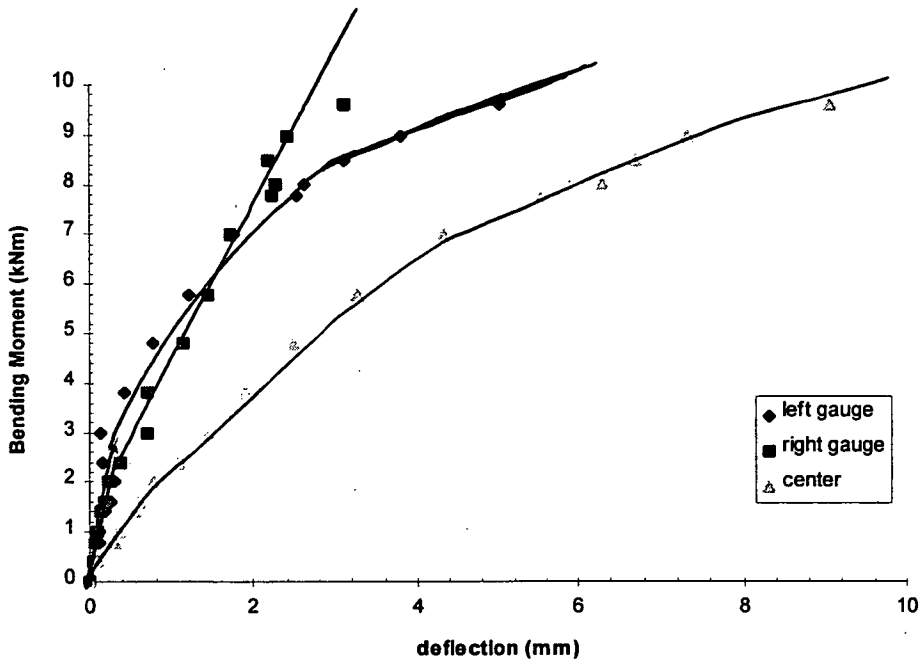

Fig 5.27 : The relationship between bending moment and the deflection along the span (RW3)

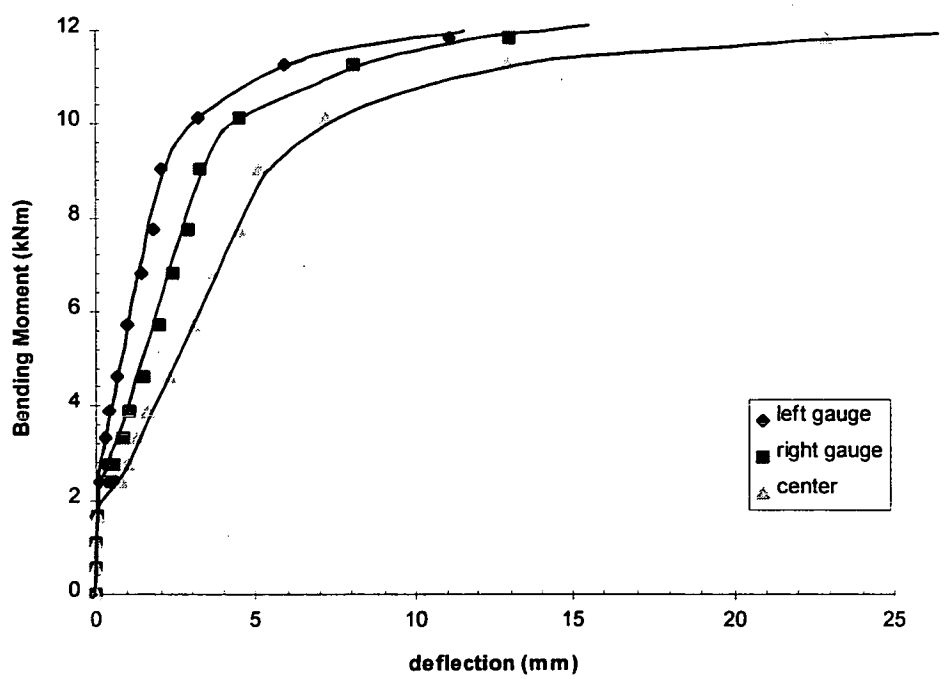

Fig 5.28 : The relationship between bending moment and the deflection along the span (RW4)

The test on RW3 was stopped much earlier than that of RW4 when it was felt that the continued taking of measurements could prove unsafe because of a strange "snapping" sound that was produced, much similar to those often obtained at the verge of collapse in brickwork prism specimens loaded in axial compression. It was therefore decided that testing should be stopped at that stage particularly because the steel had already yielded (Fig 5.29), although not severely as would normally be associated with accelerating steel strains.

The deflection of the slab at that stage was also beginning to increase more rapidly. However, the top compressive strains in brickwork at this stage were below those associated with compressive failure of the brickwork used. Nonetheless, subsequent loading to failure of this specimen was done without taking any manual strain measurements. This testing revealed that much of the reserve strength was available even after the steel had yielded severely without breaking and, some evidence of brickwork crushing was seen at the ultimate point. Failure was due to steel yielding. This experience was directly translated to the testing of RW4 which is similar to RW3 in every respect. For RW3, the top brickwork compressive strain ε_x was found to be practically uniform along the breadth before cracking. Soon after cracking, this distribution changed such that evidently more of these strains were taken up by the pocket regions of the plate relative to the other parts (Figs 5.30-32).

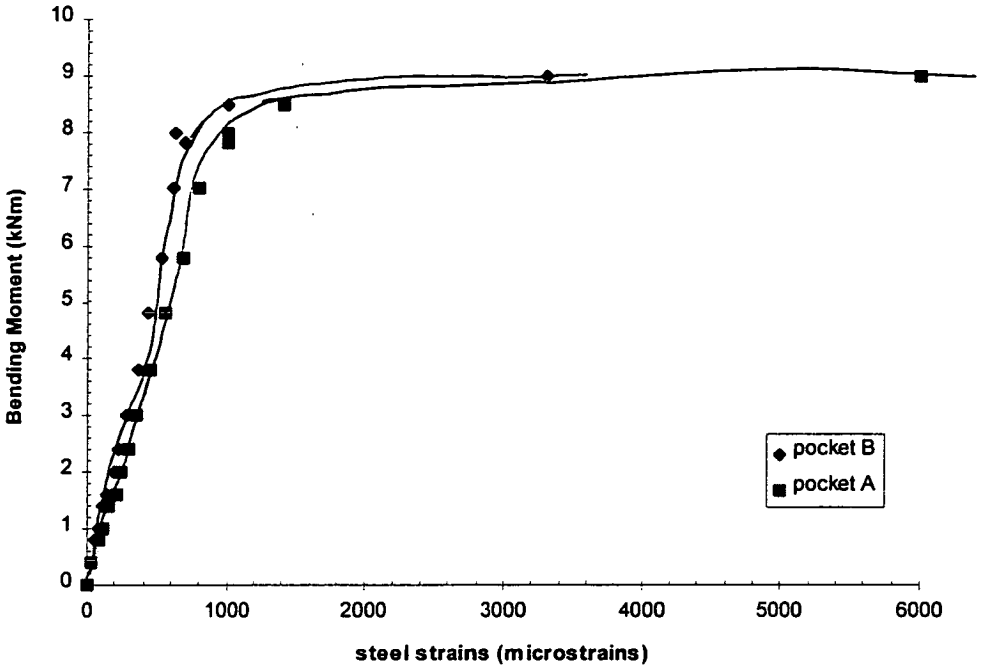

Fig 5.29 : Relationship between the bending moment and steel strains (RW3)

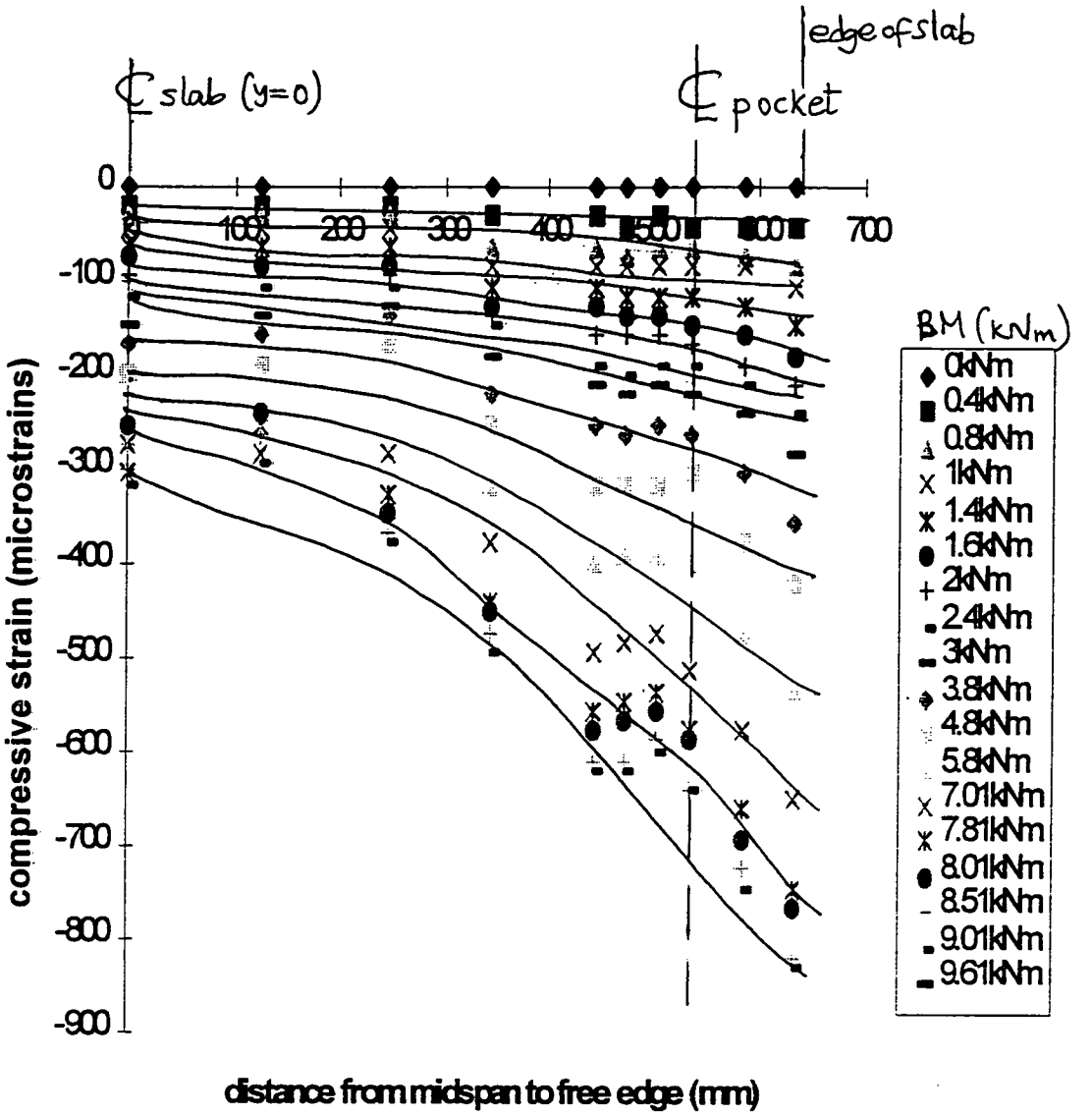

Fig 5.30 : Compressive strain in brickwork across span at various B.M. levels (RW3) - side A

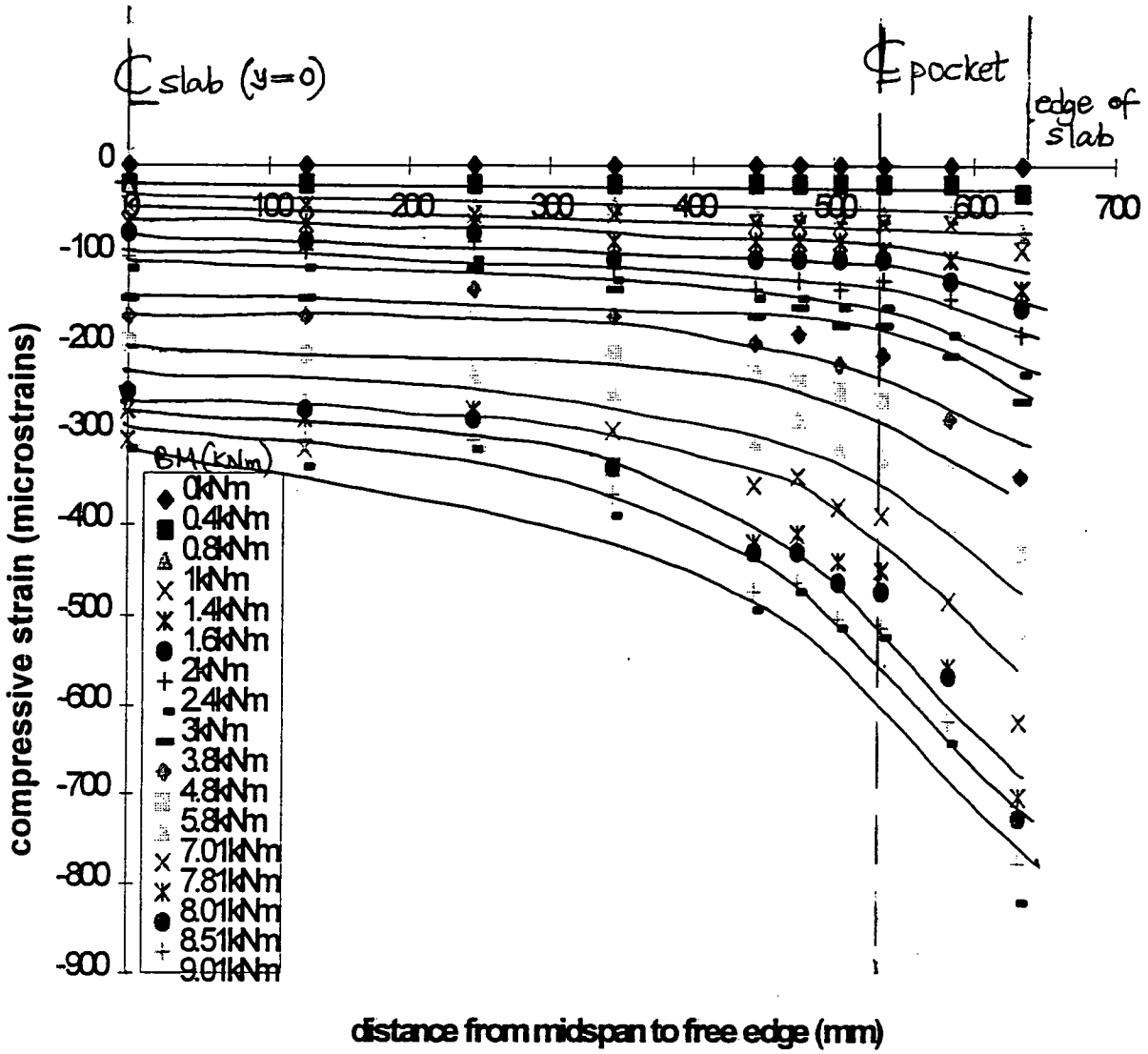

Fig 5.31 : Compressive strain in brickwork across span at various B.M. levels (RW3) - side B

A similar trend was observed for RW4 (Figs 5.33-35). Another feature of this distribution is its tendency to become more acute with increasing applied bending moment.

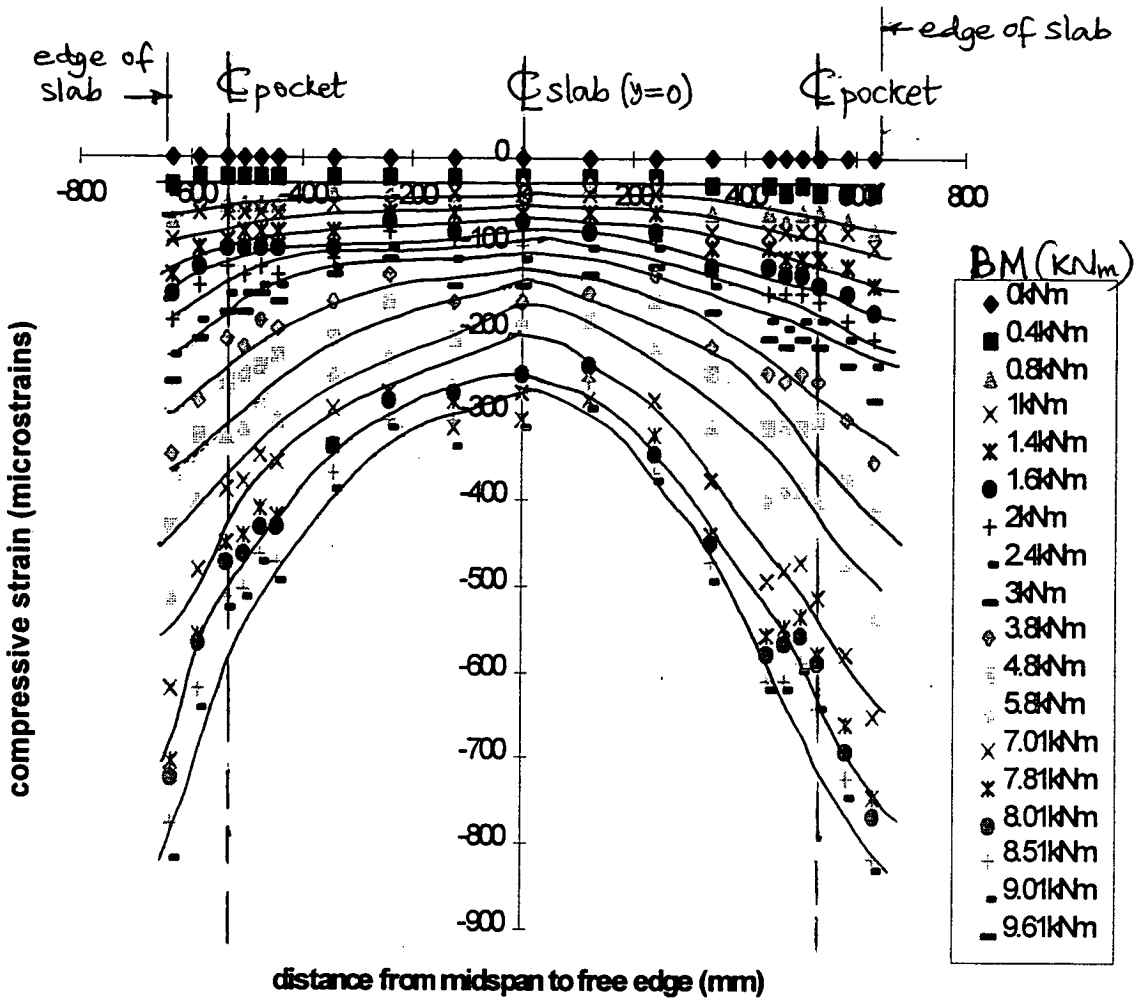

Fig 5.32 : Compressive strain in brickwork across span at various B.M. levels (RW3) - sides A & B

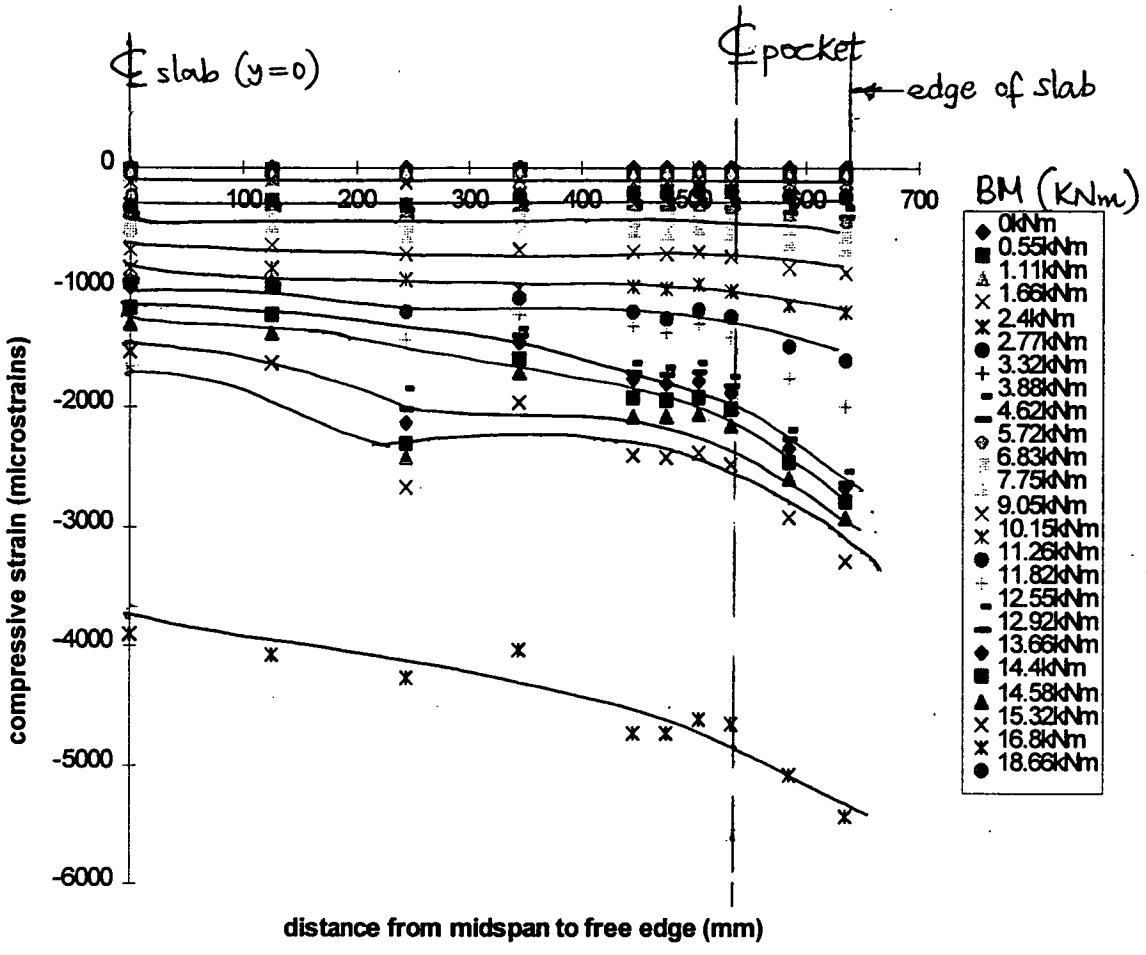

Fig 5.33 : Compressive strain in brickwork across span at various B.M. levels (RW4) - side A

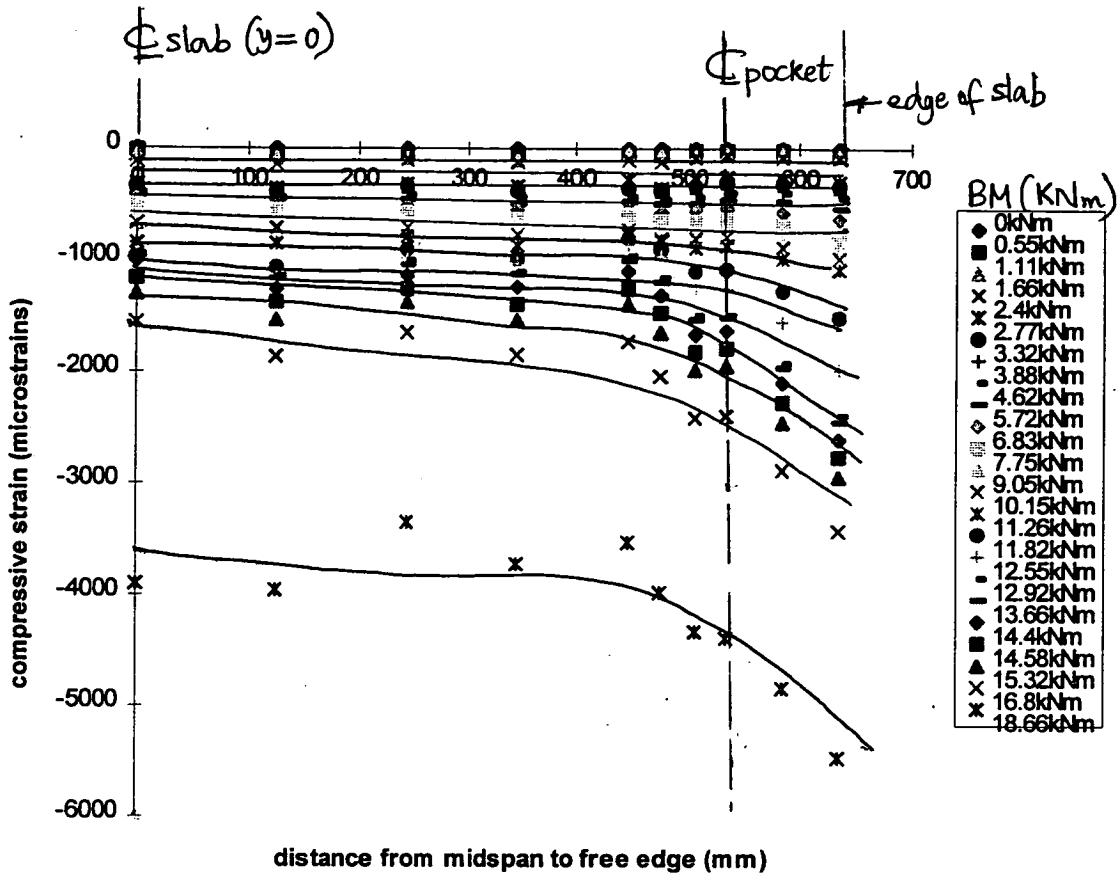

Fig 5.34 : Compressive strain in brickwork across span at various B.M. levels (RW4) - side B

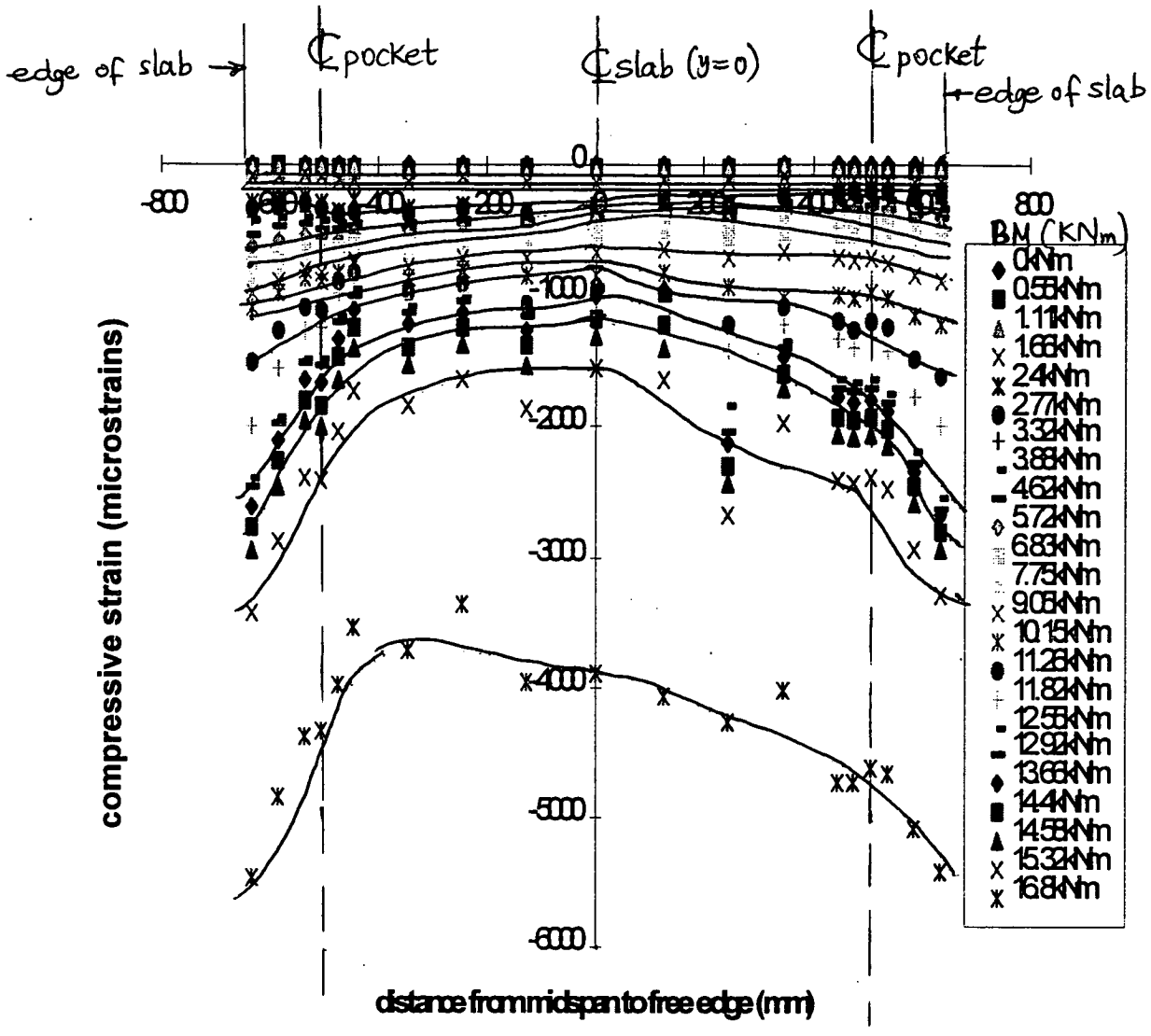

Fig 5.35 : Compressive strain in brickwork across span at various B.M. levels (RW4) - sides A & B

The behaviour of RW4 in terms of steel strain distribution is different from that of RW3. In slab RW4, at a bending moment of about 10 kNm, the steel strains suddenly began to drop off despite not having yet reached the yield point (Fig 5.36). It was observed that the growth of steel strains was especially slow after the point of cracking, compared to RW3. This is also not explainable by the behaviour of the neutral-axis depth which even tended to migrate at a faster rate towards the top of the brickwork plate in RW4 compared to RW3, a situation which should have caused higher steel strains in RW4 rather than RW3, (Figs. 5.37-40).

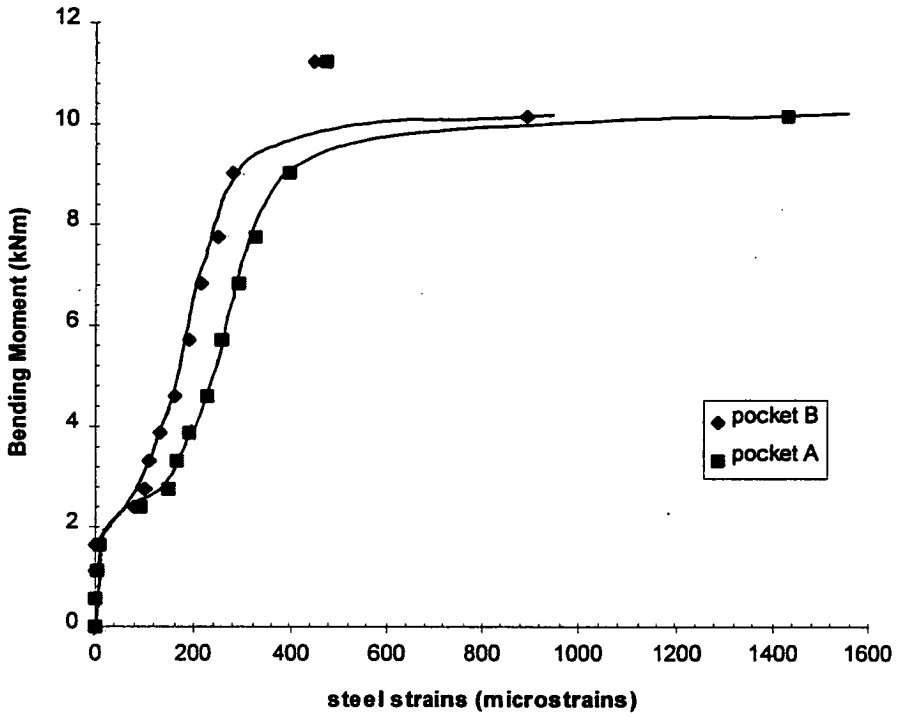

Fig 5.36 : Relationship between the bending moment and steel strains (RW4)

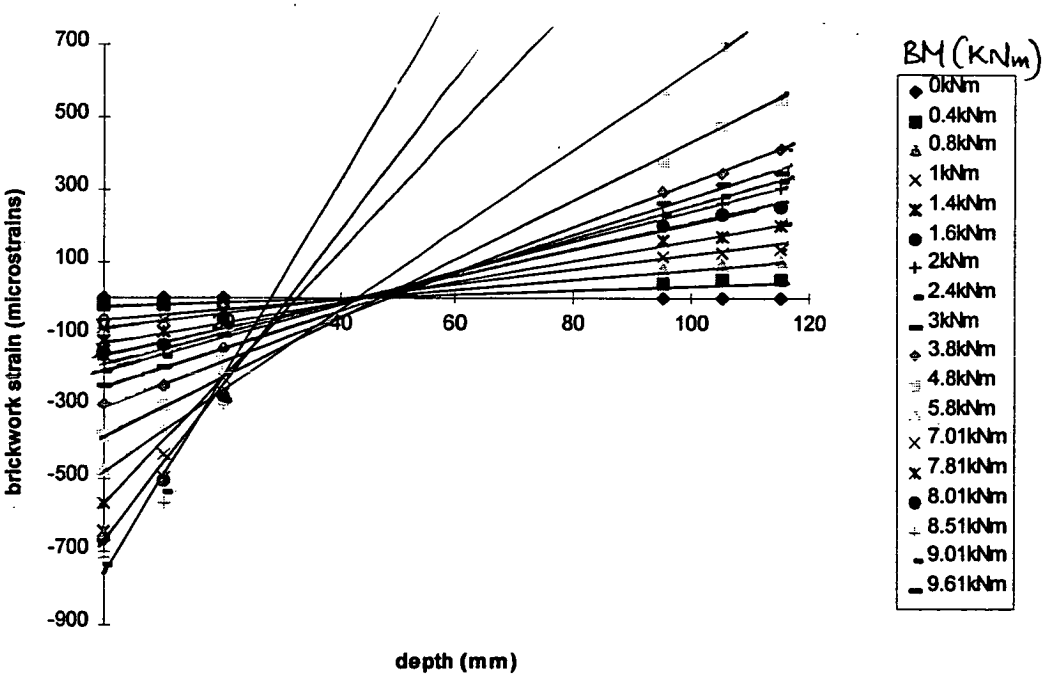

Fig 5.37 : Variation of brickwork strain through the depth (RW3)-side A

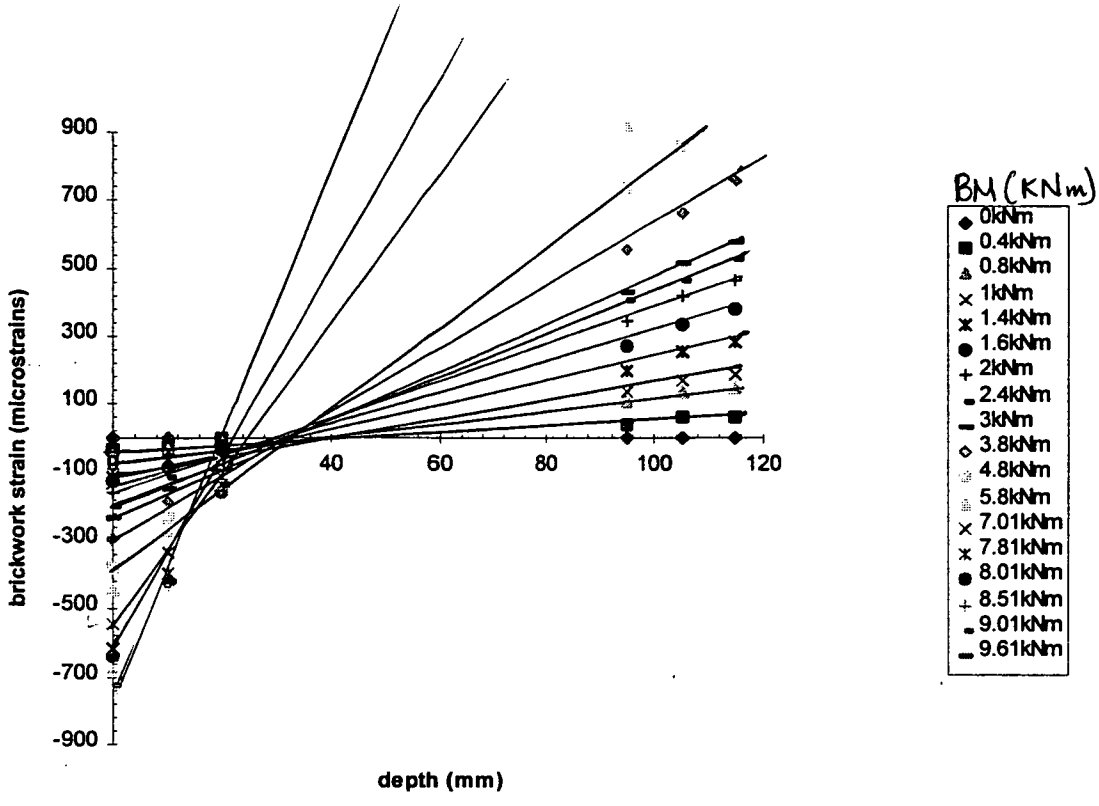

Fig 5.38 : Variation of brickwork strain through the depth (RW3)-side B

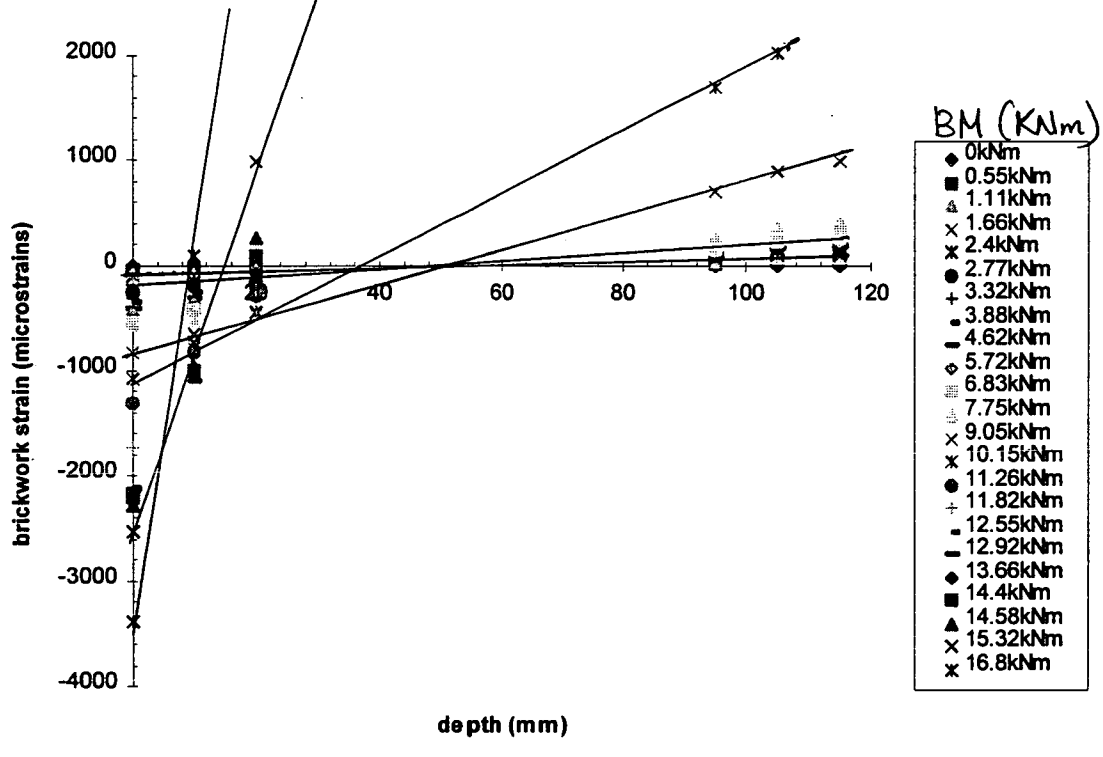

Fig 5.39 : Variation of brickwork strain through the depth (RW4)-side A

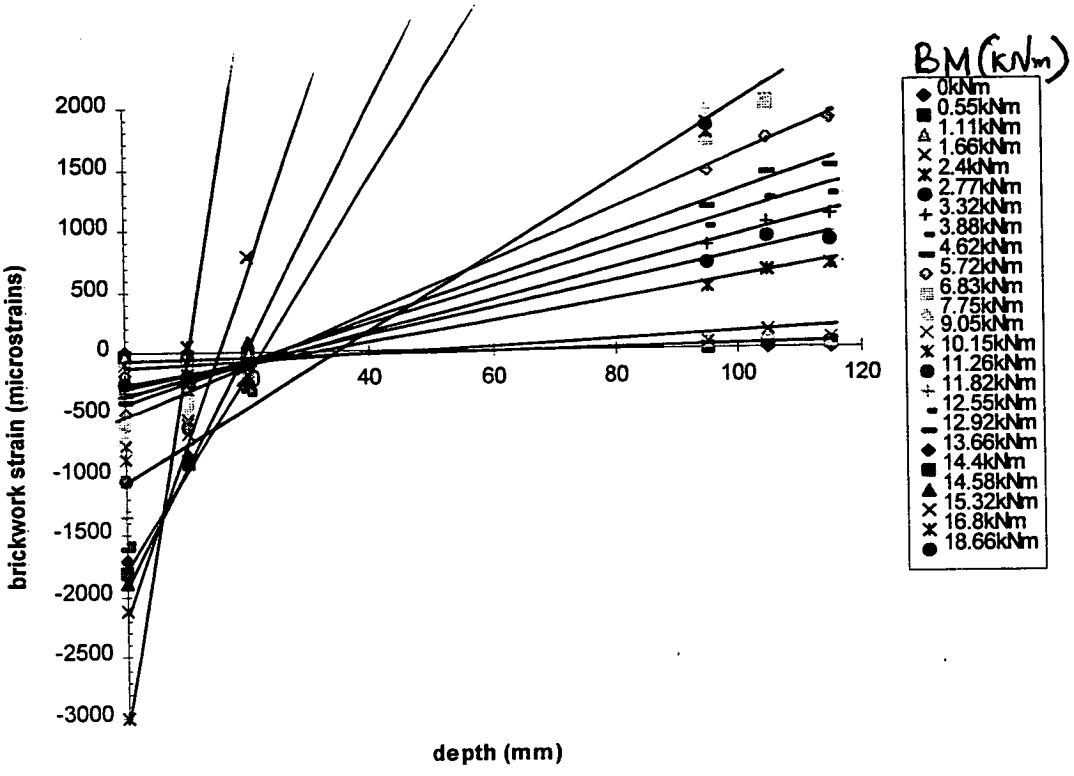

Fig 5.40 : Variation of brickwork strain through the depth (RW4)-side B

However, the compressive strain in brickwork continued to grow, and at the failure point, the order of compressive strains measured was higher than those associated with the ultimate strains in the brickwork, (Figs 5.33-35). The distribution of brickwork strain across the depth for these two walls show that (Figs. 5.37-5.40), at all levels of loading, a linear distribution existed.

The top brickwork strain distribution in the orthogonal y-direction, ε_y, even though minor compared to the x-direction and less than 15% at all stages of loading, shows that the distribution is relatively unpredictable as well. Part of the reason for this apparent unpredictable behaviour of ε_y strains is that these strains were so small that the sensitivity of the gauge could not cope with them. A typical distribution is shown in Fig 5.41.

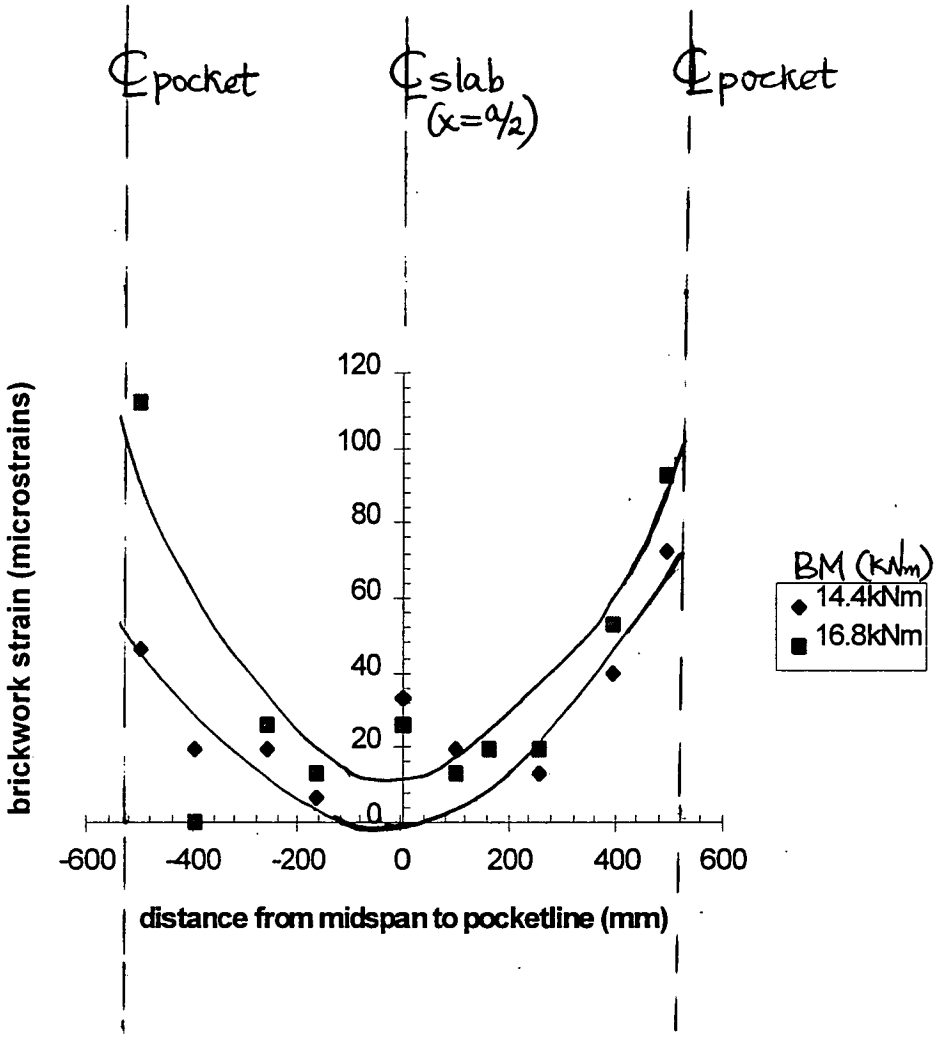

Fig 5.41 : Brickwork strain across span at various B.M. levels (RW4) - sides A & B

5.4.1.3 Walls 5 and 6 (RW5 and RW6)

The deflection behaviour of these walls is similar in many respects. A close look at the distribution of the central point deflections at different levels of applied bending moment shows these similarities (Figs. 5.42, 5.43, 5.44 and 5.45).

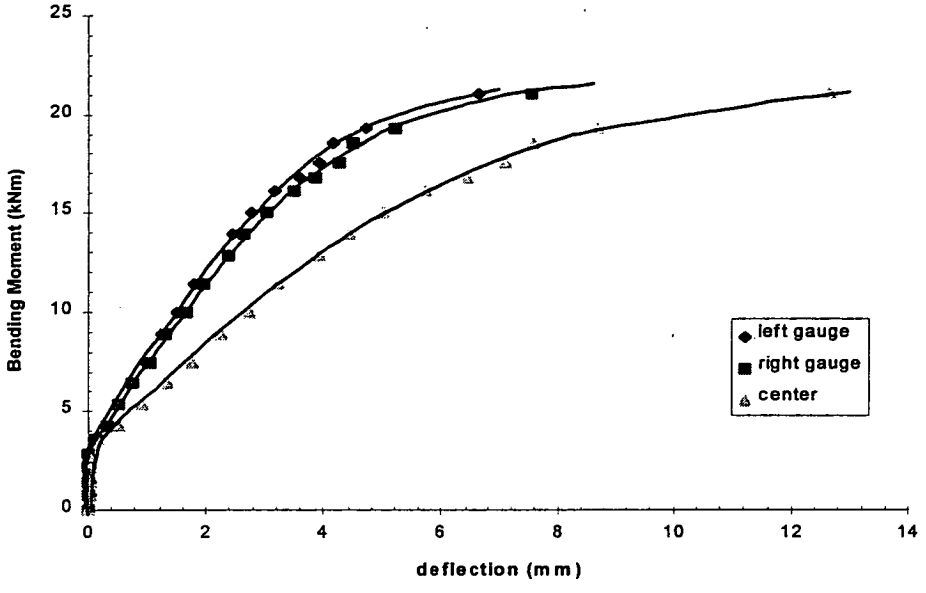

Fig 5.42 : Relationship between bending moment and the deflection along the span (RW5)

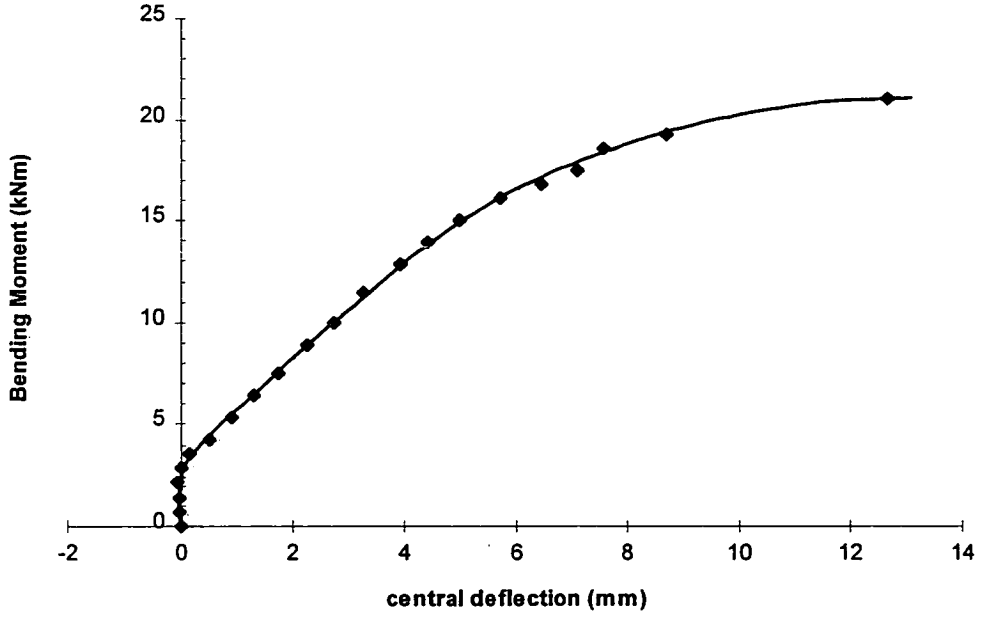

Fig 5.43 : The relationship between bending moment and the central deflection (RW5)

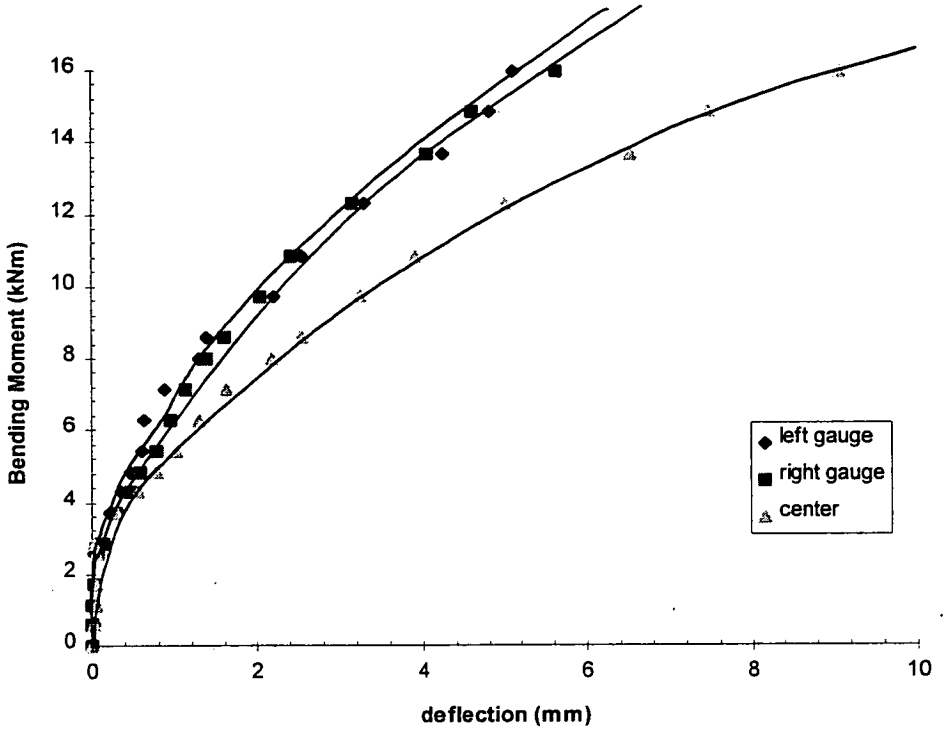

Fig 5.44 : Relationship between bending moment and the deflection along the span (RW6)

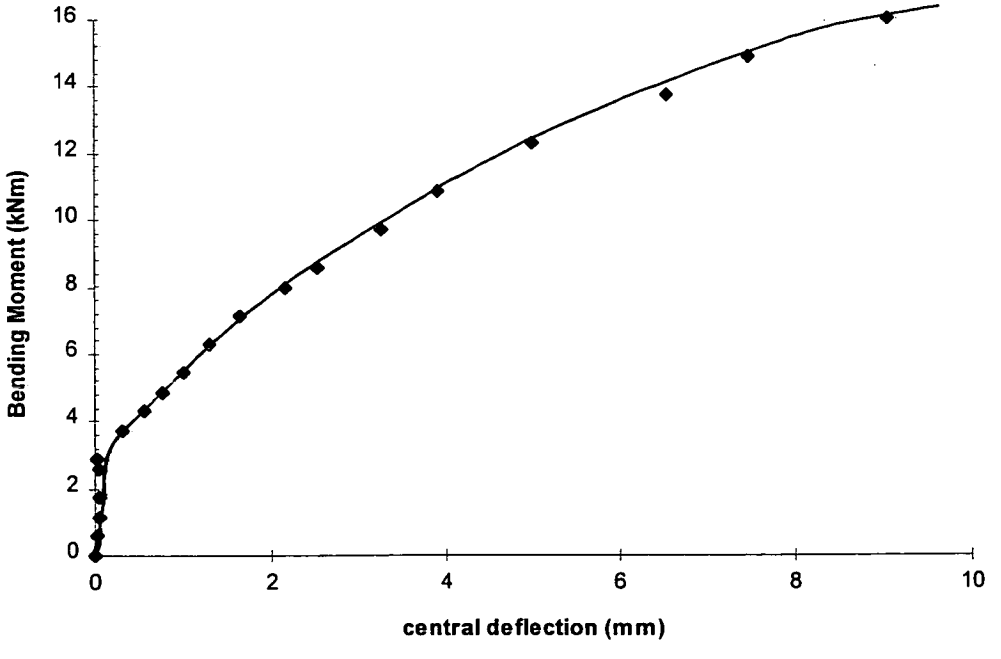

Fig 5.45 : The relationship between bending moment and the central deflection (RW6)

The characteristics of this deflection behaviour before and after cracking remained largely the same as in the preceding four walls. Deflections increased very slowly and linearly at first before the cracking point was reached. Soon after cracking, the rate of increase became faster and then, as the failure point is approached, very rapid. The behaviour of the steel strains in these two walls was also similar except that at the ultimate point, RW5 had shown serious signs of yielding whereas at failure, RW6 was just at the threshold of yielding (Fig 5.46 and 5.47).

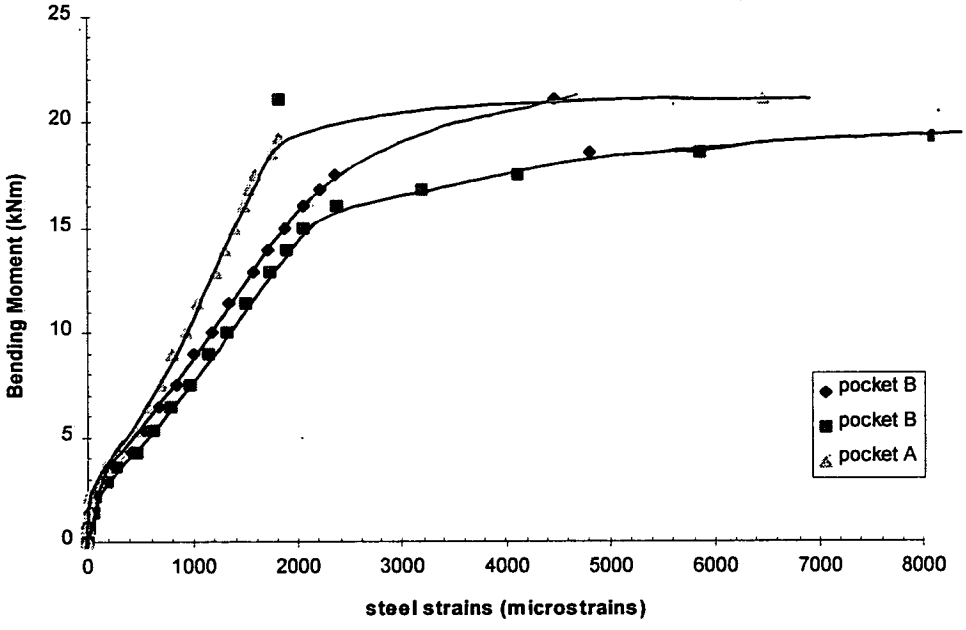

Fig 5.46 : Relationship between bending moment and steel strains (RW5)

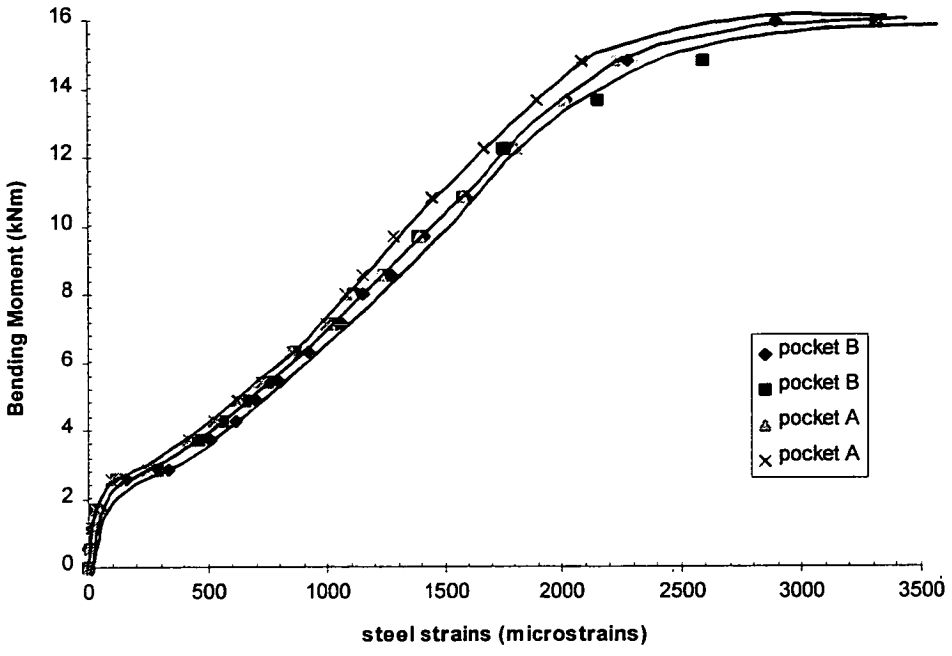

Fig 5.47 : Relationship between bending moment and steel strains (RW6)

The distribution of top brickwork compressive strains, ε_x, in these two walls were also similar, showing marked uniformity across the breadth prior to cracking. Once the cracking point was reached, a non-uniform distribution resulted with higher strains taken up by regions around the pockets and this reduced gradually at distances far removed from the pockets (Figs 5.48-5.53). Close to the failure point, the maximum ε_x strains in RW5 were in the same order of magnitude as those associated with the ultimate crushing strain for the brickwork and some evidence of crushing of the brickwork on top of the pockets could be seen, although the primary failure of this slab was due to steel yielding. RW6 failed due to local brickwork crushing in the compression zone on top of one of its two pockets.

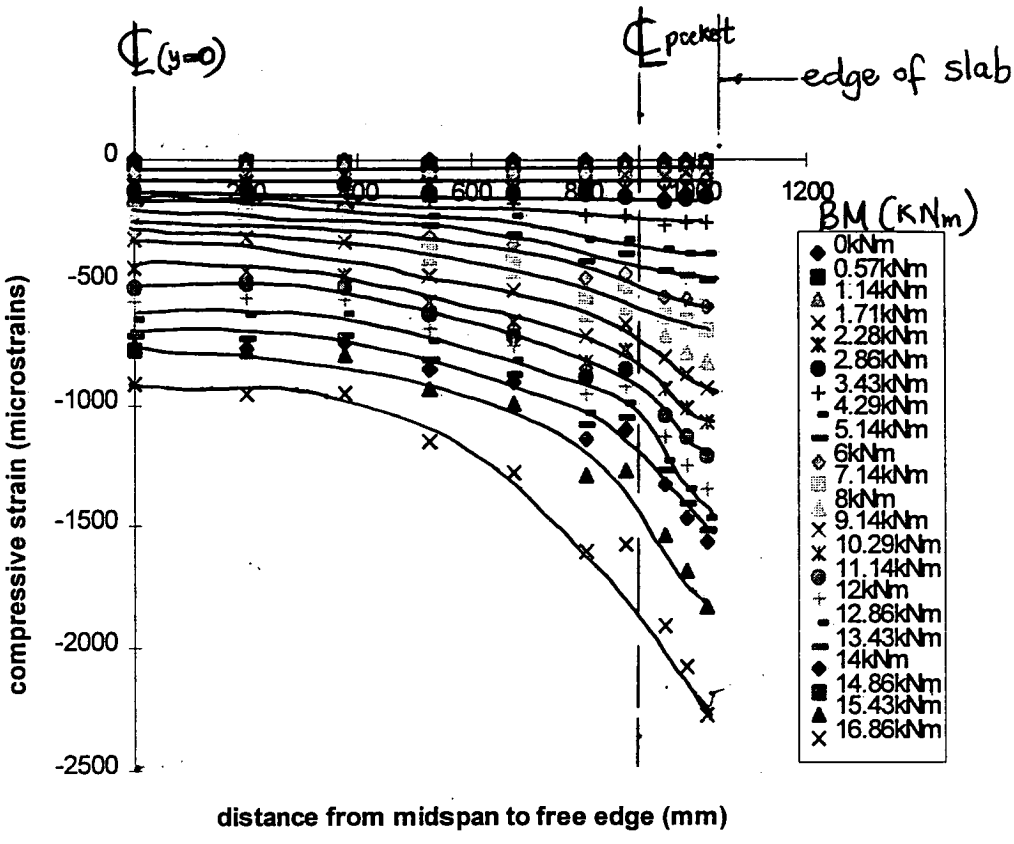

Fig 5.48 : Compressive strain in brickwork across span at various bending moment levels (RW5) - side A

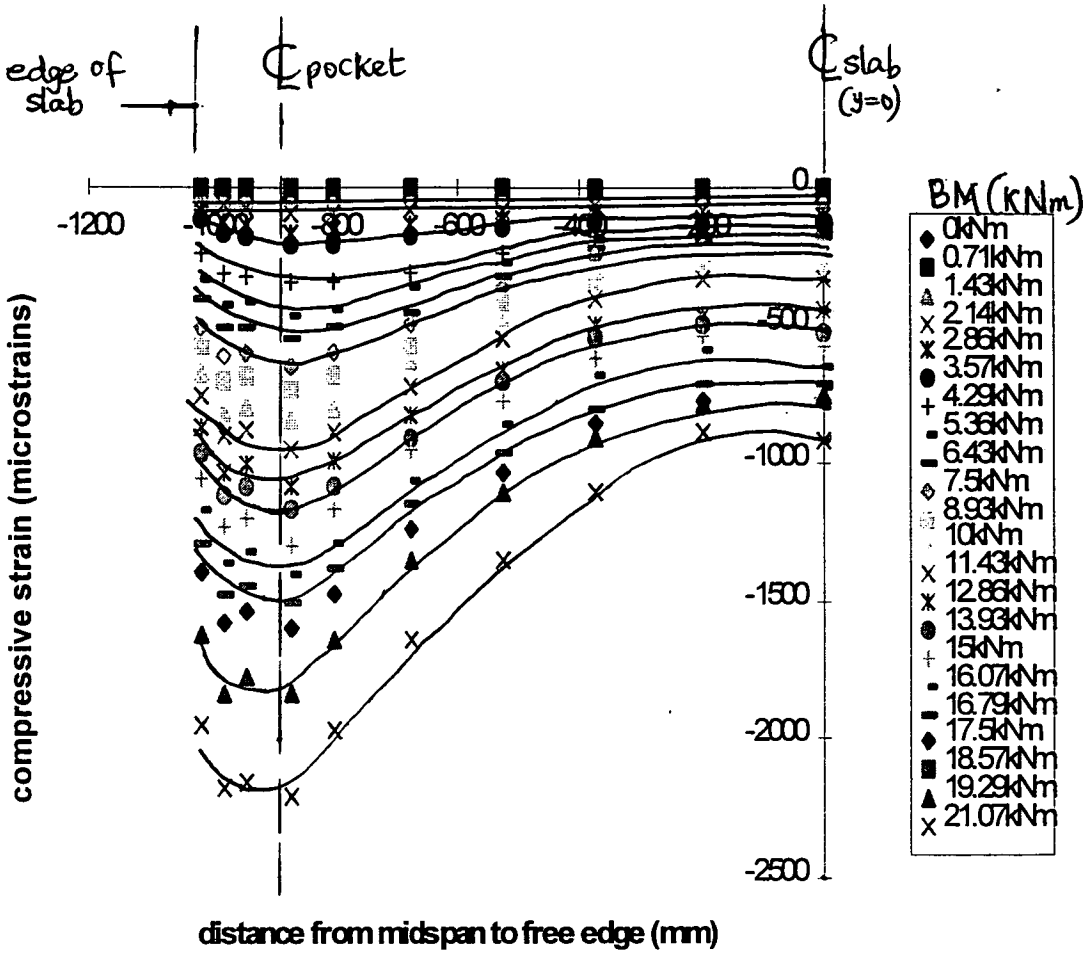

Fig 5.49 : Compressive strain in brickwork across span at various bending moment levels (RW5) - side B

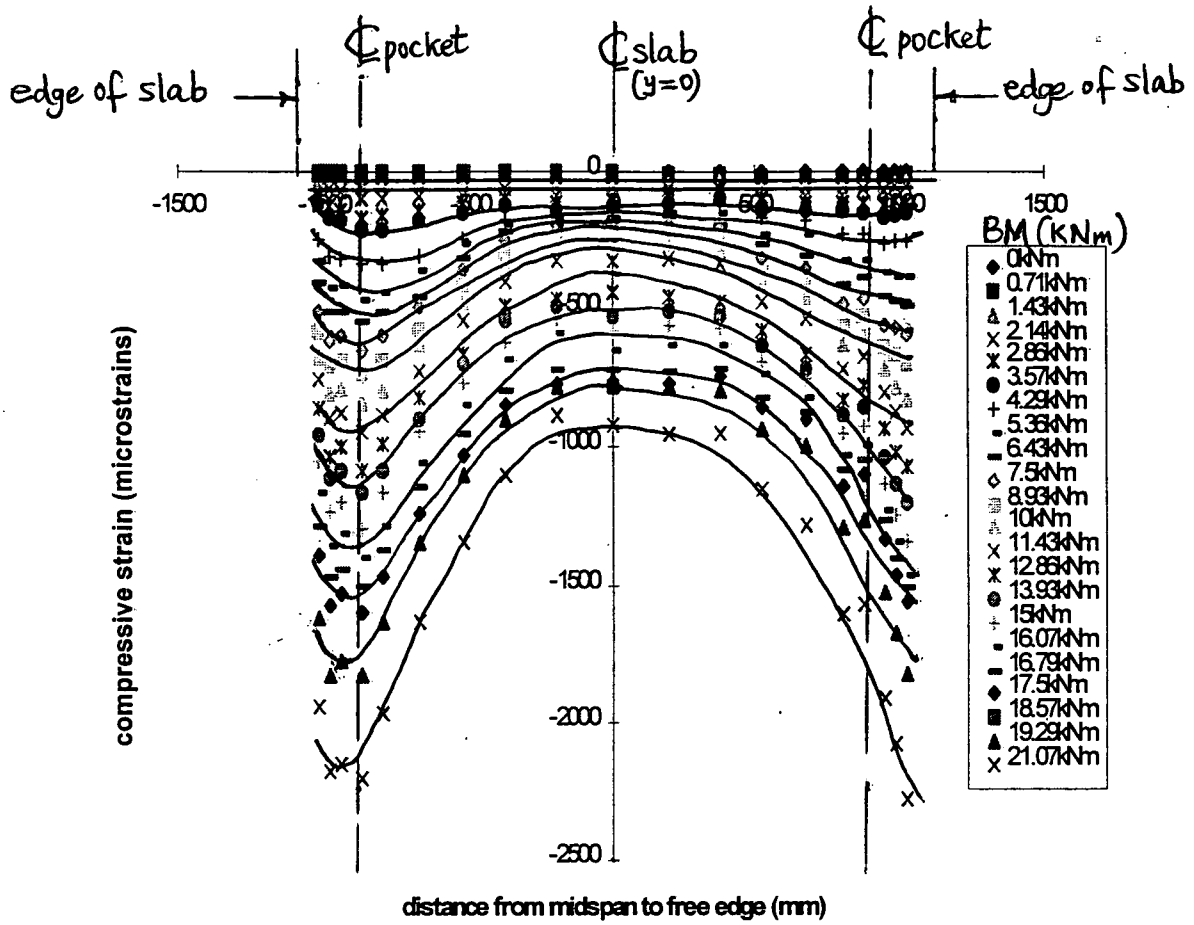

Fig 5.50 : Compressive strain in brickwork across span at various bending moment levels (RW5) - sides A & B

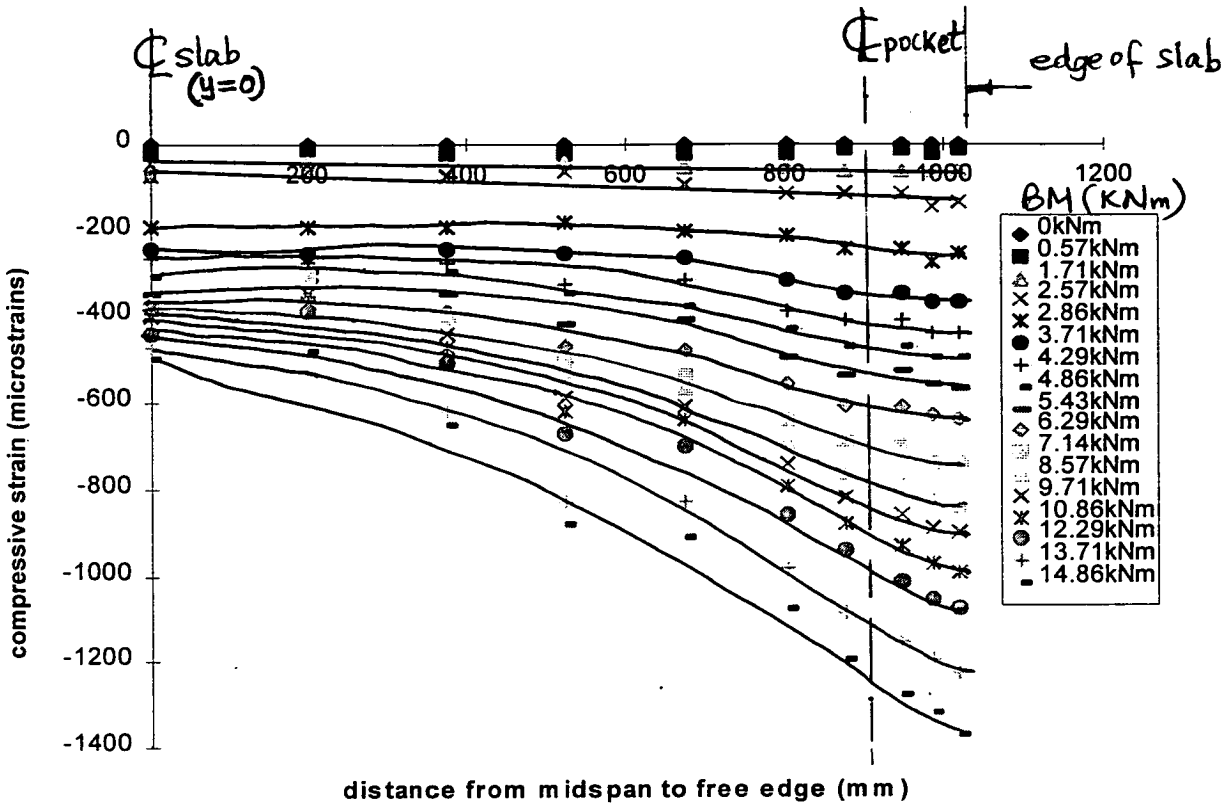

Fig 5.51 : Compressive strain in brickwork across span at various bending moment levels (RW6) - side A

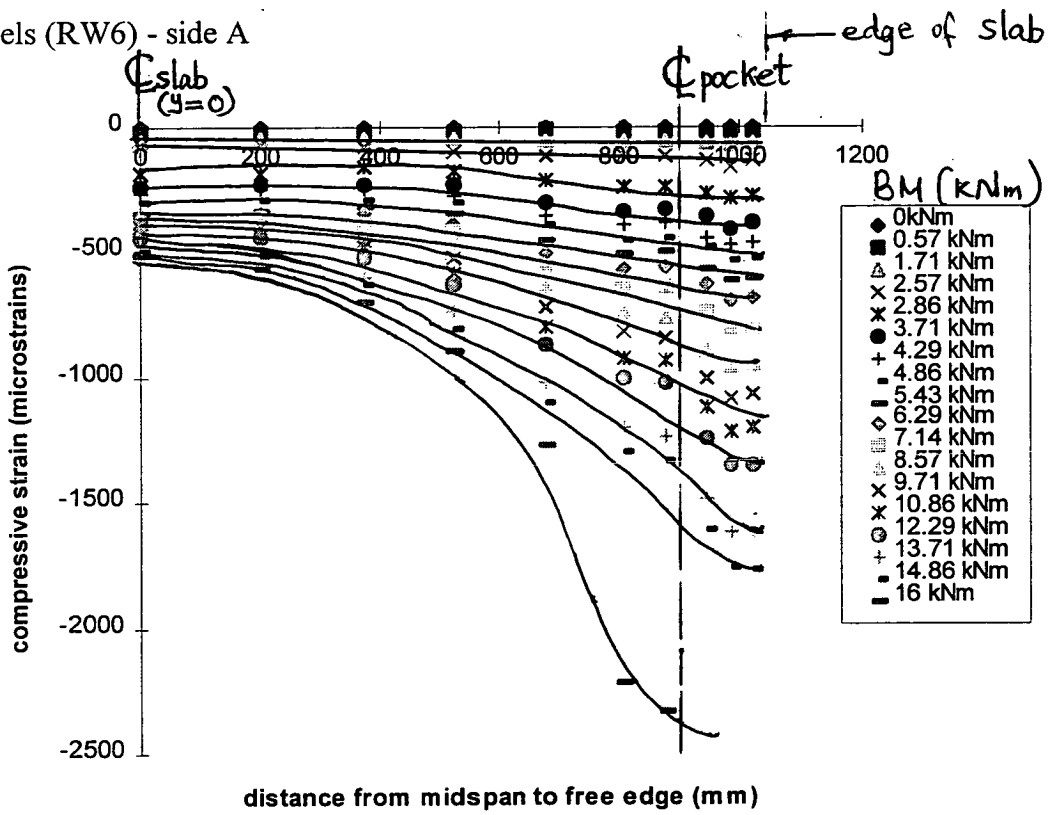

Fig 5.52 : Compressive strain in brickwork across span at various bending moment levels (RW6) - side B

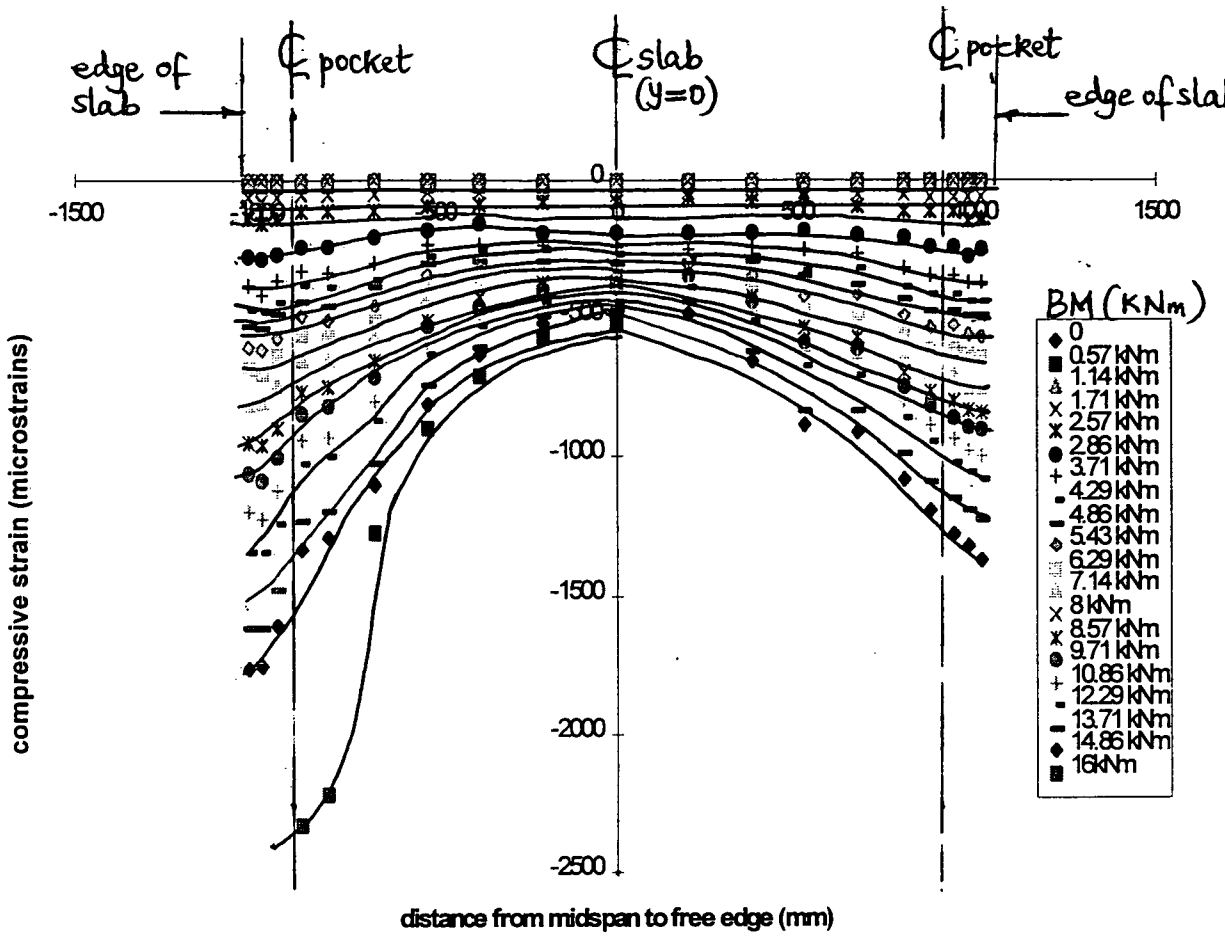

Fig 5.53 : Compressive strain in brickwork across span at various bending moment levels (RW6) - sides A & B

The magnitude of transverse strains ε_y , for the longest walls, were small compared to the orthogonal direction and the instrument was not sensitive enough to measure them. The typical distribution is shown in Fig 5.54.

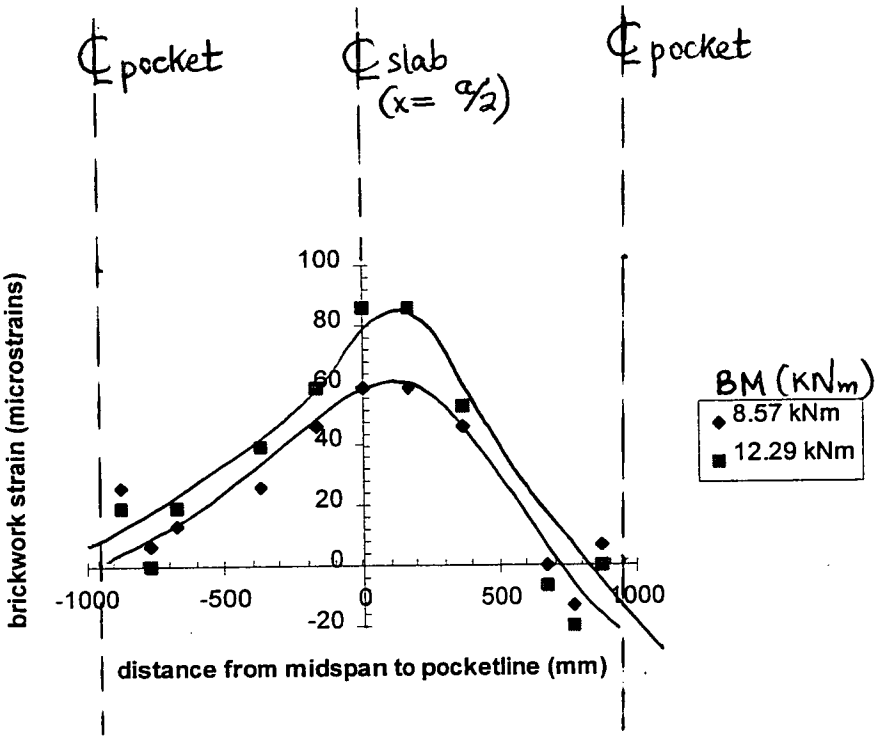

Fig 5.54 : Brickwork strain (y-dir) across span at various bending moment levels (RW6) - sides A & B

The slab RW6 failed, rather suddenly, at a pocket location (pocket B). Prior to failure, some noise was generated in this region soon after the top compressive ε_x strain measurements were taken. The taking of further readings was therefore discontinued for safety reasons. The maximum strains measured at this stage were already in the neighbourhood of those associated with the compressive failure of the brickwork used (Fig 5.53). The primary mode of failure was compression zone failure at this pocket location, a local failure which was probably due to a local strength reduction in the brickwork around this second pocket compared to other parts of the slab. The steel was just at the verge of yielding when this ultimate failure occurred. Flanged-member behaviour was also indicated for this wall since the panel of brickwork between the pockets acted effectively with the pockets to resist the applied load. The brickwork strain distribution across the depth for these two walls showed a linear distribution (Figs 5.55-58) throughout the various stages of loading up to the failure point.

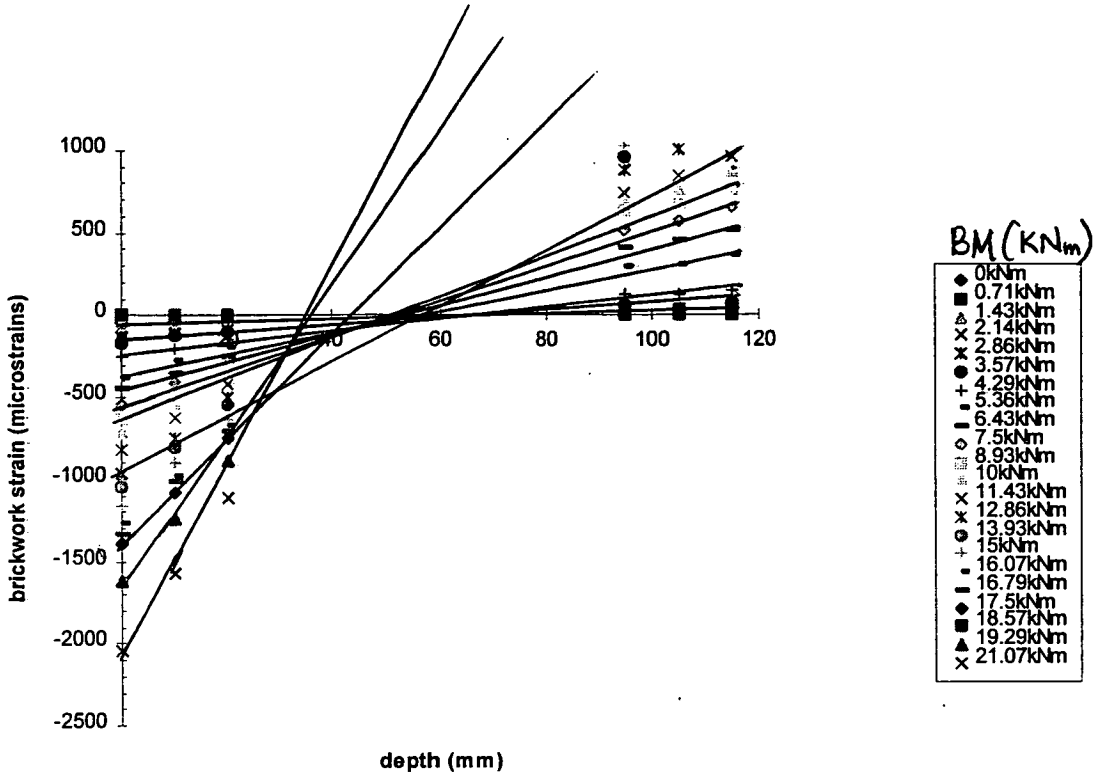

Fig 5.55 : Variation of brickwork strain through the depth (RW5) - side A

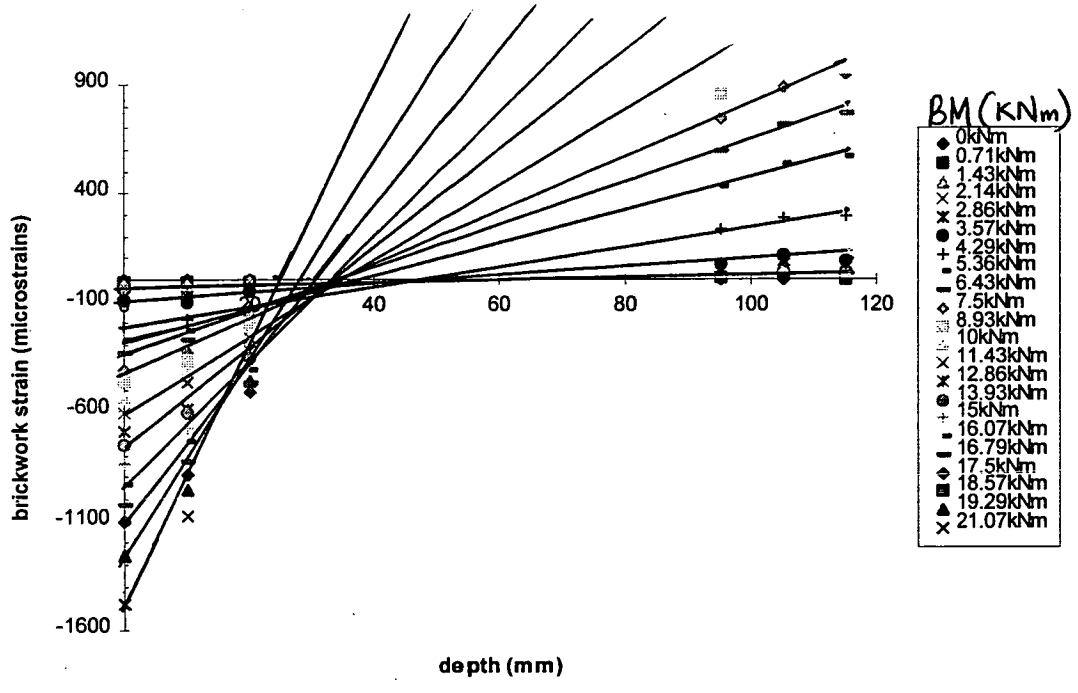

Fig 5.56 : Variation of brickwork strain through the depth (RW5) - side B

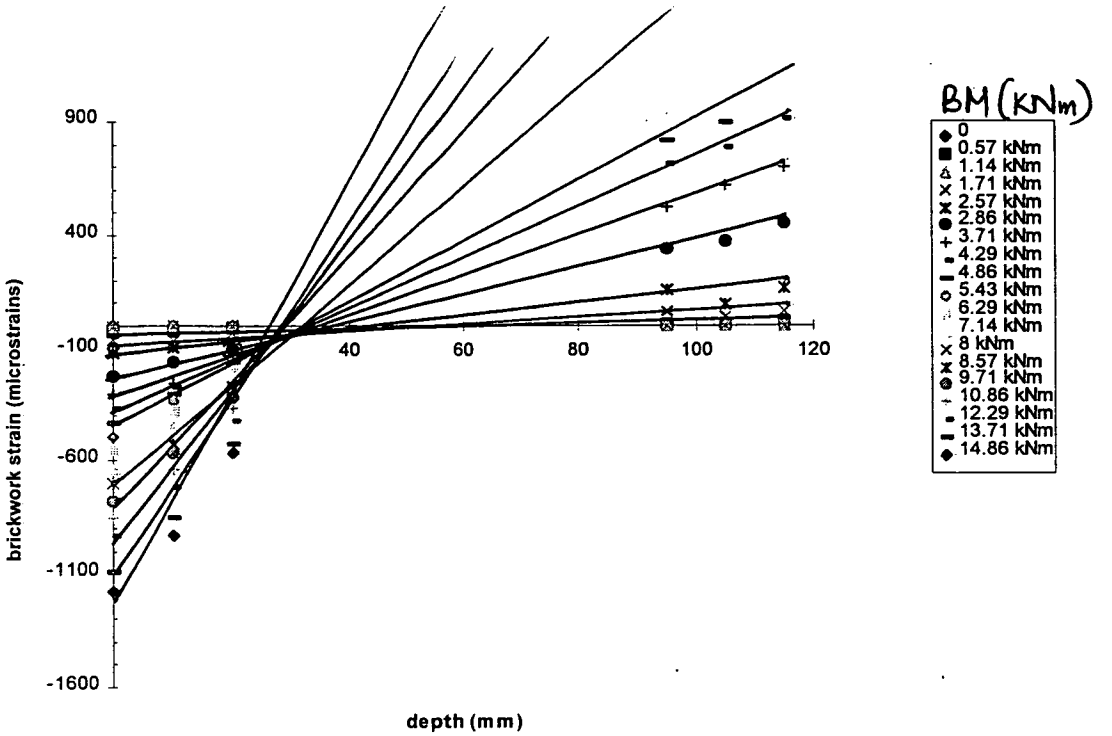

Fig 5.57 : Variation of brickwork strain through the depth (RW6) - side A

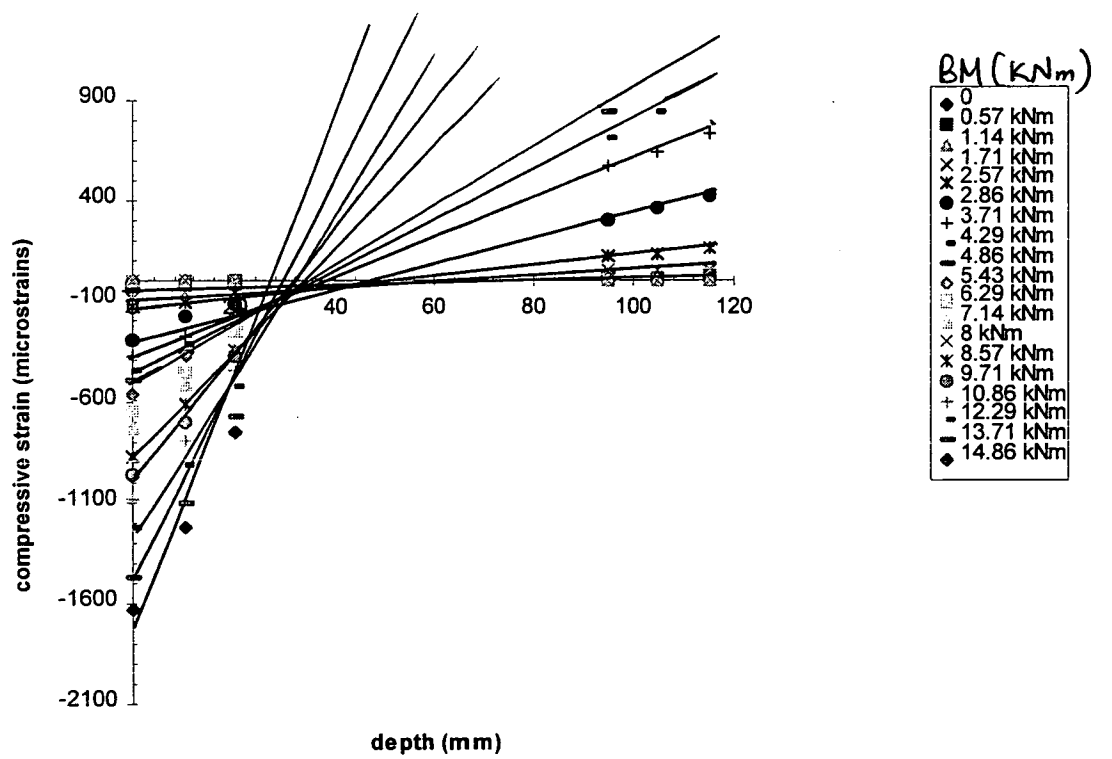

Fig 5.58 : Variation of brickwork strain through the depth (RW6) - side B

5.4.2 Estimation of Effective Width of the flange based on Experimental Measurements

The effective width associated with the different cases of pocket spacing was calculated from the analysis of all the experimental strain measurements prior to failure. It is important in the design of these walls to ensure that steel yielding, within the pockets, remains critical and that no failure of the brickwork panels between pockets occurs. It is also important to know the effective width of the flange that is associated with the ultimate conditions pertaining to steel yielding as this would ensure that excessive spacings of the pockets are not chosen in design. From the strain measurements obtained across the pockets prior to failure, the stresses corresponding to these strains were derived. The average stress-strain curve obtained for the brickwork, given in chapter 3, was used to derive these stress-distributions across the pockets just prior to failure. A curve-fitting procedure was thereafter used to determine the stress distribution in all the cases of pocket spacing. Using the stress distribution, the effective width of the flange was calculated from a knowledge of the area under the stress distribution curve and the enclosing rectangle. The summary of the results obtained are given Table 5.4.1.

Table 5.4.1 : Effective Width of Flange

		Effective width ratio, $\left(\frac{b_{eff}}{b}\right)$, in (%)			
Wall	Spacing, S (mm)	Side A (%)	Side B (%)	Average (%)	Overall average (%)
RW 1	540	97.5	97.35	97.4	96.75
RW 2	540	96	96.1	96.1	96.75
RW 3	1000	71	79	75	83.65
RW 4	1000	90.55	94	92.3	83.65
RW 5	1750	81	75	78	73
RW 6	1750	69.2	66.65	68	73

In Table 5.4.1, the calculated effective widths for the different cases have been normalized against the actual width for every case of pocket stem spacing. The ratio obtained is defined as the effective width ratio, $\left(\frac{b_{eff}}{b}\right)$. It is noted in the calculations that there exists some variation between the effective width for the two sides in the different cases of pocket spacings investigated and also, within the cases of pocket spacings itself. The variation between the two sides A and B is within a range of 10 % and is due to imperfection in the symmetrical arrangements of loading and supports. The variation observed between the individual cases, for the various pocket spacings, is due to the proximity of measurements to the ultimate; from which the stress distribution was derived. Flanged-member action is much more acute as the structural member approaches its ultimate; this is demonstrated by lower effective width ratio for RW3 compared to RW4 and also for RW6 compared to RW5. This ratio is highest for the smallest case of pocket spacing and vice versa, varying respectively from 97.4 % to 68 %. The overall average of this ratio varies from 96.75 % to 73 % for cases with spacings of 540 mm and 1750 mm respectively. These results indicate that flanged-member action occurred for all the cases investigated.

5.4.3 A Method of Solution for Investigating Flanged-Member Behaviour

5.4.3.1 Theory of Wide Beam Flanges

In the elementary theory of beam bending, equation 5.4.3-(1), it is assumed that the bending stresses are proportional to the distance from the neutral axis. This means that stresses are not a function of the width of the flange.

$$\sigma = \frac{My}{I} \qquad \text{---------- 5.4.3-(1)}$$

where M = applied bending moment

I = $bd^3/12$ (second moment of area of the cross-section of the beam)

and b = flange width.

y = distance from the neutral axis to the topmost fibre of the cross-section.

However, when this width becomes very large, it is known that parts of the flanges far removed from the web do not take up their full share in resisting the applied bending moment and this makes the beam much weaker than would be predicted by the elementary theory of beam bending. In the governing theory of the "effective width" of wide beam flanges, in which the principle of minimum energy[65] is used, it is assumed that the actual width of the beam flanges are replaceable by a certain reduced width, called the "effective width". This effective width is such that when the elementary theory of beam bending is applied to such a transformed beam cross section, one would obtain the correct value of maximum bending stress.

In providing such a theoretical basis for the determination of this effective width, certain simplifying assumptions about the beam were made : (a) That it is infinitely long and continuous on equidistant supports and; (b) it assumed that the loading arrangement is symmetrical with respect to the middle of the spans. The flange width is assumed to be infinitely large and its thickness, *h*, very small compared to the depth of the beam. On the basis of these assumptions, the flange (being assumed so thin such that it approximates a slice) is considered to experience negligible bending as a thin plate. Furthermore, it is assumed that during the bending of the beam, the forces are transmitted to the flange, by reasons of continuity and compatibility, in its middle plane so that the stress distribution in the flange presents the two-dimensional problem of plane stress. Using the boundary conditions of this problem and adopting a stress function in the form of a series, the condition is then established which makes the total strain energy of both the flange and the web attain a minimum value. This particular condition is associated with the true stress distribution being sought. The full derivation of this condition as well as the associated expression for the effective width, obtained in closed form, has already been documented[65].

Using the premises given above, the following expressions were obtained for the effective width : When the bending moment diagram is in the form of a cosine curve, equation 5.4.3-(2) is obtained and when the bending moment diagram is in the form of combinations of straight lines resulting from concentrated loads being applied to the span, equation 5.4.3-(3) is obtained.

$$2\lambda = \frac{4l}{\pi\left(3+2\upsilon-\upsilon^2\right)} \qquad \text{---------- 5.4.3-(2).}$$

$$2\lambda = 0.85\left\{\frac{4l}{\pi\left(3+2\upsilon-\upsilon^2\right)}\right\} \qquad \text{---------- 5.4.3-(3).}$$

where 2λ = effective width.

υ = Poisson's ratio

$2l$ = span.

This theory shows that using a concentrated load, placed at the middle of the span, results in a reduced effective width compared with when the resulting moment diagram from the applied load is a cosine curve.

Note that some of the assumptions used to derive these expressions for the effective width are strictly not applicable to the slab specimens tested by the author. For example, the slabs tested by the author are simply supported and are not continuous. In deriving these expressions, a continuous beam with geometric dimensions distinctly larger (in thickness terms) than the associated flange is assumed. In this work, the beam is simply supported and the thickness is not distinctly different from the corresponding flange thickness. This distinction, should naturally have some bearing on the applicability of these expressions to brickwork slabs, as a result. Nonetheless, it is suggested that the relatively thick beam section compared to the thin flange represents a similar stiffness ratio. With the uniform slab section tested in this work, in which one part of the plate is stiffer (the reinforced stem) than the remaining part (unreinforced portion).

5.5 ULTIMATE STRENGTH ANALYSIS OF THE BRICKWORK SLABS

5.5.1 Theoretical Analysis : The yield line theory by Johansen[67] has been used for the ultimate load analysis of brickwork pocket-type slab.

5.5.2 Ultimate Moment : As the Yield-Line method gives upper bound solution, several failure mechanisms were tried and the one which gives the lowest failure load is shown in Fig 5.5 -(1).

Slab (RW1-2) :

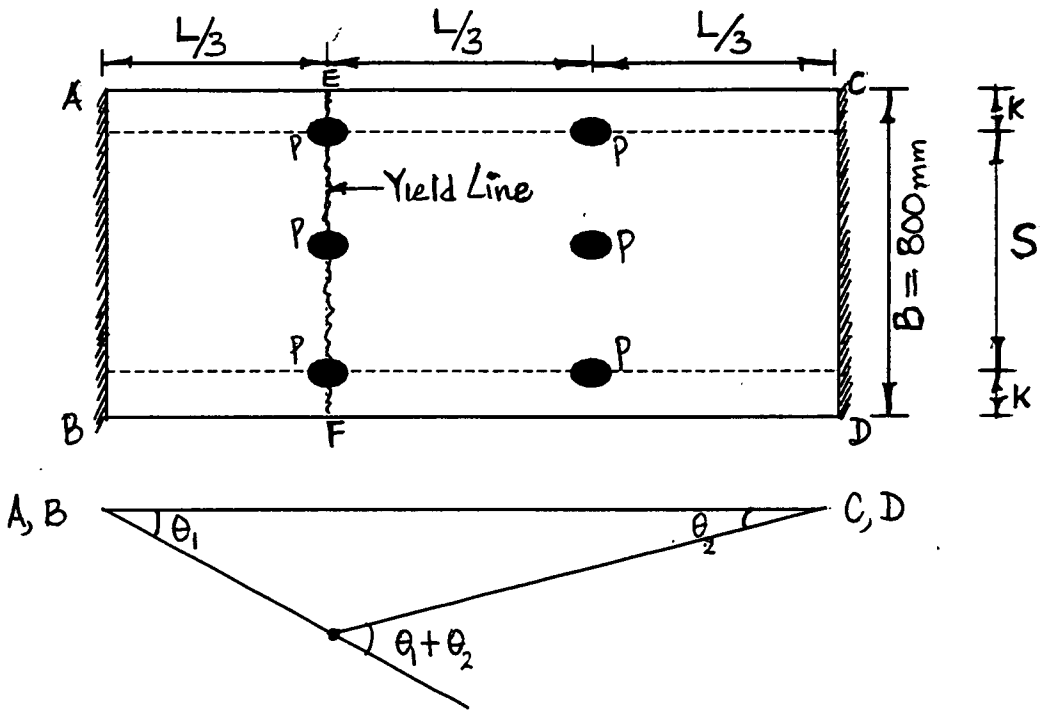

Fig 5.5-(1) : Failure mechanism assumed in ultimate load analysis of slab (RW1-2)

Consider the idealised yield line shown in Fig 5.5-(1) and give a virtual deflection of unity to the line EF.

External Work Done = $3P \times 1 + 3P \times \frac{1}{2} + \left[w \times \frac{L}{3} \times \frac{1}{2} + w \times \frac{2L}{3} \times \frac{1}{2}\right].(S+2k).t$

$$= 4.5P + \frac{wL}{2}.(S+2k).t \qquad \text{----------5.5-(1)}$$

where $w = 24\text{kN/m}^3$ (experimental value) .

Substituting the values of L, S, t, k and w gives

$$= 4.5P + \frac{24\times10^3}{10^9} \times \frac{1200}{2} \times 800 \times 115$$

$$= 4.5P + 1324.8$$

Internal work done on the yield line EF = $m_s.(\theta_1+\theta_2) + m_m.B.(\theta_1+\theta_2)$ ---- 5.5-(2)

$$= 2\left(A_s.f_y.z\right).\left[\frac{1}{L/3} + \frac{1}{2L/3}\right] + m_m.B.\left[\frac{1}{L/3} + \frac{1}{2L/3}\right]$$

$$= 2 \times 78.5 \times 500 \times 87.61 \times \left[\frac{1}{400} + \frac{1}{800}\right] + \frac{0.75\times115^2\times800}{6} \times \left[\frac{1}{400} + \frac{1}{800}\right]$$

$= 25790.2 + 4959.38 = 30749.58$ Nmm.

External work done must be equal to internal work done, hence

$$4.5P + 1324.8 = 30749.58 \qquad \text{---------- 5.5-(3)}$$

Therefore, $P = 6.54$kN ; Total load $= 6P = 39.24$kN.

Slab RW 3-6 :

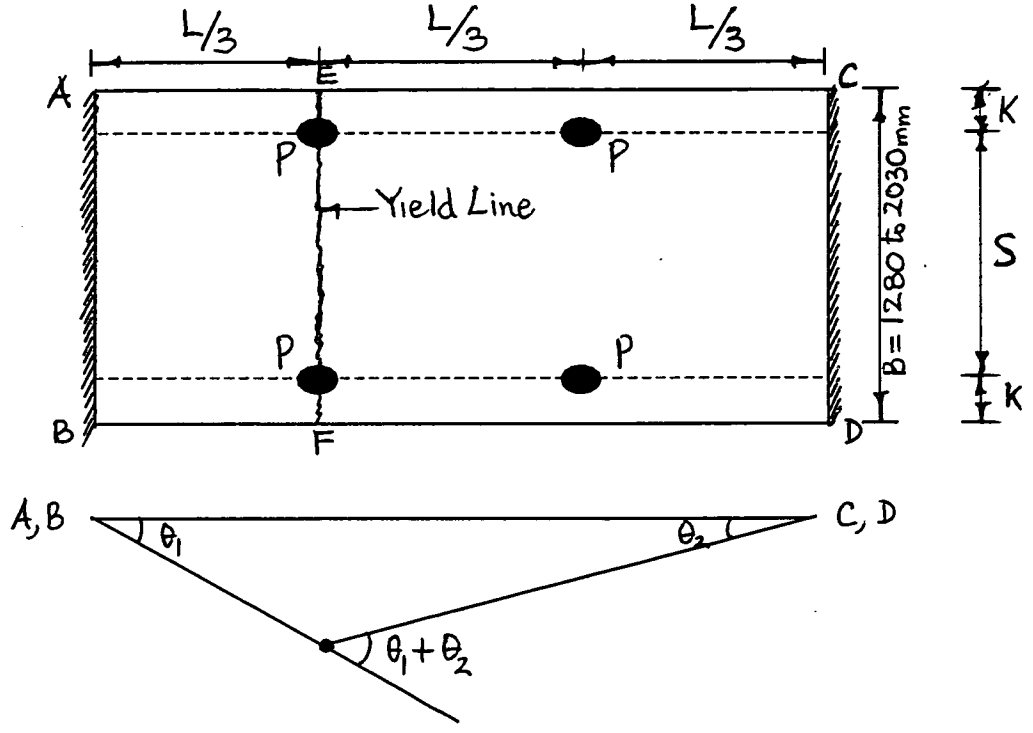

Fig 5.5-(2) : Failure mechanism assumed in ultimate load analysis of slab (RW3-6)

Similarly, from Fig 5.5-(2), for B = (S+2k) = 1280mm,

External Work Done : $3P + 2119.7 = \frac{226\times470\times87.61\times3}{800} + \frac{0.75\times115^2\times1280\times3}{6\times800}$

Internal work done has been calculated from equation 5.5-(2)

$P = 13.57$kN. ; Total load $= 4P = 54.28$kN.

Lastly, for B = (S+2k) = 2030mm,

$P = 23.32$kN. ; Total load $= 4P = 93.29$kN.

5.5.3 Calculation of Ultimate Shear : The ultimate shear has been calculated from the plastic analysis described in section 4.3.4. of chapter 4 of this thesis. The effectiveness factor for the slabs has been calculated from the equation :

$$\vartheta = \frac{0.41 f_t^{0.29}}{f_m^{0.08}} \qquad \text{(i.e. eqn. 4.3-23)}$$

A lot of flexural tests have been done previously[59] using the same brick and mortar, hence f_t has been obtained from those results. The value of f_m obtained in chapter 3 of this thesis was used and, together with f_t , the effectiveness factor for the slabs was evaluated to

$$\vartheta = \frac{0.41 \times 0.75^{0.29}}{25^{0.08}} = 0.29 \qquad \text{----------5.5-(4)}$$

The result of these calculations is given in Table 5.5-1. From the Table 5.5-1, it can be seen that there is good correlation between the experimental and theoretical result predicted by the plastic theory.

5.5.4 Deflection of pocket-reinforced slabs : The experimental deflection measurements have also been compared with theoretical predictions based on the direct method as mentioned briefly in the section 4.3.5.4 of chapter 4 and these results are shown in Figs 5.5-(3) to 5.5-(5). It is observed that the deflections are reasonably predicted by this method. The theory is used to trace deflection up to the ultimate point whereas, in the experiments, the dial gauges had to be removed close to the ultimate to prevent damage to them.

5.5.5 Discussion of experimental and theoretical results :

The yield line analysis (Table 5.5-1) gave a prediction accuracy to within 10 %. The strength of the pocket-reinforced slabs could be reasonably estimated by this technique. The Direct Method also gave reasonable prediction of the experimental results as given in Table 5.5-1. This method accounts for the stress-strain properties of

the brickwork and steel and traces the behaviour of the slab throughout its loading history. These results show that the strength of the pocket-reinforced slab could reasonably be predicted by both the Yield-Line analysis method and the Direct Method. If the equations given in the code of practice[2] are used, conservative estimates of both the moment and shear capacities of these slabs would result as given in Table 5.5-1. In the calculations based on the code equations, all the partial factors of safety have been given a value of unity. The details of these calculations are given in appendix (III). All these results are given in Table 5.5-1. Of all the methods used in analysis, the code provisions proved to be the most conservative. In view of these results, the design of these slabs should employ either the yield-line analysis or the direct method. The calculation of shear strength by the plastic theory also gave reasonable predictions and shows that the plastic method could be used to calculate the shear strength of pocket-reinforced slabs. It is evident from the analysis (Table 5.5-1) that the failure of the slabs will occur due to yielding of steel and not due to shear.

Table 5.5-1 : Comparison of experimental and theoretical results

No of Slabs	Ultimate Load (kN)				Ultimate Moment (kNm)				Shear Strength (kN)		
	Expt.	Average	Y.L. Theory	Direct Method	Expt.	Y.L. Theory	Direct Method	Code[2]	Expt.	Plastic Theory	Code[2]
1	36.0	36.78	39.24	38.36	7.36	7.85	7.67	6.71	19.72	19.8	15.34
2	37.56										
3	56.8	56.56	54.28	57.21	11.31	10.86	11.44	8.9	30.4	27.45	16.56
4	56.32										
5	88.56	85.0	93.29	95.52	17.0	18.66	19.10	14.64	45.86	47.18	19.30
6	81.4										

5.5.6 Ultimate moment based on effective width :

The ultimate moment was also calculated on the basis of the effective breadth, b_{eff}, worked out from experimental strain measurements (section 5.4.2) and the code provisions[2]. These results are compared with the other methods in Table 5.5-2. It is noted that the methods based on b_{eff} and the code[2] proved to be conservative. The strength of the pocket-reinforced slabs are much better predicted by the yield-line and the direct methods. In the absence of the test results, it may have been safe to use this method. However, in view of the present work it seems better to use either the Yield-Line analysis or the Direct Method considering the full width of the slabs in predicting the ultimate load conditions.

Table 5.5-2 : Comparison of Ultimate Moment Using Different Methods

Ultimate Moment (kNm)					
Slabs	Expt.	Y.L. Theory	Direct Method	Code[2]	Based on b_{eff} (Calculated from expt)
RW 1&2	7.36	7.85	7.67	6.71	6.88
RW 3&4	11.31	10.86	11.44	8.9	9.30
RW 5&6	17.0	18.66	19.10	14.64	16.0

In section 5.6, a qualitative comparison of results obtained from investigating flanged-action behaviour in pocket-reinforced walls is compared with two pocket-type walls tested at the BDA.

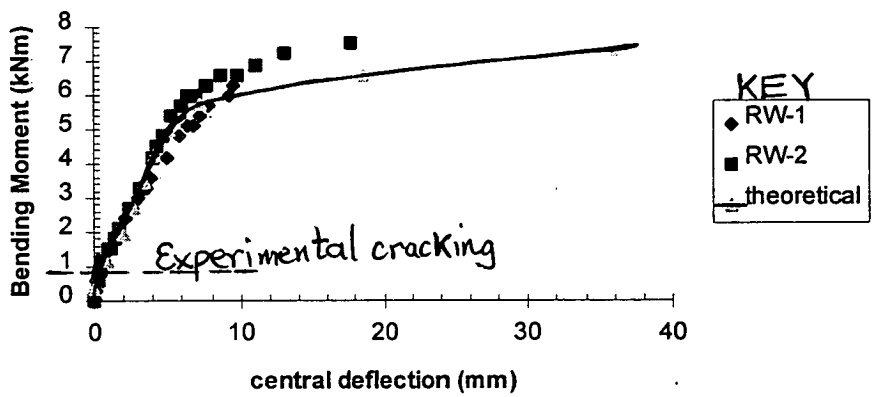

Fig 5.5-(3) : Comparison of experimental and theoretical deflections (S = 540mm)

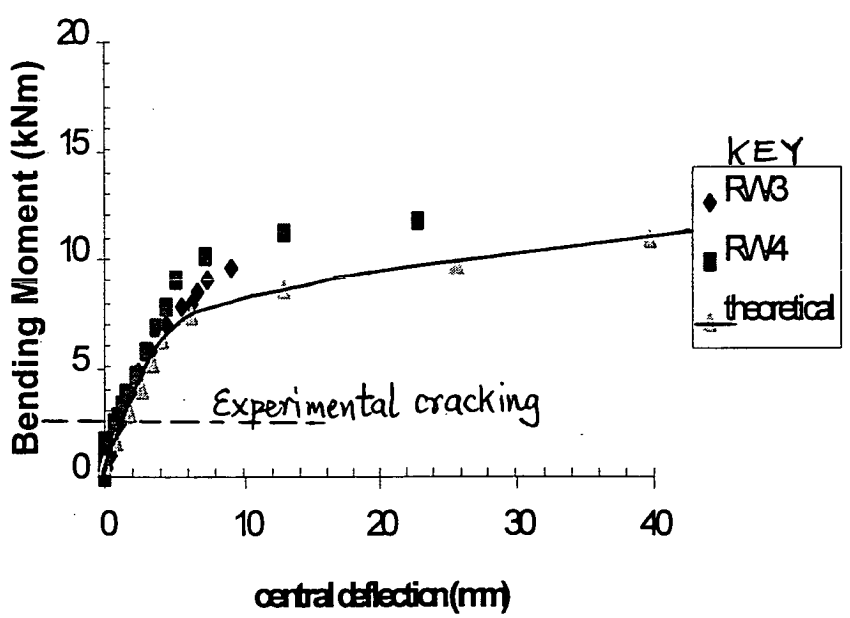

Fig 5.5-(4) : Comparison of experimental and theoretical deflections (S = 1000mm)

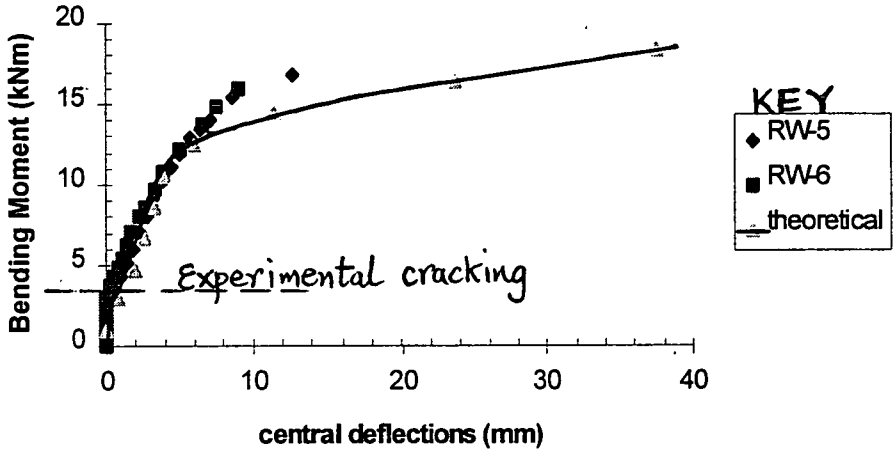

Fig 5.5-(5) : Comparison of experimental and theoretical deflections (S = 2030mm)

5.6 EVALUATION OF WORK DONE AT THE BRICK DEVELOPMENT ASSOCIATION (BDA) AGAINST THE RESULTS OBTAINED IN THE PRESENT INVESTIGATION

The results obtained from testing these reinforced slabs were compared with those obtained from roughly similar walls tested at BDA[48]. Although, the type of supports used for the full-scale tests done at BDA is different from those used here, some evaluation studies were carried out by considering the conditions at the critical sections of the BDA walls with those reported here. As only cantilever walls were tested at BDA, the critical section is at the base near the reinforced concrete footings. Examination of the brickwork and reinforcement strain profiles as well as the deflection behaviour of these walls shows similarities between results and those of the present investigation.

These walls have pocket spacings of 2.4 m and 3.0 m respectively. They both have a height of 3.0 m; are of solid rectangular cross-section of thickness 215 mm and were loaded similarly, i.e. the loading arrangement was symmetrical with respect to the two reinforced pockets. In spite of this symmetry, there was some variation in the

maximum compressive strains recorded at the pocket locations. In wall 1 (W1) having 2.4 m spacing, the right hand pocket had the higher compressive brickwork strain whereas in wall 2 (W2), it was the left-hand pocket that had the higher corresponding brickwork strain. This behaviour had no noticeable effect on the development and growth of the steel strains in W1. In this wall, the steel strain profiles in the two pockets were similar. However, in W2 with 3 m pocket spacing, the steel strain in the left-hand pocket showed a slightly higher growth rate close to the ultimate point.

In these two walls, both portal and demec gauges were used for brickwork strain measurements. The portal gauges generally recorded higher strains compared to the demec gauges for the same applied bending moment but, both types of strain gauges gave similar indication of flanged-member behaviour. The behaviour of these two walls could be divided up into three phases namely ; the early life, the middle life and the end life as done for the six walls discussed in the following paragraphs. The same phenomenon described and reported in the present investigation also applies to the two walls examined at BDA. Flanged behaviour is accentuated close to the ultimate point.

Overall, the behaviour of these walls exhibited three distinct stages of performance, namely : **(a) Stage 1 :** this marks the early stages of loading and this stage is characterized by an approximately linear relationship between the applied "load" and the corresponding "displacements". It could be considered as the early life of the wall.

(b) Stage 2 : this marks the immediate period (as well as some loading time away from cracking) after the specimen has cracked and could be considered as the middle life of the wall. The relationship between the applied loads and displacements of the wall is characterized by some measure of nonlinearity mainly due to cracking, and

(c) Stage 3 : This marks the period just prior to the ultimate failure point of the specimen. This could be considered as the end life of the wall and is characterized by an acute non-linear relationship between the applied "load" and the resulting "displacements". It is a very unstable period in the life of the wall and accurately determines the ultimate point.

5.7 CONCLUSIONS

(1) The ultimate strength of the pocket-reinforced slabs tested in this work could be reasonably predicted by a method based on yield-line analysis as well as by the direct method.

(2) The shear strength of these slabs could also be reasonably predicted by the method based on plastic analysis provided the effectiveness factor is obtained from the expression developed in this work.

(3) The deflection of these slabs are also reasonably predicted by the direct method.

(4) In all the cases of pocket spacings investigated, the failure through steel yielding was critical for the pocket-reinforced slabs. These results suggest that the design of pocket-type slabs with wide pocket spacings is permissible and would be consistent with satisfying the condition that stem failure, rather than panel failure, remain the critical design factor.

(5) Analysis of the experimental results using different theoretical prediction methods indicate that the full width of the slabs may be considered in design. The methods based on effective flange width, although reasonable, proved to be conservative. The full width of these slabs remained active and should be considered in the calculations of strength.

CHAPTER 6

SUMMARY AND CONCLUSIONS

6.1 GENERAL

This thesis presents the results of a study into the structural behaviour of pocket-reinforced brickwork sections. In total, 8 full-scale beams and 6 slab specimens made of half-scale bricks were tested. In parallel with this work, a series of small specimen tests were also undertaken to evaluate all the material properties of both the brickwork and steel which are used in the theoretical analysis. The influence of a number of important variables affecting both shear strength and flanged-member behaviour of these wall sections were thoroughly examined.

6.2 CONCLUSIONS

On the basis of this investigation, the following general conclusions are drawn :

(1) The technique of using results from axially-loaded prisms to determine the stress distribution in eccentrically-loaded prisms is shown to be valid for the brickwork format used in this work.

(2) The stress block factors λ_1 and λ_2 are not significantly different for brickwork loaded axially or eccentrically. The axially-loaded brickwork prisms provide a reliable description of the compressive properties of the brickwork beams.

(3) The modulus of elasticity for brickwork is dependent on the direction of stressing relative to the bed-joint. For the brickwork used in the present work, it is reasonably predicted by existing equations derived for (a) brickwork loaded parallel to the bed-joint and (b) brickwork in which loading is applied normal and parallel to the bed joint. It appears that the code provision for estimating the modulus of elasticity of brickwork is not conservative.

(4) Studies on shear behaviour of pocket walls show that shear strength is strongly influenced by *a/d* ratio but is only marginally affected by the percentage of longitudinal steel in the pocket stems.

(5) Pocket-reinforced sections examined by the author have ultimate shear strength values which could be reasonably predicted by the method based on plastic analysis, given that the expression for the effectiveness factor derived in this thesis is used.

(6) Both the direct method and the method based on Branson's procedure gave good prediction of deflections of pocket-reinforced beams tested in this work. The method based on the direct method gave a closer prediction than Branson's method, in most cases especially at higher bending moments.

(7) A method of prediction of ultimate strength of the pocket-reinforced slabs, based on yield-line analysis, is found to be adequate for all the slabs investigated. The use of the direct method also gave reasonable prediction of the strength of these pocket-reinforced slabs.

(8) Analysis of the experimental results using various theoretical methods revealed that the full width of the slabs should be considered in design. The methods based on effective width of the flange, although reasonable, proved to be conservative. It appears that the full width of pocket-reinforced slabs remained active and should be considered in the calculation of strength.

6.3 SUGGESTIONS FOR FURTHER RESEARCH WORK

The investigations carried out in this thesis explain the structural behaviour of pocket-reinforced brickwork slab specimens with respect to pocket stem spacing. It also provides a method of analysis which considers the non-linear material stress-strain relationship of brickwork and steel as obtained from small specimen tests. A method of calculating the effective width of the flange of the pocket beams, based on experimental strain measurements, is also formulated. The plastic method originally developed for predicting shear strength in concrete beams was adapted for predicting shear strength of reinforced brickwork pocket-type beam sections. Before these methods are applied universally, it would be worthwhile to conduct further research into the areas listed below :

(1) The use of lateral loading in the form of concentrated loads was adopted to investigate flanged-member behaviour in pocket-type reinforced walls. It is possible that the loading arrangement could have some influence on the behaviour of these wall sections. It is worthwhile to try applying a uniform loading and examine the effects on the effective width for different cases of pocket stem spacing to confirm the findings of the present work.

(2) A pocket-type slab with different pocket spacing and having other boundary conditions could be examined to check their influence on the structural behaviour of this type of reinforced brickwork sections.

REFERENCES

1. Edgell, G.J. and Templeton, W. "The Structural Performance of Pocket-Type Retaining Walls", *Laboratory Report PRWALLBDA,* October 1992, 4pp.

2. British Standards Institution, "Code of Practice for Use of Reinforced and Prestressed Masonry", BS 5628 : **Part 2** : 1995.

3. Foster, D. "Development and Applications of Reinforced and Prestressed Masonry" in "Reinforced and Prestressed Masonry", edited by Hendry, A.W. *Longman Scientific & Technical with John Wiley & Sons.,* 1991, pp 1-24.

4. Sinha, B.P. and Pedreschi, R.F. "Reinforced and Prestressed Brickwork" *IE (I) Journal*, **Vol 72,** May 1991, pp1-12.

5. Brebner, A. "Notes on Reinforced Brickwork", Technical Paper 38, **Vols 1 & 2.** *Public Works Department*, Government of India, 1919.

6. Mehta, K. C. and Fincher, D. "Structural Behaviour of Pretensioned Prestressed Masonry Beams", *Proceedings of the 2nd International Brick Masonry Conference*, Edited by H.W.H.West and K.Speed, Stoke-on-Trent, British Ceramic Research Association, 1971, pp 215-219.

7. Pedreschi, R.F. "A Study of the Behaviour of Post-tensioned Brickwork Beams", *Ph.D Thesis*, Department of Civil Engineering and Building Science, The University of Edinburgh, 1983.

8. Thomas, K. "Current Post-Tensioned and Prestressed Brickwork and Ceramics in Great Britain", *Designing, Engineering and Constructing with Masonry Products*, edited by F.B. Johnson, Gulf, Houston, Texas 1969, pp 285-301.

9. Nielsen, M.P. and Braestrup, M.W. "Shear Strength of Prestressed Concrete Beams Without Web Reinforcement", *Magazine of Concrete Research*, **Vol 30**, No 104, September, 1978.

10. Robson, I. J. Ambrose, R. J. Hulse, R., and Morton, J. "Post-Tensioned Prestressed Brickwork Beams", *Proceedings of the British Masonry* Society, **No 1**, November 1986, pp 100-105.

11. Uduehi, J. "A Comparative Study of The Structural Behaviour of Prestressed Beams of Brickwork And Concrete And The Shear Strength of Brickwork Beams" *PhD Thesis*, Department of Civil Engineering and Building Science, The University of Edinburgh, 1990.

12. Garwood, T.G. "A Comparison of the Behaviour of Reinforced, Prestressed and Partially Prestressed Brickwork Beams", *Proceedings of First International Masonry Conference*, British Masonry Society, London, December 1986.

13. Walker, P.J. "A Study of the Behaviour of Partially Prestressed Brickwork Beams", *PhD Thesis*, Department of Civil Engineering and Building Science, The University of Edinburgh, 1987.

14. Garwood, T.G. "A Comparison of the Behaviour of Reinforced, Prestressed and Partially Prestressed Brickwork Beams", *Proceedings of First International Masonry Conference*, British Masonry Society, London, December 1986.

15. Roumani, N. and Phipps, M.E. "The Ultimate Shear Strength of Unbonded Prestressed Brickwork I and T Section Simply Supported Beams", *Proceedings of The British Masonry Society,* **No 2,** April 1988, pp 82-84.

16. Roumani, N. and Phipps, M.E. "The Shear Strength of Prestressed Brickwork I and T Sections", *Proceedings of the 7th International Brick Masonry Conference*, Edited by T. McNeilly and J.C. Scrivener, Melbourne, Australia, **Vol 2,** 1985, pp 1001-1014.

17. Kotsovos, M.D. "Behaviour of Reinforced Concrete Beams With A Shear Span to Depth Ratio Between 1.0 and 2.5". *Proceedings ACI* **Vol 81**, No 3, May/June 1984, pp 279-298.

18. Kotsovos, M.D. "Compressive Force Path Concept : A Suitable Basis for Reinforced Concrete Ultimate Limit State Design", *ACI Structural Journal*, **Vol 85,** No 1, Jan.-Feb, 1988, pp 68-75.

19. Kotsovos, M.D. and Lefas, I.D. "Behaviour of Reinforced Concrete Beams Designed in Compliance with the Concept of Compressive Force Path", *ACI Structural Journal*, **Vol 87**, Title No 87-S14,1990, pp 127-139.

20. Sinha, B.P. "Structural Performance of Prestressed Brickwork Pocket-Type Retaining Walls", *Structural Engineering Review,* **Vol 4,** No 2,1992, pp 139-145.

21. Pedreschi, R.F. and Sinha, B.P. "Predicting the Flexural Strength of Prestressed Brickwork Beams", *Structural Engineering Review*, **Vol 4,** No 3, 1992, pp 211-221.

22. Davies, S. and Hodgkinson, H.R. "Compressive Strength and The Stress/Strain Relationship of Brickwork When Stressed in the directions other than normal to the bed-face", *Masonry International* **2**, Dec 1988, pp 102-106.

23. Suter, G.T. and Hendry, A.W. "Shear Strength of Reinforced Brickwork Beams", *The Structural Engineer*, June 1975, No 6, **Vol 53**, pp 249-253.

24. Sinha, B.P. "Comparative Performance of Reinforced and Prestressed Brickwork Pocket-Type Retaining Walls in Shear", *Proceedings of the 10th International Brick and Block Masonry Conference*, Calgary, Alberta, Canada 5-7th July, 1994 pp 423-430.

25. Hendry, A.W. "Structural Masonry", *Macmillan,* 1990.

26. Sahlin, S. "Structural Masonry", *Prentice-Hall, Inc.,* Englewood Cliffs, New Jersey, 1971.

27. Osman, Y and Hendry, A.W. "Shear Transmission in Reinforced Grouted Cavity Brickwork Beams", *Proceedings, 6th International Brick Masonry Conference*, Rome, May 1982, pp 817-830.

28. Suter, G. T. and Keller, H. "Shear Strength of Grouted Reinforced Masonry Beams", *Proceedings of the fourth International Brick Masonry Conference (Brugge)* 1976, Paper **4.c.2.**

29. Sinha, B.P. and de Vekay, R.C. "Factors Affecting the Shear Strength of Reinforced Grouted Brickwork Beams and Slabs", *Proceedings of the 6th International Brick Masonry Conference*, Rome, May 1982, pp 831-842.

30. Tellett, J. and Edgell, G.J. "The Shear Behaviour of Reinforced Brickwork Pocket-Type Sections", *Proceedings of the British Masonry Society,* **Masonry (1),** Edited by H.W. H. West, No 1 November 1986, pp 85-90.

31. Kani, G.N.J. "Basic Facts Concerning Shear Failure", ACI Journal, **Vol 63** (1) , No 6, June 1966, pp 675-690.

32. Kani, G.N.J. "The Riddle of Shear Failure and Its Solution" *ACI Journal , Proceedings* **Vol 61**, No 4, April 1964, pp 441-467.

33. Sinha, B.P. and Foster, D. "Behaviour of Reinforced Grouted-Cavity Brick Beams", *Vth International Brick Masonry Conference*, Washington D.C., October 1979, pp 122-125.

34. Reineck, Karl-Heinz. "Ultimate Shear Force of Strutural Concrete Members Without Transverse Reinforcement Derived From A Mechanical Model", *ACI Structural Journal,* Sept.-Oct., 1991 (Title No 88-S51), pp 592-602.

35. Kong, F.K. and Evans, R.H. "Reinforced and Prestressed Concrete", Third Edition, *Wokingham : Van Nostrand Reinhold,* 1987.

36. Horton, R.T. and Tadros, M.K. "Deflection of Reinforced Masonry Members", *ACI Structural Journal*, July-August 1990, pp 453-463.

37. Branson, D. E. "Deformation of Concrete Structures", McGraw-Hill Book Company, New York, 1977, 546pp.

38. Osman, Y.A. and Hendry, A.W. "Deflection and Cracking of Reinforced Grouted Brickwork Beams", Masonry International , **Number 6**, Dec 1985, pp 22-26.

39. Sinha, B.P. "Reinforced Grouted Cavity Brickwork", *Journal of Building Research and Practice*, July/August 1982.

40. Sinha, B.P. "Reinforced Brickwork, Grouted-Cavity : Shear Tests", *Structural Clay Products Limited*, Hertford, April 1979.

41. Garwood, T.G. and Tomlinson, A. "The Cracking, Deflection and Collapse Behaviour of a Series of Reinforced Brickwork Beams", *Proceedings of 6th IBMAC Conference*, Rome, May 1982, pp 481-492.

42. Plowman, J.M. Sutherland, R.J.M. and Couzens, M.R. "The testing of reinforced brickwork and concrete slabs forming box beams", *Structural Engineer*, **45** (11) November 1967, pp 379-394.

43. Maurenbrecher, A.H.P. "A Reinforced Brickwork Retaining Wall", *Proceedings of the Fourth International Brick Masonry Conference, (Brugge)* 1976, paper **4.c.5**

44. Sinha, B.P. "Reinforced Brickwork : Retaining Walls Long Term Tests" SCP 14, *Structural Clay Products.*, Vine Cottage, Brington Road, Old Weston, Huntingdon.

45. Tellet, J. "Pocket-Type Reinforced Brickwork Retaining Walls", *PhD Thesis*, Dept., of Engineering Science, The University of Warwick, April 1984.

46. Tellet, J. and May, I.M. "Finite Element Analysis of Pocket-Type Retaining Walls and Implications for Design", *Masonry International*, **No 5,** pp 28-37, July 1985.

47. May, I. M. and Tellett, J. "Non-Linear Finite Element Analysis of Reinforced and Unreinforced Brickwork", *Proceedings of the British Masonry Society*, **Masonry (1),** Edited by H.W. H. West, No 1 November 1986, pp 96-99.

48. Edward, P. and Dix, D. "Investigation into the Performance of Pocket-Type Retaining Walls with Wide Pocket Spacing", *Laboratory Report BDA/PWALL 2*, May 1993, 12pp.

49. Kotsovos, M.D. "Mechanics of Shear Failure", *Magazine of Concrete Research,* **Vol 35**, No 123, June 1983, pp 99-106.

50. Kotsovos, M.D. "Behaviour of Beams With Shear Span-to-Depth Ratios Greater Than 2.5", *Journal of the American Concrete Institute,* **Vol 83,** No 93, November-December 1986, pp 1026-1034.

51. Page, A.W. "The Biaxial Compressive Strength of Brickwork", Proceedings Inst., of Civil Engineers, Part 2, **Vol 71**, September 1981, pp 893-906.

52. BS 4449 : 1988 "Specifications for carbon steel bars for the reinforcement of concrete".

53. B.S.I. "Specification for Ordinary and Rapid-Hardening Portland Cement", BS 12, 1991.

54. B.S.I. "Specification for Building Limes", BS 890, 1995.

55. BS 1200, 1976 : "Specification for Building Sand from Natural Sources", British Standards Institutions London.

56. Pedreschi, R.F. and Sinha, B.P., "The Stress/Strain Relationship of Brickwork", *6th International Brick Masonry Conference*, Rome, May 1982, pp 321-334.

57. Walker, P. and Sinha, B.P. "Behaviour of Partially Prestressed Brickwork Beams", *Proceedings of the 7th International Brick Masonry Conference,* Melbourne, Australia, February 1985, pp 1015-1029.

58. Sinha, B.P. "The Shear Strength of Brickwork Beams Prestressed Normal to the Bed Joints", Masonry International **Vol 8**, No 1, 1994.

59. Ng, C. L. "Experimental And Theoretical Investigation Of The Behaviour Of Brickwork Cladding Panel Subjected To Lateral Loading", PhD Thesis, University of Edinburgh, 1996.

60. Sinha, B.P. and Hendry, A. W. "Racking test on Storey-Height Shear-Wall Structure with Opening Subjected to Precompression", in Designing, Engineering and Construction with Masonry Products, Gulf Publication, Houston, Texas 1969.

61. Tellet, J. and Edgell, G.J. "The Shear Behaviour of Reinforced Brickwork Pocket-Type Sections", *Proceedings of the British Masonry Society*, Edited by West, H.W.H. in Masonry(1), Nov 1986 pp 85-90.

62. Nielsen, M.P. Braestrup, M. W. Jensen, B.R. and Bach, F. "Concrete Plasticity Beam Shear - Shear in Joints, Punching Shear", Danish Society for Structural Science and Engineering, Special Publication, Technical University of Denmark, Copenhagen, October 1978.

63. Prager, W. "An Introduction to Plasticity", Addison-Wesley, Massachusetts, 1959.

64. Sinha, B.P. "An Ultimate Load-Analysis of Reinforced Brickwork Flexural Members", *International Journal of Masonry Construction,* **Vol 1**, No 4, 1981, p151.

65. Timoshenko, S. P and Goodier, J.N. "Theory of Elasticity", *McGraw-Hill* International Series, 1970, New York, 567 pp.

66. Timoshenko, S. and Woinowsky-Krieger, S. "Theory of Plates and Shells", *McGraw-Hill* Book Co., New York, 1959, 580 pp.

(67) Johansen, K.W. "Yield-line Formulae for Slabs". Cement and Concrete Association, London, 1972.

APPENDIX (I) : RESULTS FOR BRICKWORK CROSS-SECTIONS THAT FAILED IN SHEAR

No	Effectiveness factor	a/h ratio	Degree of reinforcement	h(mm)	f_t(N/mm^2)	fm(N/mm^2)
1	0.38	8	0.138	170	2.12	29.75
2	0.38	8	0.138	170	2.12	29.75
3	0.53	8	0.138	170	3.3	29.75
4	0.5	8	0.138	170	3.11	29.75
5	0.52	8	0.138	170	3.88	29.75
6	0.61	5.47	0.321	445	8.07	22.34
7	0.6	5.47	0.321	445	6.59	22.34
8	0.64	5.47	0.321	445	6.78	22.34
9	0.59	5.47	0.321	445	8.02	22.34
10	0.61	5.47	0.321	445	7.9	22.34
11	0.7	5.47	0.321	445	10.36	22.34
12	0.66	5.47	0.321	445	10.46	22.34
13	0.39	4.8	0.518	170	3.18	29.75
14	0.44	4.8	0.518	170	3.24	29.75
15	0.42	4.8	0.518	170	2.56	29.75
16	0.37	4.8	0.518	170	3.01	29.75
17	0.43	4.8	0.518	170	2.31	29.75
18	0.68	3.2	0.518	170	2.65	11.17
19	0.44	5.47	0.241	445	8.57	29.75
20	0.36	4.8	0.389	170	1.51	29.75
21	0.55	4.8	0.389	170	1.8	29.75
22	0.39	4.8	0.389	170	3.68	29.75
23	0.33	4.8	0.389	170	3.18	29.75
24	0.58	5.47	0.391	445	6.96	22.34
25	0.67	5.47	0.391	445	7.06	22.34
26	0.67	5.47	0.391	445	7.16	22.34
27	0.48	5.47	0.391	445	6.02	22.34
28	0.57	5.47	0.321	445	5.98	22.34
29	0.59	5.47	0.321	445	7.21	22.34
30	0.63	5.47	0.321	445	6.06	22.34
31	0.47	4.8	0.138	170	2.38	29.75

32	0.51	4.8	0.138	170	2.77	29.75
33	0.45	4.8	0.388	170	3.52	29.75
34	0.45	4.8	0.388	170	1.98	29.75
35	0.42	4.8	0.388	170	1.45	29.75
36	0.43	4.8	0.455	170	2.77	25.4
37	0.41	4.8	0.455	170	2.09	25.4
38	0.46	4.8	0.455	170	2.06	25.4
39	0.5	4.8	0.455	170	2.49	25.4
40	0.39	4.8	0.455	170	2.81	25.4
41	0.46	4.8	0.455	170	2.15	25.4
42	0.65	5.47	0.279	445	6.33	16.4
43	0.76	5.47	0.279	445	5.09	16.4
44	0.81	4.8	0.279	170	1.7	11.4
45	0.73	5.47	0.279	445	5.86	16.4
46	0.57	5.47	0.341	445	6.59	21
47	0.57	5.47	0.341	445	7.78	21
48	0.57	5.47	0.341	445	7.69	21
49	0.67	5.47	0.341	445	6.78	21
50	0.26	1.6	0.096	170	1.2	33.9
51	0.52	1.6	0.096	170	1.7	33.9
52	0.49	1.6	0.096	170	2.01	33.9
53	0.41	2.4	0.096	170	2.36	33.9
54	0.23	2.4	0.096	170	2.14	33.9
55	0.47	2.4	0.096	170	1.83	33.9
56	0.34	3.2	0.096	170	2.14	33.9
57	0.25	3.2	0.096	170	2.3	33.9
58	0.26	3.2	0.096	170	1.53	33.9
59	0.17	4	0.096	170	1.65	33.9
60	0.24	4	0.096	170	1.26	33.9
61	0.14	4	0.096	170	1.77	33.9
62	0.46	0.806	0.1224	372	1.28	7.94
63	0.4	1.21	0.1224	372	1.47	7.94
64	0.39	1.613	0.1224	372	1.37	7.72
65	0.43	2.016	0.1224	372	1.73	7.72

66	0.38	2.419	0.1224	372	1.19	7.72
67	0.46	0.806	0.9332	372	2.34	11.03
68	0.35	1.21	0.9332	372	2.83	11.03
69	0.33	1.613	0.9332	372	2.58	11.03
70	0.31	2.016	0.9332	372	3.24	10.98
71	0.36	2.419	0.9332	372	2.1	10.98
72	0.41	3.226	0.9332	372	2.86	10.98
73	0.45	4.032	0.9332	372	3.66	10.98
74	0.27	1.67	0.466	330	1.01	10.8
75	0.28	1.67	0.3	330	0.61	10.8
76	0.28	1.67	0.172	330	0.92	18.2
77	0.28	1.58	0.071	330	1.01	43.4
78	0.28	1.63	0.112	330	1.01	43.4
79	0.42	5.12	0.191	450	5.48	22.44
80	0.44	5.12	0.191	450	5.48	22.5
81	0.43	5.12	0.301	450	5.48	24.3
82	0.44	5.12	0.301	450	5.48	22.54
83	0.37	3.481	0.349	215	1.7	25.2
84	0.37	3.481	0.349	215	1.75	25.2
85	0.29	1.04	0.137	370	3.26	32.7
86	0.41	1.04	0.137	370	3.28	32.7
87	0.22	1.04	0.137	370	3.13	32.7
88	0.31	2.27	0.137	370	3.28	32.7
89	0.26	2.27	0.137	370	3.39	32.7
90	0.28	2.27	0.137	370	3.46	32.7
91	0.33	3.37	0.137	370	3.59	32.7
92	0.28	3.46	0.137	370	3.49	32.7
93	0.29	3.46	0.137	370	3.62	32.7
94	0.31	4.68	0.137	370	3.49	32.7
95	0.41	4.68	0.137	370	3.44	32.7
96	0.29	4.68	0.137	370	3.59	32.7
97	0.33	7.33	0.186	370	6.95	32.56
98	0.33	7.33	0.186	370	6.92	32.56
99	0.35	7.33	0.186	370	6.59	32.56

100	0.31	2.66	0.186	370	6.1	32.56
101	0.3	2.66	0.186	370	6.46	32.56
102	0.29	1.33	0.186	370	6.1	32.56
103	0.34	1.33	0.186	370	6	32.56
104	0.32	4.77	0.186	370	6.36	32.56
105	0.3	4.77	0.186	370	6.38	32.56
106	0.34	7.33	0.137	370	7.15	32.56
107	0.4	7.33	0.137	370	7.15	32.56
108	0.34	7.33	0.137	370	6.51	32.56
109	0.38	7.176	0.087	370	3.63	33.1
110	0.33	7.176	0.087	370	3.61	33.1
111	0.39	3.481	0.349	215	2.9	24.35
112	0.38	3.481	0.349	215	2.81	24.35
113	0.44	1.995	0.349	215	6.24	25.3
114	0.37	1.995	0.349	215	6.12	26.2
115	0.58	7.182	0.302	370	3.31	5.56
116	0.67	7.182	0.302	370	3.01	5.56

APPENDIX (II) : Table A2 : Calculated factor of safety for beams tested by Tellet[65] based on allowable shear strength results[48] .

Beam No	a/d	Shear strength (N/mm^2)		characteristic shear strength[48]	Allowable shear strength	Factor of Safety (FOS)	
		Reported results (N/mm^2)	corrected results (N/mm^2)	(N/mm^2)	(N/mm^2)	Based on reported results	Based on corrected values
1	5.09	0.46	0.91	0.54	0.27	1.7	3.37
2	5.00	0.63	1.25	0.63	0.32	1.97	3.91
3	4.75	0.30	0.59	0.52	0.26	1.15	2.27
4	3.93	0.43	0.82	0.61	0.31	1.39	2.65
5	2.00	0.81	1.60	0.80	0.40	2.03	4.00
6	5.09	0.81	1.59	0.62	0.31	2.61	5.13
7	5.28	0.90	1.78	0.71	0.36	2.50	4.94
8	5.18	0.71	1.41	0.61	0.31	2.29	4.55
9	5.00	0.32	0.64	0.50	0.25	1.28	2.56
10	5.18	0.34	0.67	0.48	0.24	1.42	2.79
11	5.28	0.84	1.51	0.71	0.36	2.33	4.19
12	2.00	0.91	1.82	1.01	0.51	1.78	3.57
13	2.00	1.33	2.67	1.01	0.51	2.61	5.24
14	1.89	1.08	2.15	1.01	0.51	2.12	4.22
15	1.96	1.71	3.47	1.19	0.6	2.85	5.78

APPENDIX (III) : CALCULATION OF BENDING MOMENT AND SHEAR CAPACITIES BASED ON BS 5628 (PART 2 : 1995)[2] .

(1) BENDING MOMENT CAPACITY :

Case 1 : (S = 540 mm)

$M_d = \frac{f_k}{\gamma_{mm}} b t_f \left(d - 0.5 t_f\right)$ (section 4.2.4.3.1) ---------- eqn. (A)

With t_f = 0.5d = 45 mm,

The width of the flange should be taken as the least of :

(a) the width of the pocket or rib plus 12 times the thickness of the flanges ;

(b) the spacing of the pockets or ribs ;

(c) one-third the height of the wall.

With option (a), b = 55 + (540) = 595 mm;

With option (b), b = 540 mm;

With option (c), b = 400 mm, hence option (c) is critical.

From eqn (A), $M_d = 21.5 \times 400 \times 45 \times \left((90 - (0.5 \times 45)\right) = 26.122500 kNm$

Also, this capacity is obtainable from

$M_d = \frac{A_s f_y z}{\gamma_{ms}}$ ---------- eqn. (B)

With $z = d\left[1 - \frac{0.5 \times 157.08 \times 500 \times 1}{400 \times 90 \times 21.5 \times 1}\right] = 90 \times (1 - 0.0507) = 85.43 mm$

where $z = d\left(1 - \frac{0.5 A_s f_y \gamma_{mm}}{b d f_k \gamma_{ms}}\right)$ (section 4.2.4.2)

hence,

$M_d = 157.08 \times 500 \times 85.43 = 6.71 kNm$

if the partial safety factors, γ_{ms} and γ_{mm} are both taken as unity.

Case 2 : (S =1000 mm)

With option (a), b = 55 + (540) = 595 mm;

With option (b), b = 1000 mm;

With option (c), b = 400 mm, hence option (c) is critical.

From eqn (A), $M_d = 21.5 \times 400 \times 45 \times \left((90 - (0.5 \times 45)\right) = 26.122500 kNm$

Also, this capacity is obtainable from

$$M_d = \frac{A_s f_y z}{\gamma_{ms}} \qquad \text{---------- eqn. (B)}$$

With $z = d\left[1 - \frac{0.5 \times 226 \times 470 \times 1}{400 \times 90 \times 21.5 \times 1}\right] = 90 \times (1 - 0.0686) = 83.83 mm$

where $z = d\left(1 - \frac{0.5 A_s f_y \gamma_{mm}}{b d f_k \gamma_{ms}}\right)$ (section 4.2.4.2)

hence,

$M_d = 226 \times 470 \times 83.83 = 8.9 kNm$

if the partial safety factors, γ_{ms} and γ_{mm} are both taken as unity.

Case 3 : (S =1750 mm)

With option (a), b = 55 + (540) = 595 mm;

With option (b), b = 1750 mm;

With option (c), b = 400 mm, hence option (c) is critical.

From eqn (A), $M_d = 21.5 \times 400 \times 45 \times \left((90 - (0.5 \times 45)\right) = 26.122500 kNm$

Also, this capacity is obtainable from

$$M_d = \frac{A_s f_y z}{\gamma_{ms}} \qquad \text{---------- eqn. (B)}$$

With $z = d\left[1 - \frac{0.5 \times (157.08 \times 500 + 226 \times 470) \times 1}{400 \times 90 \times 21.5 \times 1}\right] = 90 \times (1 - 0.119354) = 79.26 mm$

where $z = d\left(1 - \frac{0.5 A_s f_y \gamma_{mm}}{bdf_k \gamma_{ms}}\right)$ (section 4.2.4.2)

hence,

$M_d = 184760 \times 79.26 = 14.64 kNm$

if the partial safety factors, γ_{ms} and γ_{mm} are both taken as unity.

(2) SHEAR CAPACITY :

Case 1 : (S = 540 mm)

$f_v = 0.35 + 17.5\rho$ (section 3.4.1.3)

With $\rho = \frac{A_s}{bd} = \frac{2 \times 78.54}{400 \times 90} = 4.36333 \times 10^{-3}$

hence, $f_v = 0.35 + 0.07636 = 0.426\,\text{N/mm}^2$.

Therefore, $V = 0.426 \times 400 \times 90 = 15336N = 15.34kN$.

Case 2 : (S = 1000 mm)

$f_v = 0.35 + 17.5\rho$ (section 3.4.1.3)

With $\rho = \frac{A_s}{bd} = \frac{2 \times 113.09}{400 \times 90} = 6.28278 \times 10^{-3}$

hence, $f_v = 0.35 + 0.1099 = 0.460\,\text{N/mm}^2$.

Therefore, $V = 0.460 \times 400 \times 90 = 16560N = 16.56kN$.

Case 3 : (S = 1750 mm)

$f_v = 0.35 + 17.5\rho$ (section 3.4.1.3)

With $\rho = \frac{A_s}{bd} = \frac{383.27}{400 \times 90} = 0.106463 \times 10^{-1}$

hence, $f_v = 0.35 + 0.1863 = 0.536\,\text{N/mm}^2$.

Therefore, $V = 0.536 \times 400 \times 90 = 19296N = 19.30kN$.